1 2 9 0

UNIVERSIDADE D
COIMBRA

Ângela Cristina Barrôco Neves

ADVANCED MICROWAVE TECHNOLOGY IN RADIOPHARMACEUTICAL SYNTHESIS

Tese no âmbito do doutoramento em Ciências Farmacêuticas, ramo de Química Farmacêutica orientada pelo Professor Doutor Antero José Pena Afonso de Abrunhosa e pelo Professor Doutor Amílcar Celta Falcão Ramos Ferreira e apresentada à Faculdade de Farmácia da Universidade de Coimbra.

Dezembro de 2021

1 2 9 0

UNIVERSIDADE D
COIMBRA

Ângela Cristina Barrôco Neves

ADVANCED MICROWAVE TECHNOLOGY IN RADIOPHARMACEUTICAL SYNTHESIS

Tese no âmbito do doutoramento em Ciências Farmacêuticas, ramo de Química Farmacêutica orientada pelo Professor Doutor Antero José Pena Afonso de Abrunhosa pelo Professor Doutor Amílcar Celta Falcão Ramos Ferreira e apresentada à Faculdade de Farmácia da Universidade de Coimbra.

Dezembro de 2021

Acknowledgments

I would like to thank everyone who have, in one way or another, contributed to the development of this work.

I would like to express my gratitude to my supervisors, Professor Antero Abrunhosa and Professor Amílcar Falcão for the opportunity to carry out this work.

To Professor Antero, for the opportunity to develop this work at the Laboratory for Radiochemistry and Cyclotron at ICNAS-P and for all the knowledge, help, orientation, and confidence.

I am grateful for the financial support of the Foundation for Science and Technology (FCT), Ministry of Science Technology and Higher Education (MCTES), European Social Fund (FSE), European Union (UE) and to Regional Operational Program of the Centre, through the granting of the doctoral scholarship of the doctoral program “Drugs R&D”, PD/BDE/135132/2017.

To all the team at ICNAS-P for the cooperation in the development of this work. A special mention to Vítor, Ivanna, Inês, and Vanessa, for the support in the development of this project, and valuable scientific discussions. To the cyclotron team for all the cooperation and availability during all this process.

To Professor Mariette and the team at the Laboratory of Catalysis & Fine Chemistry of the University of Coimbra for the scientific support and the help with the chemical synthesis and characterizations.

To my family, friends, and colleagues, for all the support and good mood.

To António for all the support and for always being there.

Most of all, I want to thank my mother, for her unconditional support at all stages of my life, friendship, and patience, to my father (although he is no longer present) and specially to Constança, my biggest inspiration.

Abstract

Nuclear medicine is a very powerful tool in the diagnosis and treatment of multiple pathologies with important clinical and research applications in areas such as oncology, cardiology, and neurosciences. In the basis of this important clinical speciality is the use of radiopharmaceuticals, molecules that include a radioisotope in their composition and therefore allow us to map in detail molecular processes and interactions in living organisms.

Many different radionuclides have been used since the 1940's for multiple clinical applications. In the diagnostic setting, most of the efforts in recent years have been directed towards positron emitters. Of those, the most important are ^{11}C and ^{18}F with half-lives of 20 and 109 minutes, respectively. These physical characteristics make radiopharmaceutical production quite challenging. The radioactivity produced must be enough to complete chemical synthesis, purification, quality control and the clinical examination. In practice, a radiopharmaceutical synthesis process should be automatic, fast, robust, reproducible, and present good chemical and radiochemical yields.

In the work leading to this PhD thesis, we focused on two of the most difficult synthesis processes used to produce diagnostic radiopharmaceuticals today. The nucleophilic production of 6-[^{18}F]FDOPA and the radiosynthesis [^{11}C]UCB-J. Our approach was to improve current available processes, exploring the use of microwave technology, and developing GMP-compliant automated processes that could be used for routine clinical production of these important radiopharmaceuticals.

6-[^{18}F]FDOPA is a radiotracer with important clinical applications not only in neurology, but also in oncology where it can be used to image brain and neuroendocrine tumours. The synthesis process is very complex and although a few commercial implementations exist, very few centres are able to produce it, which makes it difficult for patients to have access to this important radiopharmaceutical.

In order to improve the radiosynthesis, several critical steps were converted to microwave heating such as the drying of [^{18}F]fluoride,^{18}F-fluorination of 6-[^{18}F]FDOPA precursors and hydrolysis of the protected 6-[^{18}F]FDOPA. In all steps, a reduction of reaction time was obtained, being the most significant in the hydrolysis step, from 20 to 3.4 minutes, a reduction of about 80 % in this step. Also, a new possible precursor for 6-[^{18}F]FDOPA was synthesised and fully characterised, with isolated yields of 35 %.

Another challenging process is the synthesis of [^{11}C]UCB-J, a radiopharmaceutical used to quantify synaptic density *in vivo*, whose synthesis is performed *via* the palladium-catalysed Suzuki-Miyaura cross-coupling.

The main challenges for the implementation of this production, are the reaction conditions that include de-aeration of solvents, need for constant agitation and challenging reaction

temperatures. There is no implementation of the process commercially and very few centres are able to produce it for clinical use.

Considering the 20 minutes half-life of carbon-11, optimization of synthesis and processing time is of great importance. Different solvents, reaction times, as well as the influence of precursor activation were tested. Additionally, the effect of microwave heating *vs*. conventional heating was compared. The development resulted in a robust, reproducible process, with a yield of 53 %, dc, in 55 minutes by conventional heating and, in 49.7 minutes by microwave, minus 5.3 minutes total time which, means 20 % more activity at the end of synthesis.

Following on the work described in this thesis, an application was submitted to INFARMED to produce and distribute 6-[^{18}F]FDOPA and a Marketing Authorisation (MA) was granted to ICNAS-P. This is the only 6-[^{18}F]FDOPA currently being marketed in Portugal.

Documentation is currently being prepared to initiate the use of [^{11}C]UCB-J for an international clinical trial.

Keywords: [^{18}F]FDOPA; [^{11}C]UCB-J; PET imaging; microwave; radiochemistry; automatic synthesis.

Resumo

A medicina nuclear é uma excelente ferramenta no diagnóstico de doenças, com importantes aplicações clínicas e de investigação em áreas como Oncologia, Cardiologia e Neurociências. Na base desta importante especialidade clínica está o uso de radiofármacos, moléculas que incluem um radioisótopo na sua composição e que permite mapear em detalhe processos moleculares e interações em organismos vivos.

Vários radionuclídeos têm sido utilizados para múltiplas aplicações clínicas, desde a década de 1940. No contexto de diagnóstico, a maioria dos esforços nos últimos anos têm sido direcionados para os emissores de positrões. Destes, os mais importantes são o ^{11}C e o ^{18}F, com meias-vidas de 20 e 109 minutos, respetivamente. Estas características físicas tornam a produção de radiofármacos bastante desafiante. A radioatividade produzida deve ser suficiente para efetuar a síntese química completa, o controlo de qualidade e o exame clínico.

Na prática, um processo de síntese de um radiofármaco, deve ser automático, rápido, robusto, reprodutível e apresentar bons rendimentos químicos e radioquímicos.

No trabalho conducente a esta tese de doutoramento, focamo-nos em dois dos processos de síntese mais difíceis utilizados para produzir radiofármacos de diagnóstico hoje em dia. A produção nucleofílica de 6-[^{18}F]FDOPA e a radiossíntese do [^{11}C]UCB-J. A nossa abordagem centrou-se na melhoria dos processos disponíveis atualmente, explorar a utilização da tecnologia de micro-ondas e desenvolver processos automatizados compatíveis com GMP, que pudessem ser usados para a produção de rotina destes importantes radiofármacos.

A 6-[^{18}F]FDOPA é um radiofármaco com aplicações clínicas importantes não só em neurologia, mas também em oncologia, que pode ser usado para imagem de tumores cerebrais e neuroendócrinos. O processo de síntese é muito complexo e, embora existam algumas implementações comerciais, muito poucos centros têm capacidade de o produzir, o que dificulta o acesso dos doentes a este importante radiofármaco.

A fim de melhorar o processo de síntese, o aquecimento com recurso à tecnologia de micro ondas foi aplicado em vários passos críticos, tais como a secagem de [^{18}F]fluoreto, na ^{18}F-fluoração de possíveis precursores de 6-[^{18}F]FDOPA e na hidrólise da FDOPA protegida. Em todas as etapas em que este tipo de aquecimento foi testado, obteve-se uma redução do tempo de reação, sendo a mais significativa no passo de hidrólise, de 20 para 4 minutos, o que representa uma redução de cerca de 80 % do tempo, neste passo. Além disso, foi sintetizado e completamente caracterizado um novo possível precursor para a síntese de 6-[^{18}F]FDOPA, com rendimentos isolados de 35 %.

.

Outro processo desafiante foi a síntese do [^{11}C]UCB-J, um radiofármaco usado para quantificar a densidade sináptica *in vivo*, cuja síntese é realizada através do acoplamento de Suzuki-Miyaura.

Os principais desafios para a implementação deste processo de produção, prende-se com as condições que este tipo de reações requer, tais como o desarejamento de solventes, a necessidade de constante agitação ou as desafiantes condições de temperatura.

Considerando os 20 minutos de meia-vida do carbono-11, a otimização deste processo de síntese crucial. Foram testados diferentes solventes, tempos de reação, bem como a influência da ativação do precursor. Adicionalmente, o efeito do aquecimento micro-ondas *vs* aquecimento convencional foi também comparado. O desenvolvimento resultou num processo robusto e reprodutível, com um rendimento de 53 %, dc, em 55 minutos por aquecimento convencional e, em 49.7 minutos por micro-ondas, menos 5.3 minutos de tempo total, o que significa um aumento de cerca de 20 % de atividade no fim de síntese.

No seguimento do trabalho descrito nesta tese, foi apresentado ao INFARMED um pedido de autorização de produção e distribuição de 6-[^{18}F]FDOPA, o qual foi concedido à ICNAS-P. Este é o único processo de síntese de 6-[^{18}F]FDOPA atualmente comercializado em Portugal.

Adicionalmente, está a ser preparada a documentação para iniciar o uso de [^{11}C]UCB-J num ensaio clínico internacional.

Palavras-chave: [^{18}F]FDOPA; [^{11}C]UCB-J; Imagem PET; micro-ondas; radioquímica; síntese automática.

List of abbreviations and acronyms

[^{11}C]PiB: ^{11}C-labelled Pittsburgh Compound-B

[^{11}C]UCB-J: (*R*)-1-[(3-[^{11}C] methyl-4-pyridyl)methyl]-4-(3,4,5-trifluorophenyl)pyrrolidin-2-one

[^{18}F]ASEM: 3-(1,4- diazabicyclo[3.2.2]nonan-4-yl)-6-[^{18}F]fluorodibenzo[*b*,*d*] thiophene 5,5-dioxide

[^{18}F]FAZA: [^{18}F]2-fluoroazomycin arabinoside

[^{18}F]FDG: [^{18}F]-fluoro-2-deoxy-D-glucose

[^{18}F]FMAU: 2'-deoxy-2'-[^{18}F]fluoro-5-ethyl-1-*β*-*D*-arabinofuranosyluracil

[^{18}F]FSB: *N*-succinimidyl 4-[^{18}F]fluorobenzoate

[^{18}F]NEBIFQUINIDE: [^{18}F](*R*)-*N*-(sec-Butyl)-1-(2-fluoropyridin-3-yl)-N- methylisoquinoline-3-carboxamide

[^{18}F]NS10743: [^{18}F]4-[5-(4-fluoro-phenyl)-[1,3,4]oxadia- zol-2-yl]-1,4-diazabicyclo[3.2.2]nonane

6-[^{18}F]FDOPA: 3,4-dihydroxy-6-[^{18}F]fluoro-*L*-phenylalanine

ACN: acetonitrile

A_m: Molar activity

A_s: Specific activity

ATRA: all-trans-retinoic acid

BF_3-Dm-UCB-J: (*R*)-3-(difluoroboranyl)-4-((2-oxo-4-(3,4,5-trifluorophenyl) pyrrolidine-1-yl) methyl)-pyridin-1-ium floride

Boc: tert-butyloxycarbonyl

br: broad signal

c.a. carrier-added form

cGRPP: current Good Radiopharmacy Practice

CoE: Council of Europe

cPTC: chiral Phase-Transfer Catalyst

CT: Computed Tomography

d: doublet

DBA: dibenzylidene-acetone

dc: decay corrected

DCM: Dichloromethane

dd: doublet of doublets

DMA: Dimethylacetamide

DMF: *N*,*N*-dimethylformamide

DMSO: Dimethyl sulfoxide

DOTA: 1,4,7,10-tetraazacyclododecane-1,4,7,10-tetraacetic acid

DOTANOC: DOTA-[Nal^3]-octreotide

dppf: 1,1'-bis(diohenylphosphine)ferrocene

EANM: European Association of Nuclear Medicine

EDQM: European Directorate for the Quality of Medicines and Healthcare

ee: enantiomeric excess

EMA: European Medicines Agency

EOB: end of bombardment

EOS: end of synthesis

EtOH: ethanol

EU: European Union

Eur. Ph.: European Pharmacopoeia

eV: electronvolt

EWD: electron withdrawing

GC Gas Chromatography

GHz: Gigahertz

GMP: Good Manufacturing Practices

HI: Hydriodic acid

HPGe: High Purity Germanium

HPLC: High Performance Liquid Chromatography

HRMS: High Resolution Mass Spectrometry

IAEA: International Atomic Energy Agency

ICNAS: Instituto de Ciências Nucleares Aplicadas à Saúde (Institute for Nuclear Sciences Applied to Health)

INFARMED: National Authority of Medicines and Health Products

iTLC-SG: instant Thin Layer Chromatography – Silica Gel

IU: International Units

IUPAC: International Union of Pure and Applied Chemistry

J: coupling constant

keV: kilo-electronvolt

LAL: Limulus Amebocyte Lysate

LC: liquid chromatography

m: multiplet

MA: Marketing autorisation

mCi: millicurie

mCPBA: meta-Chloroperoxybenzoic acid

MeV: mega-electronvolt

MI: Molecular Imaging

Min: Minutes

MOM: Methoxymethyl Ether

MRI: Magnetic Resonance Imaging

Ms: mesylate

Mw: Molecular Weight

n.c.a no-carrier-added form

nd: not determined

ndc: non decay corrected

NET's: Neuroendocrine tumours

NiPBPGly: 2-benzoylphenylamide of pyridine-2-carboxylic acid and glycine

NOBIN: 2-amino-2'-hydroxy-1,1'-binaphthyl

PC: Power Cycling

PET Positron Emission Tomography

Ph. Eur.: European Pharmacopoeia

PSMA prostate-specific membrane antigen

PSPA-4: (2*S*,3*R*,4*R*)-3-carboxymethyl-4-(4-methylphenylthio)pyrrolidine-2-carboxylic acid

PTC: phase transfer catalyst

PTS: Portable Test System

QC Quality Control

QMA: Quaternary methyl ammonium

R&D Research and Development

RCP: radiochemical purity

RCY Radiochemical Yield

Rt: Retention time

RT: room temperature

s: singlet

SnAr: Aromatic Nucleophilic Substitution

SPE: Solid Phase Extraction

SPECT: Single-photon emission computed tomography

t: triplet

TBA: tetrabutylammonium

TBAF: Tetra-*n*-butylammonium fluoride

Tf: triflate

THF: Tetrahydrofuran

Ts: trosilate

US: ultrasound

WHO: World Health Organization

Contents

List of Figures

List of Tables

List of schemes

Chapter 1

Introduction

Molecular imaging is a term that became very popular in medicine. However, the concept is still in discussion. In general, it could be interpretated as *"in vivo imaging of biological processes with appropriate molecular probes"* [1]. The search for the optimal molecular imaging probes is the big challenge in this area. These probes are used to visualize and measure biological processes at molecular and cellular level, in humans and other living systems.

Techniques as magnetic resonance (MRI), computed tomography (CT), ultrasound (US), optical and nuclear imaging, have been used for diagnosis and monitoring of diseases, however, nuclear imaging has unique properties, such as selectivity and specificity, that allow the visualization of molecular level events at nano- or picomolar level [2]. Nuclear imaging techniques such as PET (Positron Emission Tomography) and SPECT (single-photon emission computed tomography) were the first techniques used in the molecular imaging field [3]. The basis of these techniques is the capacity to produce a molecule able to target biological, biochemical, or pharmacological processes. The molecular imaging probe development begins with a clinical question, followed by the selection of the molecular target and the selection of a biologically active molecule appropriated for the target. Afterwards, the radionuclide is selected and the radiosynthesis performed, followed by subsequent *in vitro* and *in vivo* studies [4]. In **Figure 1.1** we present the main steps of the development of a molecular imaging probe.

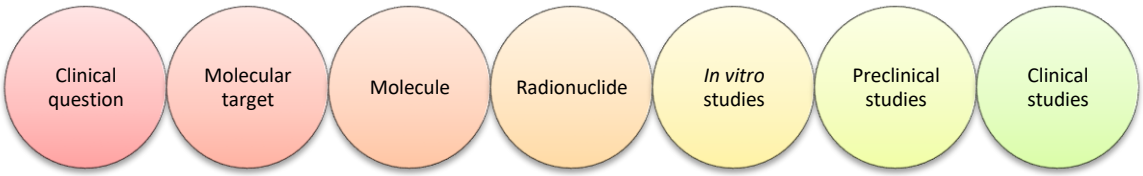

Figure 1.1: Main steps on the development of a molecular imaging probe.

The SPECT technique requires the use of an agent labelled with a gamma-emitting radionuclide, detected by a gamma camera or SPECT instrument. PET, on the other hand, requires a molecule labelled with a positron emitting radionuclide. PET has more sensitivity and better spatial resolution than SPECT and, for this reason, in the last decades, the search for the ideal PET-probe as well as PET studies performance gained substantial interest. Moreover, PET imaging allows for the quantitative mapping of a biomarker *in vivo*, which can be extremely important in evaluating whether a certain therapeutic agent can be utilized to target a receptor.

1.1 Positron Emission Tomography (PET)

1.1.1 Basic Principles

PET imaging requires the injection of a radiopharmaceutical labelled with a positron emitter radionuclide. The decay of the radionuclide results in the emission of a positron (an electron positively charged, e^+) which travels a short distance and annihilates with an electron (e^-) releasing two 511 keV gamma photons. These photons travel in opposite directions, at near 180º, being therefore detectable by the PET scanner. After acquisition, the data is fed to a computer that reconstructs the tree-dimensional tomographic images, **Figure 1.2** [5].

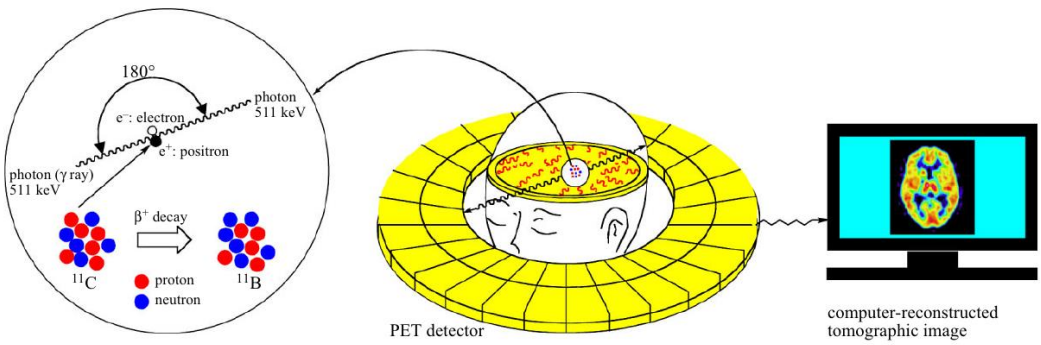

Figure 1.2: Principles of PET imaging.

PET scanners are equipped with a ring of small detectors around the patient, specifically designed to detect events only when pairs of gamma photons arrive within short time of each other. When an event is detected, the line joining the two detectors defines the origin of the annihilation without the need of a physical collimator, which results PET 100 times more sensitive than SPECT. Nowadays, PET scanners are equipped with CT (computed tomography) and, the availability of dual modality (PET/CT) has revolutionized the clinical use of PET. While PET provides functional imaging, CT gives anatomical information, which allows the visualization of molecular events and their localization in the human body [6].

For a radiopharmaceutical to be successful for molecular imaging it must have: i) hight affinity and specificity for the intended molecular target; ii) the ability to overcome the relevant biological barriers; iii) suitable kinetics to allow the binding to the target as well as a fast blood clearance; iv) and no active metabolites that can access the specific compartment so we can make quantification possible [6].

Not only the PET probe, but also the selection of the molecular target influences the success of a molecular imaging study. The target sites must have enough density to allow a strong specific signal and easy access for the PET probe. Moreover, the selection of a suitable nuclide with an adequate half-life, considering the synthesis time and the kinetics of the process being followed, is a critical issue. On the other hand, the selection of the radionuclide is important as it must preserve the physicochemical characteristics of the compound to be labelled which must be resistant to metabolism.

1.1.2 Radionuclides

Until the end of the nineteenth century, nobody knew that matter could emit radiation, except if heated or submitted to a high voltage. During the following years, a new phenomenon, called "radioactivity", was discovered [7]. The radioactivity of uranium was discovered in 1896 by Henry Becquerel. In the next years, it was found that thorium and polonium and radium, discovered by Pierre and Marie Curie, were also radioactive elements. In 1911, Ernest Rutherford performed a series of experiments in radioactivity that led to the realization that elements could be transmuted. In 1919, he managed to bombard a nitrogen nucleus with an alpha (α-) particle (from radon), transforming it into a nucleus of oxygen followed by the emission of a proton [8].

A radionuclide is a radioactive nuclide that contains an unstable arrangement of protons and neutrons, which will transform spontaneously to either a stable or another unstable combination of protons and neutrons, with a constant statistical probability. A nuclide is an atomic species characterized by the number of protons and neutrons in its nucleus and by its nuclear energy state. Nuclides with the same atomic number but different mass numbers are called isotopes, as is the case of hydrogen, which has three isotopes, **Figure 1.3**.

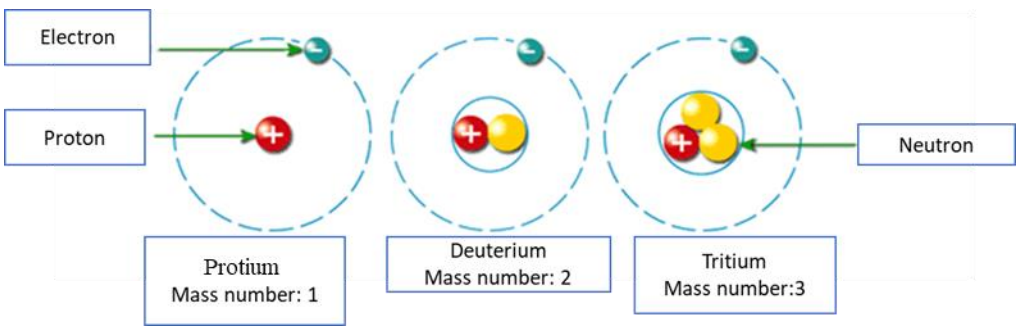

Figure 1.3: Isotopes of hydrogen.

This phenomenon is called decay or transformation of radionuclides and may involve the emission of charged particles, electron capture (EC) or isomeric transition (IT). The particles emitted from nuclei may be alpha or beta particles (negatively charged, electrons or positively charged, protons). Radionuclides with a deficit of protons usually decay by emitting electrons and those with a deficit of neutrons usually decay by electron capture or by emitting positrons, which are called positron emitters. Positrons are annihilated after interaction with electrons in the surrounding matter. The annihilation results in the emission of two gamma photons, each with energy of 0.511 MeV, generally emitted at around 180° to each other (annihilation radiation), **Figure 1.2**.

Any radionuclide decays at an exponential rate with its characteristic decay constant. The curve of exponential decay (decay curve) is described by equation (1):

$$A_t = A_0 e^{-\lambda t} \tag{1}$$

A_t= the radioactivity at time t

A_0= the radioactivity at time t = 0

λ = the decay constant, characteristic of each radionuclide

e = the base of natural logarithms.

The following equation (2) is to determine the half-life ($T_{1/2}$), the time in which a given amount of radioactivity of a radionuclide decay to half its initial value and it is related to the decay constant (λ):

$$T_{\frac{1}{2}} = \frac{\ln 2}{\lambda} \tag{2}$$

The equation of exponential decay, equation (3), can be expressed in the following way, for the estimation of the radioactivity left after elapsing time, *t*:

$$A_t = A_0 \left(\frac{1}{2}\right)^{t/T_{1/2}} \tag{3}$$

Half-life is characteristic of each radionuclide and is expressed in units of time. Also characteristic, are the nature and energy of its radiation or radiations. Their energy is expressed in electronvolts (eV), kilo-electronvolts (keV) or mega-electronvolts (MeV).

Most radionuclides used in nuclear medicine are produced artificially, since most of the ones that occur naturally are unsuitable for nuclear medicine imaging due to their long half-life or inappropriate emissions. Production of radionuclides consists in finding a mechanism to alter the nucleus of an atom to make it unstable. During the radioactive decay process, the radionuclide

returns to a stable form, and it is this process of decay that allows the localization of the radionuclide [8].

Selection of radionuclide for molecular imaging, must consider the following properties:

- Availability of the radionuclide;
- Physical properties (decay mode, emission energy, half-life) according to the application;
- Chemical properties, suitable for radiolabelling incorporation with high radiochemical yields and purities;
- A good relation between the dose received by the patient and image quality;
- An acceptable cost-efficient production.

Nowadays, most major hospitals and clinics use radiopharmaceuticals for diagnosis and therapy. The radionuclides can be obtained from the decay of longer-lived "parent" nuclides (using a generator), produced from nuclear reactions in a cyclotron or a nuclear reactor. The fundamental processes used are nuclear fission, neutron activation and irradiation with charged particles. Nuclear fission and neutron activation are performed in nuclear reactors, using the generated neutrons. Irradiation with charged particles, that lead to the nuclide's transmutation, is the process used at a cyclotron [9].

The production of fluorine-18 (^{18}F) by a cyclotron occurs through the introduction of a proton into the nucleus of the stable isotope oxygen-18 (^{18}O). Typically, this nuclear reaction is written as $^{18}O(p,n)^{18}F$, which means: target particle (incoming particle, outgoing particle) produced atom. The quantity of ^{18}F produced from ^{18}O depends on several factors such as the number of target atoms, the number of protons, the energy of protons and the probability of the occurrence of the desired nuclear reaction [8]. In **Table 1.1** we present some of the most used radionuclides for PET[10,11].

[^{18}F]Fluoride, [^{11}C]carbon, [^{15}O]oxygen, [^{13}N]nitrogen, or [^{68}Ga]gallium (**Table 1.1, Entries 1 to 5**) are the most commonly used radionuclides to label radiopharmaceuticals for PET imaging. Even in a PET centre equipped with a cyclotron, the very short half-life of radionuclides such as oxygen-15 (2 minutes) (**Table 1.1, Entry 3**) and nitrogen-13 (10 minutes) (**Table 1.1, Entry 4**) limit their clinical application.

Table 1.1: Physical properties of most commonly used radionuclides for PET.

Entry	Radionuclide	Production	Half-life (min)	Mode of decay (% β^+)	Mean Energy (β^+) (MeV)	Mean positron range* (mm)
1	^{18}F	$^{18}O(p,n)^{18}F$	110	97	0.250	0.6
2	^{11}C	$^{14}N(p,\alpha)^{11}C$	20.4	100	0.386	1.2
3	^{15}O	$^{14}N(d,n)^{15}O$	2	100	0.735	3.0
4	^{13}N	$^{16}O(p,\alpha)^{13}N$	10	100	0.492	1.8
5	^{68}Ga	$^{68}Ge/^{68}Ga$ generator $^{68}Zn(p,n)^{68}Ga$	68.3	89.1	0.836	3.1
6	^{89}Zr	$^{nat}Y(p,n)^{89}Zr$	6732	22.7	0.396	1.3

* In water.

Fluorine-18 (^{18}F) can be produced by two different ways: by the irradiation of enriched $[^{18}O]H_2O$ as target material by nuclear reaction $^{18}O(p,n)^{18}F$ to yield $[^{18}F]F^-$ or by the irradiation with deuterons ($^2H^+$) of a gas target filled with ^{20}Ne to achieve $[^{18}F]F_2$ gas, by the nuclear reaction $^{20}Ne(d,\alpha)^{18}F$ [12].

Production of carbon-11 (^{11}C), by the nuclear reaction $^{14}N(p,\alpha)^{11}C$, is performed by irradiating a gas target filled with nitrogen ($^{14}N_2$), which is mixed with trace amounts of oxygen or hydrogen to obtain $[^{11}C]CO_2$ or $[^{11}C]CH_4$, respectively.

1.1.3 Radiopharmaceuticals

Radiopharmaceuticals can be used for diagnostic applications, using imaging techniques such as PET and SPECT or, therapy where radiation can be absorbed locally, showing maximum damage to its target and minimum damage elsewhere [13]. A radiopharmaceutical is composed by two essential components: a radionuclide, that emits an appropriate ionizing radiation when it disintegrates, and a ligand (vehicle) that binds the radionuclide and transport it to the target, **Figure 1.4.**

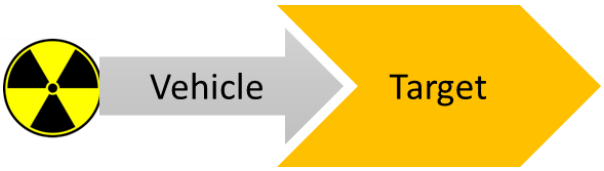

Figure 1.4: Design of a radiolabelled ligand binding to receptor target.

The vehicle is responsible for chemical and biochemical interactions within the living organism and the radionuclide provides a detectable signal enabling coincident measurements of annihilation radiation detectable by a PET scanner.

The concentration of the target molecules must be high enough, at the biological site of interest to allow the visualization and quantification. These targets can be for example: receptors, antigens, enzymes, transporters, specific metabolic alterations, up-regulated conditions, hypoxia of tissues, different energy demand of cells, changes in gene and protein expression, differences in vascularization and perfusion. The vehicle molecules can interact directly with the target or participate directly in the metabolic processes. To diagnose a pathophysiological state, the target or process have to be different compared with their healthy state [14].

There is a large spectrum of radionuclides, such as organic elements (carbon, nitrogen, oxygen, phosphorus, sulphur, or halogens) or metallic (*e.g.:* gallium, copper, or technetium), used for labelling the vehicles molecules. There are also a high variety of molecules that could be used as vehicle, such as small organic molecules, metal coordinating complex, polymers, nanoparticles, biomolecules (like peptides), carbohydrates, lipids, etc. The main challenge of the radiopharmaceutical chemist is to employ this high diversity of radionuclides and vectors, incorporate them in a suitable targeting vehicle and design a methodology to make an automated synthesis of the radiopharmaceutical according to radiological protection and GMP rules, mandatory for production of human medicines [15].

The radiopharmaceutical development starts with the identification of a biological target and the planning of the target identification strategy, which include the identification of the molecule to be radiolabelled. When choosing the molecule to be radiolabelled, it's possible to choose from: i) one that has already been developed for the same purpose; ii) one already developed for other purpose but that can interact with the desired target; or iii) one that could be the base for a new development by making some small structural changes. If it is a new target or the target was not studied yet for PET imaging, a "drug discovery" approach is required to identify new targeting vectors from a library of compounds [16]. The identification of these vectors could be based on bioactive molecules (carbohydrates, amino acids, fatty acids, nucleic acids), like 2-[^{18}F]fluoro-2-desoxy-*D*-glucose (2-[^{18}F]FDG), a glucose analogue, or 3,4-dihydroxy-6-[^{18}F]fluoro-*L*-phenylalanine (6-[^{18}F]FDOPA), an amino acid [11], **Figure 1.5**.

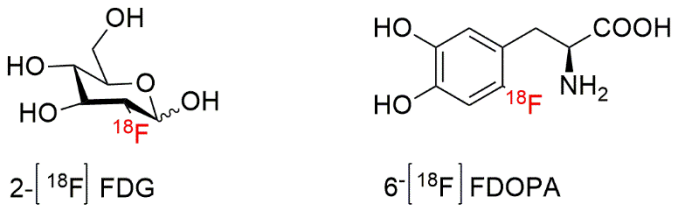

Figure 1.5: Structures of 2-[^{18}F]FDG and 6-[^{18}F]FDOPA.

Development of new radiopharmaceuticals can be also based on drugs or drug candidates, for example, prostate-specific membrane antigen (PSMA), a membrane-bound glutamate carboxypeptidase that is expressed in prostate cancer and neovasculature of solid malignancies [17]. In 2001, Kozikowski *et. al* [18] reported a class of urea-based inhibitors that targeted the enzymatic domain of PSMA, which lead to the development of PET-based PSMA radiolabelled with [^{18}F]fluoride or [^{68}Ga]gallium.

Chemical screening also could be a strategy for radiopharmaceutical development. Although this is extensively used for drug development, it is not often used for radiopharmaceutical development.

Despite the similarity between PET radiopharmaceutical development and drug development, there are some differences that allow a faster, safer, and more cost-effective route to introduce radiolabelled molecules into human studies. In **Figure 1.6** we present a comparison between pharmaceutical and radiopharmaceutical development pipelines[16].

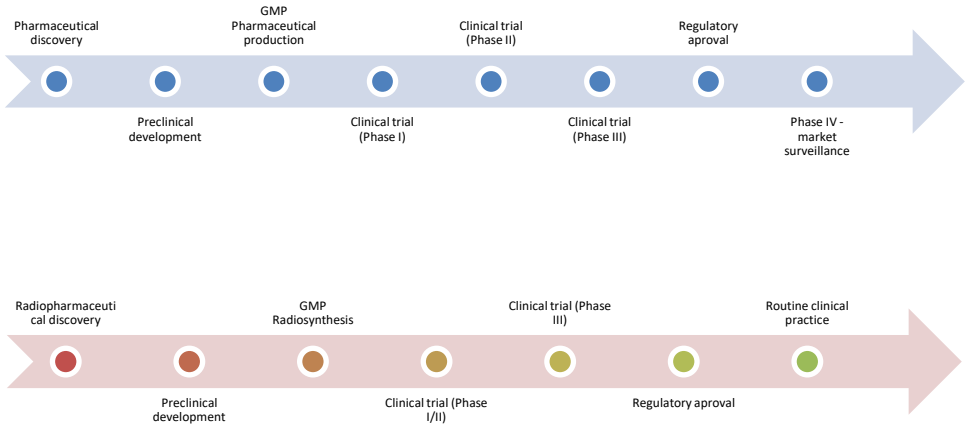

Figure 1.6: Comparison of pharmaceutical and radiopharmaceutical development.

The main reason for the differences between these two pipelines of development is that the dose administrated of a radiopharmaceutical is always below the pharmacological active dose and must never provoke a biological response. Because of this, in PET radiopharmaceutical development, it is only required a basic toxicological assessment before continuation into first-in-human studies, which shortens the development time and costs [19].

Side effects are very rare, and the concern of off-target toxicity is minimized. Beside this, physicochemical properties as oral bioavailability or therapeutic window are not applied in the field of radiopharmaceutical development. While a new drug can take 12-13 years to develop, a radiopharmaceutical can be developed, evaluated clinically, and ready for use within 8 years [16].

A good radiopharmaceutical must present the following characteristics:

- high specificity
- High binding affinity
- rapid clearance from non-target tissue
- be stable *in vivo*
- have low immunogenicity or toxicity
- must be accessible and cost effective [11].

The high specificity is crucial for the correct interpretation of images. Off-target binding must be minimized to make sure that the uptake is representative of the molecular pathology and not of a physiological process. Radiopharmaceuticals should bind with nano- or subnanomolar binding affinity to their target of interest.

High binding affinity increase the sensitivity for receptors/targets that are expressed at low density and, consequently, readily saturable.

PET radiopharmaceuticals are cleared through the renal, hepatobiliary or both pathways. The elimination route depends on multiple factors as size, lipophilicity, charge, and plasma protein binding. Rapid clearance from nontarget tissues allow the visualization of the molecular pathology. Beside this, the rapid excretion of radiopharmaceuticals reduces radiation exposure in patients.

After administration, radiopharmaceuticals circulate before reaching the target site(s). This uptake period may range from minutes to days, which makes its stability in the presence of enzymes in plasma or in target tissue a crucial parameter. The exceptions are the radiopharmaceuticals that rely on metabolic trapping as a mechanism for retention.

As already mentioned, radiopharmaceuticals are administrated in microdoses, which makes the induction of pharmacological or allergic effects unlikely. However, the potential for adverse events must still be carefully assessed as some agents will be used multiple times for response monitoring [20]. Besides all of these characteristics, the accessibility and cost effectiveness must be also taken into account: PET radiopharmaceuticals and their precursors should be readily available at low costs and available for routine clinical use [11].

Nowadays a combination of PET with an anatomical imaging technique like CT (computed tomography) or MRI (magnetic resonance imaging) results in a hybrid imaging, which combines anatomical with functional imaging. These systems allow higher spatial resolution, higher target-background contrast and accurate anatomical localization [10]. In the last years several efforts have been made in development of new radiopharmaceuticals for PET imaging and, there are several publications of its development and clinical applications. Tracers for vesicular imaging, myocardial perfusion, aminoacids for tumour imaging, tumour angiogenesis, proliferation or hypoxia as well as imaging of peptide receptors have been extensively studied and used as clinical imaging tools [10–12,14,21,22].

In **Table 1.2** are summarized examples of some PET radiopharmaceuticals, their clinical indication and molecular target [10,11,21].

2-[^{18}F]FDG (**Table 1.2, Entry 1**) is the most widely used PET radiopharmaceutical due to its versatility, as many pathological conditions present alterations in glucose metabolism. The main disadvantage of this radiopharmaceutical is its lack of specificity. Sometimes, inflammation or other benign processes are indistinguishable from tumours or the malignant mass is surrounded by tissue with high glucose metabolism and high background activity, as brain, muscles or bladder, that can make visualization difficult [23]. Besides oncological applications, it can also be used in neurological and cardiologic pathologies imaging.

Table 1.2: Examples of some PET radiopharmaceuticals, their clinical indication and molecular target.

Entry	Radiopharmaceutical	Clinical indication	Biochemical process/target	Ref.*
1	2-[^{18}F]FDG	Routine applications ı oncology, neurology, and cardiology	Glucose metabolism, myocardial glucose metabolism. Substrate for hexokinase in glucose metabolism.	23
2	6-[^{18}F]FDOPA	Oncology, neurology. Diagnosis of Parkinson's disease and neuroendocrine tumours.	Precursor for dopamine synthesis. Amino acid transport and protein synthesis.	24
3	[^{11}C]-*L*-methionine	Oncology	Amino acid transport and protein synthesis.	25
4	[^{11}C]PiB	Neurology, Alzheimer's disease.	Detection of amyloid plaques that exist in Alzheimer's disease.	26
5	[^{11}C]UCB-J	Neurological. Epilepsy, Alzheimer's disease	Density of glycoprotein SV2A	27
6	[^{11}C] acetate	Cardiology, assessing cardiac functions and metabolism, and in oncology.	Tricarboxylic acid cycle, fatty acids synthetase.	28
7	[^{13}N]NH_3	Cardiology	Myocardial blood flow	29
8	[^{18}F]Choline	Oncology, prostate tumours.	Substrates for choline kinase in choline metabolism. Phospholipid synthesis.	30
9	[^{68}Ga] PSMA-11	Oncology, prostate tumours.	Prostate-specific membrane antigen (PSMA)	31
10	[^{68}Ga]DOTANOC	Oncology. Neuroendocrine tumours.	Somatostatin receptor 2 (SSTR2)	32

* Ref.: Reference.

6-[^{18}F]FDOPA (**Table 1.2, Entry 2**) is an amino acid, and these are important structures for the survival of cells and mainly used for protein synthesis. This radiopharmaceutical has two main clinical applications: one neurological, as a biomarker of Parkinson's disease and one in oncology. When is used for detection of Parkinson disease, [^{18}F]FDOPA is taken by dopamine neurons and is decarboxylated to [^{18}F]dopamine, whereas its uptake rate is related with the number of functional dopaminergic neurons. In oncology, since tumours often show increased protein synthesis rates, enhanced uptake of amino acid tracers in tumour tissue could be observed [24]. [^{11}C]methionine (**Table 1.2**, **Entry 3**) is also an amino acid, mainly used in brain tumours [10,14,25]. One advantage of these radiopharmaceuticals is its ability to cross the blood brain barrier which allow to obtain images of cerebral pathologies.

Besides these, also (*N*-methyl-[^{11}C])-2-(4'-methylaminophenyl)-6-hydroxybenzothiazole, [^{11}C]PiB (**Table 1.2, Entry 4**) and ((*R*)-1-((3-[^{11}C]-methyl-[^{11}C]pyridin-4-yl)methyl)-4-(3,4,5-trifluorophenyl)pyrrolidine-2-one, [^{11}C]UCB-J (**Table 1.2, Entry 5**) are radiopharmaceuticals with neurological applications. [^{11}C]PiB, is used in diagnosis of Alzheimer's disease, by detecting amyloid deposits in the brain [26] and [^{11}C]UCB-J, is used to measure de density of glycoprotein SV2A, which is altered in pathologies as epilepsy or Alzheimer's disease [27].

[^{11}C]acetate (**Table 1.2**, **Entry 6**) and [^{13}N]NH_3 (**Table 1.2**, **Entry 7**) are examples of radiopharmaceuticals used for cardiac imaging.

[^{18}F] Choline (**Table 1.2, Entry 8**) is a radiopharmaceutical that is readily taken up by tumours during proliferation. Its suitable for patients with suspected prostate cancer [30]. Also [^{68}Ga]PSMA (**Table 1.2, Entry 9**) are used for diagnosis of prostate cancer through the imaging of the prostate-specific membrane antigen (PSMA) [31]. [^{68}Ga]DOTANOC (**Table 1.2, Entry 10**) is used in oncology and in the specifically binding to somatostatin receptors (SSRs), overexpressed on the surface of neuroendocrine tumours (NET) [32].

1.1.4 Regulatory aspects and quality control of radiopharmaceuticals

Radiopharmacy is the science of the design, preparation, quality assurance and clinical pharmacy of radiopharmaceuticals [13]. It is regulated and legislated by two different ways: in one hand as a radioactive substance and, on the other hand, as a medicine. Both ways sometimes enter in conflict, which leads to the necessity of obtaining a reasonable compromise between both.

From an historical perspective, **Table 1.3** presents the evolution of the regulatory framework for radiopharmaceuticals in Europe.

Table 1.3: Evolution of the regulatory framework in Europe for radiopharmaceuticals.

Document	Year	Classification	Changes to legislation	Current state
Directive 65/65/EEC [213]	1965	Directive	Establishment of the first basic structure for the assessment and granting of marketing authorization for new drugs. Also, all the procedures to be followed to obtain them.	Revoked
Directive 89/343/CEE [214]	1989	Directive	Definition of the category of radiopharmaceuticals and applicable complementary provisions.	Revoked
Note for guidance on radiopharmaceuticals [215]	1990	Guideline	Guidelines for the instruction of MA requests for radiopharmaceuticals.	Revoked
Directive 2001/83/CE [216]	2001	Directive	Single Community Code on Medicines for Human Use.	Current
Directive 2003/63/CE [217]	2003	Directive	Provides specific indications for the instruction of the application of radiopharmaceuticals (Annex 1), and specific requirements for drugs and radiopharmaceutical precursors.	Current
Directive 2003/94/CE [218]	2003	Directive	Definition of GMP principles relating to medicines for human use and experimental medicines for human use.	Current
Directive 2004/27/CE [219]	2004	Directive	Changing the definitions of drug and active substance. Definition of new GMP requirements.	Current
Guideline on radiopharmaceuticals [220]	2007	Guideline	Guidelines for the instruction of AIM requests for radiopharmaceuticals (additional information).	Current
EudraLex, Vol 4, Anex 3 [34]	2008	Guideline	Specific GMP requirements for radiopharmaceutical production and quality control.	Current
Guideline on the non-clinical requirements for radiopharmaceuticals [221]	2018	Guideline	Guidelines on non-clinical information to support the clinical development and approval of radiopharmaceuticals, considering their specificities.	Draft

AIM: Marketing Authorization Application.

In 1965, the first basic structure for the assessment and granting of marketing authorizations for new drugs was stablished by the directive 65/65/EEC [213]. Only in 1989, the term "radiopharmaceutical", was defined, for the first time, in the directive 89/343/CEE. One year after, a guideline was published which provided the requirements for a Marketing Authorization Application (MA) for radiopharmaceuticals.

The current directive 2003/63/CE [217], provides specific indications for the instruction of an application for radiopharmaceuticals, and specifies requirements for drugs and radiopharmaceutical precursors. After this directive, two guidelines for radiopharmaceuticals, in 2007 [220], 2008 [34] and in 2018 [221], were published to provide guidance for the submission of an MA of radiopharmaceuticals, specify GMP requirements for radiopharmaceutical production and quality control, and regarding the non-clinical information needed to the clinical development of radiopharmaceuticals, respectively.

European directives need to be transposed to national law. In Portuguese law, the directives are transposed as a "decree law". In **Table 1.4** we present the evolution of the Portuguese law, regarding radiopharmaceutical production.

Table 1.4: Evolution of the Portuguese law, regarding radiopharmaceutical production.

Document	Year	Classification	Changes to legislation	Current state
DL no 72/91 [222]	1991	Decree law	Creation of the first medicine statute. Transposition into national law of several community directives.	Revoked
Deliberation no1491/2004 [223]	2004	Deliberation	Contracting by hospitals of preparations intended exclusively for use in those establishments	Current
DL no 176/2006 [224]	2006	Decree law	Legal regime for an MA, amendments, manufacturing, importing, exporting, marketing, labelling and information, advertising, pharmacovigilance, and the use of medicines for human use. Definition of four categories of radiopharmaceuticals. Transposition into national law of several Community directives.	Current

According to Deliberation no 1491/2004, an hospital can contract the production of a pharmaceutical to an external company if there is an unmet clinical need, there is no alternative drug to resolve the clinical problem and, if the manufacturer complies with all the good manufacturing practices (GMP) [225].

INFARMED approves the good practices for pharmaceutical compounding under those circumstances. This includes requirements concerning personal, equipment and facilities, documentation, raw-materials, packaging, manipulation, and quality control[226]. Additionally, radiopharmaceuticals also have to comply with specific requirements, such as, dosimetry, radiation safety and labelling [225].

Production of radiopharmaceuticals must be made in accordance with the Eudralex, *"The Rules Governing Medicinal Products in the European Union"*, Volume 4, *"EU Guidelines to Good Manufacturing Practices (GMP), Medicinal Products for Human and Veterinary Use"*, and, specifically, according with Annex 3, named *"Manufacture of Radiopharmaceuticals"*, created by the European commission [33,34] All the previously mentioned documents are guidelines for production and quality control of radiopharmaceuticals, positron emitting (PET) radiopharmaceuticals, radioactive precursors for radiopharmaceutical production and radionuclide generators, produced by industrial manufacturers, nuclear centres/industries, and PET centres. Recently Gillings *et. al*. [35] published a guideline article on current good Radiopharmacy practice (cGRPP) for the small-scale preparations of radiopharmaceuticals. The guideline has been written by members of the Radiopharmacy Committee of the European Association of Nuclear Medicine (EANM) and is directed to non-commercial sites, such as hospital radiopharmacies, nuclear medicine departments or research PET centres. EANM is a professional non-profit medical association which mission is to facilitate the communication worldwide among individuals pursuing clinical and research excellence in nuclear medicine. Production of a radiopharmaceutical is, normally, divided in five main steps: reactor or cyclotron production of radionuclide, radiochemical synthesis, purification, processing, reformulation and dispensing and aseptic or final sterilization. With the exception of the first step (reactor or cyclotron production) that is not GMP, all the following steps are performed according to GMP rules.

Because of the radioactive nature of radiopharmaceuticals, manufacturing and handling can be potentially hazardous and these preparations involve adherence to regulations of radiation protection. Radiopharmaceuticals to be administered parenterally should comply with sterility requirements for parenterals and aseptic working conditions for the manufacture of sterile medicinal products as indicated in Eudralex, Volume 4, Annex 1 [36]. The short half-life of radionuclides is a specificity which allows some radiopharmaceuticals to be released before the completion of all the quality control tests. This implies a detailed description of the whole release procedure including the responsibilities of the personnel involved. Specifications and quality control testing procedures for the most used radiopharmaceuticals are specified in the European Pharmacopoeia.

Council of Europe (CoE) was founded in 1949 and is the oldest pan-European organization composed by 47 member states, representing 820 million European citizens. European Directorate for the Quality of Medicines and Healthcare (EDQM) is a directorate of the CoE and is based on the "*Convention on the elaboration of an European Pharmacopoeia"*, adopted in 1964 to harmonize quality standards for medicinal substances that, in their original state or in the form of pharmaceutical preparations, are of general interest and importance for the people of Europe. The mission of this organization is to protect public health and to contribute to equal

access to good quality medicines and healthcare, considered a basic human right for all of Europe's citizens [37]. The European Pharmacopoeia (Ph. Eur.) provides a legal and scientific reference for the quality control of medicines. All medicines marketed in the signatory member states of the Convention must comply with the quality standards of the Ph. Eur. Companies must follow these standards when applying to a national competent authority. In Portugal, the national competent authority is INFARMED, that is the national authority for medical and health products. There is also an European Medicines Agency (EMA) that is part of the European Union (EU) and is responsible for marketing authorizations across all member states. Ph. Eur. Commission is the governing body of the Ph. Eur. Each Member State and Observer is entitled to send a delegation, which consists of up to three members appointed by the respective country. Ph. Eur. is composed by general chapters and specific monographs for a specific medicine. These monographs require the use of different reference standards as benchmarks for analytical testing, which can be classified according to their intended use, qualitative or quantitative.

According to the 10th edition of Ph. Eur., monograph 07/2016:0125, "Radiopharmaceutical Preparations" [38], a radiopharmaceutical is *"any medicinal product which, when ready for use, contains one or more radionuclides (radioactive isotopes) included for a medicinal purpose."*. Radiopharmacy goes from the production and properties of the radionuclide, through its incorporation into a molecule, formulation, quality control, to adverse effects and drug interactions. It is a multidisciplinary area, employing tree major disciplines that collaborate closely to the success application of PET as molecular imaging modality: medical physics, radiopharmaceutical sciences, and clinical imaging.

In order to better understanding, the monographs of radiopharmaceuticals, Ph. Eur. 10.0, monograph 07/2016:0125[38] describe some important concepts/definitions that have to be taken into account to assure and understand the quality of the product, such as:

- **Radionuclidic purity**: "*the ratio, expressed as a percentage, of the radioactivity of the radionuclide concerned to the total radioactivity of the radiopharmaceutical preparation."*.
- **Radiochemical purity*:*** *"the ratio, expressed as a percentage, of the radioactivity of the radionuclide concerned which is present in the radiopharmaceutical preparation in the stated chemical form, to the total radioactivity of that radionuclide present in the radiopharmaceutical preparation."*.
- **Chemical purity**: *"is controlled by specifying limits for chemical impurities."*
- **Specific radioactivity**: "*the radioactivity of a radionuclide per unit mass of the element or of the chemical form concerned, e.g. becquerel per gram or becquerel per mole."*

- **Radioactive concentration**: "*the radioactivity of a radionuclide per unit volume or unit mass of the preparation. For radiopharmaceutical solutions, it is expressed as radioactivity per unit volume of the preparation.*"
- **Total radioactivity**: "*the radioactivity of the radionuclide, expressed per unit (vial, capsule, ampoule, generator, etc).*"
- **Validity**: "*the time during which specifications described in the monograph must be fulfilled.*".

Besides this general monograph, each radiopharmaceutical has one individual monograph, which refers more specific parameters, such as chemical, radiochemical or radionuclidic impurities and limits, according to the specific production methods of each radiopharmaceutical.

Concerning uniformization of the nomenclature for radiopharmaceutical chemistry, in 2015 was created an international Working Group on *"Nomenclature in Radiopharmaceutical Chemistry and related areas"*, to achieve clarification of terms and to generate consensus on the utilization of a standardised nomenclature pertinent to the field, according publishers, editors, IUPAC (International Union of Pure and Applied Chemistry), pharmacopoeias, etc.[39].
According to SI (International System of Units), "specific" refers to a physical property as a function of the mass of the material in question, while as in chemistry the amount of material is denoted in moles, chemical properties are indicated in "molar" units.

Terms as specific activity (A_s) and molar activity (A_m) were defined as:

- **Specific activity** (A_s): the measured activity per gram of compound, measured in Bq/g or GBq/mg, etc;
- **Molar activity** (A_m): the measured radioactivity per mole of compound measured in Bq/mol or GBq/µmol.

When the molecular weight cannot be determined, the term "specific activity must be used instead of "molar activity". Due to the radioactive decay, the time of measure of "molar" or "specific" activities must be stated.

These concepts are of extreme importance in synthesis of radiopharmaceuticals because they address the chemically, biologically, or pharmacologically "active" fraction of radioactive and non-radioactive materials.

Most common radionuclides used in PET, such as ^{18}F, ^{68}Ga or ^{11}C, present short half-lives, which makes the radiosynthesis of PET tracers challenging. The automation of the syntheses processes is crucial. Time and yields are other issues to consider. Microwave technology has been presented as a useful tool in the development of automated radiosynthesis processes due to its efficiency and reduction of reaction times.

1.2 Microwave technology in radiopharmaceutical synthesis

During 1940s, many research and experiments on the validation of the electromagnetic theory, were performed, in the development of microwave heating devices and in the transmission of microwaves [40]. Initially, microwaves were only used for communication, until 1946, when Percy Spencer shows the heating of materials with the use of microwave energy [41]. In the next year, he projected the first domestic microwave oven [42]. But, only in 1986, Gedye and Giguerre reported the first chemical reactions in open vessels using domestic microwave ovens [43,44]. Since then, microwave dielectric heating has been used in several chemical transformations and has revolutionized organic synthesis. Microwave heating in activation and acceleration of organic reactions has taken an exponential grow in the last few years. The way in which microwaves interact with electric dipoles and charges can be used to speed up the heating of reaction samples in ways that can't be reached by conventional heating [45].

Microwave irradiation is electromagnetic irradiation in the frequency range of 0.3 to 300GHz (vacuum wavelengths between 0.1 and 100 cm). Microwave-improved chemistry is based on the heating efficiency of materials by microwave dielectric heating, which depends on the ability of a specific material, solvent or reagent, to absorb microwave energy and convert it on to heat [46]. The electric component of the electromagnetic field is responsible by the heating by two different mechanisms: dipolar polarization and ionic conduction[47]. Microwave irradiation of a sample results in the dipoles or ions aligning in the applied electric field. The oscillation of the applied field causes the dipole or ion field attempts to realign itself with the alternating electric field. During this process, energy is lost in the form of heat through molecular friction and dielectric loss, the capacity of the sample to align itself with the frequency of the applied field, its related with the amount of heat [46,48].

Heating characteristics of a particular material under microwave irradiation conditions depends on its dielectric properties.

The so-called "loss factor", *tan δ*, is expressed by equation 4, and gives the ability of a specific material to convert electromagnetic energy into heat at a given frequency and temperature.

$$tan\ \delta = \frac{\varepsilon''}{\varepsilon'} \qquad (4)$$

ε'' is the dielectric loss, which indicates the efficiency with which electromagnetic radiation is converted into heat, and ε' is the dielectric constant describing the ability of molecules to be polarized by the electric field. High values of loss factor are required for efficient absorption, which results in a rapid heating. For example, solvents as dimethyl sulfoxide (DMSO) or 2-propanol present values of loss factor of 1.350 and 0.799 respectively, while toluene or hexane

present values of 0.04 or 0.020 respectively, at 2.45 GHz and 20ºC. Solvents without a permanent dipole such as carbon tetrachloride, benzene or dioxane are practically microwave transparent. However, even with a solvent with low values of *tan δ,* doesn't mean that it could not be used as solvent at a microwave-heated reaction. The use of polar substrates, reagents or catalysts could promote an overall dielectric property of the reaction medium, which will be enough to be heated by microwave irradiation [46].

Conventionally, organic synthesis is carried out by conductive heating, supplied by an external heat source. While microwave heating depends on the thermal conductivity of the various materials that must be penetrated. This results in the temperature of the reaction vessel being higher than that of the reaction mixture, microwave heating produces efficient internal heating by direct coupling of microwave energy with the molecules that are present in the reaction mixture [46].

Normally, reaction vessels used in microwave are made of nearly microwave transparent materials which results in an inverted temperature gradient, comparatively with conventional heating. In **Figure 1.7**, we present the differences in the heating profiles after 1 minute, of microwave irradiation (a) and treatment in an oil bath (b). Microwave irradiation raises the temperature of the whole sample (a), while in the sample heated in the oil bath, the sample in contact with the sample tube is heated first [49].

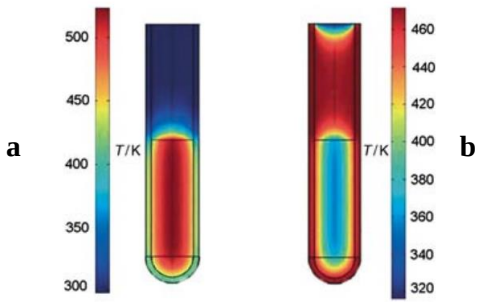

Figure 1.7: Difference in temperature gradients in microwave **a**, versus oil-bath heating **b**, after 1 minute of microwave irradiation.

In the last few decades, microwaves have proven to be a highly effective heating source; providing not only faster reactions but also better yields, cleaner product mixtures and improved reproducibility [46].

1.2.1 Microwave in PET Chemistry

The first application of microwave technology in the synthesis of radiopharmaceuticals was published in 1987 by Welch *et. al* [50], which reports the application of microwave heating into the

synthesis of a variety of labelled organic compounds that are representative of radiopharmaceuticals and observed that they can be prepared with decreased reaction times and higher radiochemical yields. In 1993, Stone-Elander[51] reported a nucleophilic aromatic ^{18}F-fluorination of aromatic rings in a microwave cavity, testing the effect of leaving groups on the aromatic ring as well as the *orto*, *meta* or *para* positions of electron-withdrawing and electron-donating substituents, obtaining higher yields and significant reduction in reaction times. The first reported radiopharmaceutical synthesis of [^{18}F]FDG using a microwave cavity in all steps, azeotropic drying, nucleophilic substitution and hydrolysis, was reported in 1996 by Taylor *et al.* [52]. They study the application of microwave cavity (Microwell 10, from Labwell AB, Uppala) in all steps separately and, comparing to conventional process, an increase in RCY, from 31 ± 8 % to 62 ± 3 % (ndc) with a reduction of 33 minutes in total synthesis time.

Early pioneering experiments were performed using a domestic microwave. However, nowadays there are mainly two types equipment's; multimode and single-mode [46]. In multimode instruments, like the domestic ovens, the microwaves that enter in the cavity are reflected by the walls and the load over a typically large cavity. In the single-mode cavities, the electromagnetic irradiation is directed through an accurately designed wave guide onto the reaction vessel, being this the preferential method used in radiochemistry[1]. After the first attempts to implement this technology in radiochemistry, the improvements in this area, namely in the development of new equipment, led to an increase of interest in this area, and application of this technology in key steps of radiopharmaceuticals synthesis, like ^{18}F-fluorination, ^{11}C-metylation or cleavage of protecting groups, were reported [53–55].

As example, PETWave, from CEM (Mathews, U.S.), presents four control options to programming a method: the standard, the dynamic, the fixed power and the power cycling.[56] These different modes allow us to control different reaction parameters. In the standard mode method, we define the temperature and reaction time. In the dynamic mode, parameters such as: maximum amount of microwave power, temperature control point, hold time, stirring function or power maximum can be selected. This is the mode which allows more flexibility to program a method. The fixed power mode can be programmed in two different ways, the power can be applied until the reaction reaches a certain temperature, which is kept during a determined time or, the power could be applied to the sample during a certain time, independently of the temperature. Other mode, commonly used in radiochemistry is the power cycling. In this mode, we define the power, a range of temperature (minimum and maximum), a heating and a cooling interval and the number of cycles. The sample is heated during a period and the microwave irradiation if turned off during another period.

In **Table 1.5** we present some microwave conditions used in azeotropic drying of [^{18}F]fluoride, in combination with nitrogen flow and vacuum.

Table 1.5: Some conditions used in [^{18}F]fluoride drying assisted by microwave heating.

Entry	Synthesised molecule	Microwave method	Power (Watts)	Temperature (ºC)	Time (minutes)	Reference
1	[^{18}F]FMAU	Dynamic	80	100	5-8	[57]
2	[^{18}F]FAZA	Power cycling	80	110	5x1	[58]
3	[^{18}F]NS10743	Power cycling	75 (20 cycles)	50-60	10-12	[59]
4	[^{18}F]ASEM	Standard	n.d.	110	2.5	[60]
5	^{18}F-fluorination of aromatic rings	Fixed Power	80	110	1	[61]

n.d: not described.

In **Table 1.5, Entry 1**, we present the method conditions used in the drying step of the synthesis of [^{18}F]FMAU, performed using a dynamic mode, where the microwave power was modulated to maintain a constant temperature of 100ºC[57].

In the procedure reported by Kumar *et al.*[58], for the synthesis of [^{18}F]FAZA, **Table 1.5, Entry 2**, the drying was performed using a power cycling mode. The power is applied only during the heating cycling. The same mode method was reported in the [^{18}F]fluoride drying step (**Table 1.5, Entry 3)** for the radiosynthesis of [^{18}F]NS10743[59].

In the fixed power mode (**Table 1.5, Entry 5**), the power is applied to the sample during a certain time. In these cases, a maximum temperature is also defined, for safety.

Typically, in aromatic ^{18}F-fluorination after the drying of [^{18}F]fluoride, the reaction takes place between the dried salt and the precursor. In **Table 1.6** we present some examples of microwave-assisted ^{18}F-fluorinations.

Table 1.6: Some condition used in aromatic ^{18}F-fluorination assisted by microwave heating.

Entry	Molecule	MW mode	Power (Watt)	Temperature (ºC)	Time (minutes)	RCY (%)	Ref.
1	[^{18}F]ASEM	Standard	50	n.d.	2.5	20.1 ± 8.9	[60]
2	[^{18}F]NEBIFQUINIDE	Standard	100	175	10	38 ± 3	[62]
3	[^{18}F]SFB	Fixed Power	50	n.d.	1	38	[63,64]
4	[^{18}F]NS10743	Power cycling	75	145-158 145-158 85-95	Maximum 15 minutes	76*	[59]
5	^{18}F-fluorination of aromatic rings	Power cycling	150	145	3x0.3	64	[61]

n.d: not described. Ref.: Reference. * Radiochemical yield of ^{18}F-fluorination.

Despite reactivity factors, which will be described in the next sections, all the works, presented in Table **1.6**, show a reduction in reaction times and an increase in radiochemical yields.

1.3 Radiolabelling strategies

With the continuous development of new PET probes for molecular imaging and the growing number of chemical compound classes used, there is a need to develop or adapt new methods of labelling, which should present the following characteristics:

- Rapid radiosynthesis with good radiochemical yields (RCY's)
- High radiochemical purity (RCP) and stability in formulation, to allow the delivery, administration to the patient and completion of the scan
- High molar activity (A_m) to ensure that the patient dose contains minimal nonradioactive compounds
- Avoid the use of reagents and solvents that are not compatible with GMP radiosynthesis and respect the limits determined by European Pharmacopeia (Ph. Eur.)
- Compatible with technology transfer to commercially available automated radiosynthesis platforms.

Short-lived positron emitters as ^{11}C or ^{18}F have been extensively used. Despite the obvious advantages of ^{18}F, due to its longer half-life, ^{11}C has the advantage to allow repeated PET studies while still allowing, to some extent, multi-step radiosynthesis sequences. Furthermore, isotopic labelling through substitution of a stable carbon atom with [^{11}C]carbon makes the corresponding

[^{11}C]labelled radiotracers indistinguishable from their stable counterparts within the biological system [65].

^{18}F is, by far, the most widely used radionuclide for routine diagnosis with PET, owing to the extensive use of 2-[^{18}F]FDG [66]. The radionuclide was produced for the first time in 1936 [67] and used in studies on fluoride-adsorption by bone and dentine, performed by Volker *et al.* in 1940 [68]. ^{18}F has favourable chemical and nuclear properties that make it a good PET nuclide. It can be produced with good yields in low-energy cyclotrons and its half-life allows multi-step synthesis, as well as the shipment to hospitals and clinics without an on-site cyclotron [66].

Usually, ^{18}F is used in analogous fluoroderivatives, where it sterically replaces an hydrogen atom. Fluorine has a Van der Waal's radius of 1.35 Å, similarly to the hydrogen (1.20 Å). However, the main differences are in electronic character. For example, when a hydrogen atom is replaced by a fluoride at an aliphatic position, the lipophilicity decreases, but if the substitution occurs in an aryl group, it will increase by two-fold. However, most of [^{18}F]labelled compounds are based in steric similarity such as 2-[^{18}F]FDG, or 6-[^{18}F]FDOPA [66,69].

1.3.1 Labelling methods with ^{18}F

Depending on the production process, ^{18}F can be obtained in 2 different chemical forms, [^{18}F]F_2 or [^{18}F]fluoride, which determines the possible reactions. The main ^{18}F-fluorination used in radiolabelling are:

1. Electrophilic substitution
2. Nucleophilic substitution
   I. Aliphatic nucleophilic ^{18}F-fluorination
   II. Aromatic nucleophilic ^{18}F-fluorination
   III. Formation of ^{18}F-labelled multifluoromethyl motifs
   IV. Non-canonical ^{18}F-labelling methods
3. ^{18}F-fluorination via build-up synthesis (via ^{18}F-fluorinated synthons or ^{18}F-fluorination via prosthetic groups)

The first two are called direct methods and the last are called indirect because the ^{18}F-fluorination occurs in the synthon or via a prosthetic group [66].

Considering the scope of this work, in the next sections will only be described the following ^{18}F-fluorination methods: Electrophilic substitutions and nucleophilic aliphatic and aromatic substitutions.

1.3.1.1 Electrophilic substitution

Electrophilic methods can only be used when high molar activities (A_m) are not required. A_m of [^{18}F]F_2 is usually in the range of 0.04 to 0.4 GBq/µmol, being the maximum about 0.6

GBq/μmol[70]. In order to improve these values, in 1997, Bergman *et al.* [71] reported the use of [^{18}F]CH_3F and a low amount of F_2, which resulted in low RCY's and poor chemo- and regioselectivities, leading to extensive purification procedures. Due to these limitations, ^{18}F-fluorination electrophilic reagents, less reactive and more selective, were prepared from [^{18}F]F_2 [69,72], including [^{18}F]XeF_2, [^{18}F]CF_3OF, [^{18}F]CH_3COOF, [^{18}F]$FClO_3$, *N*-[^{18}F]fluoropyridinium triflate, 1-[^{18}F]fluoro-2-pyridone [^{18}F]NFSI [73], and [^{18}F]Selectfluor [74,75] The most demonstrative electrophilic aromatic ^{18}F-fluorination is the synthesis of [^{18}F]FDOPA. The first attempt was the electrophilic aromatic substitution of 3,4-dihydroxy-phenyl-*L*-alanine with [^{18}F]F_2, which gave [^{18}F]FDOPA, in low RCY and low regioselectivity. Another strategy to increase the regioselectivity in arenes was the demetallation reactions of organometallic precursors. In [^{18}F]FDOPA synthesis, using this synthetic strategy, radiofluorodestannylation of tin precursors improves the RCY to 25 % and also the regioselectivity[76,77].

Scheme 1.1 presents the main electrophilic pathways for the synthesis of 6-[^{18}F]FDOPA[78–84].

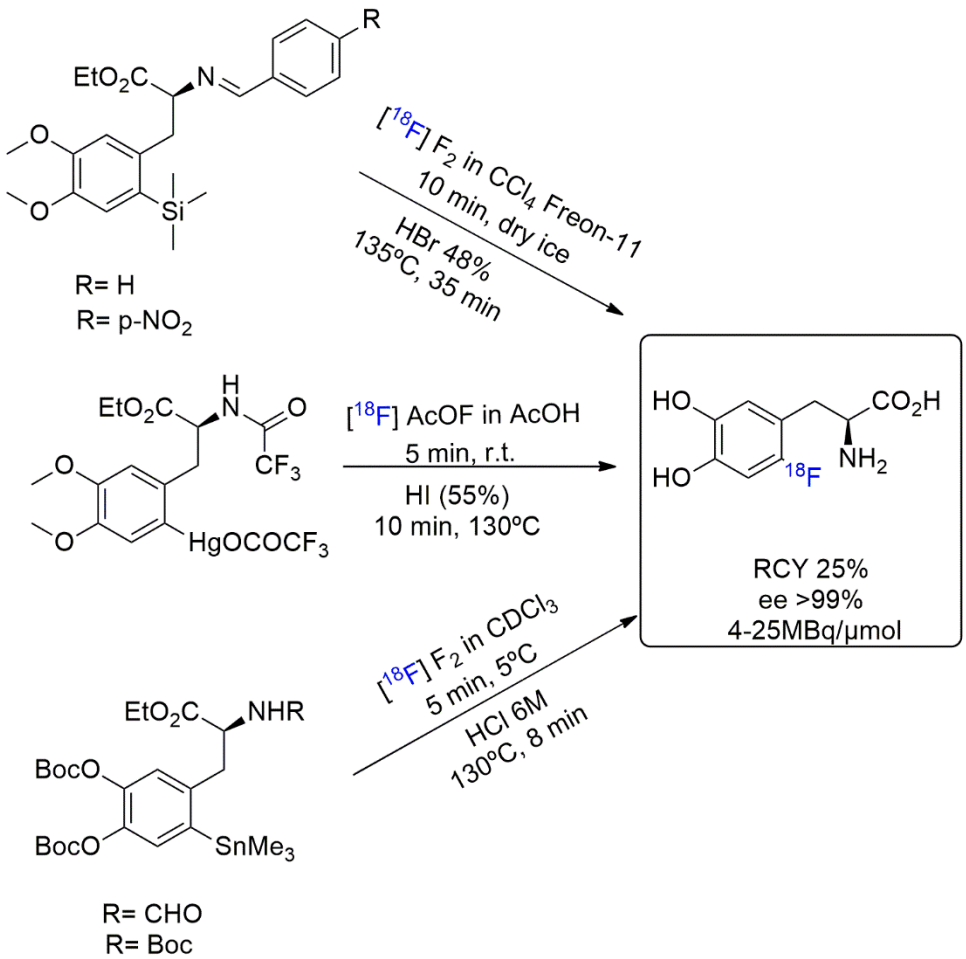

Scheme 1.1: Electrophilic synthesis of 6-[^{18}F]FDOPA.

Another possibility, is the use of [^{18}F]Selectfluor in the Ag-mediated ^{18}F-fluorination of arylstannanes or aryl boronic esters precursors [85]. Despite the higher RCY's and regioselectivity, as with all other electrophilic methods, low values of A_m restrict the use of this pathway in routine synthesis today.

1.3.1.2 Nucleophilic substitution

To overcome the limitations of the electrophilic pathway regarding A_m, the alternative is to obtain ^{18}F-labelled compounds by nucleophilic substitution based on non-carrier added (n.c.a) [^{18}F]fluoride, which is directly available from the target without any carrier addition. N.c.a. [^{18}F]fluoride is obtained by the irradiation of enriched [^{18}O]H_2O, as target material, by the nuclear reaction ^{18}O(p,n)^{18}F. [^{18}F]fluoride is obtained as an aqueous solution, but labelling must take place under polar aprotic conditions.

To separate the [^{18}F]fluoride and recover the enriched target water, anion exchange resins are used and the water is, normally, subsequently removed by azeotropic distillation with acetonitrile [86,87]. For anion activation, phase transfer catalysts (PTC) like tetraalkylammonium carbonates (hydrogen carbonates) [86,88] or the aminopolyether Kriptofix®2.2.2 [66,89] in combination with potassium carbonate or oxalate are used. Kriptofix®2.2.2, is generally preferred in most n.c.a. radiofluorination reactions.

Aliphatic nucleophilic ^{18}F-fluorination

Direct aliphatic nucleophilic substitution with [^{18}F]fluoride normally results in a C(sp^3)-^{18}F bonds with high RCY and A_m. Normally, is performed in dipolar aprotic solvents, like acetonitrile (ACN) and occurs according to an S_N2 mechanism. Reactions of this type involve the substitution of one leaving group by [^{18}F]fluoride. These leaving groups can be triflate (-OTf), tosylate (-OTs), mesylate (-Oms) or halides and the leaving capacity decreases in the following order: -OTf > -OTs ≈ -OMs > -I > -Br >-Cl [69].

Several ^{18}F-labelled PET tracers are prepared through aliphatic nucleophilic ^{18}F-fluorination which can be divided in four major chemotypes: unbranched and branched acyclic alkyl-^{18}F, cyclic alkyl-^{18}F, and alkyl-^{18}F with the [^{18}F]fluoride atom in activated positions. For example, 2-[^{18}F]FDG, the most used radiopharmaceutical, is a cyclic alkyl-^{18}F, and its synthesis starts from the substitution of the leaving group -OTf, by a [^{18}F]fluoride, of a acetylated mannose triflate precursor, in acetonitrile, followed by hydrolysis, as depicted in **Scheme 1.2** [90].

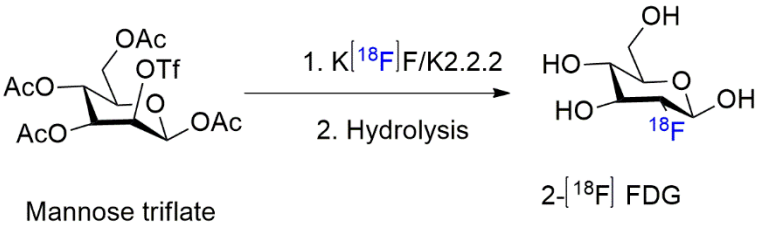

Scheme 1.2: Nucleophilic n.c.a. synthesis of 2-[^{18}F]FDG.

Synthesis of this radiopharmaceutical in routine production presents an RCY's of more than 50 % using commercially available automated modules.

Aliphatic nucleophilic ^{18}F-fluorination is usually performed in basic conditions at high temperature, which may not be compatible with highly functionalized molecules, leading to formation of undesired side products. As an alternative, transition-metal-mediated aliphatic ^{18}F-fluorination can be done in mild conditions. Palladium, iridium, cobalt or manganese are some of the transition-metals used [69].

Aromatic nucleophilic ^{18}F-fluorination

Aromatic nucleophilic substitution (S_NAr) with [^{18}F]fluoride are of great importance to radiopharmaceuticals synthesis due to the generally good metabolic stability *in vivo* of the respective radiolabelled products. It represents a direct and commonly used method to form C(sp^2)-^{18}F bonds. It's indispensable that the precursor has both a leaving group and an activating group, normally electron withdrawing (EWD) in the *ortho* or *para* positions, to promote the S_NAr reaction by stabilization of the Meisenheimer complex**, Scheme 1.3** [69].

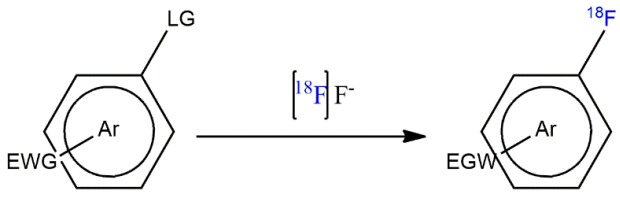

LG = $-NO_2$, -I, -Br, -Cl, $-\overset{\oplus}{S}Me_2$, $-\overset{\oplus}{N}Me_3$, (-OTs, -OTf, $-ClO_4$, I^-)

EWG = $-NO_2$, -CN, $-CF_3$, -Cl, -Br, -I or carbonyl groups etc.

Scheme 1.3: Nucleophilic aromatic ^{18}F-fluorination.

Substituents with strong electron withdrawing properties such as nitro, cyano and carbonyl groups are appropriate for the ring activation and halogens, nitro and the trimethylammonium salts shows higher reactivity as leaving groups [66]. When an arene is strongly reactive (e.g. *para*-

dinitrobenzene) ^{18}F-fluorination may occur only with addition of rubidium carbonate (Rb_2CO_3) or cesium carbonate (Cs_2CO_3) [91]. However, for less activated arenes, PTC are required. Even though the nitro-moiety is a much better leaving group than halogens, with *para*-nitrophenyl halides the nitro group will not be replaced. The same happens for *ortho*-bromo-nitroarenes [92,93].

In **Figure 1.8** we present two examples of radiopharmaceuticals synthesized via nucleophilic aromatic ^{18}F-fluorination, [^{18}F]PK10105 and [^{18}F]2FP3. In [^{18}F]PK10105, the EWG is nitro and is in a *para* position relatively to [^{18}F]fluoride and, in [^{18}F]2FP3, the EWG is in an *orto* position.

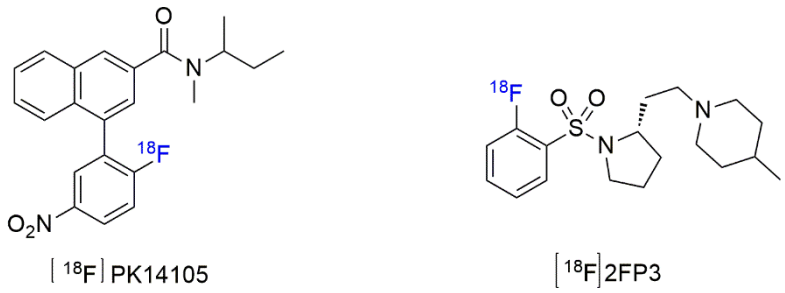

Figure 1.8: Radiopharmaceuticals, [^{18}F]PK10105 and [^{18}F]2FP3, synthesised by nucleophilic aromatic substitution.

Molecules with non-activating substituents can also be synthesised through S_NAr conversion of arenes with EWG, followed by *post*-S_NAr functional-group manipulation[94–97]. In **Scheme 1.4**, we present an example of this methodology for the synthesis of 6-[^{18}F]FDOPA [98].

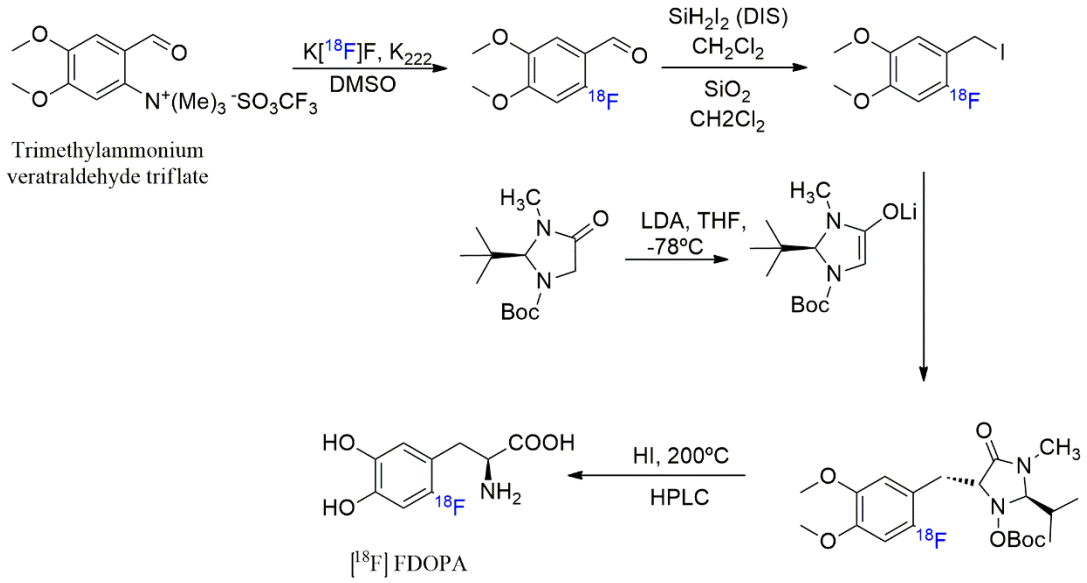

Scheme 1.4: Synthesis of 6-[^{18}F]FDOPA, starting from a trimethylammonium precursor following a post-SNAr strategy.

The process starts with the ^{18}F-fluorination of the precursor, trimethylammonium veratraldehyde triflate, activated in the *ortho* position by an aldehyde group. This step is favoured by the trimethylammonium triflate as a leaving group,a quaternary salt, which allows a time reduction of 10 min, when compared with the alternative nitro substitution reaction. After the ^{18}F-fluorination, a reductive iodination reaction is performed followed by an asymmetric inductive alkylation step, which leads to the formation of a new carbon-alpha carbon-beta bond with high diastereoselectivity. 6-[^{18}F]FDOPA, is obtained with and 17-29 % RCY and enantiomeric excess > 96 % [98].

^{18}F-fluorination of diaryliodonium salts

The need for efficient methods for the ^{18}F-fluorination of non-activated arenes lead to the development of another strategies, like such as the ^{18}F-fluorination of diaryliodonium salts, the ^{18}F-fluorination of spirocyclic iodonium ylides or the transition-metal-mediated aromatic ^{18}F-fluorination with nickel (Ni) or copper (Cu). In **Scheme 1.5** we present the schematic - ^{18}F-fluorination of diaryliodonium salts [69].

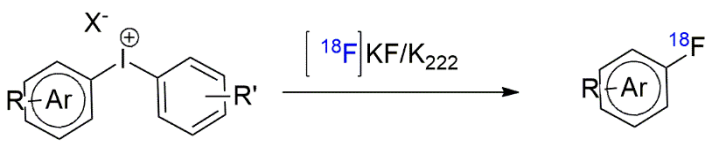

Scheme 1.5: ^{18}F-fluorination of diaryliodonium salts.

This strategy involves the ^{18}F-fluorination of a diaryliodonium salt precursor, **Scheme 1.5**, where the aryl moiety of the corresponding salt is electron-deficient and is preferentially labelled by [^{18}F]fluoride. Pike *et al.* [99] reported the first attempt to perform the ^{18}F-fluorination of a diaryliodonium salts with different substituents and counter ions activated by the Kryptofix® 2.2.2/K_2CO_3-system.

In 2011, DiMagno *et al.* [100] patented the synthesis of 6-[^{18}F]FDOPA using this synthetic methodology. In the first step, the [^{18}F]iodonium fluoride is formed in dry acetonitrile by anion exchange. After removal of the salt by filtration, the ^{18}F-fluorination of the iodonium fluoride is carried out in a non-polar solvent. The last step is the acid hydrolysis with HBr 48 %. Ground Fluor Pharmaceuticals Inc.[101] reported a similar strategy.

To improve the regioselectivity with unsymmetrical diaryliodonium salts a novel class of aryl(2-thienyl)iodonium salts were developed [102]. *Ortho*-substituents on the aryl group of

diaryliodonium salts, (**Scheme 1.6**) show a large influence in regioselectivity and the ^{18}F-fluorination occurs in the ortho-substituted arene. [103] This phenomenon is justified by the trigonal bipyramidal geometry, formed during the ^{18}F-fluorination, where the two aryl groups could rapidly exchange their positions (TS^1 and TS^2). The sterically bulky ortho-substituted aryl group is situated in an equatorial position to minimize the steric repulsion, thereby leading to a favoured reductive elimination, pathway 1, to form a C(sp^2)-^{18}F bond with the equatorial arene in both the monomeric and oligomeric states [103,104].

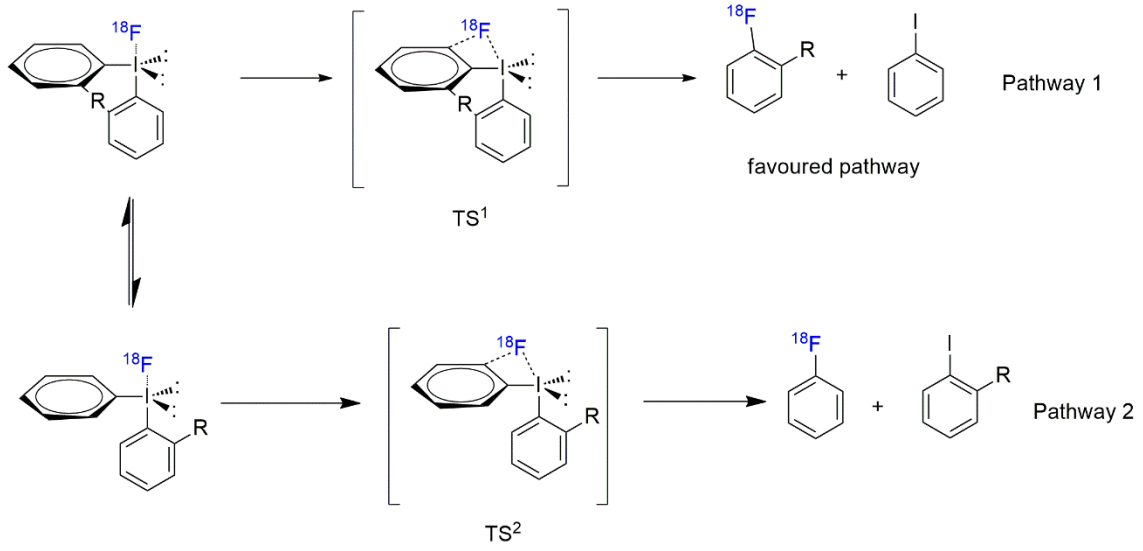

Scheme 1.6: Trigonal bipyramidal geometry of the intermediate [^{18}F]fluoride complex of the nucleophilic attack[69].

Another approach was based on the use of iodonium ylides for late ^{18}F-fluorination stage, using spirocyclic hypervalent iodine (III) complexes as precursors for one-step regioselective ^{18}F-fluorination [105]. This functionalization shows high efficiency for radiolabelling of a large range of non-activated functionalized arenes and heteroarenes, including some common radiotracers.

Transition-metal-mediated aromatic ^{18}F-fluorination has proven to be a promising alternative to other methods due to the high reactivity, selectivity, and tolerance towards other functional groups.

Transition metal catalyzed ^{18}F-fluorination

Transition-metal catalysed ^{18}F-fluorination of diaryliodonium salts was reported by several authors. For example, Ritter *et al.* [106] described a nickel-mediated nucleophilic synthesis of protected 6-[^{18}F]FDOPA, *via* oxidative ^{18}F-fluorination. The reaction is performed with aqueous

[^{18}F]fluoride with a nickel complex precursor in the presence of a hypervalent iodine as oxidant, and resulted in 15 % of product in less than 1 min. One advantage of this method is the possibility of the use of aqueous [^{18}F]fluoride, however the iodine oxidant is very unstable.

Copper-mediated aromatic radiofluorination has been widely used in aromatic ^{18}F-fluorination [107–112]. Neumann *et. al.* [107] reported a copper-mediated reaction between a diaryliodonium salt and [^{18}F]fluoride. The mixture is dissolved in a polar aprotic solvent to facilitate ion exchange between -OTf and [^{18}F]fluoride and, after solvent is removed, a nonpolar solvent is added to proceed the reductive ^{18}F-fluorination.

In 2014, Ichiishi *et al.* [109] described a strategy that uses Cu-catalyzed ^{18}F-fluorination of mesityl(aryl)iodonium salts using [^{18}F]KF. In this case, ^{18}F-C(sp^2) reductive elimination occurred on the counterpart of the steric bulky mesityl group to allow access to a variety of electron-rich, -neutral, and -deficient ^{18}F-arenes.

A cooper-mediated nucleophilic radiofluorination of arylstannanes with [^{18}F]KF was reported, [112,113] including the synthesis of 6-[^{18}F]TriBoc-*L*-DOPA methyl ester, with different reactions times and conditions, including several solvents and additives, **Scheme 1.7**.

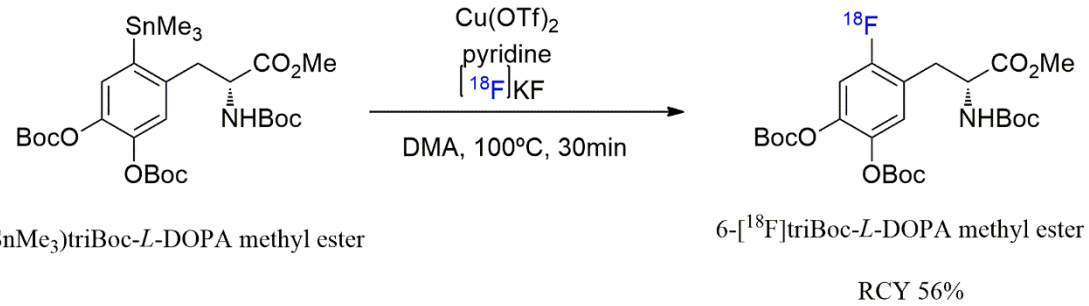

Scheme 1.7: Copper-mediated synthesis of 6-[^{18}F]triBoc-L-DOPA methyl ester [112].

The 6-[^{18}F]triBoc-*L*-DOPA methyl ester, was obtained with a 56 ± 12 % yield (**Scheme 1.7**). Similar approaches were applied for the synthesis of 6-[^{18}F]FDOPA *via* copper-mediated ^{18}F-fluorination but using aryl boronic esters[108] or pinacol boronate esters,[110,111] as precursors.

To obtain a final product with the highest possible activity, the radionuclide should be introduced in the last steps of a radiotracer synthesis. This is the case, for example, of [^{18}F]FDG, where ^{18}F-fluorination is followed only by a quick hydrolysis and an in-line cartridge purification. On the other side, complex radiosynthesis, such as, the nucleophilic pathway for 6-[^{18}F]FDOPA require lengthy processes with multiple steps and HPLC purification [98]. This makes the development of new faster and more effective ^{18}F-fluorination methods an area of big interest [66].

1.3.2 Microwave-assisted ^{18}F-fluorination

As already stated in **section 1.2.1**, several microwave-assisted nucleophilic ^{18}F-fluorinations were reported in the last few decades. [61 114 11563,6457 116 59 117]. In general, all the works reported reveal increased radiochemical yields and reduction in reaction time when compared with conventional heating.

One of the aims of this work was the implementation of this technology in key steps in synthesis of 6-[^{18}F]FDOPA.

1.3.3 Labelling methods with [^{11}C]carbon

Despite the challenge of the short half-life (20.38 minutes), [^{11}C]carbon is one of the most useful radionuclides for PET Chemistry, as it presents the opportunity to radiolabel a certain organic molecule isotopically without changing its molecular structure. [^{11}C]carbon can be produced *via* different nuclear reactions [118,119] (**Table 1.7**), however, the most used is the ^{14}N(p,α)^{11}C, by irradiation of a gas target filled with nitrogen ($^{14}N_2$), which is mixed with trace amounts of oxygen or hydrogen to obtain [^{11}C]CO_2 or [^{11}C]CH_4, respectively, **Figure 1.9**.

Table 1.7: Nuclear reactions used to produce ^{11}C and natural abundance of the irradiated stable isotope.

Entry	Nuclear reaction	Energy range (MeV)	% Natural abundance
1	^{11}B(p,n)^{11}C	5 - 20	80.1
2	^{10}B(d,n)^{11}C	3 - 12	19.9
3	^{12}C(p,pn)^{11}C	20 - 50	98.8
4	^{14}N(p, α)^{11}C	7 - 15	99.6
5	^{14}N(d,n^{4}He)^{11}C	10 - 15	99.6
6	^{12}C(^{3}He,^{4}He)^{11}C	7 - 15	98.9

Although in some special cases radiolabelling is performed with [^{11}C]CO_2 or [^{11}C]CH_4, most commonly they are converted *via* on-line synthetic pathways into more reactive species. For example, [^{11}C]CO_2 can be made to react with primary amines to give [^{11}C]ureas and [^{11}C]isocyanates [120] or with organolithium and organomagnesium compounds, as is observed in the preparation of [^{11}C]acetate via carboxylation of Grignard reagents (MeMgCl or MeMgBr), **Figure 1.9** [121]. [^{11}C]CO_2 is the most versatile primary labelling precursor because not only it can be used directly to label organic molecules, but can also be a precursor for the synthesis of more

reactive [^{11}C]carbon labelling precursors. In **Figure 1.9** we summarize different species of ^{11}C-precursors obtained from [^{11}C]CO_2 [122], such as [^{11}C]CO, [^{11}C]CS_2 or H[^{11}C]CN and others.

Among all the secondary ^{11}C-labelling precursors presented, [^{11}C]methyl iodide ([^{11}C]CH_3I) [123,124] and [^{11}C]methyl triflate ([^{11}C]CH_3OTf) [125,126] are the most used in heteroatoms methylation. These reactions could be performed using a conventional vial (in solution) or using solid supports as "on-cartridge"[127] or "in-loop" [128].

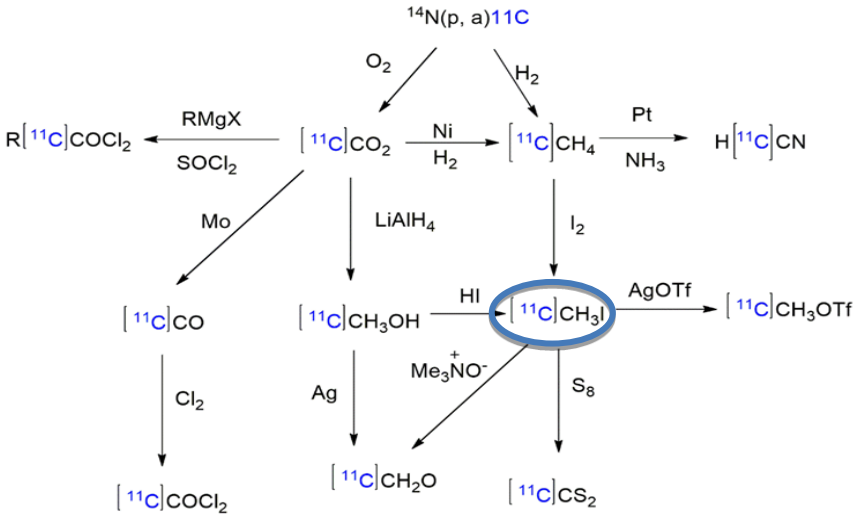

Figure 1.9: Different species of ^{11}C-precursors obtained from [^{11}C]CO.

Additionally, [^{11}C]CH_3I could also be used as an electrophile in several palladium catalysed cross-coupling reaction to form new ^{11}C-C bonds, among other applications.

In the scope of this thesis, methods which use [^{11}C]methyl iodide ([^{11}C]CH_3I) will be described, namely in palladium-mediated cross-coupling, described in **Section 1.3.3.3**..

1.3.3.1 Preparation of [^{11}C]CH_3I

[^{11}C]CH_3I is the most widely used precursor for ^{11}C-methylation. It can be synthesised by two distinct methods: one so-called "wet method" and the other "gas phase". In **Figure 1.10** we present the possible pathways for producing [^{11}C]CH_3I starting from [^{11}C]CO_2.

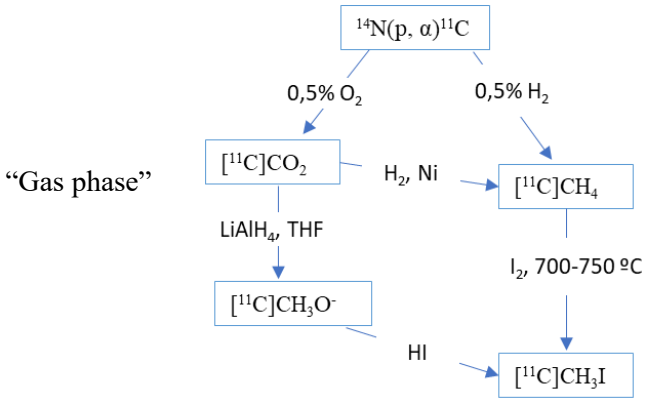

Figure 1.10: Pathways to produce $[^{11}C]CH_3I$.

In the "wet method", developed in 1973, [129,130] the cyclotron produced $[^{11}C]CO_2$ is reduced with lithium aluminium hydride in tetrahydrofuran (THF) or diethyl ether, which is after evaporated. Then hydriodic acid (HI) is added, to produce the $[^{11}C]CH_3I$ (**Figure 1.10**). After, $[^{11}C]CH_3I$ is distilled, using a stream of an inert gas, through a $NaOH/P_2O_5$ column to the vial, "*loop*" or cartridge where the methylation will occur. This method produces good radiochemical yields. However, the main disadvantage is the use of $LiAlH_4$ as a reducing agent. This reagent is a major source of cold carbon dioxide (CO_2), which decreases the A_m of the final product [131]. Also problematic, is the use of HI that causes a rapid deterioration of all the valves and tubing that are in contact with it. This method requires, therefore, extensive cleaning procedures to minimize the action of these aggressive reagents.

In contrast, the main advantages of the "gas phase" method are the high A_m and, from the technical point of view, the avoidance of the problematic $LiAlH_4$ and HI. This method converts $[^{11}C]CH_4$ into $[^{11}C]CH_3I$ by free radical iodination with iodine vapour at a temperature of 700 – 750 ºC (**Figure 1.10**) [124,132]. $[^{11}C]CH_4$ can be produced directly at cyclotron via $^{14}N(p, \alpha)^{11}C$ nuclear reaction using trace amounts of H_2 in target mixture or by hydrogen reduction of cyclotron produced $[^{11}C]CO_2$ (**Figure 1.10**) [124,132]. "Gas phase" iodination is then performed by the circulation of $[^{11}C]CH_4$ that is converted in $[^{11}C]CH_3I$ and trapped in a Porapack trap and, after the peak, the activity is heated to release the produced $[^{11}C]CH_3I$ to the place where the methylation will occur [133].

When ^{11}C-methylation with $[^{11}C]CH_3I$ is not sufficiently effective, the ^{11}C-precursor can be converted to $[^{11}C]$methyl triflate ($[^{11}C]CH_3OTf$) [126]. Besides the higher reactivity, this precursor is less volatile and more easily trapped in small volumes. The heteroatom methylation with $[^{11}C]CH_3OTf$ gives higher RCYs in shorter reaction times and allow lower reaction temperatures than $[^{11}C]CH_3I$ [125,134].

$[^{11}C]CH_3OTf$ is synthesized as an on-line process, by the passage of $[^{11}C]CH_3I$ through a silver triflate column on graphitised carbon spheres.

1.3.3.2 Heteroatom methylation with [^{11}C]CH_3I or [^{11}C]CH_3OTf

[^{11}C]CH_3I or [^{11}C]CH_3OTf are labelling agents for heteroatomic compounds *N*-, *O*- or *S*-methylation reactions under neutral or basic conditions, as depicted in **Scheme 1.8**.

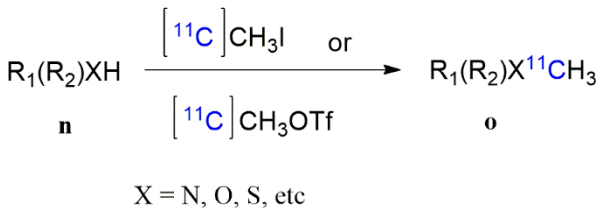

Scheme 1.8: ^{11}C-methylation via nucleophilic substitution through [^{11}C]CH_3I or [^{11}C]CH_3OTf.

These reactions are characterized by the stoichiometric relationship between the desmethyl precursor, and [^{11}C]CH_3I or [^{11}C]CH_3OTf, where the precursor is present in a substantial excess, which could reach a factor of 10^4:1 (**Scheme 1.8**). This stoichiometry results in a faster conversion rate and the radioactive labelling reagent is consumed rapidly to give good RCY's in shorter reaction times [65].

Several ^{11}C-labelled PET tracers have been synthesised by this methylation methods. [^{11}C]flumazenil or [^{11}C]-*L*-methionine are examples of ^{11}C-methylation with [^{11}C]CH_3I, while [^{11}C]PiB is an example of ^{11}C-methylation with [^{11}C]CH_3OTf. In this reaction ^{11}C-*N*-methylation is selective under neutral conditions without the protection of hydroxyl groups [135].

1.3.3.3 Palladium-mediated cross-coupling with [^{11}C]CH_3I

Palladium is one of the most versatile transition metals to promote or catalyse organic reactions and can be used in both forms, Pd(0) or Pd(II). According to **Scheme 1.9**, all catalytic processes start with Pd(0), which reacts with organic halides (or pseudohalides) R-X by an oxidative addition process, producing R-Pd(II)-X intermediates. These species can react with organometallics (*via* transmetallation) or with unsaturated compounds (*via* insertion). The regeneration of Pd(0) occurs after a reductive elimination step [136].

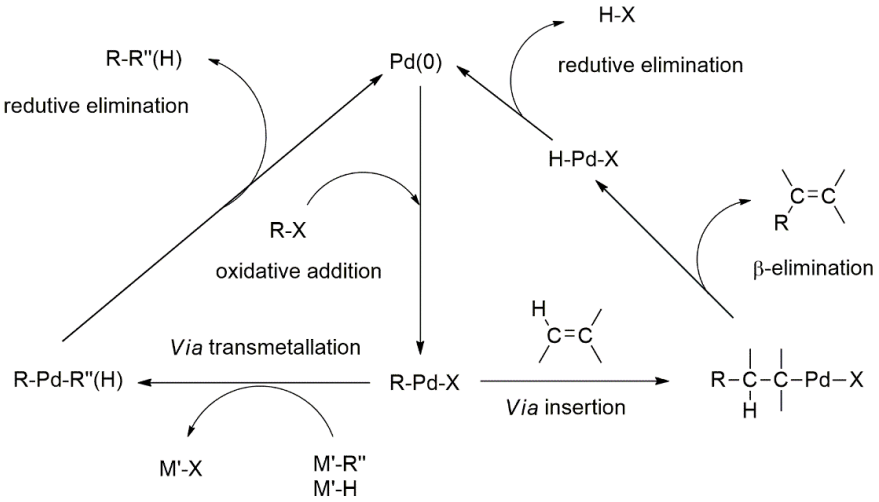

Scheme 1.9: Different pathways for Pd-mediated reactions.

These palladium catalysed reactions are tolerant to a wide range of functional groups which makes them applicable in the synthesis of multiple organic molecules. The most commercially available sources of palladium (0) are the tetrakis(triphenylphosphine)palladium (0), $Pd(PPh_3)_4$, and dibenzylidene-acetone (DBA) complexes of palladium (0), such as $Pd_2(dba)_3(dba)$ and $Pd_2(dba)_3(CHCl_3)$, which can be used to prepare other palladium-phosphine complexes by a ligand exchange reaction [136].

Palladium mediated cross-coupling, namely Stille and Suzuki reactions, have gained interest, as they allow the formation of novel ^{11}C-C bonds. In these types of reactions, tin or boron derivatives are used as substrates, in Stille or Suzuki-coupling, respectively **(Scheme 1.10)** [69]**.**

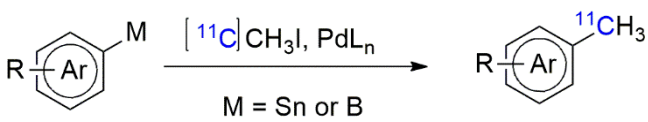

Scheme 1.10: Pd-mediated cross-coupling via $[^{11}C]CH_3I$.

Boron substrates are less toxic than the tin precursors, which is an advantage when the application is in the synthesis of pharmaceuticals. Both, electron-rich or electron-poor boronic esters and aryl boronic acids bearing a wide range of functional groups are coupled with $[^{11}C]CH_3I$ in good yields [5,137,138].

In 2009, carbon-11 methylation of organoboranes by conventional heating was reported by Suzuki *et. al.*[139]. They report the reaction of $[^{11}C]CH_3I$ with pinacol phenylboronate, in the presence of $Pd_2(dba)_3/P(o\text{-tolyl})_3/K_2CO_3$ (1:4:4) in DMF or DMF/H_2O (9:1), producing the

corresponding methylated derivatives in high yields (80-90 %). These conditions were also applied in the synthesis of other ^{11}C-labelled PET probes, such as celecoxib [140], PSPA-4 [141], dehydropravastin[142], cetrozole[143], ATRA[144] or [^{11}C]UCB-J[145].

1.3.3.4. Microwave assisted Palladium-mediated cross-coupling with [^{11}C]CH_3I

The use of microwave heating rather than conventional heating systems, as mentioned in the previous sections, is advantageous as it allows a reduction in reaction times and an increase in the yields. This is even more important in radiosynthesis, when short-lived radionuclides such as cabon-11 are used to perform challenging synthetic processes.

In **Table 1.8** we present some examples from microwave-assisted Pd-mediated Suzuki coupling reactions.

Table 1.8: Examples of microwave-assisted Pd-mediated Suzuki coupling reactions.

Entry	Temperature (ºC)	Time (minutes)	Power (Watts)	MW method	Molecule	RCY (%)	Ref.
1	60-120	1.5	50	dynamic	[^{11}C]toluenes	49-92 %[a]	[137]
2	100	1.5	50	dynamic	[^{11}C]M-MTEB	28.5 ± 2	[146]

Ref.: reference; n.d: not described. [a]decay corrected.

The first attempt to perform cross-coupling with carbon-11 was the coupling of [^{11}C]CH_3I with alkylboranes [5]. In 2005, the Merck group investigate the Pd-mediated cross-coupling of phenyl group with [^{11}C]CH_3I [137]. Authors reported the synthesis of substituted [^{11}C]toluene derivatives, by microwave heating, with high yields and radiochemical purities (**Table 1.8, Entry 1**). The [^{11}C]toluene derivatives were obtained through the reaction of [^{11}C]CH_3I with arylboranes in presence of [Pd(dppf)Cl_2] (dppf = 1,1'-bis(diphenylphosphine)ferrocene) and K_3PO_4 , in dimethylformamide (DMF), under microwave heating, in 90 seconds.

The same method was applied in the synthesis of [^{11}C]M-MTEB a PET probe for mGluR5 (**Table 1.8, Entry 2**) [146].

1.4 Radiolabelling strategies for 6-[^{18}F]FDOPA radiosynthesis

The ^{18}F-radiolabelled nonproteinogenic amino acid 6-[^{18}F]FDOPA is a powerful tool in positron emission tomography (PET) of presynaptic dopaminergic system imaging in the human brain, providing an important clinical tool for the diagnosis of several central nervous system

disorders such as schizophrenia [147,148] or Parkinson's disease [149]. The compound has two different enantiomers with *D* or *L*-configuration. As the *D*-isomer of 6-[^{18}F]FDOPA presents a lower affinity for blood-brain barrier amino acid transporters, enantiomeric purity is of great importance for PET imaging. Ideally, only the *L*-form should be synthesized [150].

As DOPA is the precursor of the neurotransmitter dopamine, the accumulation of 6-[^{18}F]FDOPA in the brain reflects the conversion of 6-[^{18}F]FDOPA in [^{18}F]fluorodopamine reflecting the functional integrity of the presynaptic dopaminergic function [151]. Accidentally, in 1996, a malignant glioma was found with 6-[^{18}F]FDOPA uptake [152], which led to an increased interest in the application of this tracer for oncology, namely in the diagnosis of malignant gliomas [151], neuroendocrine tumours [24,153–156], pheochromocytomas[157,158] and pancreatic adenocarcinomas [159]. In neuroendocrine cells, the uptake of 6-[^{18}F]FDOPA is characteristically high, because these cells store the transported and decarboxylated amines in cytoplasmic neurosecretory granules that vary in size, shape and capacity to store peptidic hormones. 6-[^{18}F]FDOPA is transported into the neuroendocrine cells *via* the sodium independent system L, mainly mediated by a large neutral amino acid transporter protein linked to the glycoprotein CD98 [24].

Synthesis of 6-[^{18}F]FDOPA is quite challenging and the existing processes are complex and typically present low radiochemical yields [160]. Several efforts have been made in the development of synthetic processes, which have been reviewed recently [94,151,160].

The development of a suitable automated synthetic process of 6-[^{18}F]FDOPA, with good radiochemical yield and enantioselectivity, according to GMP requirements, is an issue of great interest in radiochemistry and radiopharmacy. Several methods have been reported, such as isotopic exchange, electrophilic or nucleophilic ^{18}F-fluorination, already described in **Sections 1.3.1.1** and **1.3.1.2**.

One of the first attempts to produce a [^{18}F]DOPA derivative, was reported in 1973, by Firnau *et al.* [161], *via* isotopic exchange (**Scheme 1.11**).

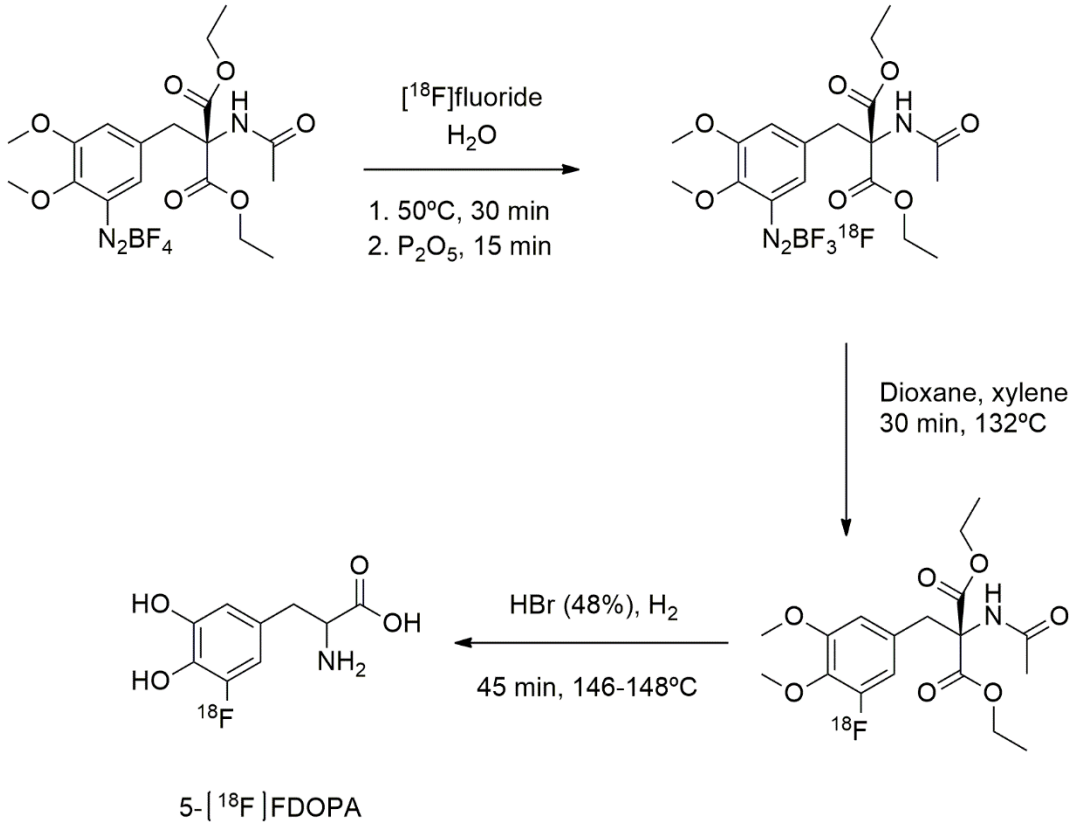

Scheme 1.11: Isotopic exchange reaction for the synthesis of 5-[^{18}F]FDOPA.

Production of [^{18}F]Fluoride was performed in a swimming pool reactor by the ^{6}Li(n,^{4}He)^{3}H and ^{16}O(^{3}H,n)^{18}F nuclear reactions in a mixture of Li_2CO in H_2SO_4 and H_2O. The produced [^{18}F]fluoride was distilled twice and the precursor, was added to this solution. After the isotopic exchange reaction occurred, water was removed, and the resulting residue was dried over P_2O_5 and was then redissolved in dioxane, filtered, and heated to 80 °C. After adding xylene, the solution was heated to 132 °C for 30 min and evaporated. After that, the protected FDOPA, was hydrolysed in the presence of HBr (48 %), yielding 5-[^{18}F]FDOPA, with A_m of 2.2 to 22 KBq/µmol and very low *in vivo* stability. Other attempts were made, by the same group by reacting [^{18}F]F_2 with *L*-DOPA, in liquid hydrogen fluoride. Only 3 % of [^{18}F]FDOPA was obtained with very low regioselectivity [162].

In 2001, Tierling *et al.*[163] presented the synthesis of 6-[^{18}F]FDOPA by isotopic exchange, with 8–10 % of radiochemical yield (RCY) (non-decay corrected (ndc)) and enantiomeric excess (ee) > 85 %, in 70 min. The labelling reaction is based on a carbonyl-activated nucleophilic aromatic substitution of fluorine-19 by fluorine-18. A similar approach was proposed by Wagner[96], which described a similar reaction for radiofluorination of a fluorine-19 precursor with tetrabutylammonium (TBA) [^{18}F]fluoride. 6-[^{18}F]FDOPA was obtained with A_m of 1.5–2.5 GBq/µmol and RCYs of 22 %. This method was automated for the GE TRACERLab MXFDG

and 6-[^{18}F]FDOPA was obtained with RCY's between 8 and 12 %, in 100 min of reaction, with radiochemical purities > 95 % and ee > 98 % [164].

In order to improve the radiochemical yields and regioselectivity of the isotopic exchange methods, synthesis methods of 6-[^{18}F]FDOPA *via* electrophilic substitution were proposed[94,151]. For many years, the only commercially available automated method for the synthesis of 6-[^{18}F]FDOPA was the electrophilic ^{18}F-fluorination[76,77] based on radiodemetallation, desilylation[165], demercuration [79–81,166] and destannylation[82–84,167] presented in **Scheme 1.1**, **Section 3.1.1**. Demercuration and destannylation gave the best results and were adapted to automated routine production [76,77]. The main route to 6-[^{18}F]FDOPA, in this approach, is the reaction of the enantiomerically pure precursors with carrier-added electrophilic fluorine-18, using an automated synthesis module [77,168]. Despite the advantages (good ee, > 99 % and low reaction times, about 50 min), these reactions present low RCY's (25 ± 3 %) and low A_m (4 to 25 MBq/μmol) due to the use of [^{18}F]F_2 which remains the major disadvantage of the electrophilic pathway [169]. When 6-[^{18}F]FDOPA is used as neurotracer, low A_m's are usually not an issue, but for the use in oncology, high molar activities are mandatory [170,171]. This is the major drawback of the electrophilic method. Low molar activities are known to produce pharmacologic effects such as carcinoid crisis by local conversion, in the tumour tissue, of 6-[^{18}F]FDOPA to noradrenaline, induced by aromatic acid decarboxylase and dopamine ß-hydroxylase enzymes [170].

To overcome this drawback, several nucleophilic synthetic processes, with high molar activity, radiochemical yields, and enantiomeric purities suitable for human PET studies, have been developed. Efforts have been made on the development of a nucleophilic incorporation of n.c.a. [^{18}F]fluoride, which can be obtained with A_m's in order of 314–43,000 GBq/μmol [160,172] and several synthetic processes have been developed.

The first nucleophilic methods developed to produce 6-[^{18}F]FDOPA, gave racemic mixtures of the *D*- and *L*- isomers and the pure *L*-isomer was purified by chiral-HPLC, but with a significant loss of activity [173,174].

Alternatively, two "multistep" synthetic routes have been explored. In the first, the reaction starts with the ^{18}F-fluorination of an aromatic ring with standard leaving groups in combination with strong EWD at *ortho* or *para* positions groups, followed by asymmetric alkylation. In the second, ^{18}F-fluorination is done *via* a chiral precursor [98,151,160,175–179].

^{18}F-fluorination occurs in precursors such as trimethylammonium veratraldehyde triflate[98], nitroveratraldehide [176,178] or nitropiperonal [173] where the groups, nitro or trimethylammonium moieties, act as leaving groups, and are activated by the aldehyde in the *para* position.

The key step of these methods is the asymmetric alkylation as this is where the enantioselectivity of 6-[^{18}F]FDOPA is determined. The European Pharmacopoeia (Eur. Ph.), limits the *D*- enantiomer to 4 % [180]. To obtain good enantioselectivities, several strategies have been developed, namely enzymatic alkylation[181], the use of chiral auxiliaries [98,173,176,178], the use

of chiral phase-transfer catalysts (PTCs) [95,97,182–184] or the alkylation under phase-transfer conditions using a substrate/catalyst pair [185].

An enzymatic reaction step was proposed by Kaneko *et al.* [181], with [^{18}F]fluorocatechol converted in 6-[^{18}F]FDOPA with an enantiomeric excess (ee) of 100 %, A_m > 200 GBq/μmol within 150 min synthesis time. However, the RCY was only 2 %.

Besides de chiral auxiliaries, shown in **Scheme 1.4, Section 1.3.1.2**, another strategy is the use of chiral phase-transfer catalysts (cPTC) in the presence of a Schiff's base in the asymmetric alkylation step. In 1997, Corey *et al.* [186] described the synthesis of *O*-(9)-ally-*N*-(9-anthracenylmethyl)-cinchonidinium bromide, a cPTC, which was then used in several asymmetric alkylation reactions [182–184,187] with different precursors and conditions. One limitation of this strategy is that, usually, the phase-transfer catalyst only allows the enantioselective construction of a new chiral carbon-carbon single bond when the reaction is performed at 0 °C [187], which could be a limitation in the automation of the process. Nevertheless, in the last few years, several cPTCs, which allow high enantioselectivities, at room temperature, were tested [97]were the ones selected to implement in automation. In **Table 1.9** we present the results obtained using this synthetic strategy for 6-[^{18}F]FDOPA synthesis.

Table 1.9: Synthesis of 6-[^{18}F]FDOPA, starting from different precursors, using cPTC and a Schiff's base in the alkylation step.

Entry	Precursor	PTC	Time (min)	RCY (%)	A_m (GBq/µmol)	ee (%)	Ref.
1	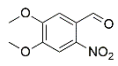 Nitroveratraldehyde	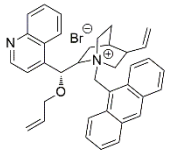	110	10-15	74-185	95	182
2	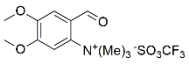 Trimethylammoniu m veratraldehyde triflate	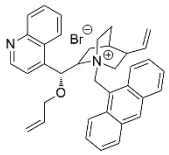	80-85	7-15*	n.d.	90	183
3	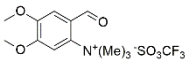 Trimethylammoniu m veratraldehyde triflate	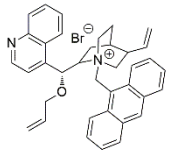	100	25-30*	n.d.	> 95	187
4	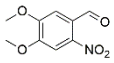 Nitroveratraldehyde	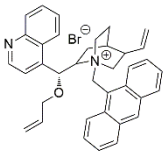	120	20 ± 4	> 50	≥ 95	184
5	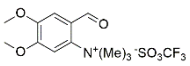 Trimethylammoniu m veratraldehyde triflate	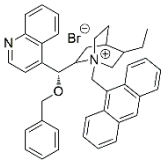 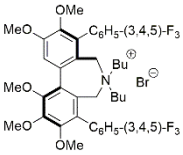	63	33-39*	>750	>97	97

Unless otherwise stated, RCYs are given non-decay corrected (ndc). *decay corrected (dc); n.d.: not determined. Ref.: Reference.

Guillouet's group reported the synthesis of 6-[^{18}F]FDOPA using nitroverathraldehyde as a precursor, a cPTC and a Schiff's base, yielding the product with a RCY of 10–15 %, A_m of 74-185 GBq/µmol, ee of 95 % in 110 min [182], (**Table 1.9, Entry 1**). After ^{18}F-fluorination, the reduction of 6-[^{18}F]fluoro-3,4-dimethoxybenzaldehyde was performed with $NaBH_4/H_2O$

followed by halogenation with gaseous HBr in a Sep-PakC18-Plus. The product was eluted from the cartridge with toluene and finally transferred to the alkylation reaction vessel. The reaction was performed at 0 °C in the presence of cPTC and a Schiff base. The acidic hydrolysis was performed at 200 °C for 20 minutes, with HI (57 %). A similar multistep procedure, using trimetylammoniun veratraldehyde triflate as precursor was performed (**Table 1.9, Entry 2**) [183]. The process involved the nucleophilic substitution, the diiodo silane reductive iodination and phase-transfer catalytic alkylation with a cPTC at room temperature, followed by HI hydrolysis. The product was obtained with low RCY's of 7–15 % (decay corrected) and ee of 90 % (**Table 1.9, Entry 2**). Based on previous reports, in 2004, Lemaire's group[187] reported an optimization of the reaction conditions. They start with the nucleophilic ^{18}F-fluorination of trimethylammonium veratraldehyde triflate, followed by the reduction and halogenation (HBr or HI) in a solid support and subsequent alkylation with a Schiff's base and cPTC. 6-[^{18}F]FDOPA was obtained with 25–30 % RCY and ee > 95 % (**Table 1.9, Entry 3**).

Shen *et al.*[184] presented a similar synthesis process for 6-[^{18}F]FDOPA using nitroveratraldehyde as a precursor, in DMF, followed by the halogenation with freshly prepared diiodosilane. The alkylation step was the same and HBr (48 %) or HI were used in the acidic hydrolysis step. The product was obtained with 20 ± 4 % RCY and ee ≥ 95 % (**Table 1.9**, **Entry 4**). The main disadvantage of this method is the instability of diiodo silane used in the reductive iodination of 4,5-dimethoxy-2-[^{18}F]fluorobenzaldehyde to 4,5-dimethoxy-2-[^{18}F]fluorobenzyliodide.

The best results were reported by Libert *et al.* in 2013[97], that used trimethylammonium veratraldehyde triflate as precursor. The ^{18}F-fluorinated aldehyde was trapped on a tC18 SPE cartridge, where the reduction of the aldehyde occurred, followed by the halogenation. After these reactions, the column was eluted with toluene into a reactor where the enantioselective alkylation, in the presence of a cPTC and a prochiral Schiff base, took place, (**Table 1.9**, **Entry 5**). Two different cPTC were tested, yielding enantioselectivities greater than 97 %. The product was obtained with 36 % RCY, A_m ≥753 GBq/μmol and ee of 97 %, in a total of 63 min synthesis time.

In 2004, Krasikova *et al.* prepared 6-[^{18}F]FDOPA under phase transfer conditions using achiral glycine derivative NiPBPGly and (*S*)-NOBIN as a novel substrate catalyst/pair in the alkylation step, under mild conditions. 6-[^{18}F]FDOPA was obtained with RCY's of 16 % and ee of 96 %. The disadvantage of this process is the complexity of the catalytic system.

Multistep reactions, using chiral auxiliaries or cPTC, have proven to solve the problem of enantioselectivity and the best results are within the limits of the pharmacopoeia requirements. However, the complexity of these processes makes them time consuming and difficult to implement in commercial automated modules.

Other alternative strategies include the ^{18}F-fluorination of diaryliodonium salts, of spirocyclic iodonium ylides or the transition-metal-mediated aromatic ^{18}F-fluorination, with Cu or Ni, as described in **section 1.3.1.2** [94,151,160].

Automation of the synthetic processes is crucial for routine clinical use and compliance with GMP requirements. Several attempts to find the ideal processes to synthesize and automate 6-[^{18}F]FDOPA production were developed, however only a few of these are, at the moment, commercially available. Those will be discussed in the next section.

1.4.1 Automated synthesis of 6-[^{18}F]FDOPA

For many years, the only commercially available automated method for the synthesis of 6-[^{18}F]FDOPA was the electrophilic destannylation [76,77], described in the previous section. However, the limitations of this method lead to a substantial interest in the development of an automated nucleophilic synthetic process able to be used in routine production.

Based on developments of Lemaire *et al.*, the cPTC strategy for 6-[^{18}F]FDOPA [97,187,188] synthesis was automated by Trasis [189]. This multistep synthesis starts from nucleophilic aromatic substitution, followed by a reduction, a halogenation, and an enantioselective carbon-carbon bond formation with a Schiff's base, in the presence of a cPTC. The protected 6-[^{18}F]FDOPA is hydrolysed and purified by semipreparative HPLC, yielding 6-[^{18}F]FDOPA with good reproducibility, RCYs > 35 %, A_m of 129,5 MBq/µmol and ee of 97 %[160]. The process is performed using a Trasis (Ans, Belgium) AllInOne® cassette-based automatic synthesis module [160].

Other automated nucleophilic method was implemented in 2013 by Martin *et al.* to a GE (Chicago, Illinois, United States) TRACERlab MX_{FDG} automated module and subsequently commercialized by ABX (Radeberg, Germany)[164]. The main difference from the previous process was the use of a chiral precursor based on SPE cartridge purification. This approach was implemented in other modules, such as the ORA Neptis® (Philippeville, Belgium) and Siemens (Munich, Germany) Explora™ One, yielding 6-[^{18}F]FDOPA with radiochemical purity (RCP) higher than 95 % and ee of 98 % [164]. Furthermore, the same process, using the non-carried precursor (*S*)-3-(5-formyl-4-methoxymethoxy-2-nitro-phenyl)-2-(trityl-amino)propionic acid tert-butyl ester was also developed for an IBA (Louvain-la-neuve, Belgium) Synthera module within a set of disposable cassettes (IFP-"Integrated Fluidic Processor"). The multistep synthesis includes trapping, elution and drying of the [^{18}F]-fluoride, nucleophilic ^{18}F-fluorination of precursor, oxidation**,** followed by the acidic hydrolysis of the protected [^{18}F]FDOPA. The purification is carried out using a set of cartridges yielding [^{18}F]FDOPA formulated in citrate buffer, with 20 ± 5 % RCY and >99 % ee. The same method was adapted for the iPHASE FlexLab

Module (Australia) by Ya-Yao Huang [190], yielding 6-[^{18}F]FDOPA with RCP > 99 %, RCY between 5-7 % in 110 minutes.

The main advantage of this method is that it can be performed in a non-cassette-based system and without the semi-preparative purification, which is expensive and time consuming. In contrast, the lower RCY when compared with the Trasis method is the main disadvantage. However, both are able to routinely produce 6-[^{18}F]FDOPA within the required specifications.

In both methods, the approach is the direct nucleophilic aromatic substitution, requiring multiple steps and leading to highly complex processes, with consequently low radiochemical yields. In the Trasis method, the fluorination occurs in nitroveratraldeyde, followed by reduction, halogenation, alkylation, hydrolysis, and semi-preparative purification. In the ABX® method, ^{18}F-fluorination occurs at a chiral precursor which encompasses an aldehyde as activating group in the *para* position, followed by a Baeyer-Villiger oxidation, to transform the aldehyde into an easily hydrolysable group.

More recently, based on the already commercially available synthetic methodologies, Pretze *et al.* [191] evaluated both multistep synthesis, from Trasis and ABX, using an Eckert&Ziegler (Berlin, Germany) modular-Lab Standard module. Trasis® strategy does not show applicability in this module. Even though the second approach shows better results, it is worse than the original performed in a IBA (Louvain-la-neuve, Belgium) Synthera® module, with an RCY of 20 ± 1 %, A_m up to 2.2 GBq/µmol and ee > 96 %.

Even more recently, Mossine *et. al.* [110,111] reported a one-pot, two steps fully automated and validated synthesis of 6-[^{18}F]FDOPA in a GE TRACERlab MX_{FN} automated synthesis module *via* copper-mediated fluorination of a pinacol boronate ester (BPin) precursor (**Scheme 1.12**) [111].

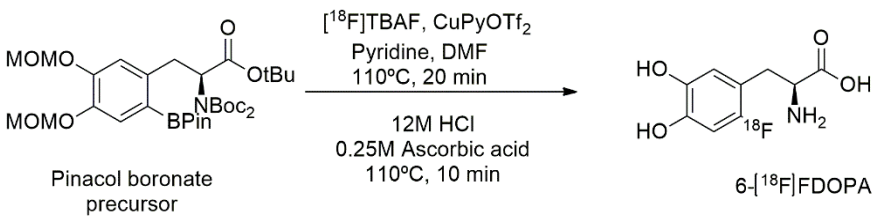

Scheme 1.12: Automated copper-mediated fluorination of a BPin precursor using a TracerLab synthesis module.

This method provides 6-[^{18}F]FDOPA with RCY of 5 %, RCP > 98 % and A_m in order of 76 TBq/mmol, is reproducible, already implemented in two different sites and validated for human use.

Despite all the commercially available processes to produce 6-[^{18}F]FDOPA, the low RCY's, long synthesis time and complexity of all methods mean that there is still a great interest in the development of new methods and the improvement of the current ones.

The first aim of this PhD project is therefore the application of microwave technology in key steps of 6-[^{18}F]FDOPA synthesis in order to improve dramatically synthesis time and yield for its production.

1.5 Radiolabelling strategies for [^{11}C]UCB-J Radiosynthesis

Another challenging process is the automated synthesis of [^{11}C]UCB-J, a PET radiotracer which allows the quantification of synaptic density *in vivo*.

Synapses are structures in brain which mediate a functional interaction between two neurons or between a neuron and another cell type [192]. They are involved in processes of higher brain functions and are targets for many psychoactive drugs. They can become defective in neurological diseases as well as psychiatric disorders such as epilepsy, Alzheimer's disease, schizophrenia, autism, depressive disorders or Huntington's disease [193–198]. Synaptic density can be used as a quantitative biomarker of synaptic pathology. Levetiracetam is a second-generation antiepileptic drug (AED), with a mechanism of action involving neuronal binding to synaptic vesicle protein 2A. This molecule could potentially be directly radiolabelled [199], however, its affinity to SV2A its too low to be used for PET imaging [200]. Other radiotracers have been developed by the company UCB to visualize SV2A *in vivo* using PET, with good affinities for SV2A. These were radiolabelled with [^{18}F]fluoride or [^{11}C]carbon.

Tracers such as [^{11}C]UCB-J, [^{11}C]UCB-A or [^{18}F]UCB-H [145,201–205] have been developed in the last few years. Based in recent studies in mice, non-human primates and healthy humans, [^{11}C]UCB-J appears to be the most promising due to its pharmacokinetic and quantification properties [145,206–208].

The first [^{11}C]UCB-J synthesis was reported by Nablusi *et.al* in 2016[145] and was performed by [^{11}C]methylation of the (*R*)-trifluoro(4-((2-oxo-4-(3,-4,5-trifluorophenyl)pyrrolidine-1-yl)methyl)pyridine-1-ium-3-yl)borate precursor (Trifluoroborate UCB-J precursor) with [^{11}C]CH_3I, in dimethylformamide (DMF) *via* the Suzuki-Miyaura cross-coupling reaction, using Tris(dibenzylideneacetone)dipalladium(0) ($Pd_2(dba)_3$), Tris(o-tolyl)phosphine ($P(o\text{-}tol)_3$) and potassium carbonate (K_2CO_3) as catalytic system (**Scheme 1.13,** *via* 1). [^{11}C]CH_3I is bubbled in the vial containing the catalytic system and after, the precursor is added.

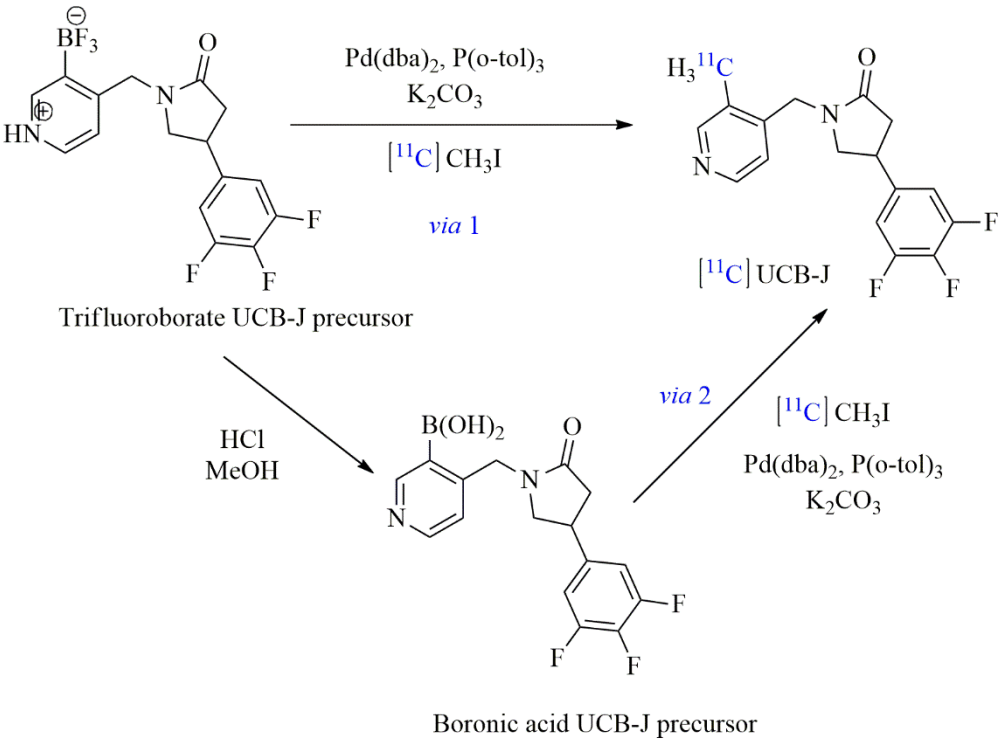

Scheme 1.13: [^{11}C]UCB-J by two different pathways, via trifluoroborate or boronic acid precursors.

In 2019, Rokka *et al.* [201] reported an improvement in the [^{11}C]UCB-J synthesis performed in one step (catalytic system and precursor) using tetrahydrofuran (THF) as solvent using an in-house developed production system (Uppsala University Hospital PET Centre, Sweden). They obtained a radiochemical yield (RCY) of 39 ± 5 % (decay corrected from [^{11}C]CH_3I). Authors attribute these results to the possible partial hydrolysis of precursor in solvent mixture THF/water, which results in a mixture of two precursors (trifluoroborate and boronic acid). More recently two other groups [202,203] reported the [^{11}C]UCB-J synthesis by *via* 2 (**Scheme 1.13**), and they believe that the hydrolysis of trifluoroborate precursor to the corresponding boronic acid precursor was important to obtain higher amounts of activity and improved RCY's [202]. In all cases, the procedures are similar. [^{11}C]CH_3I is added to the solution of the catalytic system and the precursor is added after peeking [^{11}C]CH_3I. Nevertheless, these methods still present low RCY's and require a long time to be performed [145,201,202].

The results reported until moment in synthesis of [^{11}C]UCB-J shows the difficulties to produce this radiopharmaceutical, which lead to the need to improve and automated the existent methods.

Based in all the already reported microwave-assisted Suzuki-coupling of other molecules, one of the main goals of this work was the use of microwave heating to improve the overall synthesis process of [^{11}C]UCB-J.

1.6 Aim of this thesis

The work that supports this thesis was performed at ICNAS-Produção Unipessoal, Lda (ICNAS-P), a company owned by the University of Coimbra, dedicated to the production and development of radiopharmaceuticals labelled with short-lived positron emitters. The company holds all necessary licenses for GMP pharmaceutical manufacturing and radiopharmaceutical production for clinical trials and produces radiopharmaceuticals for the portuguese market as well as for internal use at ICNAS and its own R&D projects.

The company has great interest in producing [^{18}F]FDOPA for the Portuguese market as well as to support a number of ongoing clinical research projects. ICNAS-P has two commercially automated systems able to produce [^{18}F]FDOPA: TRASIS and IBA Synthera. Both processes are complex, lengthy and produce low yields.

ICNAS-P also has an interest in producing [^{11}C]UCB-J to support ongoing clinical studies. No commercially module exists to produce this compound and all published methods are complex and lengthy what, considering the short half-life of Carbon-11, is critical for its application.

Microwave technology has proven to be advantageous over conventional heating for chemical synthesis, producing faster and cleaner reactions but is yet to be used in the routine production of radiopharmaceuticals.

The main goal of this thesis was the implementation at ICNAS-P of the synthesis processes for [^{18}F]FDOPA and [^{11}C]UCB-J and their adaptation to the use of microwave heating in key steps in order to improve yield and synthesis times of current production processes.

This project fits within the objectives of a PhD studentship in the industry.

Chapter 2

Development and implementation of an [^{18}F]FDOPA synthesis method and its improvement by microwave heating and synthesis of a nitro-DOPA precursor

As described in **Chapter 1**, 6-[^{18}F]FDOPA is used in PET for the diagnosis of central nervous system disorders [147–149], as well as in oncology, namely for the diagnosis of neuroendocrine tumors (NET's) [151–156,158,159,209].

According to the World Health Organization (WHO), *"one in four people in the world will be affected by mental or neurological disorders at some point in their lives. Around 450 million people currently suffer from such conditions, placing mental disorders among the leading causes of ill-health and disability worldwide"* [210]. Considering this scenario, diagnosis of neurological disorders is a key issue for all heath systems worldwide.

NET's, which are considered rare malignancies, are normally detected in an advanced stage of disease, as the primary lesion can remain asymptomatic for a long period of time. As an example, Darbà *et al.* [211] published a study in 2019, where 9120 patients were diagnosed with a neuroendocrine tumour, in Spain, between 2010 and 2015. They observe a 2-fold increase between 2010 and 2015, in the diagnosis of these tumours, which is mostly due the evolution of the diagnostic techniques, such as PET , which presents higher sensitivity when compared with computerized tomography (CT), magnetic resonance imaging (MRI) or other standard imaging techniques[24]. As an example, 6-[^{18}F]FDOPA PET/CT is used, not only for the diagnosis, but also to perform a molecular imaging-guided laparoscopic surgery of congenital hyperinsulinism in infants[24]. Its high sensitivity, allows the surgeon to perform a curative restricted resection of a focus without the risk of long-term diabetes[212].

The obvious characteristics and important clinical applications of this radiopharmaceutical, make him a great tool in the clinical setting. The main constrain is the lack of availability of the radiopharmaceutical. In practice, only a few very specialized production centers are able to synthesize it for routine clinical use due to the complexity of the synthesis process.

The intention to produce [^{18}F]FDOPA at ICNAS-P resulted for numerous requests form Portuguese hospitals reporting an unmet clinical need. The company has all the necessary licenses to produce radiopharmaceuticals according the good manufacturing practices (GMP)[227] and holds Marketing Authorizations to produce Fluodesoxiglucose [^{18}F] UC (2011), and GalliUC (2021)[225].

A marketing authorisation (MA) to distribute 6-[^{18}F]FDOPA (active substance: Fluorodopa (^{18}F)) in Portugal was actually submitted by the company Cis Bio International and approved by INFARMED in 2011. However, due to the complexity of its production, the product was never commercialized. There was, therefore, no alternative drug to resolve this clinical need and a compounding licence could be envisaged.

Taking into account all the documentation and procedures needed and based in all the regulations in force, the production of 6-[^{18}F]FDOPA was implemented at ICNAS-P.

In this chapter, we will discuss the implementation, and submission to authorities of the 6-[^{18}F]FDOPA synthesis process as a pharmaceutical compound.

Additionally, in order to improve the production process for 6-[^{18}F]FDOPA, the synthesis of a new precursor as well as the use of microwave heating in key steps of the radiosynthesis will be discussed.

2.1 [^{18}F]FDOPA synthesis methods

In **Scheme 2.1** we summarize the synthesis processes of 6-[^{18}F]FDOPA as automated for routine production[77,111,164,189].

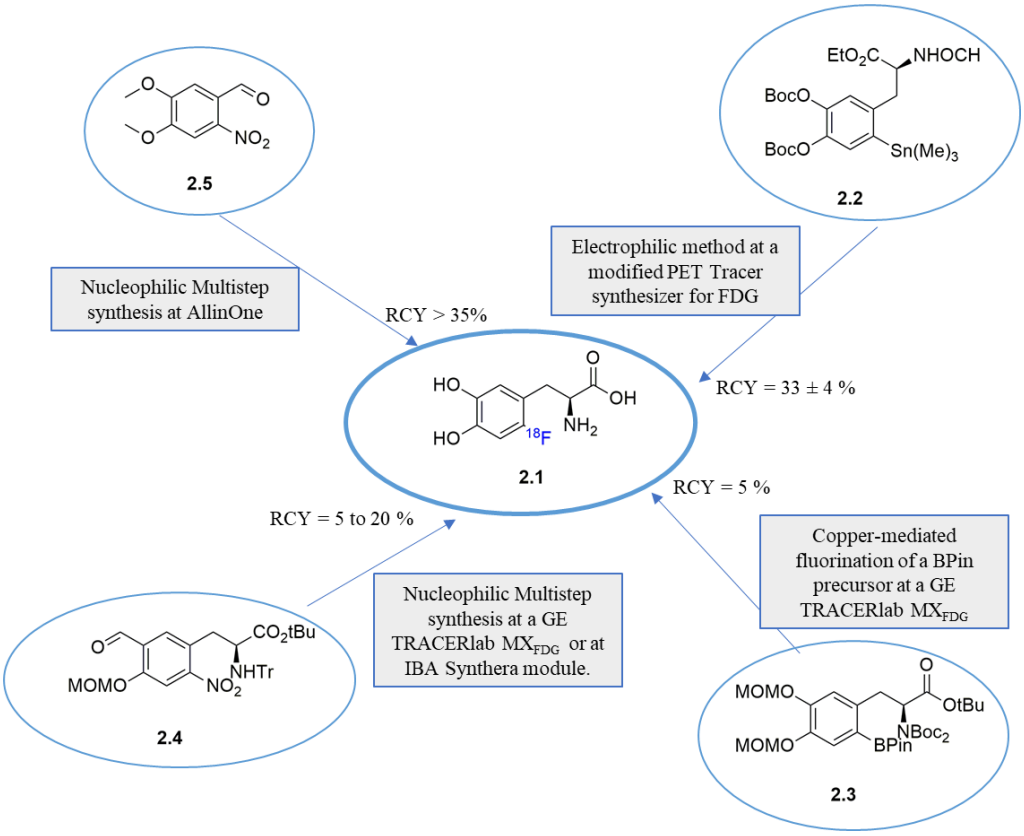

Scheme 2.1: Automated methods for the synthesis of [^{18}F]FDOPA **2.1**.

The electrophilic method [77], starting from the tin derivative precursor, **2.2**, was the only commercially available method for many years. However, the disadvantage of producing low molar activities (A_m), compromised its applicability for oncological studies.

A variety of automated nucleophilic synthesis processes were developed to overcome this drawback with RCY's ranging between 5 %, obtained with the recently developed nucleophilic

copper-mediated ^{18}F-fluorination of a pinacol boronate ester (BPin) precursor, **2.3**, method [111], and the 35 % obtained with the multistep synthesis method, starting from ^{18}F-fluorination of nitrobenzaldehyde, **2.5** [189].

The other multistep synthesis method, starting with the ^{18}F-fluorination of a chiral precursor, **2.4** [164], was implemented in several automated modules, such as IBA Synthera®, TRACERlab MX_{FDG}, ORA Neptis®, Siemens Explora™ IPhase FlexLAb Module and in an Eckert & Ziegler module. The RCY's of these methods varies between 5 and 12 % non-decay corrected (ndc).

ICNAS-P is equipped with two automated modules capable of [^{18}F]FDOPA production: AllinOne® from Trasis and IBA Synthera®.

2.2 First implementation of [^{18}F]FDOPA synthesis at ICNAS-P

2.2.1 Production

Due to the availability of IBA Synthera® modules at ICNAS-P, **Figure 2.1,** the first attempts to implement [^{18}F]FDOPA, **2.1** followed the nucleophilic method developed by ABX (Germany) for these modules [164].

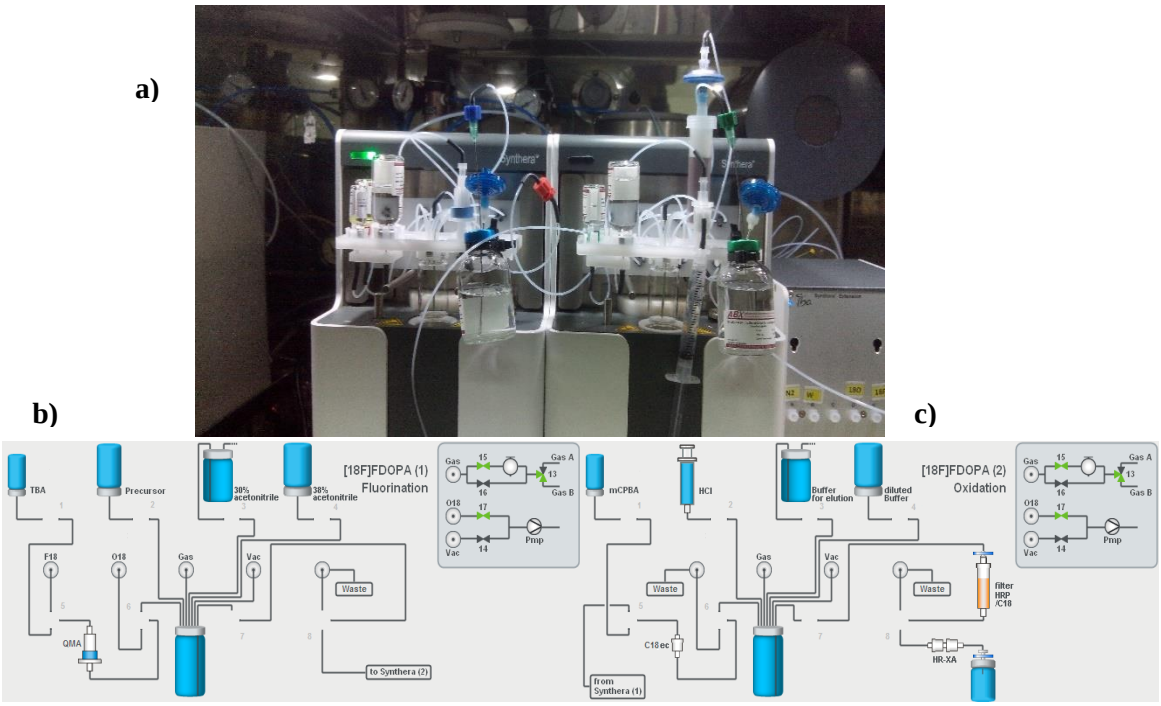

Figure 2.1: IBA Synthera® module for the synthesis of **2.1** using the ABX synthesis method. **a**) IFP's with reagents installed. **b**) script for the ^{18}F-fluorination synthesis step. **c**) script for the oxidation and hydrolysis step.

6-[^{18}F]FDOPA synthesis requires two modules (**Figure 2.1**, **a)**, which are controlled by their respective scripts (**Figure 2.1**, **b)**, the first one for ^{18}F-fluorination, and the second for oxidation, and hydrolysis (**Figure 2.1, c)**.

[^{18}F]Fluoride is produced *via* the ^{18}O(p,n)^{18}F nuclear reaction by irradiation of [^{18}O]H_2O in a IBA Cyclone® 18/9 or in an IBA Cyclone® KIUVE® (variable energy) cyclotron (Louvain-la-Neuve, Belgium). After irradiation, the [^{18}F]fluoride aqueous solution is transferred to a vial located in an hot cell and then passed through a quaternary methylammonium (QMA) column (Sep-Pak Accell Plus QMA Carbonate Plus Light) containing a silica-based, hydrophilic, strong anion-exchanger and a carbonate counter-ion. The [^{18}F]fluoride is retained in the column and [^{18}O]H_2O passes to a waste vial. Subsequently, the column is eluted with tetrabutylammonium hydrogen carbonate (0.075M) – aqueous solution, stabilized with ethanol (TBA.HCO_3), to originate the tetrabutylammonium fluoride (TBAF) salt which is azeotropically dried. Afterwards, the precursor is added to the salt and the ^{18}F-fluorination occurs. The schematic synthetic process is presented in **Scheme 2.2**.

This synthetic strategy starts with ^{18}F-fluorination of the (*S*)-3-(5-Formyl-4-methoxymethoxy-2-nitro-phenyl)-2-(trityl-amino)-propionic acid tert-butyl ester, **2.4**, to give **2.6**, which is after oxidized by a Bayer-Villiger oxidation to compound **2.7**. **2.7** is after hydrolysed by an HCl 6 M solution, yielding [^{18}F]FDOPA, **2.1**.

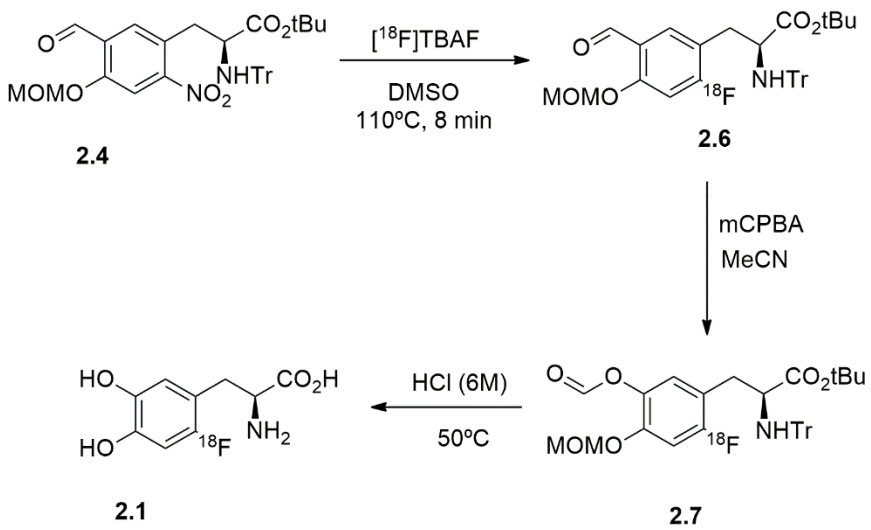

Scheme 2.2: Automated synthesis of [^{18}F]FDOPA **2.1**, using the ABX method[164].

In the first step, the ^{18}F-nucleophilic fluorination occurs at position 6 of the aromatic ring, by the substitution of a nitro leaving group. To permit the nucleophilic aromatic substitution at this position, the aromatic ring must include, besides the leaving group, an activating group,

normally an electron withdrawing, located in *ortho* or *para* positions to promote the nucleophilic aromatic substitution by stabilization of the Meisenheimer complex. In the molecule **2.4**, this group is in the *para* position relatively to the leaving group, **Scheme 2.2**.

After the ^{18}F-fluorination, the intermediate **2.6** is oxidized with *m*-chloroperbenzoic acid (mCPBA) to transform the aldehyde (the activating group) into a hydrolysable group, molecule **2.7**, **Scheme 2.2**. This step is followed by an acidic hydrolysis with a mixture of HCl 6M and ethanol.

The main advantage of this method, when compared with other nucleophilic methods, is the purification by solid-phase extraction (SPE) instead of the traditional semi-preparative HPLC. A set of columns were mounted sequentially: i) a custom-made HR-P (polymer-based RP materials), to remove the HCl used in hydrolysis step; ii) a Sep-Pack Plus C18 to remove the non-polar by-products and the precipitates and iii) an OASIS WAX cartridge. The diluted reaction mixture is passed through the columns that are cleaned with water. [^{18}F]FDOPA is then eluted to the final product vial with a citrate or phosphate buffer solution containing 3 % of ethanol and stabilizers, yielding [^{18}F]FDOPA **2.1**, with RCY's of 6.8 ± 1.3 % (n = 5), in 81 minutes, (**Figure 2.2**). Two main factors contribute to the low radiochemical yields: the Baeyer-Villiger oxidation step and the clogging of the cartridges during the purification. According to published works [228,229], the Baeyer-Villiger oxidation step is determinant for the RCY of the final reaction. On the other hand, the use of mCPBA, leads to the formation of precipitates upon the hydrolysis reaction, which leads to the main problem of this synthesis method, the clogging of the cartridges during the purification. Sometimes, this results in a failed production, making this method unreliable for routine production.

2.2.2 Quality control

Quality control tests are implemented according to the pharmacopoeia monograph for the electrophilic method [230], when applicable, which were the only available when this implementation was performed at ICNAS-P. Tests as appearance, pH, radionuclidic and enantiomeric purities or biological impurities are common to both methods. All the other tests, chemical and radiochemical purities and residual solvents are adapted to this production method.

Chemical purities are determined by TLC, to analyse the presence of tetrabutylammonium hydroxide, and by HPLC to analyse the other chemical impurities.

Radiochemical, and enantiomeric purities were determined by analytical HPLC according to the methods described in the **Chapter 5**. Radiochemical yields are determined by the relation between the total amount of activity at end of bombardment (EOB) and the activity of [^{18}F]FDOPA at end of synthesis (EOS).

In **Figure 2.2** we present the results of 5 runs of [^{18}F]FDOPA synthesis using the ABX

method. Radiochemical Yield (RCY), Radiochemical purity (RCP) and percentage of *L*-[^{18}F]FDOPA are indicated.

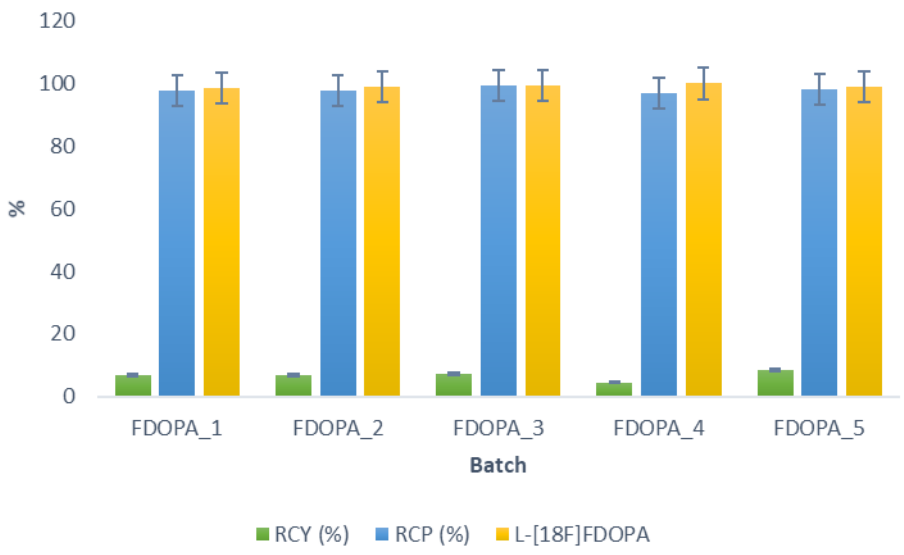

Figure 2.2: Results obtained with the ABX synthesis process performed in a IBA Synthera® module (n=5). Radiochemical Yield (RCY), radiochemical purity (RCP) and percentage of the *L*-enantiomer.

Residual solvents ethanol (EtOH), acetonitrile (ACN) and dimethylsulfoxide (DMSO), are determined by gas chromatography and their concentration is determined by a calibration curve or by comparison with a standard solution prepared with the solvents to analyse at the limit concentration, injected right before the analysis. According to European Pharmacopoeia (Eur. Ph.) [231], ACN, a class 2 residual solvent, must be limited in pharmaceuticals due to its inherent toxicity. The limit of this solvent is 4.1 mg/day. EtOH and DMSO are solvents with low toxic potential, of class 3. The limits of these solvents are, generally, of 50 mg/day. In all the analysis, residual solvents are below the limits.

Radionuclidic purities are determined by measuring the half-life and by gamma-ray spectrometry, where the peaks in the gamma ray spectrum corresponding to photons with an energy different from 0.511 MeV or 1.022 MeV must be lower than 0.1 % [232].

Despite the good results regarding radiochemical purity, 98.0 ± 0.8 % (n=5), and enantiomeric purity, 99.1 ± 0.5 % (n=5), (**Figure 2.2**), the low RCY and the clogging problems lead to the necessity to implement another synthesis process.

2.3 Second implementation of [^{18}F]FDOPA synthesis at ICNAS-P

To overcome the problems of the ABX process, a multistep strategy, based in an alkylation step in the presence of a cPTC (chiral phase-transfer catalyst) [95,97,188], automated by Trasis (Ans, Belgium) was implemented and validated at ICNAS-P. The production was performed using an AllinOne® synthesis module (**Figure 2.3, a)**. In **Figure 2.3**, **b)**, we present the script which controls the synthesis process for [^{18}F]FDOPA, **2.1.**

a) **b)**

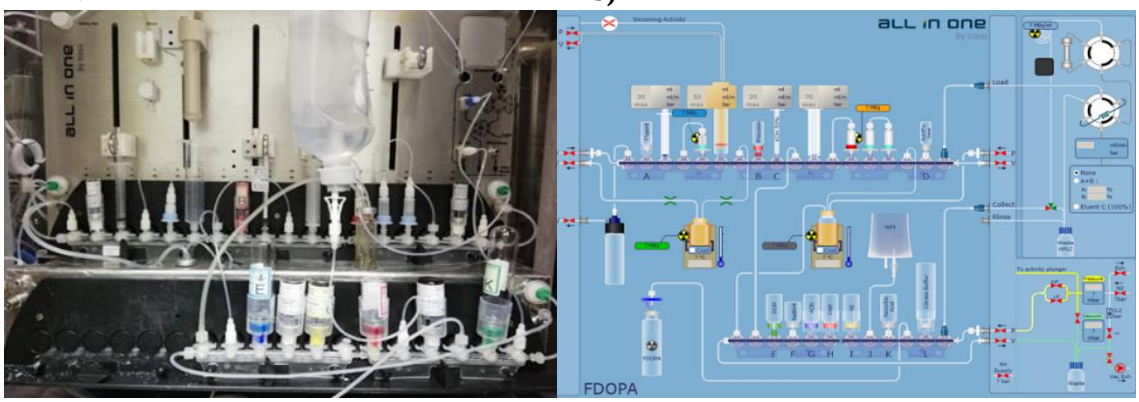

Figure 2.3: **a**) Automated module AllinOne® by Trasis, a) and; **b**) the script which controls the [^{18}F]FDOPA production.

To minimize exposure to radiation, the synthesis process is performed without isolation of intermediates.

The method developed by Trasis and implemented at ICNAS-P is similar to the method developed by Libert *et al.* [97], but using the nitro precursor, **2.5**, instead of 6-trimethylammonium veratraldehyde triflate, and DCM as solvent at the alkylation step, instead of toluene (**Scheme 2.3**).

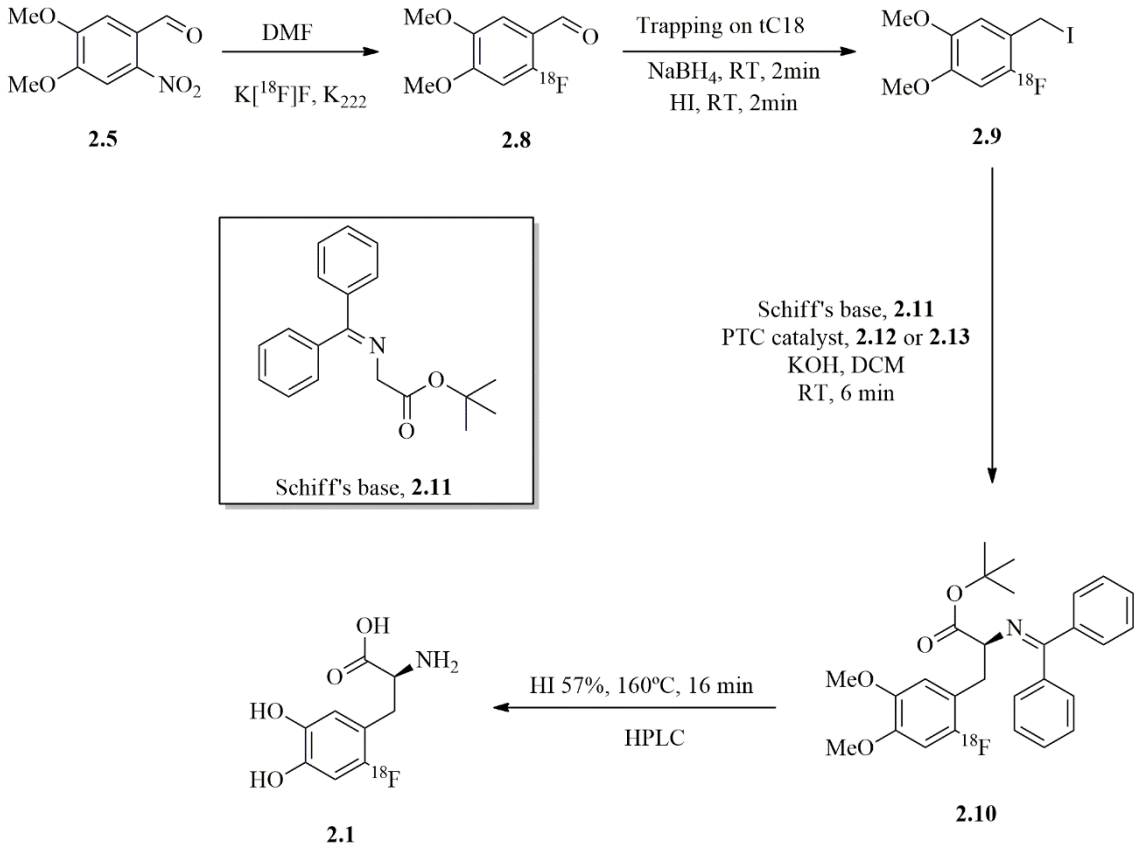

Scheme 2.3: Automated synthesis of 6-[^{18}F]FDOPA **2.1** by Trasis method[189].

According to several authors [38,42], 6-trimethylammonium veratraldehyde triflate has great advantages over the 6-nitroverathraldeyde, **2.5**, needing less reaction time (2 minutes), and its solubility in water facilitates purification by a tC18 cartridge[97]. However, 6-trimethylammonium veratraldehyde triflate is not stable for a very long period even when stored at 0-4ºC. According to Zhang *et al.* [183], after 6 months, the labelling yields are reduced to lower than 10 %, which make this precursor a bad candidate for a commercial method.

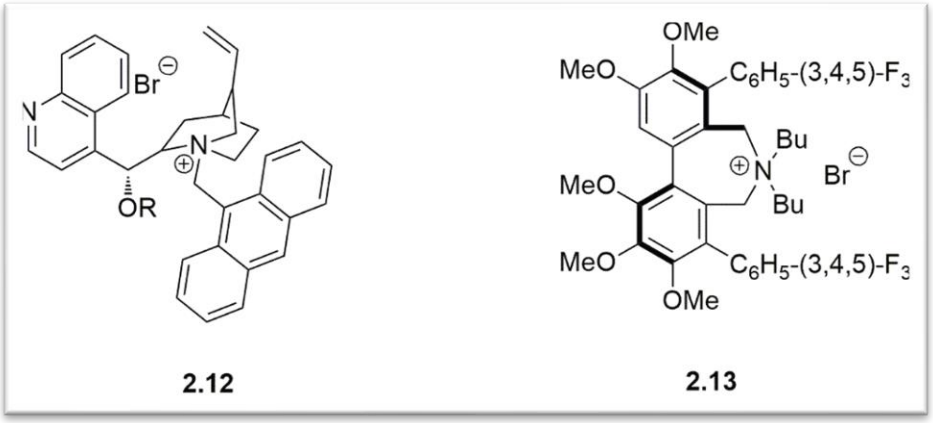

Figure 2.4: Phase transfer catalysts (PTC) used in asymmetric alkylation of glycine imines.

The process starts with the production of [^{18}F]fluoride, as described previously, that is transferred to the hot-cell and trapped in the Sep-Pak Accell Plus QMA Carbonate Plus Light. After retention of the [^{18}F]fluoride, the column is eluted with a Kriptofix$_{222}$ (K_{222}) solution, 0.2 M in acetonitrile and K_2CO_3 0.1 M in water onto a reaction vessel and then the K[^{18}F]-K_{222} is azeotropically dried. This method is widely used in ^{18}F-fluorination by S_N2 or S_NAr [233] ^{18}F-fluorination reactions. After, the precursor **2.5**, diluted in dimethylformamide (DMF), is added to the dry salt K[^{18}F]-K_{222} and the ^{18}F-fluorination occurs at 160ºC for 5 minutes, yielding the intermediate 2-[^{18}F]fluoro-4,5-dimethoxybenzaldehyde **2.8**, with a radiochemical conversion yield of 50 % [97].

After ^{18}F-fluorination, the crude reaction mixture is diluted with water and **2.8** is trapped onto a tC18 cartridge where the aldehyde group is quantitatively reduced to alcohol by reaction with sodium borohydride ($NaBH_4$). By exposure to a solution of hydriodic acid (HI) 57 % through the cartridge, the alcohol group is replaced by and iodine group, resulting in 1-[^{18}F]fluoro-2-(iodomethyl)-4,5-dimethoxybenzene, **2.9**.

This intermediate is then eluted from the cartridge with dichloromethane and dried over potassium carbonate cartridges to the second reactor. Then, a strong base, KOH, Schiff's base, **2.11**, and a chiral phase-transfer catalyst (**2.12** or **2.13, Figure 2.4**) is added to perform the asymmetric alkylation yielding the protected [^{18}F]FDOPA, **2.10**. In this step, a new carbon-carbon single bond is formed and the enantioselectivity of [^{18}F]FDOPA is defined. Asymmetric synthesis of α-amino acids, by phase-transfer catalysed alkylation of prochiral glycine derivatives has been widely used [234–236]. A critical factor is the choice of a phase-transfer catalysts (PTC's) which provides the desired enantiomeric purity [186,234,235,237–239]. According to Eur. Ph. [230], the percentage of the *L*- enantiomer must be higher than 96 %. In 1997, Corey *et al.* [186] report, for the first time, *N*-antracenylmethyl substituted cinchona alkaloids, **2.12**, as phase transfer alkylation of glycine imines (**Figure 2.4**) with good enantiomeric excesses in the range of 92-99.5 %.

As stated in **Chapter 1**, many efforts have been made in the search for the best system to perform the asymmetric alkylation in the synthesis of [^{18}F]FDOPA **2.1**. Guillouet *et al.* [182] reported, for the first time, the use of catalyst **2.12** in the production of [^{18}F]FDOPA, **2.1**, with an enantiomeric excess (ee) of 95 %. The same catalyst was reported by other groups, with different precursors, obtaining enantiomeric excesses varying from 90 to 96 %. In 2013, Libert *et al.* [97] report an automated multistep approach, using a trimethylammonium precursor, instead of the nitro precursor. They studied the use of catalysts **2.12** and **2.13** in the alkylation step with the Schiff's base *N*-(diphenylmethylene)glycine *tert*-butyl ester **2.11**, at room temperature and they obtain an ee of 97 %. One of the most challenging steps for automation is the enantioselective alkylation step. Normally, to produce a good ee, the reaction must be performed at low

temperatures, negative or close to 0ºC. They optimized the alkylation step testing different PTC's, bases, solvent, and temperature. The best results were obtained when the alkylation was catalyzed by PTC's **2.12** and **2.13** in presence of KOH 9N and using toluene as solvent. However, in the Trasis method the solvent is dichloromethane and the enantiomeric purity of *L*-[^{18}F]FDOPA **2.1**, is 96.6 ± 0.4 %.

The last steps are the hydrolysis of **2.10** and the semi-preparative purification, yielding [^{18}F]FDOPA, **2.1**, with RCY of 36 ± 3 % (decay corrected). The production method was performed at a FASTlab module.

The full process, implemented at ICNAS-P was performed following the steps presented in **Figure 2.5**.

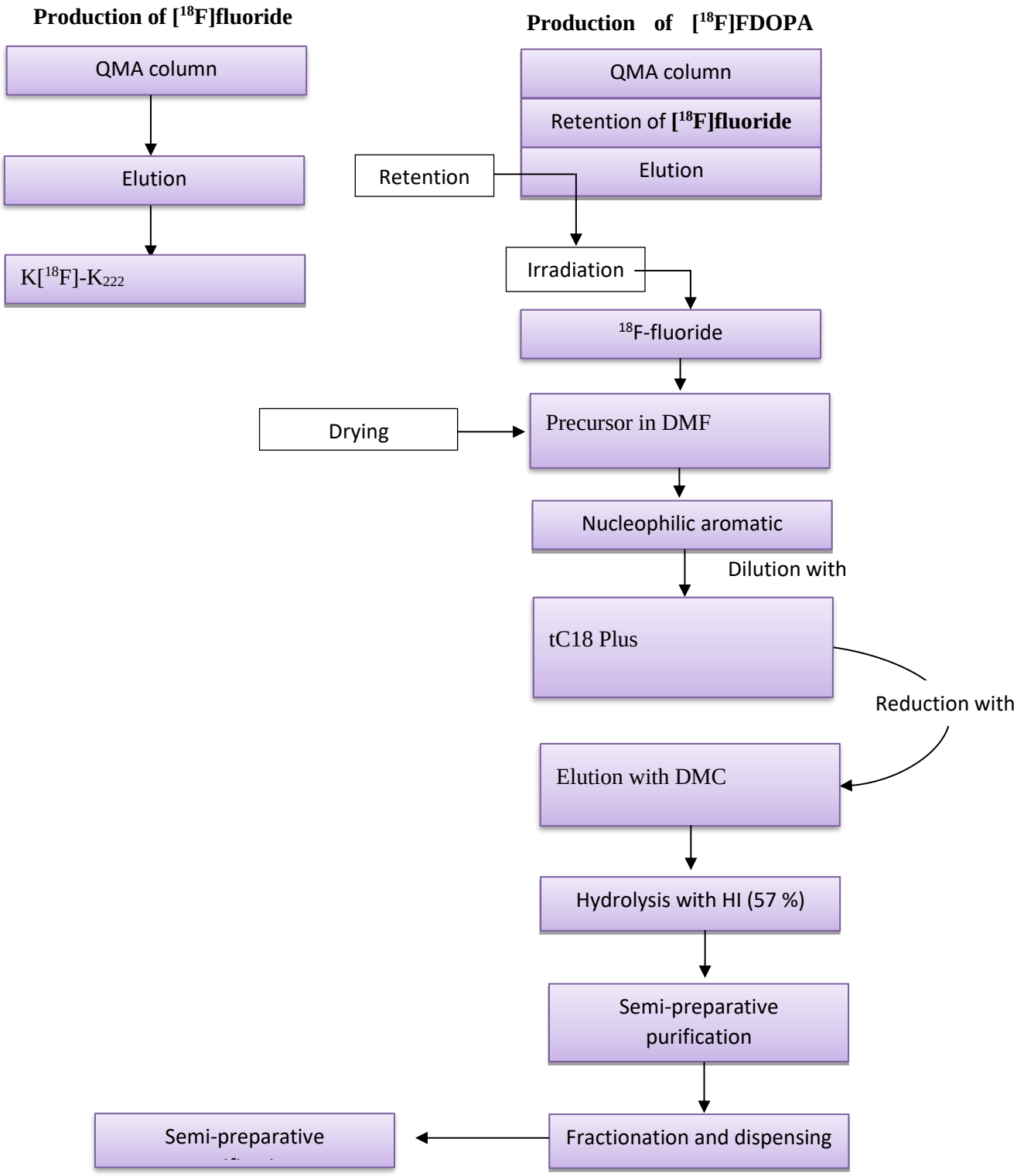

Figure 2.5: Flowchart of the 6-[^{18}F]FDOPA **2.1** production.

The reagents kits and cassettes were supplied by Trasis (**Figure 2.6**, **a** and **b**). Additionally, two bags of water for injectables (WFI), bulk vial for dilution and a Theodorico kit W (**Figure 2.6, c**) were also needed.

a) **b)** **c)**

Figure 2.6: Consumables necessary to produce [^{18}F]FDOPA: **a**) disposable cassette for [^{18}F]FDOPA synthesis; **b**) reagent kits and water for injections; **c**) theodorico disposable kit.

In the automated synthesis module, the process starts with the selection of the method for [^{18}F]FDOPA**.** After initiation, the script starts by testing the module (vacuum, pressure, valve rotation and syringe actuation) to ensure that all is working correctly.

In parallel, the cyclotron starts with the irradiation of [^{18}O]H_2O using the IBA Cyclone® 18/9 or the KIUBE® to produce the [^{18}F]fluoride.

The cassette is installed, and all the valves, heaters and cassette connections are tested. After, reagents and mobile phase for the semi-preparative HPLC are installed. Then, the following preliminary steps are performed:

i. the alkylation vial, which contains the PTC and the Schiff's base is solubilized with DCM
ii. the tC18 cartridge is conditioned with EtOH and WFI; after, the entire manifold is flushed and purged with inert gas high flow, to be sure that there is not any liquid in the manifold
iii. the lines of the HPLC eluents are purged.

After these preliminary steps, the module is ready to receive the activity.

After receiving the activity, the entire process runs in an automated way, according to the script (**Figure 2.3, b**). The only operator action is the collection of the [^{18}F]FDOPA **2.1** peak, during the semi-preparative purification. Column used was a Sunfire Prep C18, 5 µm, 10x250 mm using as mobile phase a solution containing acetic acid, sodium acetate titriplex III and ascorbic acid, at 5 mL/min.

In **Figure 2.7** we present a sample chromatogram of the semi-preparative of the [^{18}F]FDOPA **2.1** production.

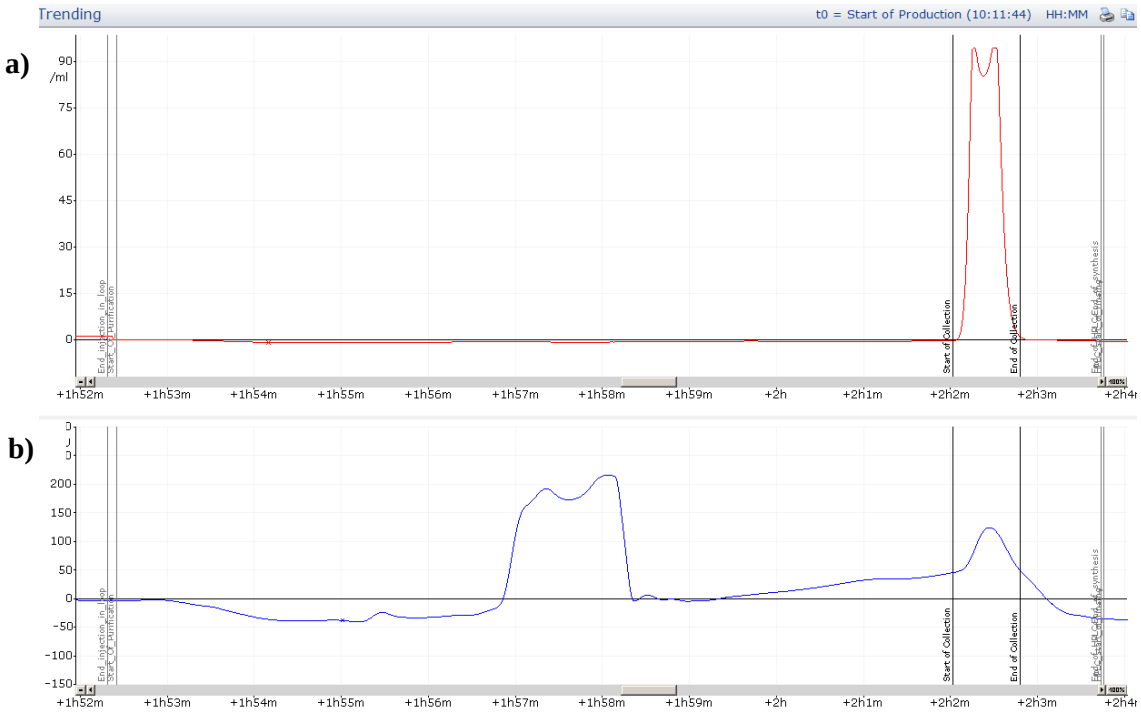

Figure 2.7: Chromatogram of the semi-preparative HPLC for [^{18}F]FDOPA **2.1**, production. **a**) Radioactivity. **b**) UV at 285 nm. Retention time (Rt) is about 10 minutes.

The retention time (Rt) for 6-[^{18}F]FDOPA**, 2.1,** is around 10 minutes. When the peak is collected, the solution is transferred to the automated fractionating module (Theodorico®) and reformulated in a citrate buffer solution. Ascorbic acid is also added as a radical scavenger to help with the stability of the final formulation. In **Chapter 5**, we describe the installation of the Theodorico kit W and how the fractionating process is performed.

At the end of synthesis, a production report is generated. In **Figure 2.8** we present a sample chart with the main variables such as pressure, vacuum and temperatures throughout all process.

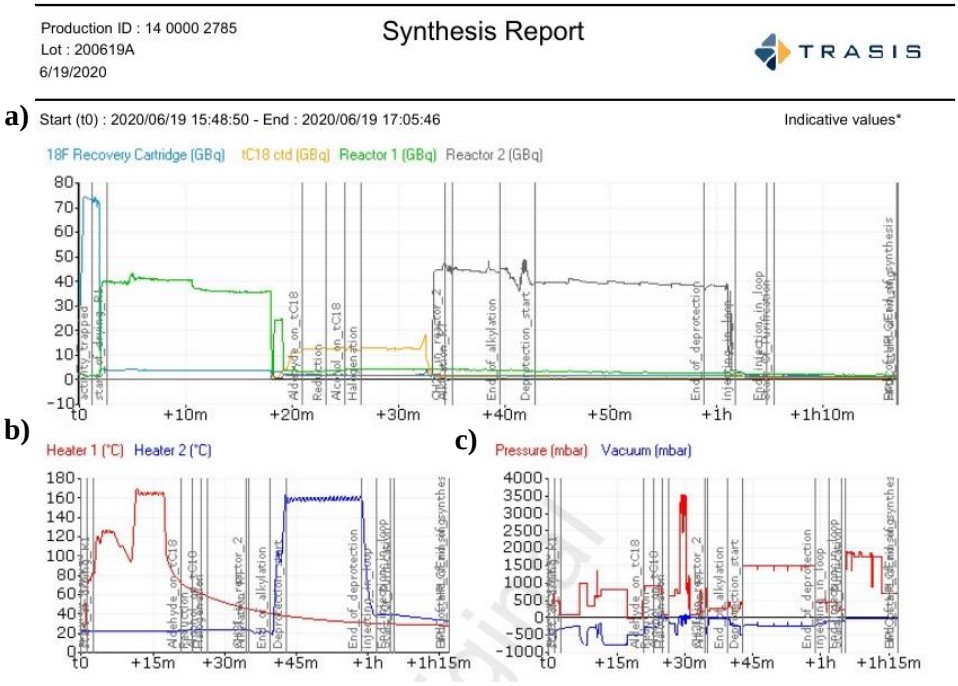

Figure 2.8: Graphs illustrative of **a**) activity, **b**) oven temperature, **c**) vacuum (blue line) and pressure (red line), during 6-[^{18}F]FDOPA, **2.1** production.

In **Figure 2.8,** graph **a),** presents the activity in different points of the synthesis, QMA (light blue line), heater 1(green line), tC18 cartridge (orange line) and at heater 2 (black line). This allows us to follow the activity during the process and observe if everything is running as normal. The same happens with graphs of **b)** temperatures and **c)** pressure and vacuum**.**

2.3.1 Production Validation

To obtain the authorization to produce 6-[^{18}F]FDOPA, the company had to produce the radiopharmaceutical according the already stated procedures, in order to obtain the product with the required quality.

The validation process was divided into 4 main parts:

- Test the production procedure and the quality control tests
- Execution of 3 full production runs including quality control.
- Stability tests
- Documentation to submit to authorities.

The first step was the tests of production, fractioning and quality control tests, to define the procedures of production and quality control. Then, Standard Operating Procedures (SOPs) were written for production, and quality control.

The production SOP is a guide to the operator, in which all the necessary steps to perform the production of [^{18}F]FDOPA**,** including fractioning and documentation, are described. All these steps are detailed in **Chapter 5.**

In the SOP for quality control, we describe all the physico-chemical and microbiological analysis of the final solution of [^{18}F]FDOPA. Likewise, these tests are detailed described in **Chapter 5.**

Also, the logs, for production and quality control (discussed in the next section) were produced. During production the log registers all the relevant production data, from the production of the radionuclide to the final verification of labels.

The document must include the following information:

- Production number
- Batch
- Date and time of production
- Data relative to radionuclide production at cyclotron, target, $H_2{}^{18}O$ batch and expire date, intensity of current, irradiation time
- Activity and time of end of bombardment (EOB), as well as activity and time of EOS, RCY, batch volume, calibration time and expiry time
- Registration of visual inspection of module conditions, gas, pressure, cassette, reagents, ancillaries, or line clearance
- Batch numbers of HPLC semi-preparative column, mobile phase, cassette, and all the reagents necessary to perform the synthesis and dispensing
- Bubble point test
- In process controls, production chart and temperature log
- Batch size, number of vials, internal and external
- External packaging, lead pot, box, and seal.

For validation process, three production runs in three consecutive days were performed. In **Table 2.1**, we present the data relative to the first step, the radionuclide production on the cyclotron.

Table 2.1: Data regarding radionuclide production on the cyclotron.

Batch	FDOPA_6	FDOPA_7	FDOPA_8
Irradiation time (hour)	0.26	0.3	0.4
Current at target (µA)	49.2	56	44
Integrated current (µA.h)	12.8	16.8	17.6

[^{18}F]fluoride is produced as described above. Irradiation time is adapted according to the clinical needs for each day. For validation batches, the irradiation times were 16, 18 and 22 minutes.

Considering the reformulation solution, citrate buffer and the 5 mL collected from the semi-preparative the final volume is 25 mL. The maximum limit for the volume in a vial is 10 mL. This is also the maximum volume of solution injectable per day.

In **Table 2.2** we present the activities at end of bombardment (EOB) and at end of synthesis (EOS), as well as the radiochemical yields obtained for the validation batches.

Table 2.2: Production data for validation batches of [^{18}F]FDOPA, **2.1**.

Batch	FDOPA_6	FDOPA_7	FDOPA_8
Activity EOB (GBq)	28	37	58
Activity at EOS (GBq)	5.3	15.4	16.6
RCY* (%)	19.0	41.5	28.6

EOB: end of bombardment; EOS: end of synthesis; RCY: radiochemical yield. *non decay corrected (ndc).

RCY's, non-decay corrected (ndc) obtained were 29.7 ± 9.2 % (n=3), with a total synthesis time of 90 minutes.

Fractioning and dispensing of the 6-[^{18}F]FDOPA solution was performed using an automated robotic arm (Theodorico®, Comecer). For the validation batches, 5 vials were dispensed: 4 with 0.5 mL; one retention vial; one to perform the bacterial endotoxins test; one for sterility and one for quality control at t0; and one with 10mL for quality control after 12 hours (stability test).

The detailed procedure for dispensing is described in **Chapter 5**. **Figure 2.9** shows the core section of the robotic dispensing system.

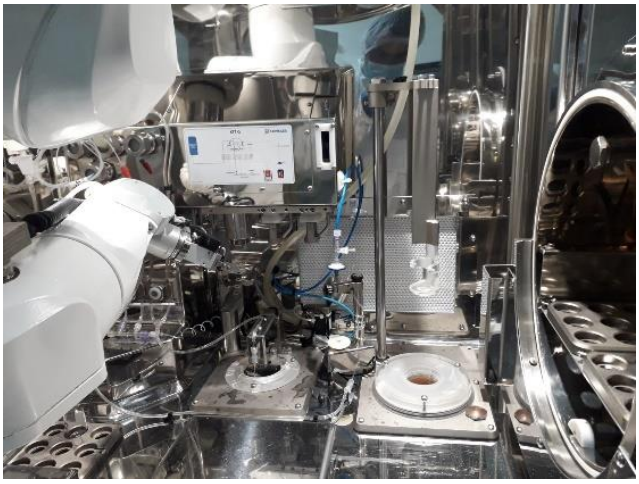

Figure 2.9: Theodorico® robotic arm, performing fractioning and dispensing.

To confirm the integrity of the sterile filter, a bubble point test is performed before and after the fractioning process. This test is performed by bubbling a needle located after the filter, inside of a vial with NaCl 0.9 %. The pressure of the inert gas passed through the filter is increased until bubbling starts. The pressure at this point is registered at the production log.

2.3.2 Quality Control

Quality control analytical procedures for [^{18}F]FDOPA, are performed according to the specifications of the monograph 04/2019:2481, Fluorodopa (^{18}F) (Prepared by nucleophilic substitution) [180], of the European Pharmacopoeia (Eur. Ph.).

According to this monograph, the product is defined as: "*Sterile solution of (2S)-2-amino-3-(2-[^{18}F]fluoro-4,5-dihydroxiphenyl)propanoic acid (6-[^{18}F]fluorodopa. It may contain stabilisers such as ascorbic acid or edetic acid(….) Content: - fluorine-18: 90 per cent to 110 per cent of the declared fluorine-18 radioactivity at the date and time stated on the label; - 6-fluorolevodopa: maximum 0.1 mg per maximum recommended dose in mililitres*"[180].

The quality control log must include:

- Tests to be performed
- Method by which the tests are to be performed
- Specifications
- Results.

An SOP for Quality Control was produced to guide the operators on how to perform the physical-chemical tests.

In **Table 2.3** we present the tests, methods, and specifications for Quality Control of the 6-[^{18}F]FDOPA solution.

Table 2.3: Quality control tests, methods and specifications for the [^{18}F]FDOPA solution.

Tests	Specifications
Appearance	Clear, colorless solution
pH after dilution	4.0 to 5.5
Aminopolyether (Kryptofix)	≤ 2.2 mg/10 mL
Total peak area of 6-fluoro-*L*-dopa	≤ 0.1 mg/10mL
Impurity D (*D*,*L*-DOPA)	≤ 0.1 mg/10mL
Impurity E (6-hydroxy-*DL*-dopa)	≤ 0.05 mg/mL
Any unspecified impurity	≤ 0.1 mg/mL
Total impurities	≤ 0.5 mg/10mL
Identification	Rt of major peak corresponds to the Rt of *L*-DOPA reference standard
Identification	Rt of major peak corresponds to the Rt of *L*-DOPA reference standard
Total peak area of 6-[^{18}F]fluoro-*L*-DOPA	≥ 95 %
^{18}F-Fluorine in the form of fluoride of 6-[^{18}F]fluoro-*L*-DOPA (Impurity I)	≤ 5 %
Total peak area of 6-[^{18}F]fluoro-*L*-DOPA	≥ 96 %
Total peak area of 6-[^{18}F]fluoro-D-DOPA	≤ 5 %
Radionuclidic identification - Energy photons ϒ	The only gamma photons have energy of 0.511MeV. A sum peak of 1.022 MeV may be observed
Half-life	105 to 115 min
Total radioactivity due to radionuclidic impurities*	≤ 0.1 %
Ethanol	≤ 2500 mg/10mL
DCM	≤ 6.0 mg/10mL
DMF	≤ 8.8 mg/10mL
Sterility*	No evidence of microbial growth should be found
Bacterial endotoxins*	≤ 175 IU/10mL

*According to Ph. Eur., these tests are carried out after batch release for use.

pH is measured using a pH meter or with pH strips and must be between 4.0-5.5 [180]. The values obtained in the three validations batches were 4.1, 4.2 and 4.0. A low pH is important to keep the molecule in the formulation.

The presence of Kryptofix$_{222}$ in the final solution is determined by TLC spot method. The detection of this impurity is very critical due to its low LD_{50} of 35 mg/Kg. This test is performed by a colorimetric semi-quantitative method by comparing the sample which a reference solution containing the limit indicated in the Eur. Ph. for Kryptofix$_{222}$ in the [^{18}F]FDOPA solution: 2.2 mg/10 mL. In **Figure 2.10** we present a plate with the Kryptofix$_{222}$ test: on the left is the spot with the reference solution (2.2 mg/10mL) and on the right is the test solution. The spot corresponding to the test solution (right) is not more intense than the spot due to the reference solution (left).

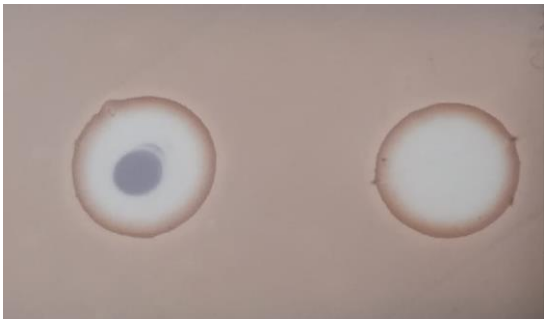

Figure 2.10: Determination of Kryptofix$_{222}$. **Left**: reference solution, **right**: test solution.

In specific case of [^{18}F]FDOPA, the presence of Kriptofix$_{222}$ is very unlikely, due to the semi-preparative purification, where only the [^{18}F]FDOPA peak is collected to the final product vial.

Chemical and radiochemical purities were determined by HPLC according to the method described in **Chapter 5**.

Before the analysis of the [^{18}F]FDOPA **2.1,** solution, a reference solution, containing the 6-fluorolevodopa (FDOPA) and the possible identified impurities, according Eur.Ph.[180], at the maximum allowed concentration, 0.1 mg/10mL of 6-fluorolevodopa (FDOPA), 0.1 mg/10 mL of (2*RS*)-2amino-3-(3,4-hydroxyphenyl)propanoic acid (*D*,*L*-DOPA, **2.14**) (**impurity D**, according Eur. Ph.) and 0.05 mg/10mL of (2*RS*)-2amino-3-(2,4,5-trihydroxyphenyl)propanoic acid (6-hidroxy-*D*,*L*-DOPA, **2.15**) (**impurity E**, according Eur. Ph.) are injected. In **Figure 2.11** we present a chromatogram of the reference solution.

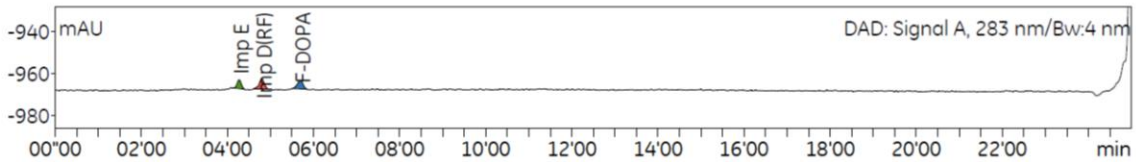

Figure 2.11: HPLC Chromatogram of reference solution containing the maximum allowed concentration of impurity E (**2.14**), impurity D (**2.15**) and FDOPA. Mobile phase of trifluoroacetic acid 1.22 g/L and acetonitrile, at 1mL/min. λ at 283nm. Column Xterra RP18 is used as stationary phase.

Retention times for impurities E, D and FDOPA are 4.00, 4.28 and 4.93 minutes, , and the peak area is 2.41, 154.51 and 128.96 mAU*1000, respectively. The peak areas for the [^{18}F]FDOPA solution must be lower that the peak area for the reference solution. In **Figure 2.12** we present an example of a chromatogram for the final [^{18}F]FDOPA solution.

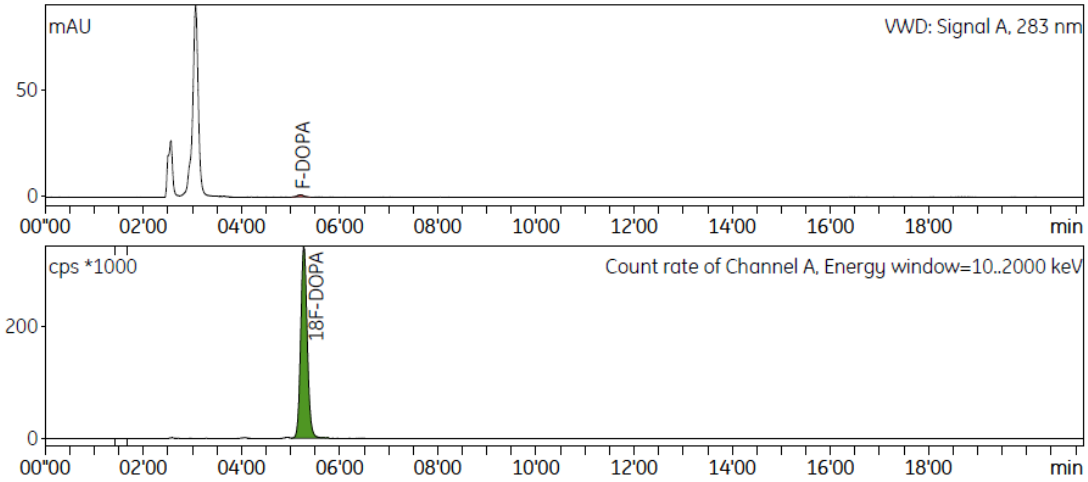

Figure 2.12: Chromatogram of a [^{18}F]FDOPA solution. Mobile phase of trifluoroacetic acid 1.22 g/L and acetonitrile, at 1mL/min. λ at 283nm. Column Xterra RP18.

The two peaks observed between 2 and 4 minutes in the UV chromatogram, are derived from the buffer. In **Figure 2.13** we present the chromatogram obtained by injecting the buffer.

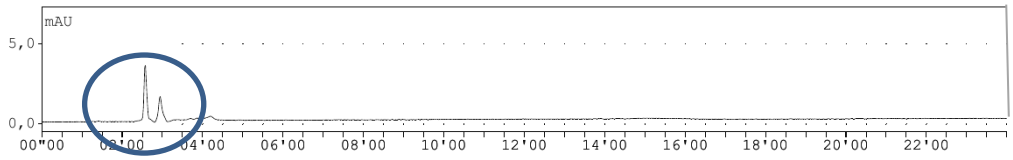

Figure 2.13: Chromatogram for the buffer. Mobile phase of trifluoroacetic acid 1.22 g/L and acetonitrile, at 1mL/min. λ at 283nm. Column Xterra RP18.

In **Figure 2.14** we present the structures of the impurities *D* and *E*. As we can observe from the chemical structure of the molecule **2.14**, and **2.15**, they may result from the presence of water in the solution. The molecule **2.15** can result from a nucleophilic substitution in which the OH group acts as nucleophile. **2.14** can result from the elimination of a water molecule which can occurs in acidic medium if molecule **2.15** is present.

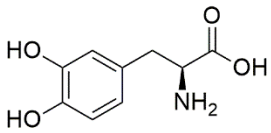

D,*L*-DOPA, **2.14**
Impurity D

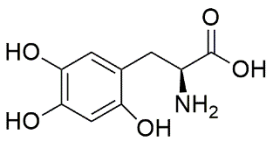

6-hydroxy-*D*,*L*-DOPA, **2.15**
Impurity E

Figure 2.14: *D*,*L*-DOPA, **2.14** and 6-hydroxy-*D*,*L*-DOPA, **2.15**.

Usually, none of these impurities were detected in the chromatogram of the final [^{18}F]FDOPA solution (**Figure 2.12**), which means that the product is according to the required specifications.

Radiochemical purity (RCP) is determined by comparing the main peak in the radiochromatogram with all other peaks. As an example, in the radiochromatogram presented in **Figure 2.12** the RCP was 99.8 %.

Another impurity which can be present, according to Eur. Ph., is the [^{18}F]fluoride, which must be lower than 5 % of the total radioactivity. The detection is performed by thin-layer chromatography. In all batches, [^{18}F]fluoride was lower than 1 %. In **Figure 2.15** we present an example of a radio-TLC for this test.

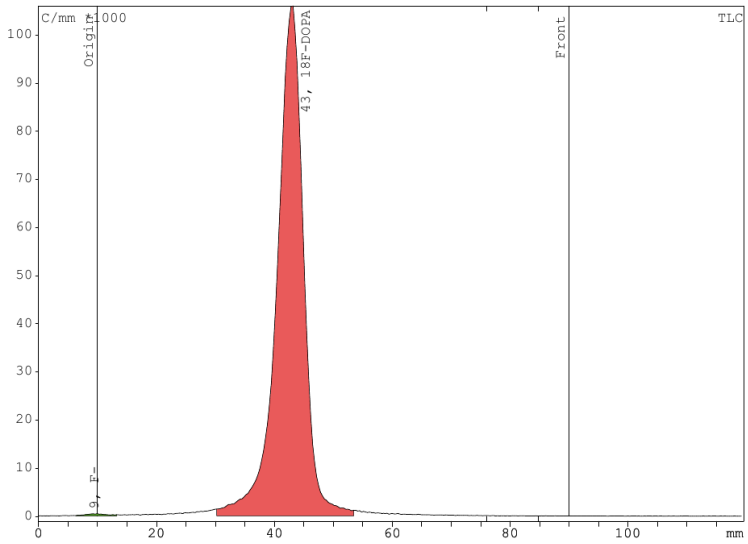

Figure 2.15: Radio-TLC of the final 6-[^{18}F]FDOPA solution. TLC was performed with TLC silica gel 60 plates. Rf [^{18}F]F^{-} = 9.30 mm, Rf 6-[^{18}F]FDOPA = 42.86 mm.

The enantiomeric purity was also determined. 6-[^{18}F]FDOPA can be present in two different conformations: *D* or *L*-enantiomer. The *D*-isomer of 6-[^{18}F]FDOPA **2.1** presents low affinity for blood-brain barrier amino acid transporters, so, the enantiomeric purity is essential for PET imaging [150]. The enantiomeric purity is determined by HPLC using a chiral column as stationary phase. The column is composed by silica modified with chiral crown ethers. This column presents good performances when the compounds have a primary amino groups near the chiral centre, such as amino acids [240]. The chiral separation results by the formation of a complex between the crown ether and ammonium ion (-NH_3), under acidic conditions. With CROWNPAK® CR(+) the *D*-form of aminoacids always elutes at the first position. The mobile phase is a perchloric acid 2.9 g/L. Before the analysis of the 6-[^{18}F]FDOPA solution, a mixture of both (*D*) and (*L*) enantiomers was injected to assure that the method maintain the separation performance. In **Figure 2.16** we present the chromatogram of the racemic mixture injection.

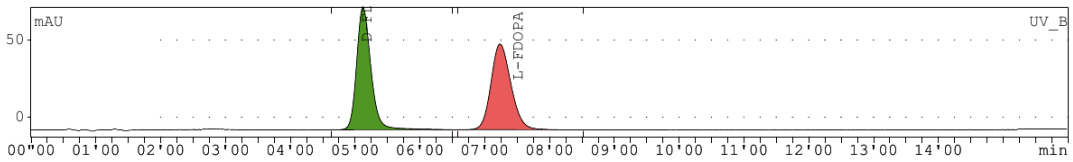

Figure 2.16: Reference solution of *D*,*L*-DOPA. Mobile phase: isocratic, perchloric acid, 2.9 g/ at 1mL/min, λ of 283 nm. Chiral column Crownpack CR (+).

In **Figure 2.17** we present a chiral chromatogram obtained with the 6-[^{18}F]FDOPA final solution.

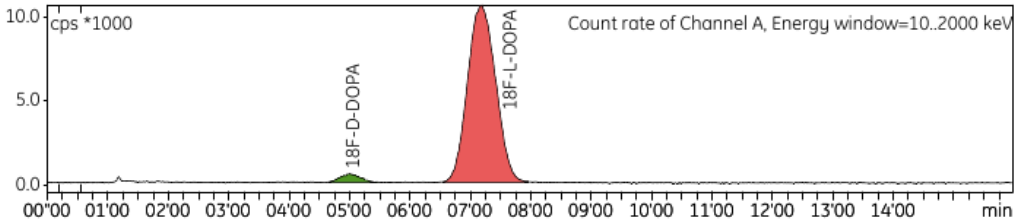

Figure 2.17: Chiral chromatogram of the 6-[^{18}F]FDOPA final solution. Mobile phase: isocratic, perchloric acid, 2.9 g/ at 1mL/min, λ of 283 nm. Chiral column Crownpack CR(+).

The values of the *L*-enantiomer were always higher than 96 %. In **Figure 2.18** we present the results of, RCY, RCP and percentage of *L*-enantiomer for the validation batches of 6-[^{18}F]FDOPA, using the Trasis module.

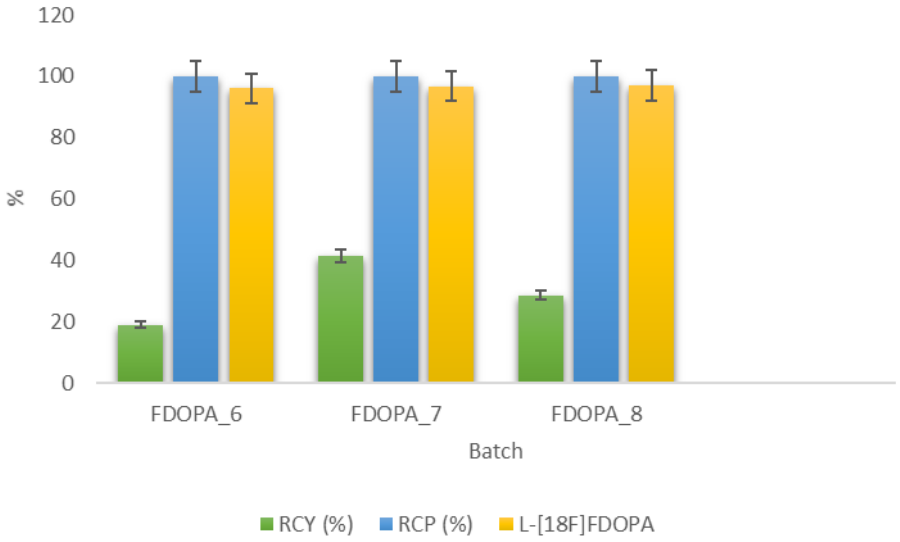

Figure 2.18: Results obtained with the [^{18}F]FDOPA process using the Trasis AllinOne module (n=3). Radiochemical Yield (RCY), radiochemical purity (RCP) and *L*-enantiomer percentage.

RCY's of 29.7 ± 9.3 %, RCP's of 100.00 ± 0.09 % and a percentages of *L*-enantiomer of 96.6 ± 0.4 % were obtained.

Radionuclidic impurities can arise from the target irradiation ([^{18}O]H_2O or target walls) and, consequently, be transferred with the target solution to the hot cell in the chemistry laboratory. To avoid these contaminants, the solution is passed through a QMA Sep-Pack cartridge where most (or all) of them are eliminated.

To test the radionuclidic purity three different analyses are performed. The half-life is determined using a dose calibrator (ISOMED 2010) and the result must be between 105 and 115 minutes. The half-life of ^{18}F is 109.8 minutes and an error of 5 % is considered. The results for

the half-life of 6-[^{18}F]FDOPA solution regarding the three validation batches are within the specifications.

The other tests are a gamma-ray spectrum, using a High Purity Germanium (HPGe) detector, at EOS and another 24 hours later, to ensure that there are no other radionuclides with longer half-life that could be shadowed by the high ^{18}F activity at EOS.

In the first spectrum, obtained at EOS, the 0.511 MeV photons from the annihilation radiation dominate and a sum peak of 1.022 MeV may be observed. If any other peak is observed, it should be lower than 0.1 % of the total radioactivity. At the second spectrum, no peaks should be observed. In **Figure 2.19**, we present a sample spectrum for the final solution of 6-[^{18}F]FDOPA.

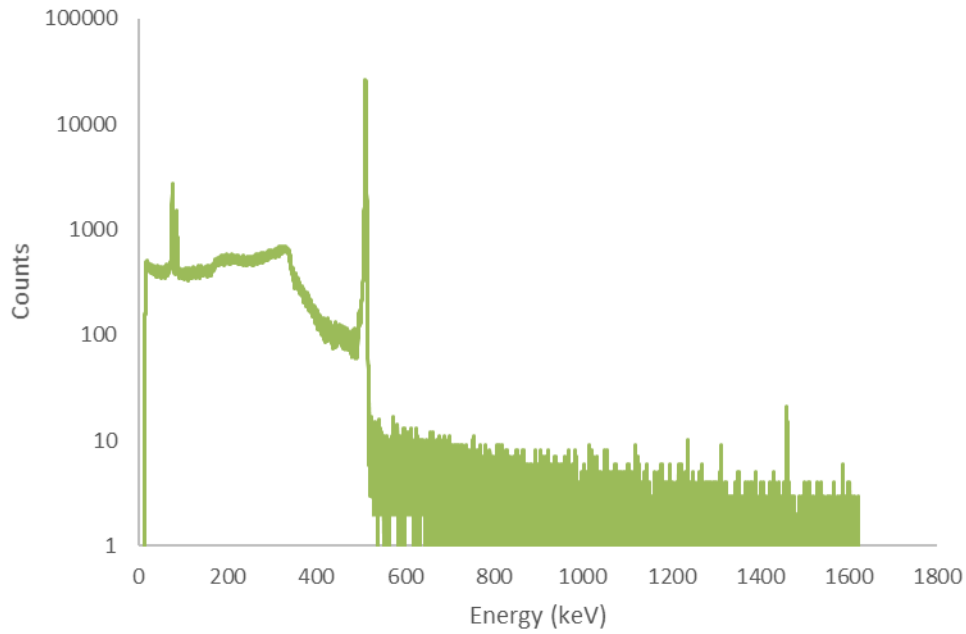

Figure 2.19: Gamma-ray spectrum of 6-[^{18}F]FDOPA solution, by HPGe, at end of synthesis (EOS).

During the synthesis process for 6-[^{18}F]FDOPA**,** some solvents, such as DMF, dichloromethane and ethanol are used, which have to be monitored to guarantee the safety of the patient. This analysis is performed by gas chromatography. Firstly, we inject a reference solution containing the solvents that can be present in test solution, at the maximum allowed concentrations. According to the monograph 04/2019:2481[180] of Eur. Ph. the limit for residual solvent ethanol is 2500 mg/10 mL, maximum 10 % V/V, 2.5 mg per administration taking density to be 0.790 g/mL, being 10 mL the maximum volume administered per day. The limits for the other residual solvents, DMF and DCM are described in the general chapter, "Residual Solvents"[231] of Eur. Ph.. According to this general chapter, the residual solvents are divided into

3 classes, 1, 2 and 3, *"solvents to be avoid"*, *"solvents to be limited"* and *"solvents with low toxicity"*, respectively. DMF and DCM both belongs to class 2 solvents and their limits are 6 and 8 mg/10mL, respectively.

In **Table 2.4** we present the results obtained for residual solvents in the 3 validation batches.

In all the validation batches, the residual solvents, are within the limits. Furthermore, the quantities detected are very low. Ethanol is used to condition the tC18 column, DCM is used as solvent in the alkylation step and DMF is the solvent where the precursor is dissolved. The multistep process and the semi-preparative purification allow for the use of this solvents without compromising the quality of the final product.

Table 2.4: Results for residual solvents in the 3 validation batches.

Residual solvents (mg /10 mL)	**FDOPA_7**	**FDOPA_8**	**FDOPA_9**
Ethanol	3.8	2.4	2.4
DCM	0.1	0.1	0.0
DMF	0.1	0.2	0.2

6-[^{18}F]FDOPA**,** as injectable solution, is a sterile product and is subjected to special requirements to minimize the risk of microbiological and of particulate and pyrogen contaminations. At ICNAS-P, 6-[^{18}F]FDOPA solution is prepared using an aseptic process. This process has to comply with several requirements related to personnel, premises, equipment's, sanitation, and processing [34]. As the product is a radiopharmaceutical, a parametric release is performed, meaning that the sterility and bacterial endotoxins tests are performed after the release of the product. This is only possible because a validation of aseptic process was previously performed and, it's well stablished, that if all the instructions were followed, the product should be sterile.

When all the activity decays, a sample of each 6-[^{18}F]FDOPA batch is sent to an external laboratory to be tested for sterility.

IU/Bacterial endotoxins test is performed using a spectrometer and the endotoxins must be lower than 175 IU/10mL.

To study the stability of the 6-[^{18}F]FDOPA solution, all the quality control testes are performed after 12 hours and the results have to be maintained according to specifications. Based in this results, the expire time for 6-[^{18}F]FDOPA was set to 12 hours after EOS.

This method was reproducible, and all the batches were according to the specifications of quality control.

2.3.3 Molar activity (A_m)

As mentioned previously, A_m of the 6-[^{18}F]FDOPA solution is an important issue because of its use is oncology [170]. Low molar activities could produce pharmacological effects such as carcinoid crisis by local conversion of 6-[^{18}F]FDOPA to noradrenaline, promoted by the aromatic acid decarboxylase and dopamine β-hydroxylase enzymes, in the tumor tissue [170].

Although this parameter is not included in the quality control tests, it is calculated periodically to assure that its levels are appropriate according to the intended use.

A_m is calculated by HPLC through a calibration curve given by the concentration as a function of the peak area. Several solutions of know concentrations are prepared and injected to obtain a line, by which the concentration of 6-[^{18}F]DOPA is determined. **Figure 2.20** depicts the calibration line obtained to determine the A_m of 6-[^{18}F]FDOPA.

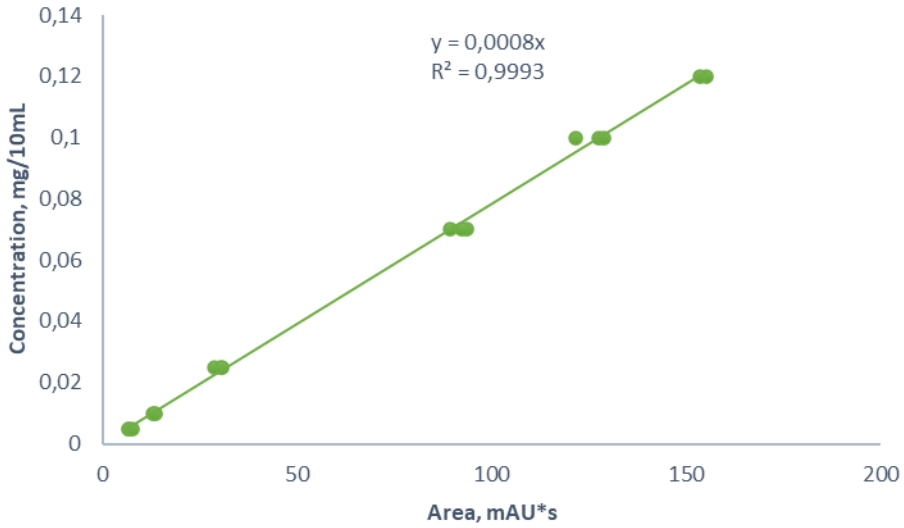

Figure 2.20: Calibration line used to calculate A_m of 6-[^{18}F]FDOPA.

Molar activity is given by the reason between activity and the number of moles, in GBq/µmol, and it is calculated at EOS. However, as we can observe from **Figure 2.12**, most of the time the peak of FDOPA is not detectable by the UV/vis sensor, which means that it is very low and, consequently, the A_m, is very high. The A_m obtained at ICNAS-P (for n=4) is of 467.10 ± 67.32 GBq/µmol.

Considering the results presented, not only in quality control, but also in production, it's clear that this process is substantially better than the first one, (ABX). With this method, we can perform several patient studies internally and eventually distribute to nearby hospitals. However,

the complexity of process and the low RCY's of 29.7 ± 9.2 % (n=3), make it a very expensive process and limit the number of patient doses produced in each run.

Keeping this in mind, one of the main goals of this PhD work was the improvement of the 6-[^{18}F]FDOPA synthesis in two ways: by developing a new synthesis process starting from a new precursor which could allow the radiosynthesis of 6-[^{18}F]FDOPA in three main steps, drying [^{18}F]fluoride, ^{18}F-fluorination and hydrolysis and by using microwave-heating in key steps of the process.

2.4 Synthesis of a nitro-*L*-DOPA precursor by asymmetric alkylation

Asymmetric phase-transfer catalytic alkylation, using chiral quaternary ammonium salts as phase-transfer catalyst, such as **2.12** and **2.13**, is widely used for the asymmetric synthesis of non-proteinogenic amino acids [86,234]. This synthetic strategy has been extensively used due to its enormous advantages such as: i) the economy of the catalyst and reagents; ii) the reduction of the use of organic solvents; iii) separation of biphasic system which allows the recycling of catalysts; iv) the high yields and purity and; v) the simplicity of the procedures [186,234,235,241,242]. Phase-transfer catalysis allows the reaction between two reagents in two different phases, when the reaction is inhibited because the reagents cannot easily come together. The role of PTC is to transfer one of the reagents to a location where it can conveniently react with another one[243]. To perform asymmetric phase-transfer catalytic alkylation a chiral catalyst is used. Chiral quaternary ammonium salts derived from cinchona alkaloids are the most used PTC's for asymmetric transformations [186,242,244–248].

In **Figure 2.21** we present a mechanism for the symmetric alkylation of a glycine Schiff's base, proposed by Maruoka *et al.* [249].

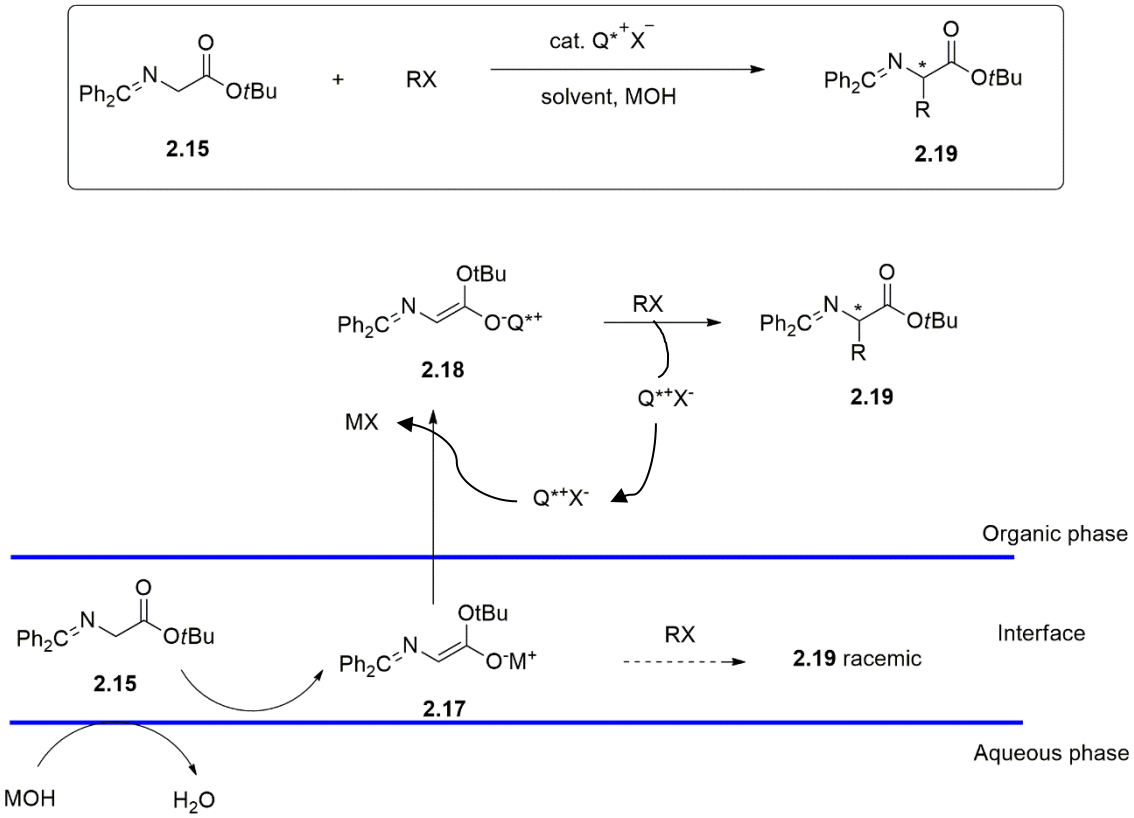

Figure 2.21: General mechanism for the symmetric alkylation of a glycine Schiff's base [249].

These reactions generally follow an interfacial mechanism. The first step of the alkylation is the interfacial deprotonation of the hydrogen of the α-carbon of the Schiff's base **2.11**, with base (MOH) to give the metal enolate **2.11a**, which is located at the interface of the two layers. Then, the ion-exchange of the anion with the catalyst ($Q^{*+}X^{-}$) generates the lipophilic chiral onium enolate **2.11b**. After this step, the enolate goes to the organic phase, to react with the RX, which in our process is the molecule **2.17**, **Scheme 2.4**, resulting the product **2.16a**.

The success of these reactions depends on the faster interaction of the chiral onium cation (Q^{*+}) to generate the highly reactive chiral onium enolate **2.11b, Figure 2.21**, through sufficiently fast ion-exchange and effective shielding of one of the two enantiotopic faces of the enolate anion. This interaction minimizes the direct alkylation of metal enolate to give the **2.16a** racemic[249].

An important issue in this type of reactions is the effect of the strongly basic conditions, which could cause decomposition of the catalyst, hydrolysis of the substrate, product racemization or dialkylation. To prevent these possible problems is mandatory to do the correct choice of the protecting groups. The structure of **2.11**, **Figure 2.21**, have a *tert*-butyl ester, as protecting group, which can resist to the saponification and the benzophenone imine moiety facilitates the initial deprotonation and protect the α proton.

Based in the Corey strategy [186], a new molecule was synthesized and characterized by Inês Fonseca and Ivanna Hrynchak, at the Laboratory of Catalysis and Fine Chemistry of University of Coimbra.

In **Scheme 2.4** we present the synthesis of (*S*)-tert-butyl-3-(4,5-dimethoxy-2-nitrophenyl)-2-((diphenylmethylene)amino)propanoate **2.16,** synthesized by phase-transfer catalytic alkylation of a glycine derivative, *N*-(diphenylmethylene)glycine tert-butyl ester (**2.11**), using *O*-allyl-*N*-(9-anthracenylmethyl)cinchonidium bromide (**2.12**) as PTC**,** according to the already described procedures [95,97,186].

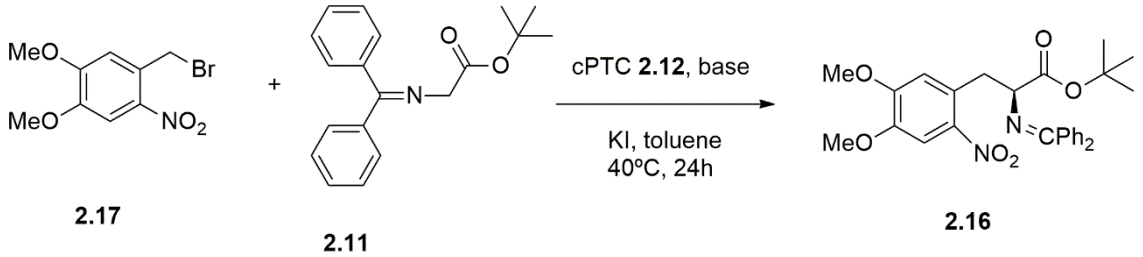

Scheme 2.4: Synthesis of nitro-*L*-DOPA precursor, **2.16**, by asymmetric phase-transfer catalytic alkylation.

In general, 4,5-dimethoxy-2-nitrobenzyl bromide, **2.17**, reacts with the Schiff's base, a glycine derivative, **2.11**, in presence of PTC **2.12** and a base in toluene. Also, the addition of potassium iodide (KI) was tested. Different **2.17**:**2.11** ratios, different bases at 9M, concentrations of reagents, and reaction times were tested, to obtain the best reaction conditions. In **Table 2.5** we present the optimizations performed. Reactions were performed according to the workup described in **Chapter 5**.

Table 2.5: Optimization of parameters in the synthesis of molecule **2.16**.

Entry	2.17:2.11 ratio[a]	Base	Volume / mL	Addition of KI	Temperature / ºC	Time / hours	Yield / %
1	1:0.8	$CsOH.H_2O$, 9M	7	No	40	24	21.7 ± 8.7 (n=2)[b]
2	1:0.8	$CsOH.H_2O$, 9M	7	Yes	40	24	35.5 ± 17.5 (n=2)[b]
3	1:0.8	$CsOH.H_2O$, 9M	7	Yes	40	48	18[b]
4	1:1.2	$CsOH.H_2O$, 9M	7	Yes	40	24	23[b]
5	1:0.8	KOH, 9M	7	Yes	40	24 50	15.8[c] 12[b]
6	1:0.8	Cs_2CO_3, 9M	7	Yes	40	24 70	2.6[c] 5.4[b]

[a] starting from 0.36 mmol of **2.17;** [b] Isolated yield; [c] Conversion by HPLC.

In the first attempts to synthesise the new precursor **2.16,** 0.36 mmol of **2.17** with 0.8 equivalents of **2.11,** in the presence of 0.06 equivalents of **2.12** and 10.6 equivalents of $CsOH.H_2O$ (9M solution) (**Table 2.5**, **Entry 1**). This mixture was stirred for 24 hours at 40ºC. At the end, the reaction was stopped, and the product was extracted with DCM, dried over Na_2SO_4 and the solvent was evaporated achieving a yellow solid in 21.7 ± 8.7 %, isolated yield (**Table 2.5, Entry 1**). The product was isolated by HPLC semi-preparative column according to the procedures described in **Chapter 5**.

In an attempt to increase the yield, 0.1 equivalents of KI were added. Because iodine (-I) is a better leaving group than bromide (-Br), the addition of KI has the purpose of changing the -Br from an -I to increase the reactivity of **2.17**. In **Table 2.5**, **Entry 2** we present the results obtained and, in fact, an increase of yield from 21.7 to 35.5 % was observed. These conditions lead to the best isolated yield obtained.

The reaction evolution was followed by analytical HPLC after 1, 3, 19 and 24 hours, using as mobile phase, a mixture of acetonitrile ACN/water and an analytical column Xterra RP18 column using an isocratic method. To perform the analysis, a sample was taken from the reaction mixture and was extracted with dichloromethane (DCM), dried over Na_2SO_4, and filtered.

An example of the evolution of reaction, by HPLC analysis, with time, is presented in **Figure 2.22**.

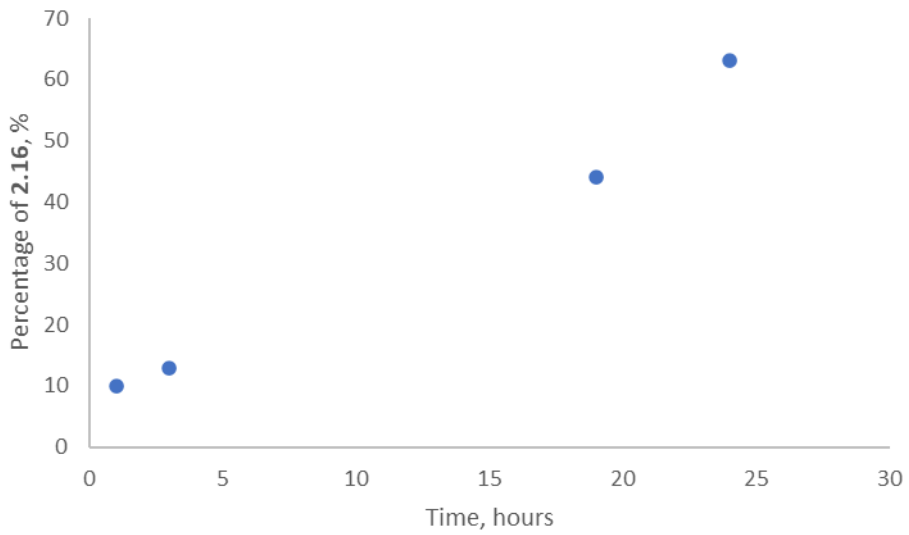

Figure 2.22: Evolution of the formation of **2.16** with time, as checked by HPLC analysis.

As it can be observed in **Figure 2.22,** the yield of conversion into **2.16** increases with time and, after 24 hours, the RCY is 63.1 %, by HPLC. A reaction in the same conditions was stirred for 48 hours (**Table 2.5**, **Entry 3**) and the isolated yield was 17 % lower than after 24 hours. This can occur due to possible degradation of the product during time, in a basic environment.

Another parameter studied was the ratio between the precursor **2.17** and the Schiff's base **2.11** (**Table 2.5**, **Entry 4**). The quantity of the Schiff's base was increased from 0.8 to 1.2 equivalents. As it can be observed, the isolated yield was reduced from 35.5 to 23 %.

Other bases already reported in literature [235,248,249], such as potassium hydroxide (KOH) and cesium carbonate ($CsCO_3$) were also tested, in the same concentration than $CsOH.H_2O$, 9M. With KOH, after 24 hours, by HPLC analysis, the conversion was only 15.8 %. The reaction was kept for 50 hours, and, at the end, the isolated yield was only 12 %, **Table 2.5 Entry 5**. $CsCO_3$ was even inferior, with a conversion of 2.6 % by HPLC after 24 hours and isolated yield of 5.4 % after 70 hours (**Table 2.5**, **Entry 6**).

In **Figure 2.23** we present an HPLC chromatogram of the reaction mixture after 24 hours. Conditions as described in **Table 2.5**, **Entry 2**.

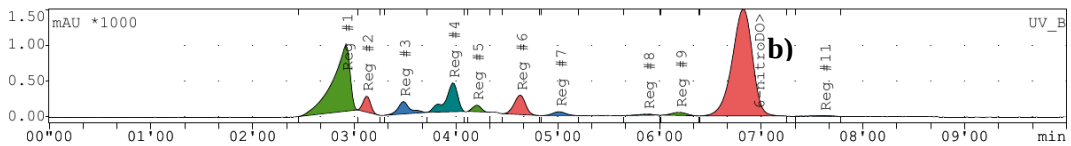

Figure 2.23: Analytical HPLC chromatogram obtained from the reaction mixture after 24 hours with conditions presented in **Table 2.5**, **Entry 2** (λ= 285 nm).

To analyze the evolution of reaction, all the reagents were injected on an HPLC using the same method. The retention times were 2.1, 2.2, two peaks at 2.3 and 2.6, 3.9, 6.0, for **2.12,** KI, $CsOH.H_2O$, **2.17**, **2.11**, respectively. The retention time of the desired product, **2.16** was 6.8. By HPLC analysis of the crude reaction after 24 hours, the product **2.16** represents 49.98 % of the total mixture, **Figure 2.23**. In **Figure 2.24** we present the chromatograms of the reagents **2.12**, **2.17**, **2.11**, KI and $CsOH.H_2O$.

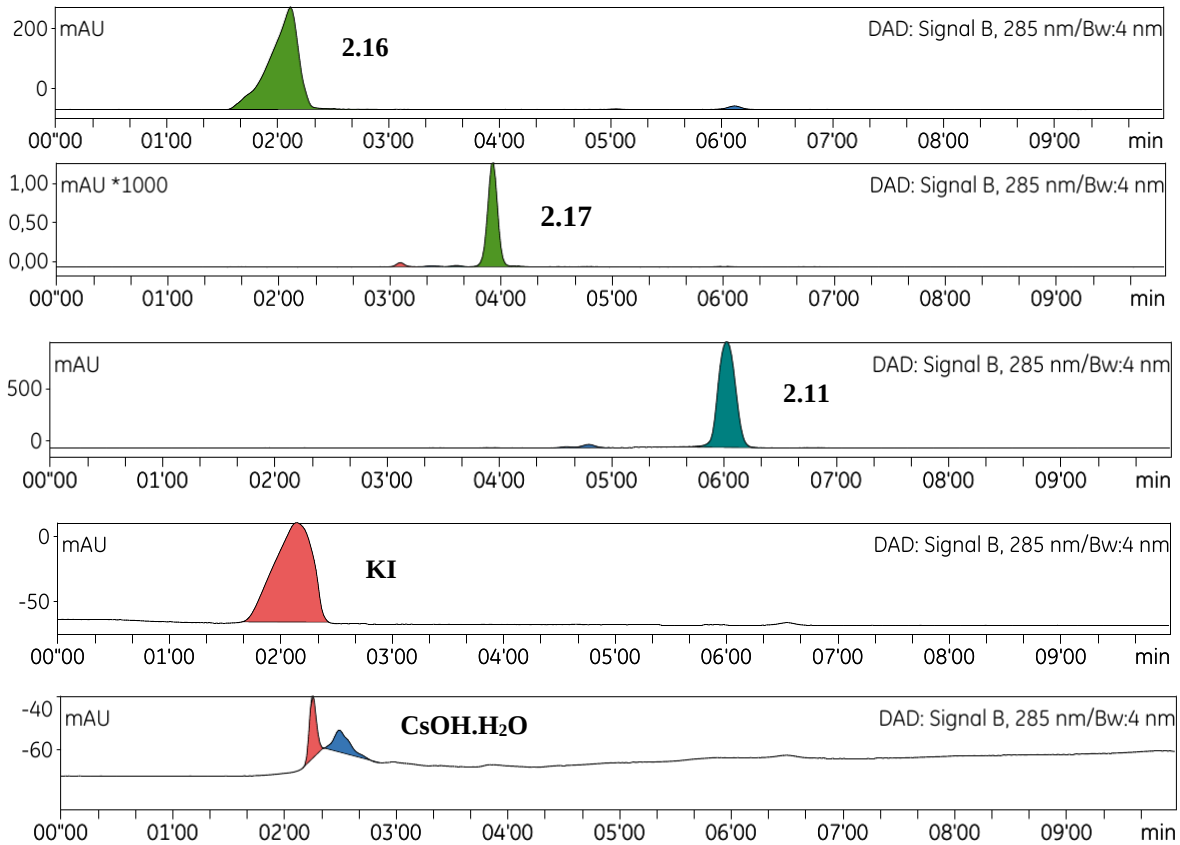

Figure 2.24: Analytical HPLC chromatograms of the reagents **2.12**, **2.17**, **2.11**, KI and $CsOH.H_2O$, respectively, used as reference for reaction control, (λ= 285 nm).

As we can observe on the chromatogram of the final reaction mixture, presented in **Figure 2.23**, a good purification method is required to isolate the product. The complex reaction mixture,

with a lot of impurities, which must be eliminated, was an additional challenge in the synthesis of this product, which was also optimized.

2.4.1 Optimization of purification conditions

To isolate **2.16**, two different chromatographic techniques were evaluated, flash chromatography, a technique available at laboratory of Catalysis & Fine Chemistry of University of Coimbra, and by semi preparative HPLC, installed at the automated synthesis module, Trasis, available at ICNAS-P.

In the first technique we used, as stationary phase, a flash column F0004-PF-C_{18}HP**.** In the second we used a semi-preparative column, Waters Sunfire Prep C18 5µm – 10 x 250 mm. Based on the analytical HPLC method, a mixture of ACN/water was used as mobile phase. To optimize the purification, different ratios and/or gradients were tested. In **Table 2.6** we present those optimizations.

Table 2.6: Optimization of purification conditions for molecule **2.16**.

Entry	Technique	Mobile phase (ratio eluent)	Elution method	Flow (mL/min)
1	Flash chromatography	ACN:H_2O (10:90)	Gradient 1	2
2	Flash chromatography	ACN:H_2O (02:98)	Gradient 2	2
3	Semi-preparative HPLC	ACN:H_2O (95:05)	Isocratic	4
4	Semi-preparative HPLC	ACN:H_2O (95:05)	Isocratic	5
5	Semi-preparative HPLC	ACN:H_2O (90:10)	Isocratic	4
6	Semi-preparative HPLC	ACN:H_2O (90:10)	Isocratic	5
7	Semi-preparative HPLC	ACN:H_2O (70:30)	Isocratic	5
8	Semi-preparative HPLC	ACN:H_2O (60:40)	Isocratic	5

* ACN – acetonitrile; flash column: F0004-PF-C_{18}HP; semi-preparative column: Waters Sunfire Prep C18 5µm – 10 x 250 mm. Gradient 1 and Gradient 2 are described in **Table 2.9.**

In **Table 2.6, Entries 1** and **2**, we present the ratios of solvent mixtures used in flash chromatography, **Gradients 1** and **2**. The first gradient starts with a ratio of 10:90 of ACN:H_2O and the second starts with a ratio of 02:98. Both with a flow of 2 mL/min. The gradients 1 and 2 we present in **Table 2.7**.

The conditions presented in **Table 2.6**, **Entries 3** to **8** are referred to the semi-preparative method.

Table 2.7: Gradients 1 and 2, tested in purification by flash chromatography.

Flash method	Time (min)	Acetonitrile (%)	Water (%)
Gradient 1	0	10	90
	30	90	10
	50	90	10
Gradient 2	0	2	98
	8	2	98
	10	5	95
	15	5	95
	20	95	5
	40	95	5
	60	100	0

Wavelength in both techniques was 285 nm.

In both gradients 1 and 2, the purification starts with a more aqueous mobile phase and is changed to a more organic (90 and 100 % of ACN). The main difference is that in the gradient 2 this change was slower to try separate better the product from the impurities.

In **Figure 2.25** we present the chromatograms for the purification obtained by flash chromatography with the gradient 1 (left) and 2 (right).

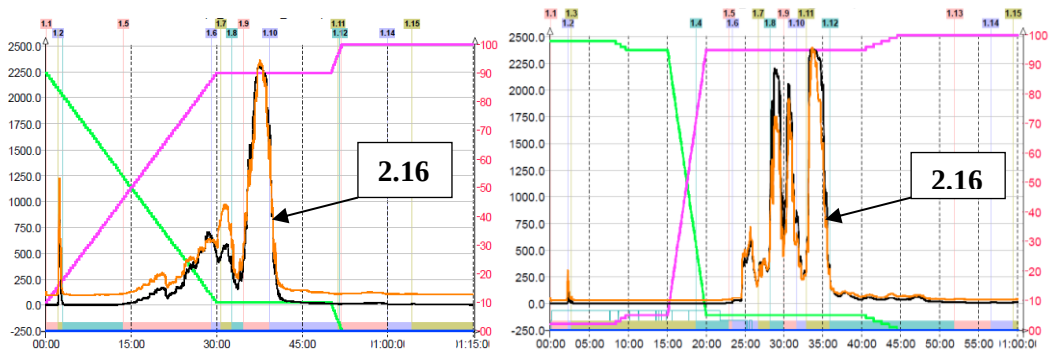

Figure 2.25: Flash chromatography gradient 1 (left) and 2 (right). The pink line represents the solvent ACN and the green H_2O. The black and orange lines are the λ between 200-800 nm, and 285 nm, respectively.

lel

with the desired purity. When the gradient 1 was used, only 70.4 % of purity was obtained. The gradient was changed to **gradient 2** (**Figure 2.25**, **right**) to try to isolate the product. Even the purity increases to 93 % was not sufficient.

As described in **Section 2.3**, in the automated synthesis of 6-[^{18}F]FDOPA **2.1**, a semipreparative purification was performed at the end of synthesis to isolate the desired product. Based on this experience this methodology was tested in the purification of the crude mixture of the synthesis of **2.16**. Different chromatographic conditions were tested and were presented in **Table 2.6**. The conditions presented in **Table 2.6, Entry 8**, gave the best separation. In **Figure 2.26** we present a chromatogram of the purification of product **2.16** by semi-preparative HPLC.

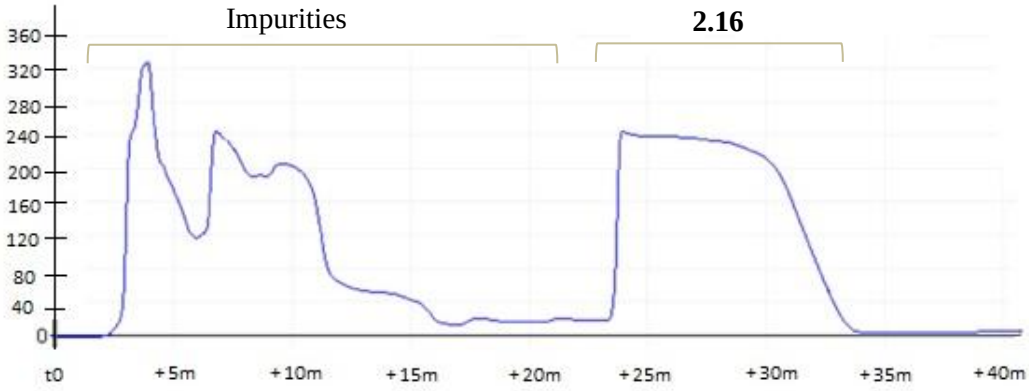

Figure 2.26: Chromatogram of the crude purification by semi-preparative HPLC, using a Sunfire Prep C18, 5 µm, 10x250 mm column, with λ = 285 nm. Chromatographic conditions presented in **Table 2.6**, **Entry 8**.

During the purification all the fractions were collected from the beginning of the purification to 36 minutes, and all were analysed by HPLC, using the same method already described in the reaction control. The fractions which chromatogram presents a percentage of

product **2.16** higher tant 98 %, were collected, generally, between the 23 and 30 minutes. In **Figure 2.27** we present the analytical chromatogram of the final product **2.16**.

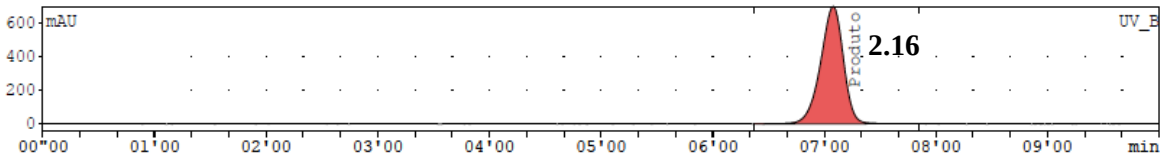

Figure 2.27: Analytical chromatogram of the final purified product **2.16**. Mobile phase: water/ acetonitrile, isocratic at 1mL/min (λ at 285nm). A column Xterra RP18 is used as stationary phase.

The selected fractions were added together, diluted in water and passed through a Sep-Pack® Plus C18 cartridge, previously activated with 10mL of ethanol and 10 mL of water. As the product **2.16** is retained, the cartridge is dried by a stream of nitrogen and is eluted after with acetonitrile. Sequentially, the solvent is evaporated and compound **2.16** is obtained as a yellow solid with 98 % of purity and 35.5 ± 17.5 % of yield, for n=2 (**Table 2.5**, **Entry 2**).

To confirm the identity of **2.16** the molecule was fully characterized.

2.4.2 Characterization of nitro-*L*-DOPA precursor, 2.16

The fully characterization of **2.16** was performed by spectroscopic techniques, described with detail in **Chapter 5**. ^{1}H-NMR, ^{13}C-NMR infrared and mass spectrometry, were used to confirm the identity of molecule **2.16**. Optical rotation and melting point were also determined.

In **Figure 2.28 a** we present the ^{1}H-NMR spectrum of the new nitro-*L*-DOPA precursor, **2.16**. By analysis of the ^{1}H-NMR spectrum, it was possible attribute each signal with the respective protons of structure of **2.16**. Protons of *t*-butyl group show their resonance as a singlet at δ 1.45 ppm, integrating a total of 9 protons. At δ 3.32 ppm 1 proton of the methylene group 7a appears as double duplet and the other, 7b appears at δ 3.76 ppm. The 3 protons of the *O*-methyl groups, 11 and 12 appear at singlets at δ 3.74 and δ 3.91, respectively. Since protons 12 are in meta position of the electron-withdrawing nitro group, the resonance appears more deshielded, when compared with 3 protons of position 11. The same influence of the nitro group is observed for the protons located at positions 6 and 3, which show their resonance at δ 6.80 and δ 7.53 as singlets. The aromatic zone is expanded in **Figure 2.28 b** from δ 7.20 to 7.65 and, the protons in that zone integrate the remaining 9 protons.

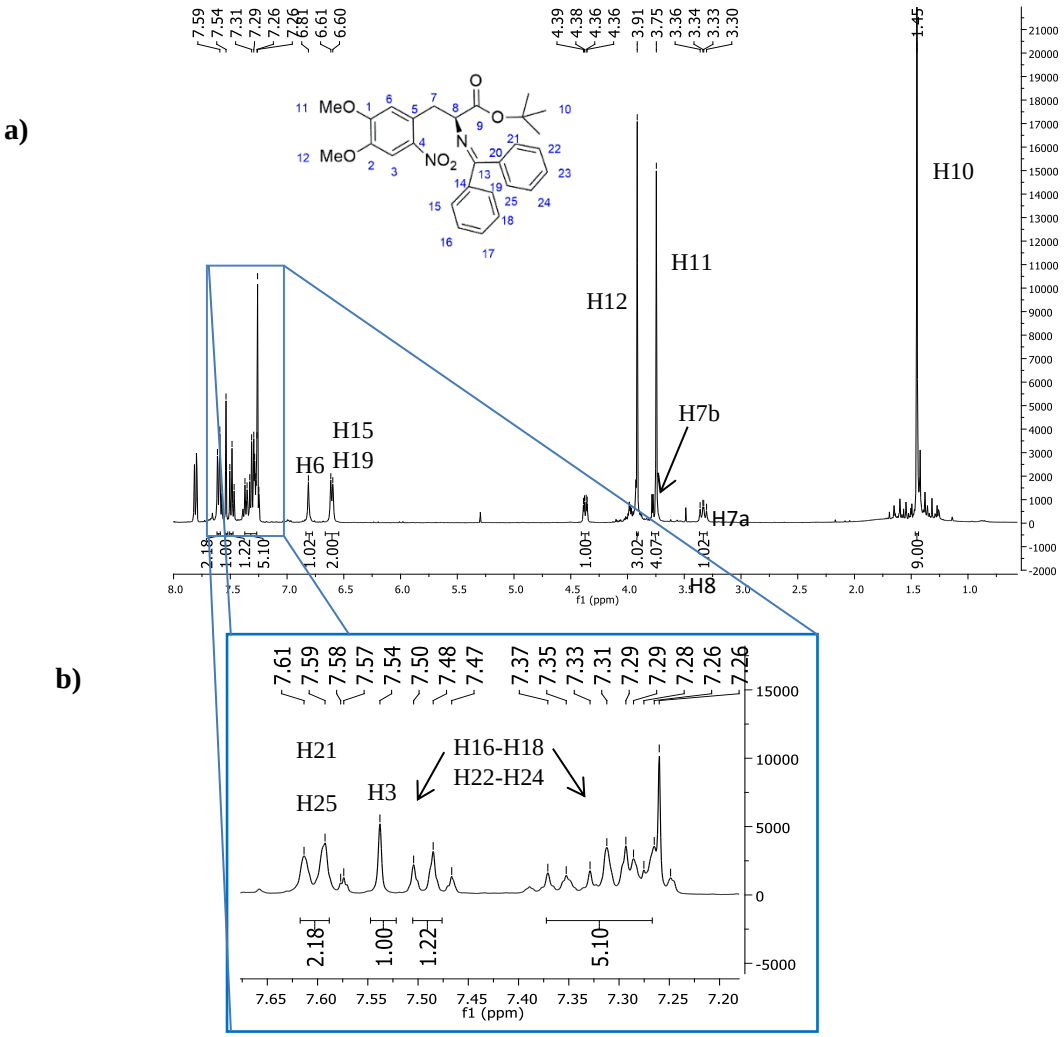

Figure 2.28: **a**) Total ^{1}H-NMR spectrum of **2.16** in $CDCl_3$; **b**) selected expansion of ^{1}H-NMR in $CDCl_3$, 400 MHz.

^{13}C-NMR was also acquired, to confirm the structure and is presented in **Figure 2.29**. Also, by this technique, all the carbons were identified and are according to the expected structure of **2.16**.

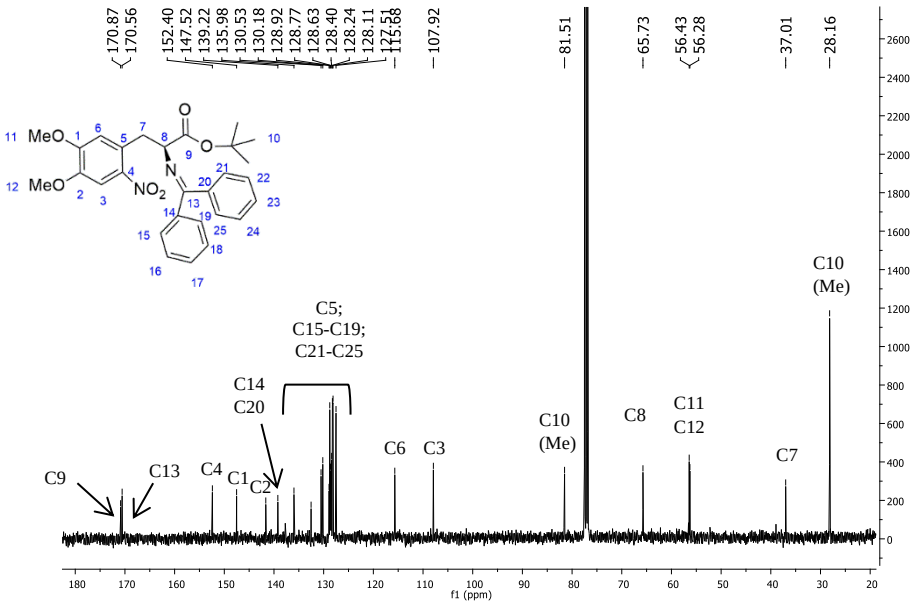

Figure 2.29: ^{13}C-NMR spectrum of **2.16** in $CDCl_3$,100 MHz.

In **Figure 2.30** we present the IR spectrum of a sample of **2.16**. The infrared (IR) spectrum obtained by Attenuated Total Reflection (ATR) shows absorbance bands at 2750, 2510, 2490, 1800, 1725, 1510 and 1225 cm^{-1}, characteristics of the bonds C-H aromatic, C-H, C=N, C=C aromatic, CN, NO and CO, respectively.

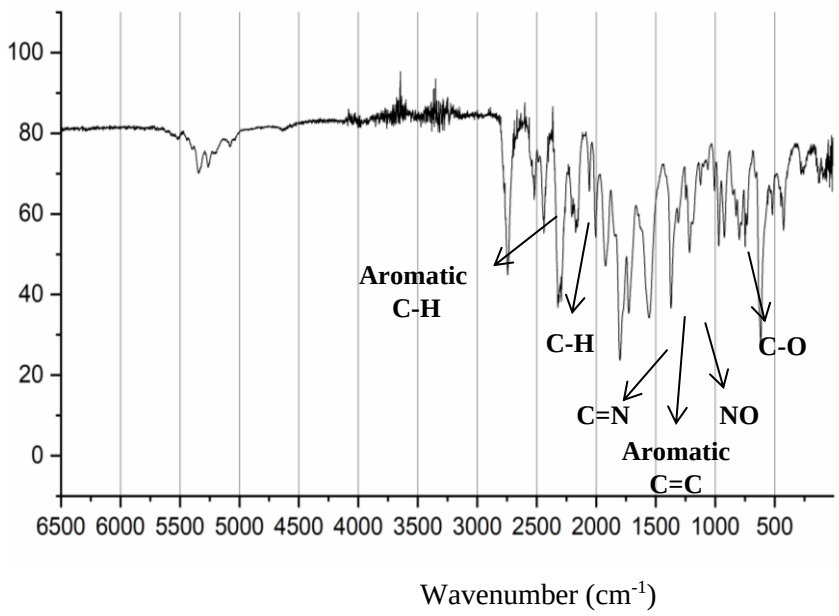

Figure 2.30: IR [ATR, cm-1] spectrum of **2.16**.

Using mass spectrometry analysis, **Figure 2.31**, the obtained mass corresponds to the ion $[M+H]^+$ and the isotopic distribution is according to the theoretically expected.

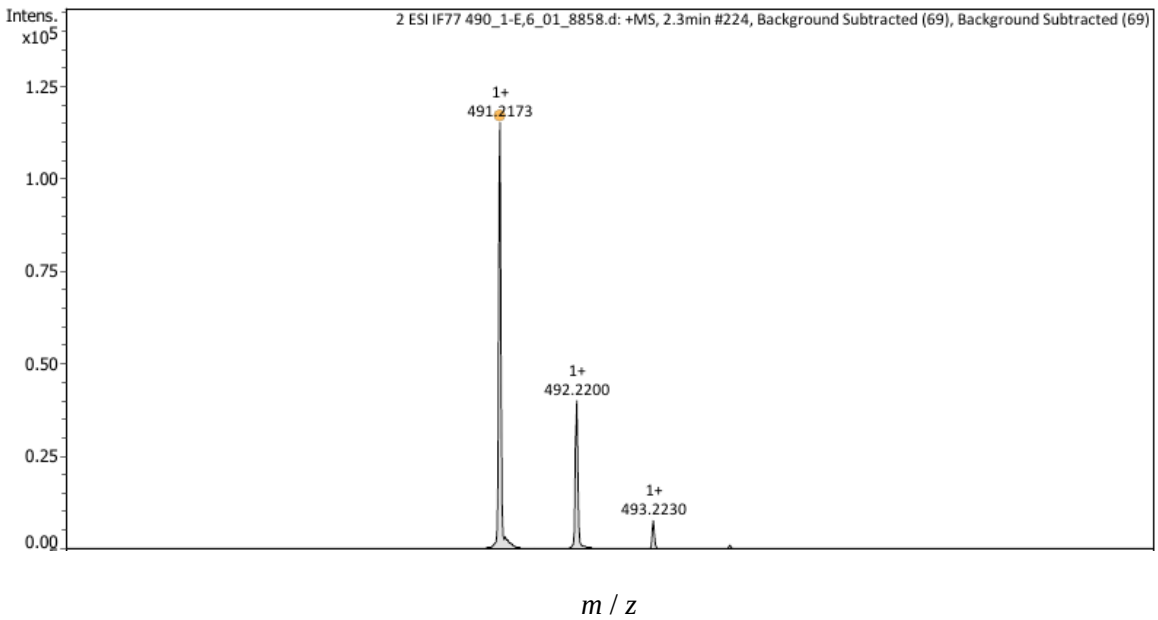

Figure 2.31: ESI mass spectrum (positive mode) of **2.16**.

After several optimizations, in the synthesis and in the purification, we obtained a reliable process to produce **2.16** with a yield of 35.5 %.

The main purpose for synthesising **2.16** was to use it as a precursor for [^{18}F]FDOPA and as starting reagent to microwave-mediated hydrolysis optimizations at ICNAS-P. An important issue, for this purpose, is its stability.

2.4.3 Stability of the new nitro-*L*-DOPA precursor, 2.16

The stability of molecule **2.16** was tested under storage conditions in solution and when submitted to microwave heating.

Two different solvents were tested, ACN and dimethylformamide (DMF). Acetonitrile because it is used for purification and DMF because it is used in the aromatic nucleophilic ^{18}F-fluorination.

2.16 was kept for 2 days in acetonitrile at -20ºC, and after analysed by HPLC, **Figure 2.32**. The chromatogram confirms that the purity of the product (98 %) is maintained. This is an important information because we can prepare a stock solution to be used later.

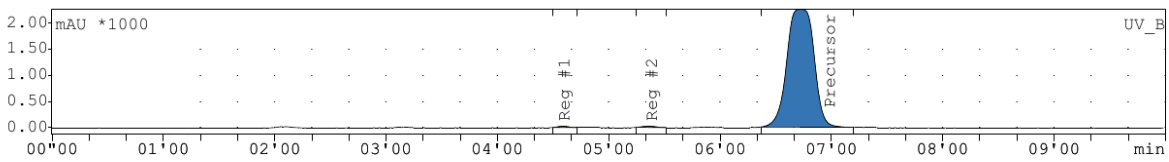

Figure 2.32: HPLC chromatogram of **2.16** after 2 days stored in solution at -20 ºC.

As already mentioned, the main purpose of synthesising **2.16** was to use it as a new precursor for ^{18}F-fluorination followed by hydrolysis under microwave heating. As already mentioned in **Chapter 1**, microwave heating is a more efficient heating source than conventional heating. On the other hand, the faster reactions, lead to cleaner mixtures because, as the reactions are shorter, the probability of degradation is lower. To confirm this, the solution of **2.16** in acetonitrile was submitted to microwave heating using the Power Cycling method, as described in **Table 2.8**.

Table 2.8: Microwave Power cycling methods used in stability tests of molecule **2.16**.

Power cycling method	1st method	2nd method
Power (W)	70	70
Heating time (seconds)	60	60
Cooling time (seconds)	5	5
Maximum temperature (ºC)	120	145
Minimum temperature (ºC)	70	95
Number of cycles	6	6

Percentage of **2.16** drops only 1 %, from 98 to 97 % (**Figure 2.33**). After the acetonitrile was evaporated by nitrogen/vacuum flow and 0.5 mL of DMF was added. The same MW method was tested, and the purity decrease from 97 to 87 %, **Figure 2.33**. Moreover, when the 2nd method (**Table 2.10**), was applied, the purity dropped to 75 % (**Figure 2.33**)

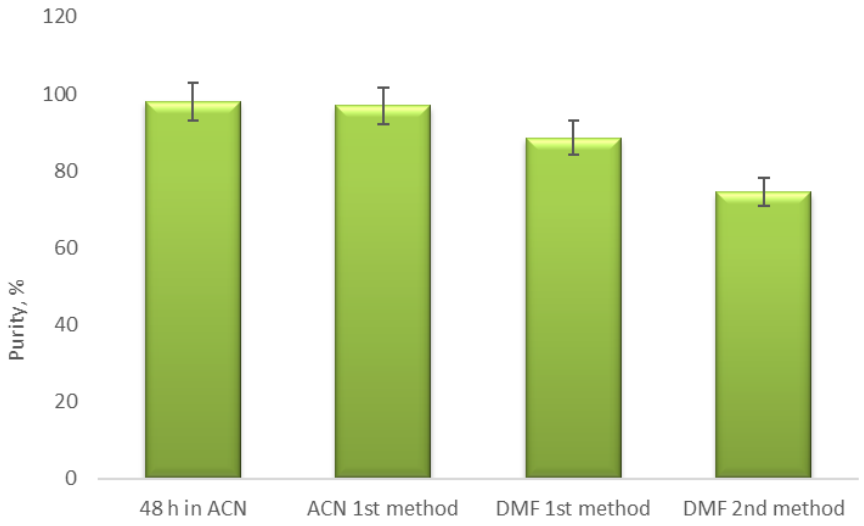

Figure 2.33: Stability tests of **2.16**. Purity determined by HPLC analysis.

In summary, **2.16** demonstrated to be stable in acetonitrile when stored at -20 ºC for, at least, 2 days. When submitted to microwave heating in ACN the purity its almost kept, however, when submitted to higher temperatures in presence of DMF, the purity drops to 75 %.

2.5 Optimization of microwave heating conditions

Microwave heating has proven to be an excellent alternative to conventional heating methods, due its heating efficiency. As already mentioned, microwave heating has been extensively investigated in several chemical transformations, particularly in organic chemistry. Nevertheless, despite the obvious advantages of shortening reaction time and improving yields, this technology was never applied to the routine production of radiopharmaceuticals.

The main purpose of this PhD work was the implementation of the microwave technology in two of the most complex synthesis in radiochemistry, 6-[^{18}F]FDOPA by the nucleophilic pathway and [^{11}C]UCB-J.

Regarding 6-[^{18}F]FDOPA, 3 main steps were identified that could benefit from microwave technology: i) drying of [^{18}F]fluoride; ii) ^{18}F-fluorination; iii) hydrolysis.

To evaluate the potential advantage of the technology, conventional heating will be compared with microwave heating using a single-mode cavity in the key steps mentioned above as well as in the evaluation of several possible alternative precursors for synthesis of this radiopharmaceutical.

As described in **Section 2.1**, there are currently only four commercially available automated methods for 6-[^{18}F]FDOPA production, the electrophilic method and three nucleophilic multistep strategies.

Both nucleophilic approaches, are multistep synthesis and, consequently very long and complexes synthesis processes yielding 6-[^{18}F]FDOPA **2.1**, in very low radiochemical yields (RCY's). In **Figure 2.34** we present the steps for each of these processes, *via 1* and *via 2*, starting from a chiral precursor, **2.4**, and from 6-nitroverathraldehyde, **2.5**, respectively.

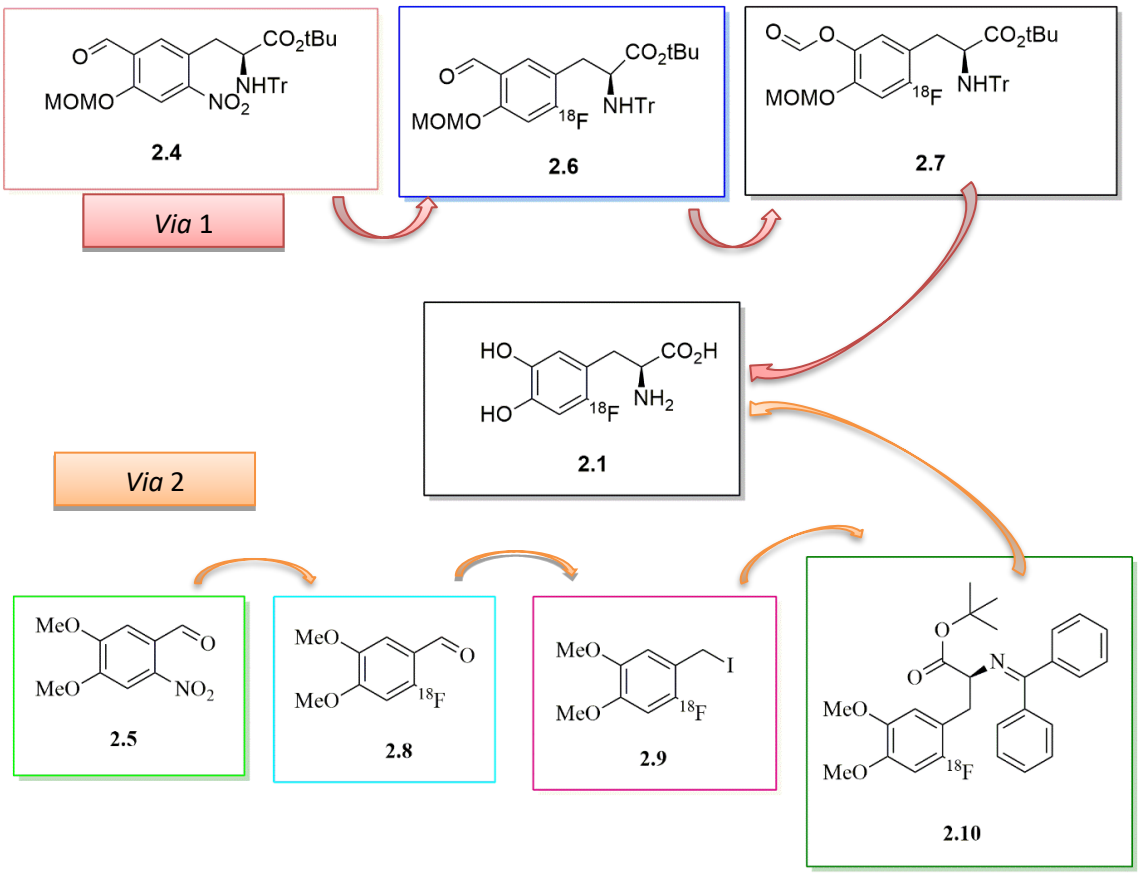

Figure 2.34: Nucleophilic multistep 6-[^{18}F]FDOPA synthesis: *via 1* – starting from a chiral precursor, **2.4** and *via 2* – starting from 6-nitroverathraldehyde, **2.5**.

The first step of any typical ^{18}F-fluorination process is the drying of [^{18}F]fluoride produced by the cyclotron.

2.5.1 Microwave-assisted azeotropic drying of [^{18}F]Fluoride

At the end of irradiation, the [^{18}F]fluoride solution is transferred to a hot cell located in the chemistry laboratory and is passed through a QMA column, which retains the [^{18}F]fluoride while

the [^{18}O]H_2O is collected in a waste container. The column is then dried by a nitrogen flow and the [^{18}F]fluoride is then eluted to the microwave cavity or to a conventional reactor with K_2CO_3/Kryptofix$_{222}$ or TBA.HCO_3 aqueous solution. This solutions is then dried resulting in the salts [^{18}F]KF/K_{222} and [^{18}F]TBAF, respectively. In **Figure 2.35** we schematize the purification of [^{18}F]fluoride using the QMA column.

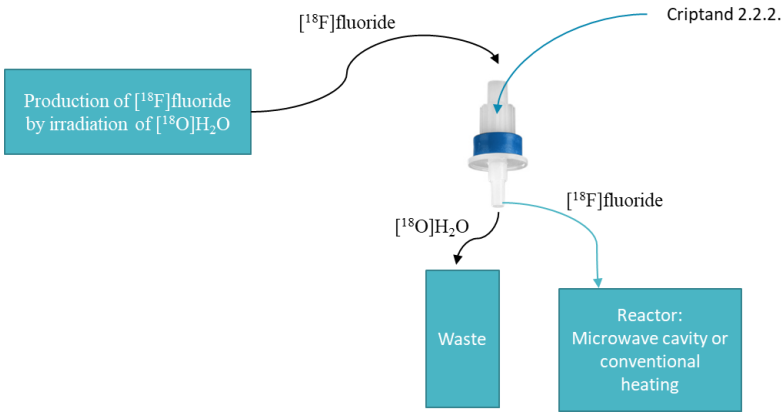

Figure 2.35: Schematic representation of [^{18}F]fluoride recovery, from cyclotron production to the reactor.

The drying of [^{18}F]KF/K_{222} or [^{18}F]TBAF and the ^{18}F-fluorination assisted by microwave heating were tested and compared with the obtained by conventional heating.

Initial tests were performed using only the solvents to determine the optimal heating conditions. Solvents to be used in the labelling reactions, such as acetonitrile (ACN), dimethylsulfoxide (DMSO), *N*,*N*-dimethylformamide (DMF) and water were submitted to microwave heating using different microwave heating methods, dynamic or standard. Higher temperatures in shorter times were reached when DMSO was used, which agrees with the dielectric properties of the solvent. However, as described in **Chapter 1**, when the reagents are used, the capacity of converting electromagnetic energy into heat, doesn't depend uniquely on the solvent, but from the total reaction mixture.

Due the diversity of microwave heating methods, the fixed power, standard, dynamic, and power cycling methods were tested for drying [^{18}F]KF/K_{222}, to select the most adequate for the azeotropic drying.

In each microwave heating method, different conditions were tested, based in previously reported studies in literature [57–60]. To assure that the solution was dry, at the end of microwave run, the presence of a white solid had to be observed.

First method tested was the Fixed Power. In this method the power (100 watts), the time and a safety maximum temperature (110ºC) were defined, being the power constant from the beginning to the end of the reaction. Two different reaction times were tested: 5 and 7 minutes. The dry solid was only obtained after 7 minutes. This compares unfavorably with the conventional heating where this result is achieved in 5 minutes.

After, the standard microwave heating method was tested (**Table 2.9**). In this method, temperature and the reaction time were defined. The method starts with a ramping to reach to the selected temperature. The reaction time only starts when the defined temperature is reached.

Table 2.9: Drying of the [^{18}F]KF/K_{222} solution under different conditions using the Standard method.

Conditions	1	2[b]	3	4
Temperature (ºC)	100	90	90	90
Reaction time (minutes)	3[a]	1	2	3
Total time (minutes)	4.0	2.6	5.4 ± 0.3	6.8 ± 3.0
n	1	1	3	3

Pre-heating maximum of 20 minutes. [a)] Temperature defined (100ºC) was not reached. [b)] Not dry.

With the first conditions tested (**Table 2.9, conditions 1**), 100 ºC for 3 minutes, the temperature was not reached, and the method was stopped after 4 minutes. At the end, the solution was dry. The temperature was then set to 90 ºC. Initially, 1 minute of reaction was defined. After a total time of 2.6 minutes, the salt [^{18}F]KF/K_{222} was not dry. Keeping the same temperature but increasing the reaction time to 2 and 3 minutes, the dry salt was obtained after 5.4 ± 0.3 and 6.8 ± 3.0 minutes of total time, respectively.

Searching for the optimal process, the dynamic method was also tested. This method allows the control of maximum power, temperature, hold time and stirring. In **Table 2.10** we present the results obtained with the drying of [^{18}F]fluoride using the dynamic method.

Table 2.10: Drying of the [^{18}F]KF/K_{222} solution using the dynamic method.

Conditions	1	2	3	4	5	6	7	8
Power (W)	80	80	80	80	80	80	90	90
Temperature (ºC)	110	100	90	90	70	80	80	80
Time (minutes)	2	2	3	2	3	3	3	2
Total time (minutes)	4.0[a]	6.4[a]	6.9 ± 1.8	5.6 ± 2.4	4.8 ± 1.5[b]	4.3 ± 0.2	6.6 ± 1.4	4.3 ± 0.7
n	1	1	3	3	3	3	3	3

Pre-heating maximum: 20 minutes. [a] Temperature was not reached. [b] The solution don't dry.

In the first attempts to dry the [^{18}F]KF/K_{222} solution using the dynamic method, the temperatures defined were 110 and 100ºC, respectively (**Table 2.10, conditions 1** and **2**). In both cases, the temperature defined was not reached and the runs were stopped after 3.98 and 6.4 minutes, respectively.

Similarly to the standard method, the highest temperature reached by the solution was 90 ºC. For this reason, keeping the same power, this temperature was tested with the parameters presented in **Table 2.10, conditions 3 and 4**. With 3 minutes of reaction, the total time needed to dry the solution was 6.9 ± 1.8 minutes, being reduced to 5.6 ± 2.4 minutes when the reaction time was 2 minutes. This means that the time needed to reach the 90ºC was 3.9 and 3.6 minutes, respectively. Based in these results, lower temperatures were tested, 70 and 80ºC (**Table 2.10, conditions 5 to 9**). With 70 ºC, the solution doesn't dry (**Table 2.10**, **conditions 5**). When the drying was performed at 80ºC, the solution dries in 4.3 ± 0.2 minutes, and the solution takes 1.3 minutes to reach the defined temperature.

Looking for the best conditions, keeping the temperature to 80ºC the power was increased to 90 W. Defining reaction times to 3 and 2 minutes, the solution was dried in 6.6±1.4 and 4.3±0.7 minutes, respectively.

With both microwave heating methods standard and dynamic, the reaction time was preceded by a ramping time, which results in drying times similarly to the times needed to dry the solution by conventional heating (around 5 minutes).

Finally, the Power Cycling method was tested. With this method, the following parameters were defined: the power; the heating and cooling time intervals; the maximum and minimum temperatures; and the number of cycles. Besides the drying of [^{18}F]KF/K_{222}, also the drying of the [^{18}F]TBAF solutions was tested with this microwave heating method.

In **Table 2.11,** we describe the drying conditions of [^{18}F]KF/K_{222} solutions tested with the power cycling method.

Table 2.11: Drying of [^{18}F]KF/K_{222} solutions using the Power Cycling method.

Conditions	1	2	3	4	5
Power (W)	50	50	70	70	70
Heating time (seconds)	60	60	60	60	60
Colling time (seconds)	30	30	5	5	5
Maximum temperature (ºC)	110	110	110	110	70
Minimum temperature (ºC)	60	50	70	45	30
Number of cycles	3	3	4	4	3
Total time (minutes)	3.6	3.3 ± 0.3	4.0 ± 0.0	4.00 ± 0.01	3.1 ± 0.4
n	1	4	2	3	6

Based on previously reported conditions from the literature,[58,60] we started to test the maximum temperature of 110 ºC (**Table 2.11, conditions 1 to 5**). The solid was obtained in lower times than the previous methods, however, similarly to the results obtained in previous methods, the maximum temperature of 110ºC was not reached. For this reason, the parameters indicated in **condition 5** were tested and the solid was obtained in 3.13 ± 0.4 minutes, less 2 minutes than in conventional heating.

In **Figure 2.36** we present the report of drying [^{18}F]KF/K_{222} solution at microwave cavity using conditions presented in **Table 2.11, conditions 5.**

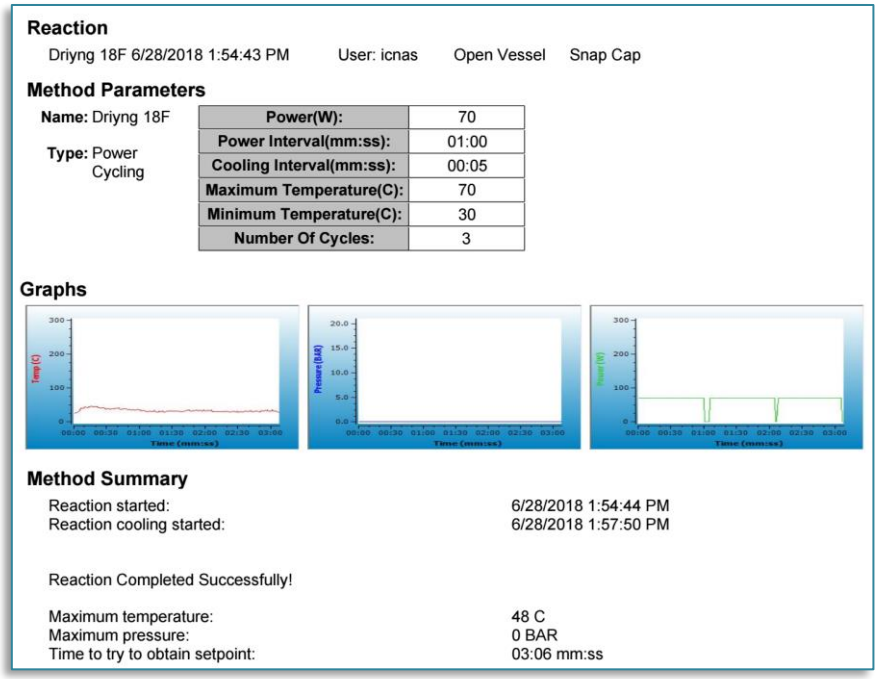

Reaction

Driyng 18F 6/28/2018 1:54:43 PM User: icnas Open Vessel Snap Cap

Method Parameters

Name: Driyng 18F

Type: Power Cycling

Power(W):	70
Power Interval(mm:ss):	01:00
Cooling Interval(mm:ss):	00:05
Maximum Temperature(C):	70
Minimum Temperature(C):	30
Number Of Cycles:	3

Graphs

Method Summary

Reaction started: 6/28/2018 1:54:44 PM
Reaction cooling started: 6/28/2018 1:57:50 PM

Reaction Completed Successfully!

Maximum temperature: 48 C
Maximum pressure: 0 BAR
Time to try to obtain setpoint: 03:06 mm:ss

Figure 2.36: Report of microwave run method of azeotropic drying of [^{18}F]KF/K_{222} solution (**conditions 5, Table 2.11**).

The best conditions for the azeotropic drying of [^{18}F]KF/K_{222} solution were obtained with the Power Cycling microwave heating method and the same conditions were used to perform the azeotropic drying of [^{18}F]TBAF solution (**Table 2.12**).

Table 2.12: Dry of [^{18}F]TBAF solution conditions tested in Power Cycling microwave heating method.

Condition	**1**
Power (W)	70
Heating time (seconds)	60
Colling time (seconds)	5
Maximum temperature (ºC)	70
Minimum temperature (ºC)	30
Number of cycles	3
Total time (minutes)	5.55 ± 2.01 (n=3)

In case of [^{18}F]TBAF, the resulting salt is not a white solid but an unclear oil. This is a difficulty for the visual control of the drying process, in contrast with [^{18}F]KF/K_{222} salt. However, by the results presented in **Table 2.12**, it is clear that [^{18}F]TBAF needs more time to completely dry the salt, 5.55 ± 2.01 minutes, instead of 3.13 ± 0.4 minutes, for the [^{18}F]KF/K_{222} salt.

The best method conditions for drying were selected to perform the further ^{18}F-fluorination studies.

2.5.2 Nucleophilic aromatic ^{18}F-Fluorination of [^{18}F]FDOPA precursors by microwave heating

After the optimization of the microwave-assisted dying, the microwave-assisted ^{18}F-fluorinations of the precursors (*S*)-3-(5-Formyl-4-methoxymethoxy-2-nitro-phenyl)-2-(trityl-amino)-propionic acid tert-butyl ester), **2.4** and 6-nitroveratraldehyde, **2.5** (**Figure 2.37)**, were also optimized.

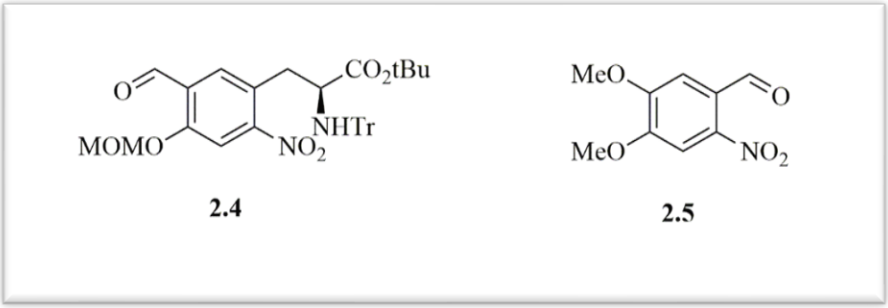

Figure 2.37: Structures of precursors **2.4** and **2.5** which were labelled with [^{18}F]fluoride.

Based on the results obtained with microwave-heating for azeotropic drying and previously reported studies already summarized in **Chapter 1**[59,61], only dynamic and power cycling microwave heating methods were selected to optimize the [^{18}F]fluorination of possible [^{18}F]FDOPA precursors.

Analysis of ^{18}F-fluorination conversions of precursors **2.4** and **2.5** was performed using analytical HPLC. The experimental details are described in **Chapter 5**.

Molecule **2.5**, which is the precursor used in the routine production of 6-[^{18}F]FDOPA, was selected to start the optimizations of microwave-assisted^{18}F-fluorination using a Kriptofix$_{222}$ solution as QMA eluent, according to the reaction presented in **Scheme 2.5**.

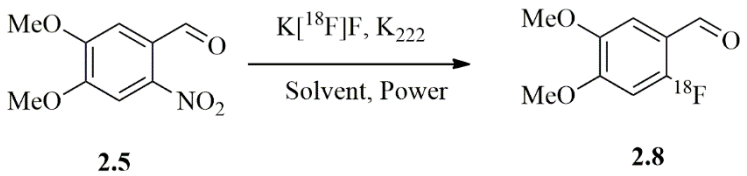

Scheme 2.5: Microwave assisted ^{18}F-fluorination of 6-nitroverathraldehyde, **2.5**.

Typically, the following parameters were defined in the following microwave heating methods:

- Dynamic method conditions:
  - Power;
  - Temperature;
  - Reaction time.
- Power Cycling (PC) method conditions:
  - Power;
  - Heating time;
  - Cooling time;
  - Maximum temperature;
  - Minimum temperature;
  - Number of cycles.

At the end of the reaction, a sample is collected to be analysed by analytical HPLC and the ^{18}F-fluorination radiochemical yields are determined as the percentage of the desired product relatively to all the other activity peaks in the chromatogram.

In routine production, ^{18}F-fluorination of precursor **2.5**, was performed in DMF, while ^{18}F-fluorination of precursor **2.4** was performed in DMSO. The loss factor of these solvents makes them a good choice for microwave applications. In all the experiments (unless otherwise stated) the precursors were dissolved in 0.5 mL of their respective solvent.

In **Table 2.13** we present the results obtained with two different microwave heating methods, Dynamic and Power Cycling, in ^{18}F-fluorination of **2.5** in DMF, using [^{18}F]KF/K_{222}, as fluorination agent.

Table 2.13: ^{18}F-Fluorination of **2.5**, in DMF, with different microwave heating methods.

Entry	MW Method	Temperature (ºC)	Power (watts)	Time (min)	Total time (min)	Number of cycles	^{18}F-Fluorination Yield (%)[a]
1	Dynamic	145	75	7.5	13.8 ± 3.3	n.a.	26.6 ± 23.4 (n = 2)
2	PC[b]	145/65	70	n.a	3.3	6	80 (n = 1)
3	PC[b]	145/65	70	n.a.	6.4 ± 0.8	12	83.3 ± 13.7 (n = 3)

[a]^{18}F-fluorination yield based in HPLC analysis. n.a.: not applicable. General conditions: Dynamic method: 75W, 145ºC; [b]PC (Power Cycling): 70W; heating time 60s; cooling 2 seconds; 145ºC of maximum temperature and 65ºC of minimum temperature.

The ^{18}F-fluorination, using the dynamic method, produced lower yields in longer time when compared with the power cycling method, 26.6 ± 23.4 % in 13.8 ± 3.3 minutes and 83.3 ± 13.7 % in 6.4 ± 0.8 minutes, respectively (**Table 2.13**, **Entries 1** and **3**). The influence of the number of cycles was also evaluated with the Power Cycling method (**Table 2.13**, **Entries 2** and **3**) and we observed that the ^{18}F-fluorination yield was similar.

Based in these results, forward optimizations were performed using the Power Cycling (PC) microwave heating method with both solvents and using two different QMA eluents, K_2CO_3/Kriptofix$_{222}$ and TBA.HCO_3 solutions, which results in two different [^{18}F]salts ([^{18}F]KF/K_{222} and [^{18}F]TBAF, respectively), in the ^{18}F-fluorination of **2.5**. In **Table 2.14** we present the results obtained.

Table 2.14: ^{18}F-Fluorination of **2.5** by Power Cycling microwave heating method, using two different [^{18}F]salts and solvents.

Entry	Solvent (ml)	[^{18}F]salt	Temperature (ºC)	Power (watts)	Total time (min)	Number of cycles	^{18}F-Fluorination Yield (%)[a]
1	DMF	[^{18}F]KF/K_{222}	145/65	70	6.4 ± 0.8	12	83.3 ± 13.7 (n=3)
2	DMSO	[^{18}F]KF/K_{222}	145/65	70	6.4	12	100
3	DMSO	[^{18}F]KF/K_{222}	145/65	70	2.5 ± 0.2	2	100 ± 0 (n=2)
4	DMSO	[^{18}F]TBAF	145/65	70	6.5	6	75

[a]^{18}F-fluorination yield based in HPLC analysis. PC (Power Cycling) method: 70W; heating time 60s; cooling 2 seconds; 145ºC of maximum temperature and 65ºC of minimum temperature.

Based in the best result obtained in ^{18}F-fluorination of 6-nitroveratraldehyde, **2.5**, dissolved in DMF, (**Table 2.14, Entry 1**), the same method was tested using DMSO as solvent (**Table 2.14**, **Entry 2**). The ^{18}F-Fluorination yield increased from to 83.3 ± 13.7 to 100 %, with 12 cycles. The number of cycles was reduced to 2 (**Table 2.14**, **Entry 3**), yielding the product **2.8** in 100 ± 0 % in only 2.5 ± 0.2 minutes.

The same conditions were tested with [^{18}F]TBAF (**Table 2.14, Entry 4**), and the ^{18}F-fluorination yield dropped from 100 to 75 %. .

According to **Table 2.14**, it is clear that the best results, producing the higher ^{18}F-fluorination yields in shorter times, were the ones presented in **Entry 3**. ^{18}F-fluorination of **2.5**, with [^{18}F]KF/K_{222} in DMSO, heated by Power Cycling microwave heating method yielded **2.8** with a conversion of 100 % in only 2.5 ± 0.2 minutes, 2 microwave cycles and temperatures in the range of 145 and 65 ºC.

Concerning the solvents, DMSO and DMF, the conversion of **2.5** into **2.8** drops from 100.0 ± 0.0 % with DMSO in 2 cycles, to 83.3 ± 13.7 % with DMF in 12 cycles. This occurs due to the capacity of the solvents to convert electromagnetic energy into heat, the "loss factor", tan δ, for DMSO is 0.825 and for DMF is 0.161, which justify, the lower yield when the second solvent was used.

In conclusion, the reduction of the ^{18}F-fluorination from 5 minutes in conventional heating to 2.5 ± 0.2 minutes with microwave heating, results in a saving of about 50 % in time. Besides the reduction in time, also a significant increase in the RCY (from 50 to 100%) was achieved.

In **Figure 2.38** we present, as example, of a chromatogram of the precursor **2.5** (**a**) and the reaction mixture at the end of ^{18}F-fluorination performed in DMF: **b**) UV detector, **c**) radiation detector). Retention time of [^{18}F]fluoride, based in **Figure 2.38**, was around 2.03 minutes, and for **2.8** was around 3.17 minutes.

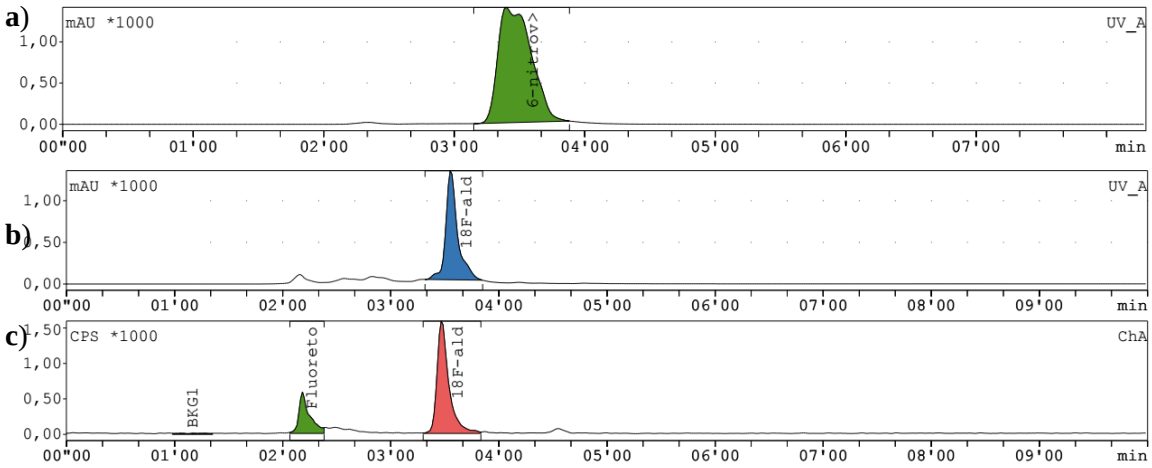

Figure 2.38: Chromatograms: (**a**) UV chromatogram of precursor **2.5**, at 283 nm; (**b**) UV chromatogram at the end of ^{18}F-fluorination, at 283 nm; (**c**) radioactivity detector of reaction mixture at the end of ^{18}F-fluorination.

The studies proceeded with the precursor **2.4**, a molecule initially developed by Rene-Martin *et al.* [164] and used in the automated process by ABX. The ^{18}F-fluorination of this precursor was also tested with microwave heating, according to the reaction schematized in **Scheme 2.6**.

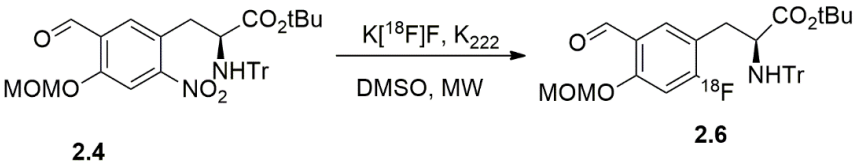

Scheme 2.6: Microwave assisted ^{18}F-fluorination of precursor **2.4**.

In the routine production of 6-[^{18}F]FDOPA by the ABX method the precursor is dissolved in DMSO. Additionally, the best results obtained with the microwave-assisted ^{18}F-fluorination of **2.5** were also with this solvent. In **Table 2.15** we present the results obtained in the microwave assisted^{18}F-fluorination of **2.4**, in DMSO**.**

Table 2.15: ^{18}F-Fluorination of **2.4** by Power Cycling microwave heating method.

Entry	Solvent	[^{18}F]salt	Temperature (ºC)	Power (watts)	Time (min)	Number of cycles	^{18}F-Fluorination Yield (%)[a]
1[b]	DMSO	[^{18}F]KF/K_{222}	145/65	70	1.8 ± 0.2	2	85.45 ± 3.65 (n=2)
2	DMSO	[^{18}F]KF/K_{222}	145/100	80	6.2	6	86
3	DMSO	[^{18}F]KF/K_{222}	145/100	100	8.0	4	89

[a]^{18}F-fluorination yield based on HPLC analysis. [b]PC (Power Cycling) method: 70W; heating time 60s; cooling 2 seconds; 145ºC of maximum temperature and 65ºC of minimum temperature.

Repeating the conditions that previously produced the best results (**Table 2.15, Entry 1**), yielded 85.45 ± 3.65 % of **2.6** in only 1.8 ± 0.2 minutes. In search of the best conditions, changes in power and number of cycles were tested. However, even with a significant increase of the reaction time, the conversions increased only slightly from 85.45 to 89 % (**Table 2.15**, **Entries 1** and **3**).

These attempts to improve the automated 6-[^{18}F]FDOPA **2.1** synthesis were performed in parallel with the synthesis of **2.16**, as described in **Section 2.4**.

As referred previously, one of the objectives of this work was the synthesis of a new precursor which allowed us to perform the synthesis in only three reaction steps: i) drying; ii) ^{18}F-fluorination; iii) hydrolysis, according to the reactions depicted in **Scheme 2.7**.

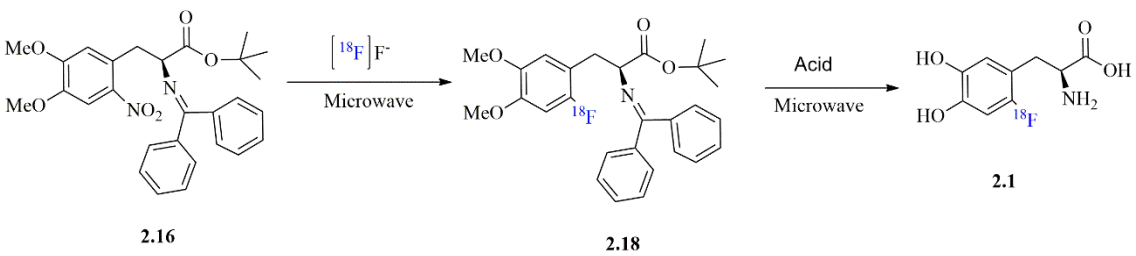

Scheme 2.7: Proposed 6-[^{18}F]FDOPA **2.1**, synthesis using microwave heating.

Besides a good leaving group (-NO_2), a nucleophilic aromatic substitution also requires an electron-withdrawing group in the *ortho* or *para* positions to promote the reaction by stabilization of the Meisenheimer complex. Stone-Elander [51], reported a nucleophilic aromatic ^{18}F-fluorination of aromatic rings using a microwave cavity, testing the effect of leaving groups on the aromatic ring and the effect of the *orto*, *meta* or *para* positions of electron-withdrawing and electron-

donating substituents. Molecule **2.16** contains a good leaving group, and the objective was trying to circumvent that limitation with microwave-heating.

The ^{18}F-fluorination of **2.16** with [^{18}F]TBAF was tried, initially, using conventional heating, dissolved in DMF for 10 minutes at 120ºC. The conversion into **2.18** was 0 %, as expected by the chemical structure of **2.16**.

Microwave heating was also tested in the ^{18}F-fluorination of **2.16** using DMSO and DMF as solvents and also both [^{18}F]salts, [^{18}F]KF/K_{222} and [^{18}F]TBAF. For DMSO, the microwave heating method was the same used in ^{18}F-fluorination of **2.5**. The results obtained are presented in **Table 2.16**.

Table 2.16: ^{18}F-Fluorination of **2.16** by Power Cycling microwave heating method.

Entry	Solvent	[^{18}F]salt	Temperature (ºC) maximum/minimum	Power (watts)	Time (min)	Number of cycles	^{18}F-Fluorination Yield (%)[a]
1	DMSO	[^{18}F]KF/K_{222}	145/65	70	4.2 ± 0.2	6	0.0 ± 0.0 (n=3)
2	DMSO	[^{18}F]TBAF	145/65	70	4.4	6	0
3	DMSO	[^{18}F]TBAF	145/65	70	16.1	12	0
4	DMF	[^{18}F]KF/K_{222}	145/95	70	5.5	6	0
5	DMF	[^{18}F]KF/K_{222}	170/120	70	7.0	6	0
6	DMF	[^{18}F]TBAF	145/95	70	7.9	6	0
7	DMF	[^{18}F]TBAF	120/70	70	5.0	6	0

[a] ^{18}F-fluorination yield based on HPLC analysis.

Several attempts were performed to perform the reaction however, ^{18}F-Fluorination of **2.16** never occurred. This means that, even with microwave heating the electron-withdrawing group in the *ortho* or *para* positions group is mandatory.

Besides the microwave-assisted ^{18}F-fluorination of precursors **2.5, 2.4** and **2.16**, also the hydrolysis steps of the process were optimized by microwave heating and will be discussed in the next section.

2.5.3 Hydrolysis of protected FDOPA by microwave heating

Application of microwave heating in the cleavage of protecting groups of radiopharmaceuticals was reviewed in 2002 by Stone-Elander [250], which was mainly focused in understanding the differences between the several single mode devices, developed for PET applications, with a commercial purpose. It's clear that the reaction times and yields are different when performed in different devices, but also which have obvious advantages over conventional

heating methods. The first single-mode microwave device used for radiolabelling, was firstly reported in 1991 [251]. More recently a remarkable reduction in the hydrolysis time in the synthesis of [^{18}F]-fluoroestardiol was reported, from 20 to 3 minutes[117].

In the processes described in **Scheme 2.2, Section 2.2,** and **Scheme 2.3**, **Section 2.3**, the hydrolysis reaction was the step that takes more time in the process, around 20 minutes in each one.

To optimize this step, the hydrolysis of precursors **2.4** and **2.16** was performed according to the reactions represented in **Schemes 2.8** and **2.9**, respectively.

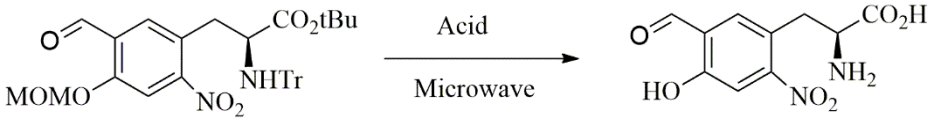

2.4 **2.19**

Scheme 2.8: Hydrolysis of **2.4**, by microwave heating.

The conversion of the hydrolysed products was confirmed by HPLC by comparison with reference standards of 6-nitro-Formyl-DOPA hydrochloride, **2.19**, and 6-nitro-*L*-DOPA hydrogensulfate, **2.20**, using the same HPLC conditions described in **Section 2.5.2** for ^{18}F-fluorination of **2.4** and **2.16**.

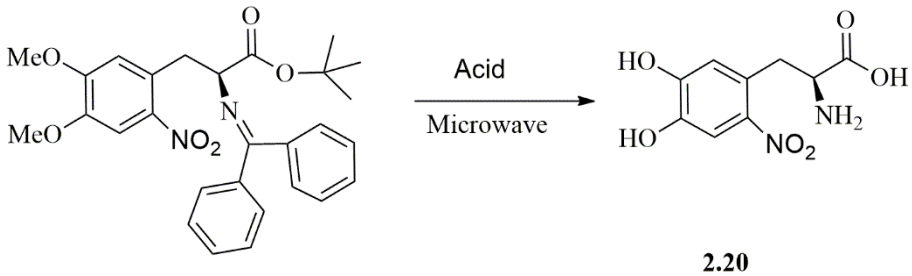

2.16 **2.20**

Scheme 0.9: Hydrolysis of **2.16**, by microwave heating.

In **Table 2.17** we present the results obtained.

Table 2.17: Optimization of microwave-assisted hydrolysis of **2.16** and **2.4**.

Entry	Precursor	Solvent (ml)	Acid solution	Time (min)	Yield (%)
1	**2.4**	-	HI 37 %	3.3	85.6
2	**2.4**	DMSO	HCl 4M	4.9	100
3	**2.16**	-	HI 37 %	5.6 ± 0.9	81 ± 15 (n=2)
4	**2.16**	-	HCl 4M	4.5 ± 0.4	85 ± 4 (n=3)
5	**2.16**	DMF	HI 37 %	4 ± 0	74 ± 10 (n=2)
6	**2.16**	DMF	HCl 4M	4	53.9

Microwave hydrolysis conditions – Method: Power cycling, Power=60W, heating 00:45, cooling=00:10, Tmax=120ºC, Tmín=70ºC, 5 cycles.

The improvement of the method which starts with the **2.4** precursor was tested. Similarly to the tests of ^{18}F-fluorination of **2.4**, also its hydrolysis was optimized, with HI 37 % without solvent and with HCl 4M previously dissolved in DMSO. The dissolution of precursor in DMSO results in a complete conversion of **2.4** into **2.19** in 4.9 minutes

The best hydrolysis conditions of **2.16,** yields **2.20**, with 85 ± 4 % in 4.5 ± 0.4 minutes (**Table 2.17, Entry 4**). Besides the good yield, also a significative reduction in the time, when compared with conventional heating, from 20 to 4.5 minutes was observed. In the routine production method (**Scheme 2.2**), before the hydrolysis of the corresponding ^{18}F-fluorinated **2.7**, the solvent used in the previous step was evaporated and, for that reason, we start to test the hydrolysis without solvent. To evaluate the influence of the presence of the solvent, a previous dissolution of precursor **2.16** in DMF was also tested (**Table 2.17**, **Entries 5** and **6**). The dissolutions do not produce any improvement in the hydrolysis yield.

Considering the results obtained, not only in ^{18}F-fluorination, but also in hydrolysis step, the advantages of microwave heating over conventional heating are evident.

2.6 Conclusions

The necessity to implement a 6-[^{18}F]FDOPA synthesis method at ICNAS-P lead us to try to implement two commercially available different methods. The first, which starts by the ^{18}F-fluorinationan of an already chiral precursor, **2.4** (ABX method) produced very low yields and also, proved to be quite unreliable.

The second 6-[^{18}F]FDOPA synthesis method, which starts by ^{18}F-fluorinationan of 6-nitroverathraldeyde, **2.5**, (Trasis method) is reproducible with RCY's of 29.7 ± 9.2 % (ndc), and radiochemical purities ≥ 95 % in 90 minutes total synthesis time.

Production and quality control of this method was implemented at ICNAS-P, and documentation was compiled and submitted to the Portuguese authorities. The process was successful, and the company obtained authorization to commercialize the product since 28 June of 2019.

With this method, it is possible to perform a few patients internally and distribute to nearby hospitals. However, the multistep synthesis method is complex, expensive and very time consuming. These drawbacks limit the rentability of the process.

With the aim to develop a new synthesis process, a synthesis method of a new possible 6-[^{18}F]FDOPA precursor, **2.16**, was developed. Besides all the optimizations of reaction conditions, we arrive to a reliable synthesis process yielding **2.16** with a yield of 35 %.

The product was fully characterized, and its structure confirmed by different characterization techniques. Also, the stability of **2.16**, in solution was evaluated and the purity of 98 % was kept after, at least, 2 days in solution.

The purpose of synthesising a new precursor was the development of a new 6-[^{18}F]FDOPA synthesis process which could be performed in only 3 steps by microwave heating. Unfortunately, the non-activation of the aromatic ring in the structure of new molecule **2.16** did not allow the ^{18}F-fluorination, even when microwave heating was applied.

To improve the already existent 6-[^{18}F]FDOPA synthesis methods, microwave heating was used in key steps of the process, such as drying [^{18}F]fluoride, ^{18}F-fluorinatio and hydrolysis. In all these steps, reduction in the times, was observed.

In **Figure 2.39** are summarized the main results of conventional *vs* microwave heating in the different reaction steps of the 6-[^{18}F]FDOPA process implemented at ICNAS-P.

The use of microwave heating in the first two steps of the process, drying [^{18}F]fluoride and ^{18}F-fluorinatin, allowed for a reduction of 44 % in time.

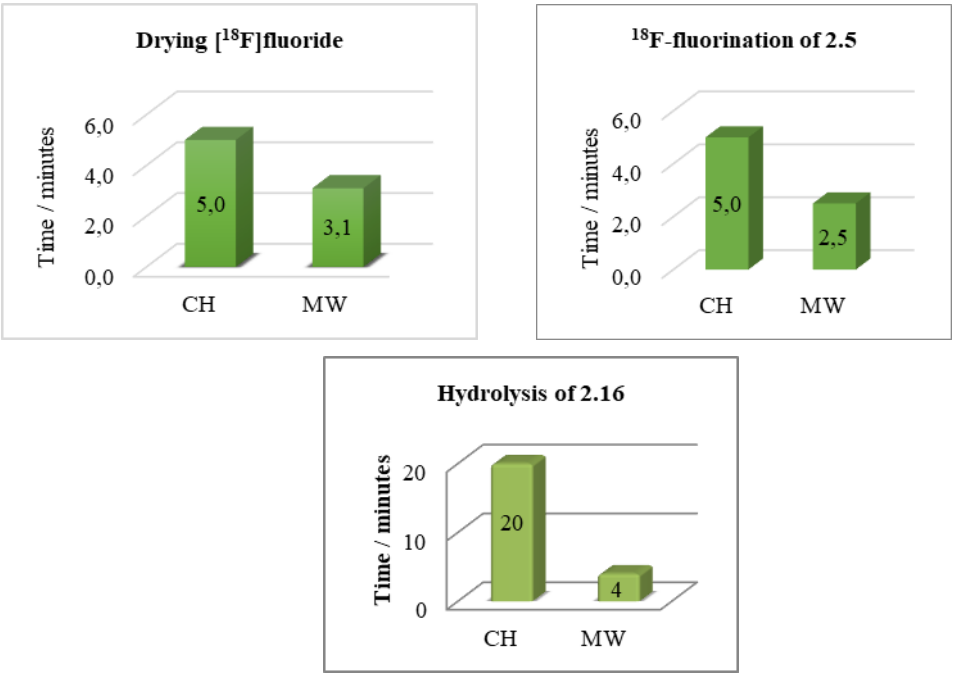

Figure 2.39: Conventional *vs* microwave heating in drying of [^{18}F]fluoride, ^{18}F-fluorination of **2.5** and hydrolysis of **2.16**.

Furthermore, when the hydrolysis step was performed by microwave heating, a reduction of 80 % in time was obtained, from 20 to 4 minutes. In radiosynthesis with short-lived radiopharmaceuticals all the minutes are important. Due to the half-life of 109 minutes of ^{18}F, the reduction of 2 minutes in the two first steps are not very significative. However, the reduction in 16 minutes in hydrolysis step is a very substantial reduction in time, 80 %.

Chapter 3

Improvement of [^{11}C]UCB-J radiosynthesis by microwave heating

As mentioned in **Chapter 1**, the most common strategy to synthesise ^{11}C-labelled compounds is the methylation of N-, O-, and S- heteroatoms, with methyl iodide ([^{11}C]CH_3I) or methyl triflate ([^{11}C]CH_3OTf) [125,126].

At ICNAS-P, radiopharmaceuticals such as [^{11}C]PiB, [^{11}C]flumazenil or [^{11}C]methionine are produced routinely, by methylation of the N- heteroatom with [^{11}C]CH_3OTf, in case of [^{11}C]PiB and with [^{11}C]CH_3I, in the other cases. In **Figure 3.1** we present, as example, the three structures of the mentioned ^{11}C-labelled radiopharmaceuticals produced at ICNAS-P.

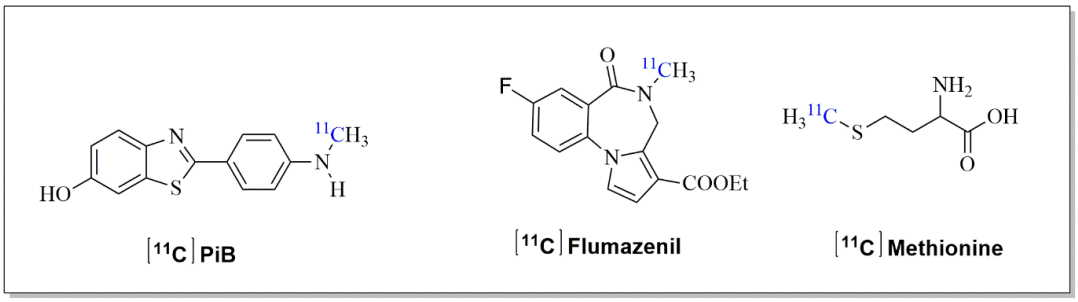

Figure 3.1: Examples of ^{11}C-labelled compounds produced at ICNAS-P.

Radiolabelling of [^{11}C]PiB and [^{11}C]flumazenil precursors is performed "*in-loop" a* method where the precursor, typically dissolved in a solvent such as dimethylformamide (DMF), dimethylsulfoxide (DMSO), acetone or acetonitrile (ACN), is pre-loaded into an HPLC loop. A base (sodium hydroxide, sodium hydride, potassium carbonate or tetrabutylammonium) is usually added to deprotonate the functional group (amino or thiol). [^{11}C]CH_3I is then distilled through the loop and allowed to react, for a short period of time, at room temperature.

In the production of [^{11}C]methionine, a cartridge is used. The precursor is dissolved in a solution of H_2O/methanol(1:1) and made to react with [^{11}C]CH_3I, also at room temperature.

The production of [^{11}C]UCB-J is more complex and it requires heating, so a reactor is required. Traditionally, heating is done with a conventional oven, a process that is time consuming, a critical issue considering the short half-life of Carbon-11 (20.4 min). In this work, we tested the use of a microwave cavity to perform this synthesis comparing it with conventional oven heating.

3.1 Synthesis of [^{11}C]UCB-J

As described in **Chapter 1**, synapses can become defective in neurological as well as in psychiatric disorders such as epilepsy, Alzheimer's disease, schizophrenia, autism, depressive disorders or Huntington's disease [192,194–198]. [^{11}C]UCB-J **3.3** appears to be the most promising PET probe for in SV2A PET imaging, considering its pharmacokinetic and quantification properties [145,206–208]. Typically, [^{11}C]UCB-J is synthesized *via* a Suzuki-Miyaura cross-coupling mediated by a palladium catalyst.

In **Table 3.1** we present the reaction conditions and results reported in the literature for the radiosynthesis of [^{11}C]UCB-J.

Table 3.1: Reaction conditions and results for [^{11}C]UCB-J radiosynthesis.

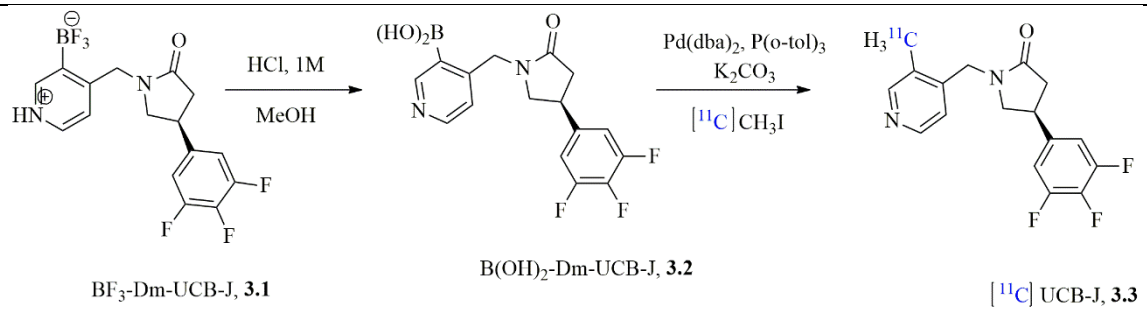

Entry	Precursor -BF_3, 3.1$^-$	Precursor -$B(OH)_2$, 3.2	Solvent mixture	Temperature, ºC	Reaction time, min	RCY, %[c]	Ref.
1[a]	✓	-	DMF/H_2O	100 ºC	5	11 ± 4	145
2[b]	✓	-	THF/H_2O	70ºC	4	39 ± 5	201
3[a]	-	✓	DMF/H_2O	100 ºC	5	35 ± 4	202

n.r.: not reported; Ref.: Reference. [a] [^{11}C]CH_3I was trapped in a solution of Pd_2dba_3/(o-tolyl)$_3$P, K_2CO_3. **3.1** was added after trapping; [b] [^{11}C]CH_3I was trapped in a solution of Pd_2dba_3/(o-tolyl)$_3$P, K_2CO_3/**3.1**. [c] decay corrected (dc) to [^{11}C]CH_3I.

In 2016, Nablusi *et al.* [145] reported the first [^{11}C]UCB-J **3.3** synthesis performed by ^{11}C-methylation of the precursor (*R*)-3-(difluoroboranyl)-4-((2-oxo-4-(3,4,5-trifluorophenyl) pyrrolidine-1-yl) methyl)-pyridin-1-ium fluoride (BF_3-Dm-UCB-J) **3.1** with [^{11}C]CH_3I, in a mixture of dimethylformamide (DMF)/water (8:1) (**Table 3.1**, **Entry 1**). [^{11}C]CH_3I was trapped into a reactor containing Tris(dibenzylideneacetone)dipalladium(0) ($Pd_2(dba)_3$), Tris(o-tolyl)phosphine (P(o-tol)$_3$) and potassium carbonate (K_2CO_3) dissolved in DMF/H_2O (8:1). Then, a solution of **3.1**, dissolved in the same mixture, was added and the reaction proceeded at 100ºC for 5 minutes, under stirring, with a global RCY of 11 ± 4 % (dc to [^{11}C]CH_3I).

Later, Rokka *et al.* [201], report the attempt to reproduce the Nabulsi method [145] but, without success, and, consequently, develop a new procedure (**Table 3.1**, **Entry 2**). The main differences between the methods are the solvent mixture, which was changed from DMF/H_2O (8:1) to tetrahydrofuran (THF)/H_2O (8:1), and the experimental procedure. The [^{11}C]CH_3I trapping was performed on a solution containing $Pd_2(dba)_3$, P(o-tolyl)$_3$, K_2CO_3, and the precursor **3.1**. The solution was stirred for 4 minutes at 70 ºC. They report a RCY of 39 ± 5 % (dc to [^{11}C]CH_3I). Authors attributes the better yield, to a possible *in situ* conversion of **3.1**, into the corresponding boronic acid derivative, **3.2**, a common precursor for Suzuki cross-coupling.

Based in these findings, Sephton *et al.* [202] reported a procedure in which, the corresponding boronic acid derivative, **3.2**, was previously generated by dissolving **3.1** in a mixture of methanol (MeOH)/HCl 1M, and was stirred for 60 minutes at 60ºC. In **Scheme 3.1** we present the hydrolysis of **3.1**.

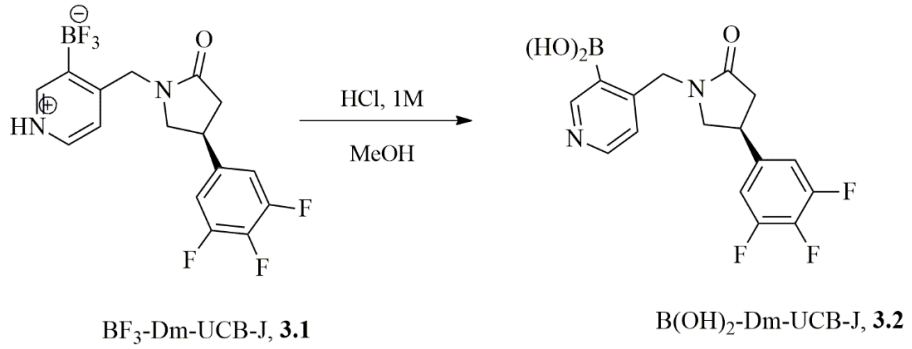

Scheme 3.1: Hydrolysis of **3.1** to give the corresponding boronic acid derivative, **3.2**.

As in the Nabulsi's method [145], in the Sephton's process, [^{11}C]CH_3I trapping is performed in a solution containing $Pd_2(dba)_3$, P(o-tolyl)$_3$ and K_2CO_3. After trapping, the solution of **3.2** in DMF/H_2O is stirred for 5 minutes, at 100ºC, with an overall RCY of 35 ± 4 % (dc to [^{11}C]CH_3I), in 35 minutes from end of bombardment (EOB) (**Table 3.1**, **Entry 3**).

The clinical interest to perform SV2A PET studies at our Institute, lead us to implement a production method of [^{11}C]UCB-J **3.3**. Considering the low RCY's reported in the literature, an improvement of the process was required to produce clinical doses of the radiotracer.

In this Chapter will be described the development of an automated and reproducible synthesis process of [^{11}C]UCB-J **3.3** radiosynthesis, and respective optimizations by conventional and by microwave heating.

In general, the synthesis process for [^{11}C]UCB-J **3.3**, comprises several independent steps that are performed sequentially (**Figure 3.2**).

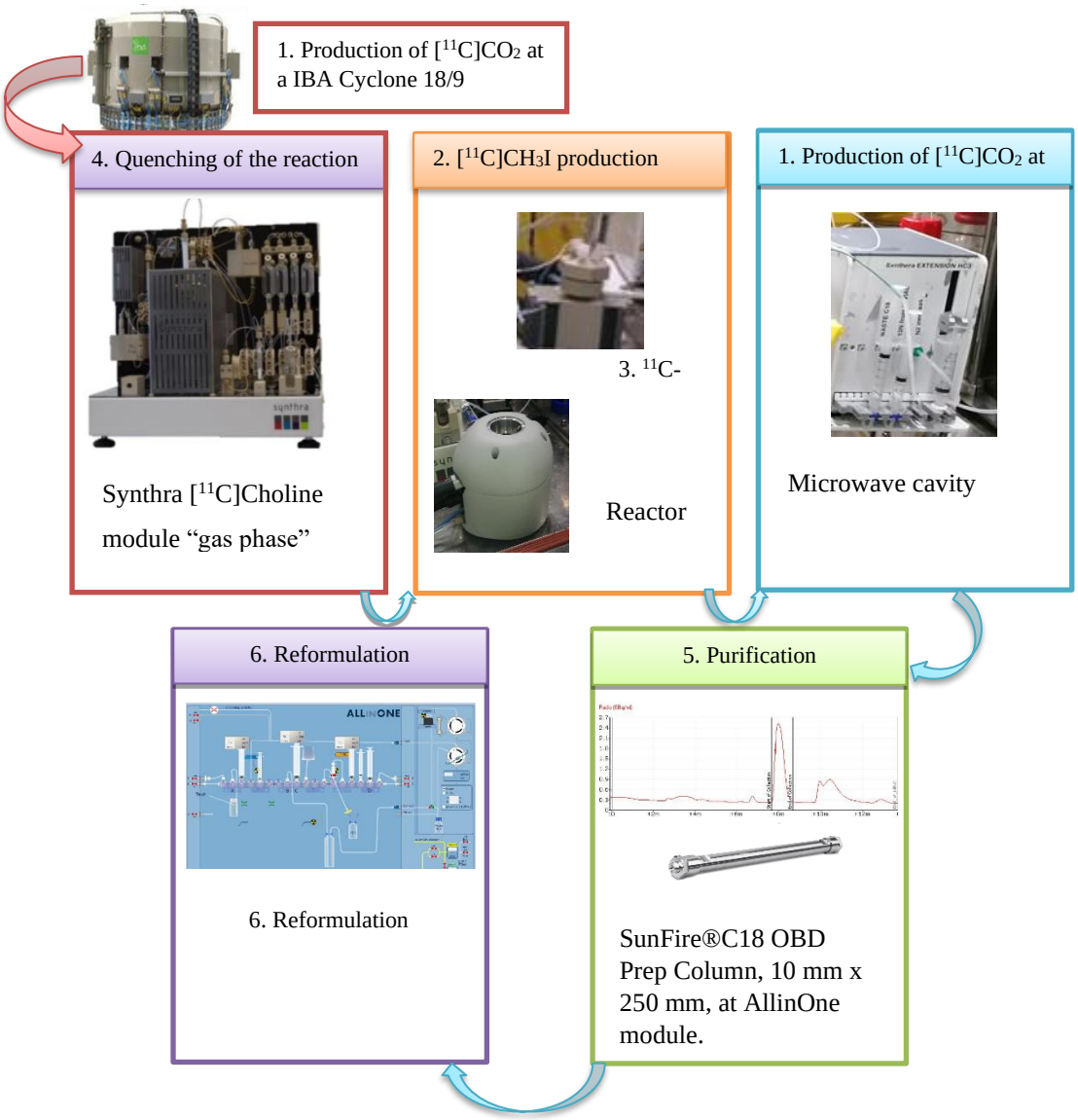

Figure 3.2: Overview of the [^{11}C]UCB-J synthesis procedures.

The full process requires six different steps, performed in five different automated modules:

1. Production of [^{11}C]CO_2 by the irradiation of a gaseous N_2 + 0.5 % O_2 target in the cyclotron

2. Conversion of the produced [^{11}C]CO_2 to [^{11}C]CH_3I in an automated synthesis module, Synthra [^{11}C]Choline

3. ^{11}C-methylation reaction

4. Quenching of the reaction crude, on the automated module IBA Synthera Extension®

5. Purification of the ^{11}C-labelled product in an HPLC semi-preparative system (AllinOne module)

6. Reformulation of the product, originating an injectable solution.

In the next sections, these steps, and their respective optimizations will be detailed.

3.1.2 Production of [^{11}C]CH_3I

The first step in a radiosynthesis is the production of radionuclide. In our site, carbon-11 labelling starts with [^{11}C]CO_2, which is produced by the nuclear reaction $^{14}N(p,\alpha)^{11}C$ using an IBA Cyclone 18/9 cyclotron. Typically, irradiations are performed during 45 minutes with a current of 20 µA. At the end, the produced [^{11}C]CO_2 is transferred, via capillary tubing, to a synthesis module, located inside a shielded isolator (hot cell), in a clean room.

In the hot-cell [^{11}C]CO_2 is converted to [^{11}C]CH_3I, in the gas phase [132], using the Synthra [^{11}C]Choline® commercial module (**Figure 3.3**).

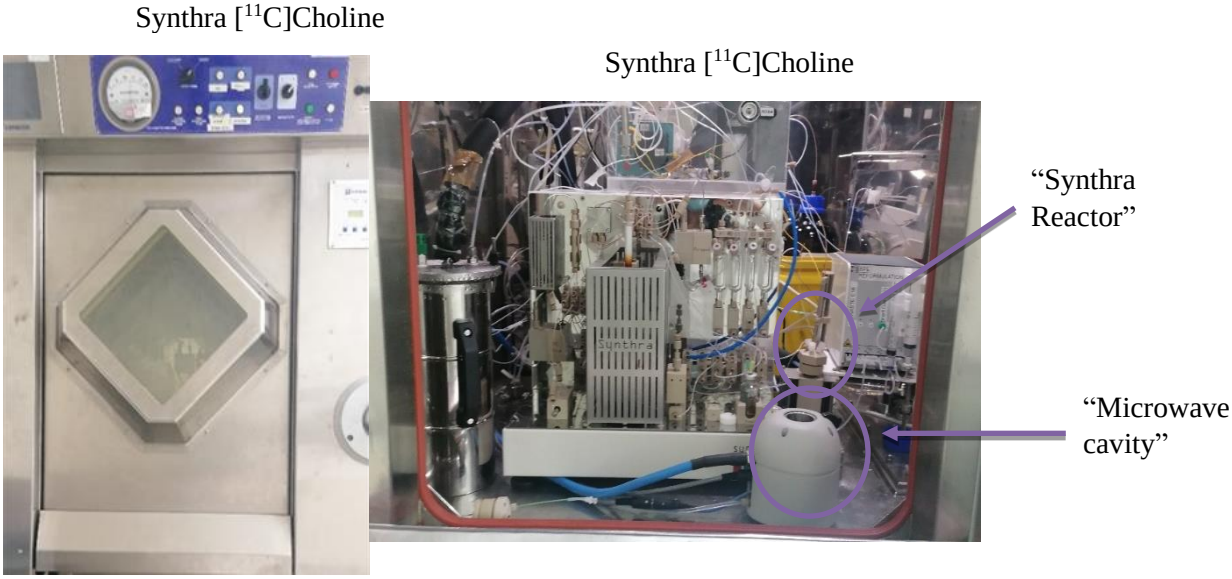

Figure 3.3: View of the commercially available Synthra [^{11}C]Choline, located inside a shielded MIP1-1P hot cell.

The automated module is controlled by a dedicated software, the SynthraView® Software. In **Figure 3.4** we depict the user interface of SynthraView® for the Synthra [^{11}C]Choline module used for the radiosynthesis of [^{11}C]CH_3I.

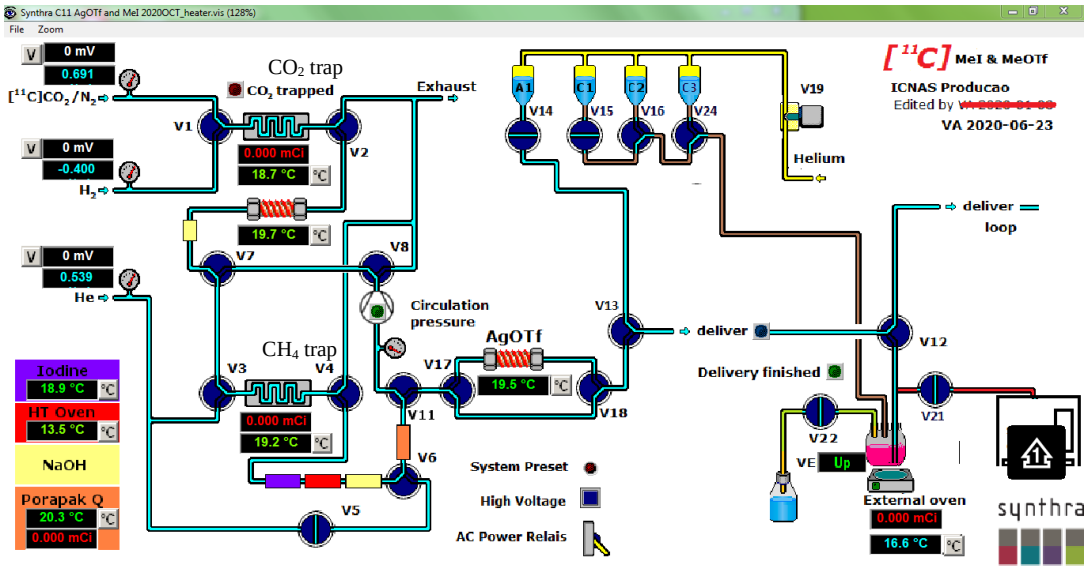

Figure 3.4: User interface of the SynthraView Software on the Synthra [^{11}C]Choline module used for the radiosynthesis of [^{11}C]CH_3I.

Before receiving the activity produced at the cyclotron, the column where the [^{11}C]CO_2 will be trapped is cooled at -180ºC, with liquid nitrogen, to collect all the activity. After trapping, the column is heated up to 50ºC and the [^{11}C]CO_2 is converted to [^{11}C]CH_4 by allowing it to react with H_2, on a nickel catalyst, at 425 ºC. After this reaction, water and unreacted [^{11}C]CO_2 are removed by an intermediate NaOH column and the [^{11}C]CH_4 is collected with a trap, previously cooled at -120ºC with liquid nitrogen. This trap is then heated to 120ºC to release the [^{11}C]CH_4 which will react with gaseous I_2, at 750ºC yielding [^{11}C]CH_3I which is collected on a Porapack® cartridge.

In **Figure 3.5** we present the [^{11}C]CH_3I production activity profile as measured in the different components, along the synthesis: [^{11}C]CO_2 trap, [^{11}C]CH_4 trap and Porapack® cartridge.

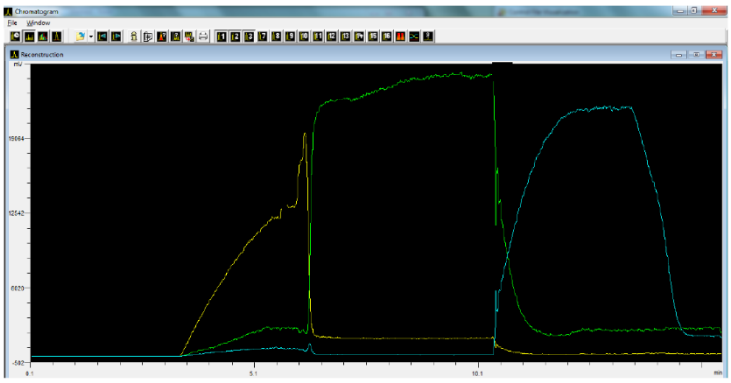

Figure 3.5: [^{11}C]CH_3I production activity profile during the synthesis as measured in the different components: [^{11}C]CO_2 trap (yellow), [^{11}C]CH_4 trap (green) and Porapack® cartridge (blue).

Just before the implementation of this process, labelling with [^{11}C]CH_3I or [^{11}C]CH_3OTf was performed at room temperature using the *"loop*". The process was not efficient, so we decided to install a reactor, coupled to the Synthra [^{11}C]Choline, referred to as "Synthra reactor" (**Figures 3.2** and **3.3**). Besides heating, this new device also allows us to stir the solution.

Produced [^{11}C]CH_3I is released using a helium flow of 5 mL/min to the Synthra reactor or to a remote microwave cavity.

Before the labelling experiments, HPLC methods for analytical analysis and purification were optimized.

3.1.3 Optimization of HPLC conditions

Analytical conditions

Chemical and radiochemical analysis were performed by analytical HPLC. Firstly, to optimize the analytical methods, standards of product, **3.3** and possible impurities, **3.1** and **3.4**, and [^{11}C]CH_3I, were injected. The wavelength selected was 254 nm. In **Figure 3.6** we present the structures of the injected standards.

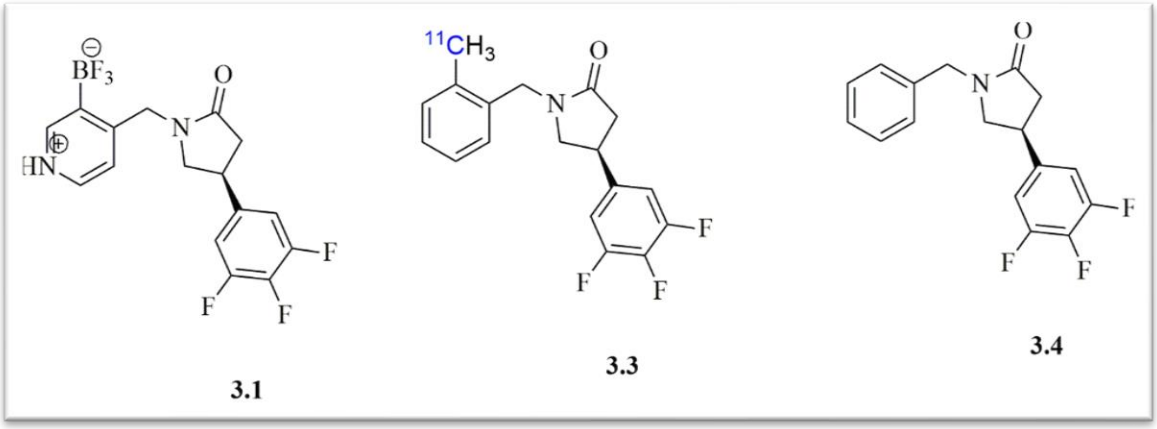

Figure 3.6: Structures of possible molecules present at [^{11}C]UCB-J final solution, identified by HPLC.

Initial optimizations were performed using a Zorbax Eclipse XDB-C18 (4.6x250mm, 5µm) analytical column. The choice of mobile phase, a mixture of acetonitrile (ACN), ammonium formate (AMF) and acetic acid, was based in the previously reported procedures and adapted to the described column [145,201]. Different percentages of this solvent mixture and flows were tested and the results are presented in **Table 3.2**.

Considering the results presented in **Table 3.2**, the main problem is the weak separation between compounds **3.3** and **3.4** which is, at best, 1 second (**Table 3.2, Entries 3** and **4**).

Table 3.2: Optimization of analytical HPLC conditions for analysis using the Zorbax Eclipse XDB®-C18 column.

Entry	Mobile Phase (v/v)	Flow, mL/min	Rt, 3.1, (minutes)	Rt, 3.3, (minutes)	Rt, 3.4, (minutes)	Rt, [^{11}C]CH_3I, (minutes)
1	38 % ACN 62 % 0.1M AMF 0.5 % acetic acid	2	1.9	1.3	nd	3.2
2	38 % ACN 62 % 0.1M AMF pH=3.5, adjusted with acetic acid	2	1.9	1.3	1.3	3.2
3	38 % ACN 62 % 0.1M AMF pH=3.5, adjusted with acetic acid	1.5	2.5	1.7	1.8	nd
4	38 % ACN 62% 0.1M AMF pH=3.5, adjusted with acetic acid	1.0	nd	2.5	2.6	nd

ACN: acetonitrile; AMF: ammonium formate; nd: not determined; Rt: retention time.

To improve the separation between **3.3** and **3.4,** the XBridge® C18 column[202] was tested, using as mobile phase a mixture of acetonitrile and NaH_2PO_4 10 mM solution, at different relations and flows. The results are presented in **Table 3.3**.

In the first two methods tested (**Table 3.3**, **Entries 1** and **2**), the retention time of UCB-J was 17.7 and 14.1 minutes, respectively. In practice, theses times were too long for a radiopharmaceutical labelled with carbon-11, a radionuclide with a half-life of 20.4 minutes. For molecules labelled with short lived radionuclides, it's very important to find a compromise between a good separation and a "fast" run. A retention time of 17 minutes is almost one half-life of the radionuclide.

The third method tested (**Table 3.3**, **Entry 3**), was reasonable. With an increase of 5 % in ACN, we managed to advance the retention time (Rt) of the product more than 3 minutes, keeping a good separation from the other impurities.

Table 3.3: Optimization of analytical HPLC conditions using the XBridge® C18 column.

Entry	Mobile Phase (v/v)	Flow (mL/min)	Rt, 3.1 (minutes)	Rt, 3.3 (minutes)	Rt, 3.4 (minutes)	Rt, $[^{11}C]CH_3I$ (minutes)
1	70 % NaH_2PO_4 10 mM 30 %ACN	0.8	nd	17.7	13.4	nd
2	70 % NaH_2PO_4 10 mM 30 %ACN	1	nd	14.1	10.7	nd
3	65 % NaH_2PO_4 10 mM 35 % ACN	1	4.9	8.1	6.3	6.2
4	60 % NaH_2PO_4 10 mM 40 % ACN	1	3.4	5.1	4.3	5.5

ACN: acetonitrile; AMF: ammonium formate; nd: not determined; Rt: retention time.

The best separation between the different analytes, using the XBridge® C18 column, was obtained when 60 % NaH_2PO_4 10 mM/40 % ACN was used as mobile phase, with a flow of 1 mL/min (**Table 3.3, Entry 4**). The peaks with the closest retention time were the **3.3** and CH_3I, with a relative retention time of 26 seconds. However, for quality control of the final product, this is not an issue because the $[^{11}C]CH_3I$ intermediate never appears in the final product vial. As $[^{11}C]CH_3I$ is a volatile compound (boiling point of 42ºC), and the reactions are heated and stirred in an open vessel, any unreacted $[^{11}C]CH_3I$ would evaporate. Even if it manages to remain in solution after the reaction, two additional purification steps are performed, semi-preparative and SPE, which will be discussed in the next sections. However, when a new process is developed, all the possibilities must be considered.

These conditions were then selected to perform the quality control of $[^{11}C]$UCB-J final solution. In **Figure 3.7** we present the chromatograms of the standards, injected using the selected method (**Table 3.3**, **Entry 4**).

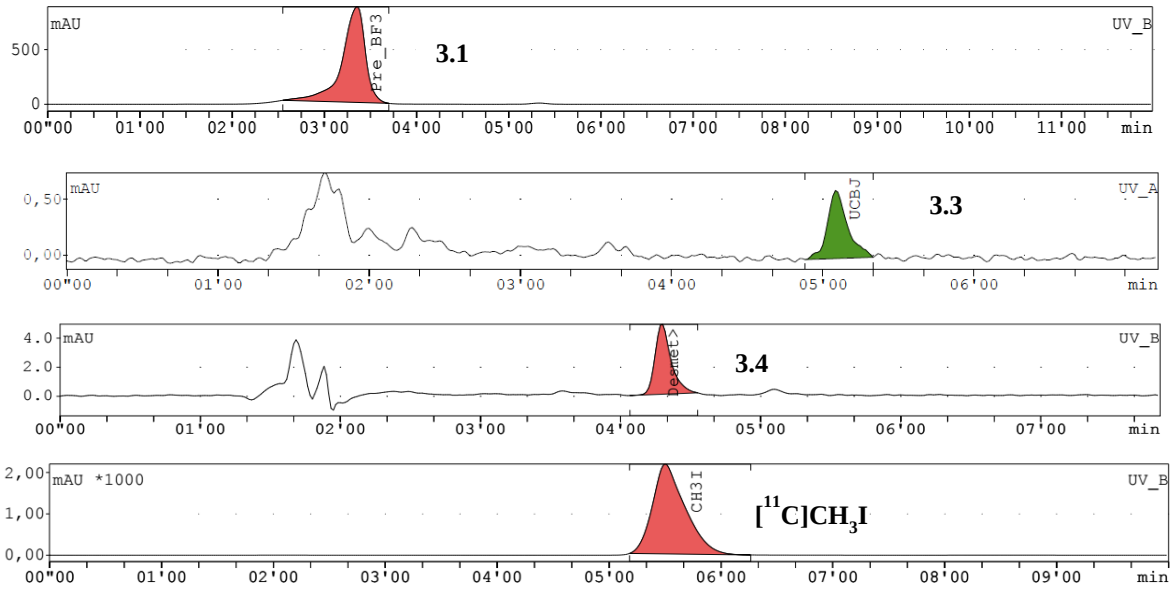

Figure 3.7: Chromatograms of standards, **3.1**, **3.3**, **3.4** and [11C]CH3I at selected [^{11}C]UCB-J analytical method. Mobile Phase: 60 % NaH2PO4 10 mM/40 % ACN, flow 1 mL/min, λ=254 nm.

The impurity desmethyl UCB-J, **3.4**, originating from the desmethylation of the unreacted precursor, is probably the major chemical side product. This impurity has high SV2A affinity, and, because of this, its concentration should be lower than 1.5 µg/dose. Furthermore, also for [^{11}C]UCB-J **3.3**, the maximum allowed dose is 10 µg/dose. This limit was stablished based on an animal toxicity studies [202].

Despite the precursor molecule **3.1**, already having a chiral center, to be sure that the enantiomeric purity of the molecule was kept, optimization of a chiral method was performed using a chiral HPLC column, a Chiralpack IA-3® (4.6x150mm), by the injection of 20 µL of both the enantiomers (*R*) and (*S*)-UCB-J.

The mobile phase tested was a mixture of 75 % *n*-hexane/25 % ethanol/0.1 % NEt_3 at different flows. Results are present in **Table 3.4**.

Table 3.4: Optimization of chiral HPLC conditions for the Chiralpack IA-3® column.

Entry	Mobile Phase (v/v)	Flow (mL/min)	Rt of (*S*) enantiomer (minutes)	Rt of (*R*) enantiomer, (minutes)
1	75 % *n*-hexane 25 % ethanol 0.1 % Net_3	1	3.9	4.3
2	75 % *n*-hexane 25 % ethanol 0.1 % NEt_3	0.7	7.3	9.7

NEt_3 – triethylamine; Rt: retention time.

Firstly, the enantiomers are injected separately, and after, the mixture is analyzed. In **Figure 3.8** we present the chromatogram obtained by injecting the mixture of both enantiomers, (*R)* and (*S)*-UCB-J with conditions as presented in **Table 3.4, Entry 2**.

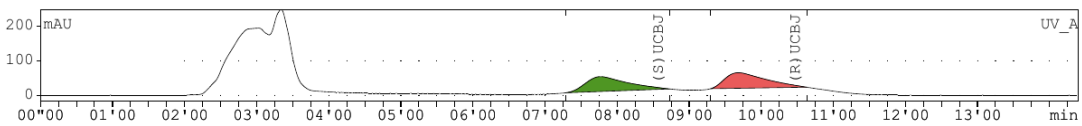

Figure 3.8: Chromatogram of a mixture of enantiomers (*R*) and (*S*)-UCB-J.

The retention time of the *(R*) enantiomer in the radiation detector was similar of that obtained at the UV detector with the injection of standard. The *(R*) enantiomer of [^{11}C]UCB-J in the final solution, has an enantiomeric purity of 100 %.

Semi-preparative purification conditions

As mentioned in **Section 3.3**, [^{11}C]UCB-J synthesis was performed *via* Pd-mediated Suzuki cross-coupling. At end of labelling, all the reagents, $Pd_2(dba)_3$, $P(o\text{-}tol)_3$, K_2CO_3, unreacted precursor, [^{11}C]CH_3I, or side products of reaction can be present in the final solution. The reaction mixture is then purified by semi-preparative chromatography.

For this purpose, optimization of the semi-preparative purification method was performed, by injecting the standards: UCB-J precursor **3.1**, non-radioactive UCB-J **3.3** and CH_3I.

The semi-preparative column was installed in the AllinOne module, which is equipped with a 10 mL injector in the loop, a UV detector and a radiation detector, the same described in **Chapter 2** for the purification of the [^{18}F]FDOPA mixture. Two different semi-preparative columns were tested, a Sunfire™C18 OBD Prep column and a Phenomenex Luna™ C18(2). In

Table 3.5 were presented the conditions tested for the semi-preparative purification by the injection of standards.

Table 3.5: Optimization of semi-preparative HPLC conditions for the purification of [^{11}C]UCB-J, **3.3**, reaction mixture.

Entry	Column	Mobile Phase (v/v)	Flow (mL/min)	Rt of 3.1, (minutes)	Rt of 3.3, (minutes)	Rt of CH_3I, (minutes)
1	Sunfire™C18 OBD Prep	35 % ACN 65 % 0.1M AMF 1.3 % NaOH	2 (first 2 minutes) 5 (after)	7.0-8.0	13.0	12.0-13.0
2	Sunfire™C18 OBD Prep	40 % ACN 60 % 0.1M AMF (pH=10, with 37 % ammonia)	5	5.0-6.0	7.0-9.0	12.0-15.0
3	Sunfire™C18 OBD Prep	40 % ACN 60 % 0.1M AMF	5	5.0-6.0	7.0-9.0	10.0-12.0
4	Phenomenex Luna™ C18(2)	40 % ACN 60 % 0.1M AMF	5	5.0-6.0	9.0-10.0	6.0-7.0

ACN: acetonitrile; AMF: ammonium formate; nd: not determined; Rt: retention time.

The first semi-preparative column tested was the Sunfire™C18 OBD Prep. The mobile-phases tested were based in previously described procedures [145,201,202] (**Table 3.5, Entries 1** and **2**). The first one tested (**Table 3.5**, **Entry 1**) shows poor separation between **3.3** and CH_3I, but the second one works quite well (**Table 3.5**, **Entry 2**).

After the labelling reaction, which will be described in **Section 3.1.5**, the quenching was performed with HCl 1M, making the reaction media quite acidic. Instead of neutralizing the reaction media, authors report the use of a mobile phase with pH around 10. However, due to several technical problems with some parts of the semi-preparative pump, due to the high pH, the

same solvent mixture, without pH adjustment was tested (**Table 3.5, Entry 3**). The retention times of all standards are kept.

The same solvent mixture was tested in the semi-preparative column Phenomenex Luna™ C18(2) (**Table 3.5**, **Entry 4**). However, the retention times of the product **3.1** and CH_3I were very similar.

The best separation was obtained with conditions presented in **Table 4.5**, **Entry 3** and this option was selected for further tests.

The main purpose of the semi-preparative purification was to isolate the product **3.3**. However, when we collect the peak of the [^{11}C]UCB-J, it is present in a mixture of the semi-preparative mobile phase solvents, not as an injectable solution. Therefore, after the collection of the peak, a reformulation of the product is performed to obtain an injectable solution for human use.

In the next section, we will describe the optimization of the reformulation conditions.

3.1.4 Optimization of reformulation conditions

Another parameter optimized was the choice of the best column to eliminate the mobile phase components, in which the product was dissolved, after collection from the semi-preparative purification. Usually, this second purification is performed by concentrating the product in a Sep-Pack cartridge to separate if from the mobile phase.

To evaluate the most adequate Sep-Pack column to purify the collected product, three different C18 Sep-Pack columns were tested: C18 Plus, tC18 Plus and a C18 light cartridges. All the columns are pre-activated with 10 mL ethanol, 10 mL of water and dry with air before use. To assure that the losses are minimized, each column are loaded with the solution of [^{11}C]UCB-J collected from the semi-preparative and diluted with 10 mL of water. Typically, are collected between 5 to 10 mL of mobile phase, which as to be diluted with water to assure that the column retains the product.

The efficiency of the column was calculated by the ratio between the activity loaded and the activity at final product vial. In **Figure 3.9** we present the percentage of [^{11}C]UCB-J **3.3** at final product vial, for each column tested.

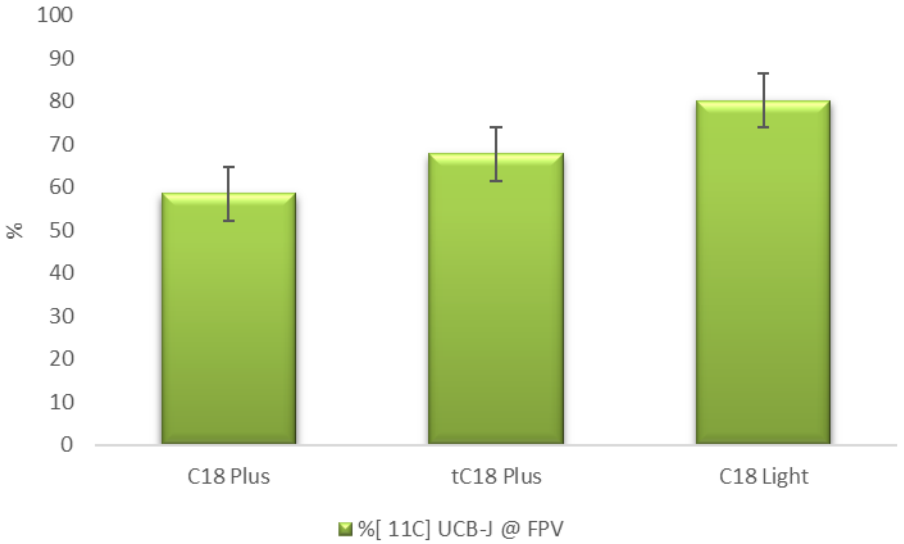

Figure 3.9: Efficiency of three C18 Sep-Pack cartridges in [^{11}C]UCB-J purification.

According **Figure 3.9**, the more efficient column for this process was the Sep-Pack C18 light cartridge, with a [^{11}C]UCB-J recovery of 80 %. This cartridge was selected for further tests.

After optimization of all the analytical analysis and the purification and reformulation steps, we proceed with the optimizations of the labelling reaction by conventional and microwave heating.

3.1.5 Labelling of [^{11}C]UCB-J

As already mentioned, synthesis of [^{11}C]UCB-J **3.3**, was performed by Suzuki-Miyaura cross-coupling, by the reaction of BF_3-Dm-UCB-J, **3.1**, or a mixture of this with the corresponding boronic acid derivative, **3.2**. The mechanism of these reactions, already described in **Chapter 1** (**Scheme 1.9**), starts with an oxidative addition of the [^{11}C]CH_3I to Pd(0). followed by a transmetallation, and by a reductive elimination to yield the product [^{11}C]UCB-J, **3.2**.

Compared with the simple methylation reactions which were previously performed at ICNAS-P, this labelling process was challenging, not only in terms of chemical synthesis, but also because it required different reaction conditions, such as temperature and stirring.

Taking into account the already reported synthesis procedures[145,201,202], **Section 3.1**, (**Table 3.1**), the main differences between the methods tested were:

- The order of addition of the precursor, before or after trapping of [^{11}C]CH_3I
- Precursor species, BF_3-Dm-UCB-J **3.1**, or a mixture of the two species, **3.1** and the corresponding boronic acid derivative **3.2**
- The solvent mixture, organic solvent/H_2O (8:1).

All these parameters were tested using the two different heating methods: conventional and microwave.

3.1.5.1 Labelling reaction general procedure

As already presented, to obtain a mixture of **3.1** and **3.2**, the precursor **3.1** was stirred in MeOH and HCl 1M, at 60ºC for 1 hour, to give the boronic acid derivative, **3.2** (**Scheme 3.1**). Then, the mixture was dried and the solid redissolved in the solvent mixture which was after used in the ^{11}C-labelling. This reaction was performed right before the production. The use of the precursor activated in the previous days, usually gave poor results.

To assure that the conversion of **3.1** in **3.2** occurs, the final product, of two different hydrolysis reactions, were analysed by ^{1}H-NMR and ^{19}F-NMR. By analysing the respective spectrums, we conclude that the ratio **3.1**:**3.2**. was 2:1, respectively. In fact, previous studies[202] have shown that 3-10 % of the boronic acid derivative, **3.2**, was enough to improve the labelling yield[201].

In general, $Pd_2(dba)_3$, P(*o*-tol)$_3$ and K_2CO_3 are diluted with the solvent mixture resulting in a dark red solution (**Figure 3.10**, **left**). Then, a solution of precursor **3.1** or the resulting mixture of **3.1**/**3.2** was added to the first solution and stirred at 40ºC to form the complex. The solution must pass from the dark red color to a light yellow (**Figure 3.10, right**), due to the alteration of oxidation state of palladium. Usually, this color change takes less than 5 minutes. If the color doesn't turn light yellow, another solution must be prepared, with new reagents.

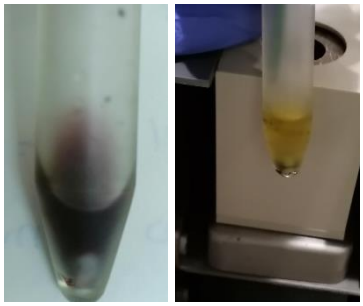

Figure 3.10: Evolution of the color of the reactor solution.

When the solution is light yellow, the hot cell is closed and the [^{11}C]CO_2 is transferred to start the production of [^{11}C]CH_3I, as described is **Section 3.1.2**.

[^{11}C]CH_3I is trapped in the solution at room temperature. When the activity peaks, the reactor is heated to the desire temperature ant is stirred during the reaction time. At the end, the reactor is cooled down to 25ºC and 1 mL of HCl 1M is added to stop the reaction. A solution of 40 % ACN / 60 % 0.1M AMF, pH=10, adjusted with 37 % ammonia, is added to neutralize the acidic solution. Before purification, the solution is filtered to remove the Pd particles present. The quenching and filtration steps are performed using an IBA Synthera Extension® automated module (**Figure 3.11, A**), with a disposable kit installed in a dedicated cassette (**Figure 3.11, B**).

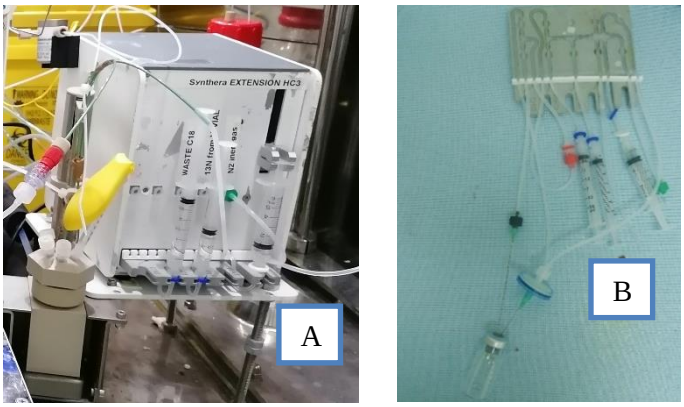

Figure 3.11: IBA Synthera Extension®, automated module used for quenching of reaction. **A**: quenching kit installed with all the necessary reagents, tubes, and connections; **B**: disposable kit installed in the dedicated cassette.

After, the filtered solution is transferred to another vial located at the hot cell housing the AllinOne® synthesis module (**Figure 3.12**, **top**). The purification and formulation process is controlled by a script developed specifically for this purpose for the software Trasis Supervision® (**Figure 3.12, bottom**).

The disposable kit is composed by:

i. 3 in line manifolds with 6 valves each
ii. 3 work syringes located at positions 3, 9 and 15
iii. a syringe with semi-preparative mobile phase, at position 5
iv. a bag with water for injections (WFI)
v. a collect vial
vi. Sep-Pack C18 column
vii. 1 mL of ethanol
viii. 9 ml of NaCl 0.9 %, and a final product vial.

All the components are installed before starting the synthesis. When all the activity arrives to the first vial (*"From Synthera Extension")*, the script is activated to start the purification. The content of the vial is injected in the semi-preparative loop, followed by injection of another 1 ml of mobile phase (pH=10) to clean lines. The product, **3.3**, is collected between 7 to 9 minutes to the collection vial.

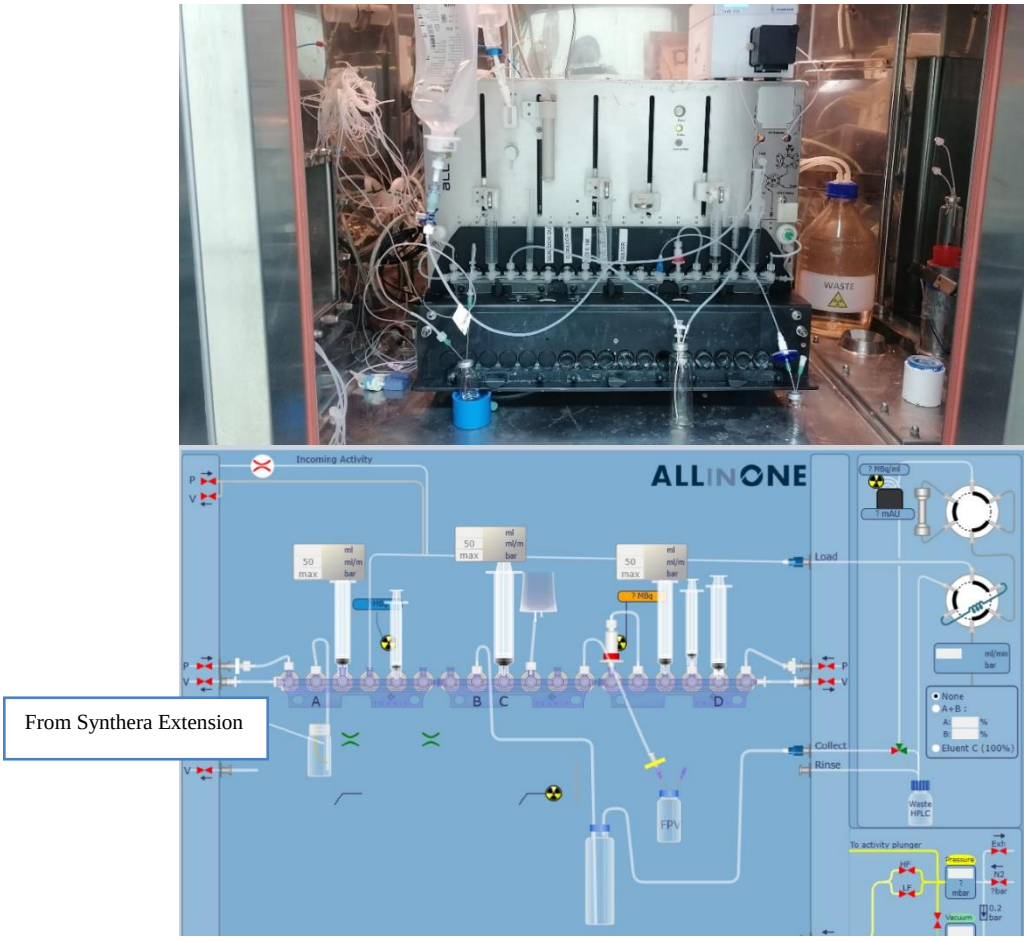

Figure 3.12: Layout of AllinOne® to perform purification and reformulation of [^{11}C]UCB-J.

An example of a semi-preparative HPLC chromatogram obtained with the radioactivity detector is illustrated in **Figure 3.13**.

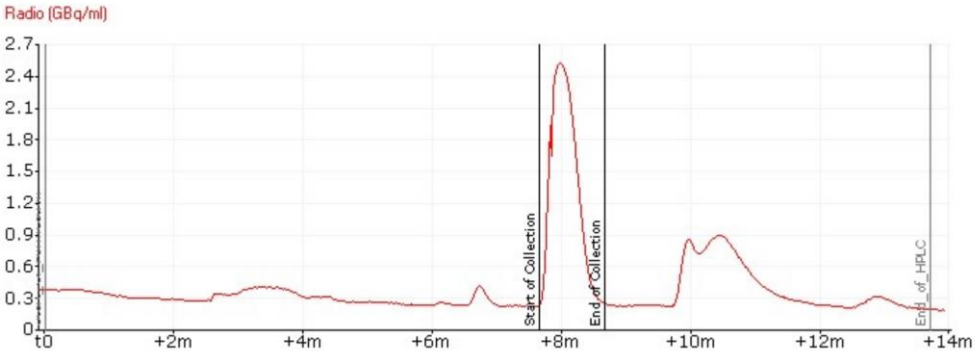

Figure 3.13: Radioactivity semi-preparative chromatogram of [^{11}C]UCB-J.

The collected peak corresponding to [^{11}C]UCB-J **3.3** is diluted with 10 mL of water for injectables (WFI) and is retained in a C18 Sep-Pack, as the mobile phase goes to the waste. Then, the column is cleaned with an additional 10 mL of WFI to assure that all the mobile phase components and any [^{11}C]CH_3I present goes to the waste. After, the Sep-Pack is dried with nitrogen for 1 minute and the [^{11}C]UCB-J, **3.3,** is eluted with 1 mL of ethanol to the final product vial through a 0.22 µm sterile filter. Then, the product is reformulated with 9 mL of saline solution (NaCl, 0.9 %), yielding an injectable solution of [^{11}C]UCB-J **3.3**.

The radiochemical yields (RCY's) are calculated by the ratio between the activity measured at final product vial at end of synthesis (EOS), decay corrected (dc) to [^{11}C]CH_3I, measured in the Porapack® cartridge.

3.1.5.2 Optimization of [^{11}C]UCB-J labelling conditions, by conventional heating

Initially, we tried to follow the process reported by Nabulsi [207] and Sephton [202], described in **Section 3.1**, in which the precursor **3.1** is added to the solution after [^{11}C]CH_3I trapping in the reactor. However, in our case, no conversion was observed.

Further reactions were all performed by trapping [^{11}C]CH_3I in the reaction mixture which already contains the precursor, as described in **Section 3.1.5.1**.

The influence of precursor hydrolysis (**Table 3.6**, **Entries 1** and **2, 7** and **9**, and, **11** and **12**), reaction times (**Table 3.6**, **Entries 2** and **3** and **Entries 4** and **5**), reaction temperature (**Table 3.6**, **Entries 2** and **5** and **Entries 3** and **4**) were evaluated using different solvent mixtures, at different reaction temperatures and times.

In **Table 3.6** we present the optimization results obtained when the reaction was performed using conventional heating.

Table 3.6: Optimization of [^{11}C]UCB-J reaction conditions using conventional heating.

Entry	Precursor	Time (minutes)	Temperature (ºC)	Solvent mixture[a]	RCY[b] (%)	n[c]
1	**3.1**	5	100	DMF/H_2O	3.0	1
2	**3.1/3.2**	5	100	DMF/H_2O	13.6	1
3	**3.1/3.2**	10	100	DMF/H_2O	23.6	1
4	**3.1/3.2**	10	60	DMF/H_2O	32.6	1
5	**3.1/3.2**	5	60	DMF/H_2O	5.5	1
6	**3.1**	10	70	THF/H_2O	3.7	1
7	**3.1**	5	60	THF/H_2O	12.9	1
8	**3.1/3.2**	5	70	THF/H_2O	7.0	1
9	**3.1/3.2**	5	60	THF/H_2O	40.4	1
10	**3.1/3.2**	10	60	THF/H_2O	12.7	1
11	**3.1**	10	80	DME/H_2O	0.2 ± 0.2	2
12	**3.1/3.2**	**10**	**80**	**DME/H_2O**	**53.6 ± 0.4**	**3**
13	**3.1/3.2**	5	80	DME/H_2O	20.1 ± 1.5	2
14	**3.1/3.2**	10	60	DME/H_2O	2.5	1
15	**3.1/3.2**	5	80	DME	11.9	1

[a] organic solvent/water (8:1). [b] RCY reformulated, based in [^{11}C]CH_3I. [c] number of experiments.

Conditions were based on the methods reported in the literature[145,201,202], adapted to our specific procedures.

Considering the results presented in **Table 3.6**, it's clear that, independently of the solvent mixture used, the RCY increase when we use the mixture containing the boronic derivative precursor **3.1/3.2 (Table 3.6**, **Entries 1** and **2**, **7** and **9** and, **11** and **12)**.

Suzuki-Miyaura coupling is a palladium catalysed reaction between an halide or a pseudohalide (R_1-X, where X=I, Br, OTf, etc) with an organometallic compound, usually with the generic structure $B(OR)_2$[136]. The -BF_3 group BF_3-Dm-UCB-J **3.1**, is not a usual precursor for this type of reaction. Nevertheless, the results obtained in **Table 3.6** are in line with the previously described in the literature [201,202].

Initial optimizations were performed with the mixture DMF/H_2O (8:1), according to Nabulsi and Sephton work [145,202] (**Table 3.6**, **Entries 1** to **5**). Based on the previous results reported with this solvent mixture [145,202], the reaction was stirred at 100ºC for 5 minutes (**Table**

3.6, **Entries 1** and **2**). Using as precursor the mixture **3.1**/**3.2**, in the referred conditions, the RCY achieved was 13.6 %. Nevertheless, when the reaction time was increased to 10 minutes, the RCY increased to 23.6 % (Table **3.6**, **Entry 3**). Considering the reaction time, at the same temperature (60 ºC), the RCY decreased to 5.5 % when the reaction was stirred for only 5 minutes, (**Table 3.6**, **Entry 5**).

Based in the Rokka procedure[201], the mixture THF/H_2O (8:1) was also tested (**Table 3.6**, **Entries 6** to **10**). The authors performed the reaction at 70ºC. However, reaction in the Synthra reactor is performed on an open vessel which limits the temperature due to the boiling point of the solvent. To compare the influence of the solvent, at a constant temperature, a lowest temperature of 60 ºC, limited by the boiling point of THF (66 ºC), was selected for all the solvent mixtures tested, (**Table 3.6, Entries 4**, **5**, **7**, **9**, **10** and **14**).

In the case of DMF/H_2O (8:1), the temperature reduction from 100ºC to 60ºC, also increased the RCY to 32.6 %, **Table 3.6**, **Entry 4**, in 10 minutes.

We started to test THF/water (8:1) at 70 ºC, based on previously reported procedures[201], however, as our reactor is not closed, the activity was lost during the reaction (**Table 3.6**, **Entries 6 and 8**). Using the same reaction conditions, but at 60 ºC, the RCY's increased from 3.7 to 12 % and from 7 to 40 % (**Table 3.6**, **Entries 6** and **7** and, **8** and **9**) with precursor **3.1** and mixture **3.1/3.2**, respectively. Keeping the same conditions but increasing the reaction time from 5 to 10 minutes (**Table 3.6**, **Entry 10**) resulted in a decrease in the RCY, from 40.4 % to 12.7 %.

To understand the effect of a similar solvent which allows us to perform the reaction at higher temperatures we decided to try DME, which has a boiling point of 85ºC instead of the 66ºC of THF, a linear ether. The results are presented in **Table 3.6** (**Entries 11** to **14)**. DME allows us to perform the reaction at 80ºC, without significative losses when the temperature of the reaction is increased. The reaction performed in the solvent mixture DME/H_2O (8:1) at 80 ºC yields [^{11}C]UCB-J **3.3** with a RCY of 53.6 ± 0.4 %. The reduction of temperature to 60 ºC, keeping the same conditions, decreases the RCY to only 2.5 %.

The use of DME alone as solvent (**Table 3.6, Entry 15**), resulted in a reduction of 50 % in RCY due to the low solubility of the K_2CO_3 in DME. Furthermore, we don't dry the solvents previously, so the 11 % of conversion obtained is probably due to the presence of some water in solution.

Moreover, the effect of reaction time was also tested. And, when the solvent mixtures DMF and DME/H_2O (8:1) were used, the RCY (dc), increased from 5 to 10 minutes (**Table 3.6**, **Entries 2** and **3**, **5** and **4**, **10** and **9** and, **13** and **12**). However, the same doesn't happen with the solvent mixture THF/H_2O (8:1) (**Table 3.6**, **Entries 9** and **10**), where a decrease in the RCY from 40.4 % to 12.7 % was observed.

Additionally other palladium system, Pd(II)acetate, was tested. The main difference is that we start with Pd(II) instead of Pd(0). Palladium (II) acetate ($Pd(OAc)_2$), triphenylphosphine

(PPh_3) in the presence of the same base, K_2CO_3 was tested, however, the conversion was only 6 %.

In conclusion, the best conditions, using conventional heating, were the presented in **Table 3.6**, **Entry 12**, using DME/water as solvent mixture and 10 minutes of reaction time. This yielded [^{11}C]UCB-J with 53.6 ± 0.4 % of RCY and A_m of 369.7 ± 68.17 GBq/µmol. The total synthesis time was 55 minutes, from EOB and 49 minutes from [^{11}C]CH_3I.

To improve the RCY and to reduce the reaction time, optimization by microwave heating was performed, which will be discussed in the next section.

3.1.5.3 Labelling of [^{11}C]UCB-J with microwave-heating

The advantages of microwave heating over conventional heating were already discussed, in **Chapter 2**, for ^{18}F-radiochemistry. Considering that carbon-11 has an even shorter half-life (20.4 minutes), any reduction in reaction times can have an even greater impact in the activity obtained at the final product vial.

The use of microwave heating in some Pd-mediated Suzuki coupling reactions was already described in **Chapter 1**, with good results in the synthesis of [^{11}C]toluenes [137] and [^{11}C]M-MTEB [146]. These reactions were performed using a dynamic method, with 50 watts, for 1.5 minutes. Based on this and on our previous experience with ^{18}F-fluorination, two different microwave heating methods were used, Power Cycling (PC) and dynamic.

The synthesis procedures were the same as described in **Section 3.1.5.2** but, instead of a reactor, we used a microwave cavity to perform the ^{11}C-labelling reaction. Furthermore, due to the established advantage of using the precursor mixture **3.1**/**3.2**, for microwave heating optimizations only this mixture was used.

We started by testing the dynamic heating method. The reactional mixture, dissolved in a mixture DME:H_2O (8:1), was heated during 4 minutes, at 70 watts, yielding the reformulated product **3.3,** with a RCY of 29 % (dc to [^{11}C]CH_3I). This is less 24 % than what we obtained under similar conditions with conventional heating (**Table 3.6**, **Entry 12**).

As described in **Chapter 2**, the microwave heating which gave better results was the Power Cycling, in which heating intervals (power) are alternated with cooling intervals for a certain period of time. The intervals, as well as the maximum and minimum temperatures and the power are defined by the operator.

The PETwave® doesn't allow us to control the pressure. Therefore, similarly to the tests with conventional, heating was performed using an open vial. In **Figure 3.14** we present an image of the microwave cavity of the PETwave® with the reactor installed.

Figure 3.14: PETWave® microwave cavity with reactor installed.

This technical issue led us to adapt the reaction temperatures to the boiling point of the solvents used. The same solvents used in conventional heating, DMF, DME and THF, where tested also in the microwave-assisted Pd-catalysed synthesis of [^{11}C]UCB-J **3.3**.

Four different Power Cycling (PC) microwave heating methods were used. Those were the following:

- **Method 1 (PC1)**: Power: 50 watts; heating: 60 seconds; cooling: 2 seconds; maximum/minimum temperatures: 80/60ºC; number of cycles: 6.
- **Method 2 (PC2)**: Power: 50 watts; heating: 60 seconds; cooling: 2 seconds; maximum/minimum temperatures: 70/50ºC; number of cycles: 6.
- **Method 3 (PC3)**: Power: 50 watts; heating: 60 seconds; cooling: 2 seconds; maximum/minimum temperatures: 170/120ºC; number of cycles: 6.
- **Method 4 (PC4)**: Power: 50 watts; heating: 60 seconds; cooling: 2 seconds; maximum/minimum temperatures: 120/90ºC; number of cycles: 6.

In **Table 3.7** we present the results obtained with the microwave-assisted [^{11}C]UCB-J synthesis.

Table 3.7: Optimizations of microwave-assisted of [^{11}C]UCB-J synthesis.

Entry	Precursor	PC Method	Time (minutes)	Solvent mixture	RCY[a] (%)	n[b]
1	**3.1/3.2**	PC1	5.4	THF/ H_2O	3.2	1
2	**3.1/3.2**	PC2	4.2 ± 1.3	THF/ H_2O	17.8 ± 1.4	2
3	**3.1/3.2**	PC1	1.7	DMF/ H_2O	25.9	1
4	**3.1/3.2**	PC3	7.5	DMF/ H_2O	41.5	1
5	**3.1/3.2**	PC4	2.7	DMF/ H_2O	38.9	1
6	**3.1/3.2**	PC1	4.73 ± 0.86	DME/H_2O	53.03 ± 5.09	3

[a]RCY reformulated and decay corrected to [^{11}C]CH_3I.[b] Number of experiments.

Considering the capacity of the solvents to convert dielectric energy into heat, we expected the best results to be achieved with the mixture DMF/water (8:1).

The Power Cycling microwave heating **Method 1 (PC1)**, described previously, was tested with all the solvents mixtures evaluated. In THF/water (8:1) the RCY was only 3.2 % (**Table 3.7**, **Entry 1**). Considering the boiling point of this solvent, **Method 2 (PC2)**, with maximum temperature of 70ºC, and minimum of 50ºC was also tested (**Table 3.7**, **Entry 2** and, the RCY's increases to 17.8 ± 1.4 % (**Table 3.7**, **Entry 2**).

Considering the solvent mixture DMF/water (8:1), the best results obtained were with **Method 3 (PC3)**, (**Table 3.7**, **Entry 4**), however, similarly to the results obtained by conventional heating, the best results were obtained with the solvent mixture DME/H_2O (8:1) (**Table 3.7**, **Entry 6**). Comparing with similar conditions in conventional heating, we observe that the dc RCY (53.3 ± 5.09 %) was similar than the one obtained in the conventional heating (53.6 ± 0.4 %). Moreover, the total synthesis time was 49.7 minutes, instead of the 55 minutes in conventional heating. This represents a 20 % increase in the activity at the final product vial at EOS when compared with the conventional heating.

After optimization of the reaction conditions, the best one, presented in **Table 3.7** (**Entry 6**), was selected for further tests and three consecutive batches were produced and subjected to quality control to validate the injectable solution of [^{11}C]UCB-J formulated in a sterile saline solution with 10 % ethanol.

Besides the RCY's, another important parameter is the molar activity (A_m). Low A_m's represent the injection of "cold" (nonradioactive) compounds that compete for same the binding sites of the radiotracer, resulting on a poor quality of the final image.

As discussed in **Chapter 1**, the production of [^{11}C]CH_3I by the called "gas phase" leads to higher A_m's than those obtained with the "wet method". However, other factors such as the

precursor quantities and the long reaction times could result in a decrease of A_m's due to the decay of carbon-11.

The calculation of A_m is performed by the ratio between the activity at EOS per mol of compound. The moles of compound at the final solution can be calculated through a calibration curve (as described for [^{18}F]FDOPA, **2.1**, in **Chapter 2)** or by injecting a standard with a well know concentration value. The concentration of a certain sample is then determined by comparing it's peak area with the one of a standard solution. This was the approach used for [^{11}C]UCB-J as multiple HPLC systems were used throughout the tests.

The results for the three validation batches are presented in **Table 3.8**.

Table 3.8: Molar activities (A_m) of the three validation batches.

Batch	[^{11}C]UCB-J-1	[^{11}C]UCB-J-2	[^{11}C]UCB-J-3
Molar activity (A_m) (GBq/µmol)	396.7	267.5	433.0

* Decay corrected.

The injection of the standard is also used to confirm the identity of [^{11}C]UCB-J **3.3** peak and to assure that the concentration limits are respected. This will be discussed in the next section.

3.2 Quality Control of [^{11}C]UCB-J

To insure the quality of the product, quality control tests of [^{11}C]UCB-J were performed according to the procedures described in the European Pharmacopoeia (Eur. Ph.)[252]. The analytical details were described in **Chapter 5**.

After production, a vial containing 10 mL of [^{11}C]UCB-J injectable solution is sent to quality control where a visual inspection is performed, behind a lead shielded window, to assure that the solution is clear and colourless.

The pH of the product is measured. The value obtained for the injectable solution must be between 4.5 to 8.5.

Chemical, radiochemical, and enantiomeric purities are determined by analytical HPLC with the best conditions obtained by the optimization described in **Section 3.1.3**.

Radiochemical purity is determined as the percentage of the [^{11}C]UCB-J peak relative to other radiochemical impurities. Chemical purity is determined by quantification and relative comparison of the corresponding UV absorbance peaks of the QC samples and the reference standards of know concentrations. The reference solutions, at maximum allowed concentrations, are injected before the analysis, 10 ug /10 mL for UCB-J and 1.5 µg /10 mL for desmethylUCB-J. The limit for desmethylUCB-J is constrained to 1.5 µg /10 mL because this molecule competes

with UCB-J for the binding sites [202]. The limit imposed for UCB-J was based in animal toxicity studies[202].

Furthermore, the injection of UCB-J standard is also used to identify the product, by comparing the retention time of the standard with the corresponding [^{11}C]UCB-J, **3.3**, peak and, as discussed, to calculate the A_m of the final solution. In **Figure 3.15** we present an example of a chromatogram of the final solution of [^{11}C]UCB-J.

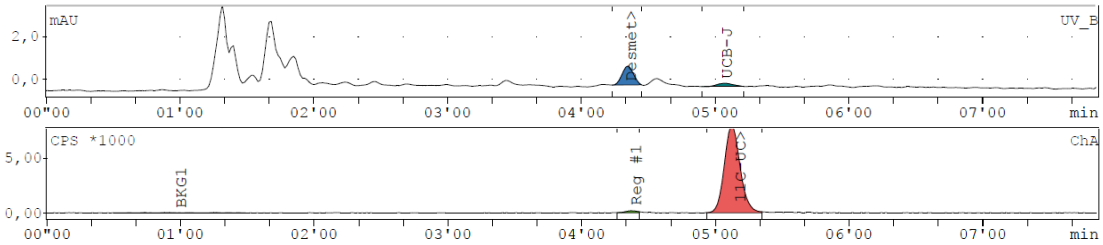

Figure 3.15: HPLC of a final solution of [^{11}C]UCB-J. Analytical column X-Bridge C18. Mobile Phase: 60 % NaH_2PO_4 10 mM/40 % ACN, flow 1 mL/min, λ=254 nm.

Enantiomeric purity was analyzed by HPLC using a chiral column, with the already described conditions. In the literature, a limit for the enantiomeric purity is not defined however, it should be determined because, as it was already reported for [^{18}F]UCB-H, the (*R*)-enantiomer has a 10-fold higher affinity to SV2A than the (*S*)-enantiomer [253]. We always obtained 100 % of the (*R*)-enantiomer. In **Figure 3.16** we present an example of a chiral chromatogram of the final solution of [^{11}C]UCB-J.

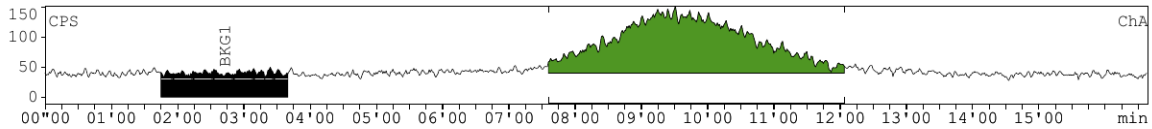

Figure 3.16: Chiral chromatogram of a final solution of [^{11}C]UCB-J.

Residual solvents were determined by gas chromatography according to the general chapter of Eur.Ph., "Residual Solvents" [231]. Acetonitrile is included in Class 2 and ethanol is included in Class 3, being limited to 4 and 2500 mg/10 mL, respectively.

Radionuclidic purity was confirmed by half-life determination and gamma ray spectroscopy. The gamma ray spectrum should only contain the 0.511 MeV line and, eventually, a sum peak at 1.022 MeV. The half-life was determined using a dose calibrator and the result must be between 19.9 and 20.9 minutes. The interval considers the error of the analysis.

As with any injectable solution, biological tests are mandatory. However, as with other radiopharmaceuticals, these tests are not required before injection and are performed after complete decay of radioactivity in solution. Bacterial endotoxins content is determined using the LAL test, and Sterility test is performed by an external certified laboratory. To confirm the biological safety of the final [^{11}C]UCB-J solution, three lots were analyzed.

In **Table 3.9** we present the specifications and results of the quality control for the three validation batches of [^{11}C]UCB-J injectable solution.

Table 3.9: Quality Control tests and specifications for [^{11}C]UCB-J injectable solution.

Tests	Specifications	[^{11}C]UCB-J 1	[^{11}C]UCB-J 2	[^{11}C]UCB-J 3
Appearance	Clear, colourless solution	Comply	Comply	Comply
pH after dilution	4.5 to 8.5	6	6	6
Chemical purity				
UCB-J	≤ 10 µg/10 mL	Comply	Comply	Comply
Desmethyl UCB-J	≤ 1.5 µg/10 mL	Comply	Comply	Comply
Total unidentified impurities	≤ 3 µg/10 mL	Comply	Comply	Comply
Radiochemical purity				
[^{11}C]UCB-J	≥ 95 %	100	99.6	100
Enantiomeric purity				
R enantiomer	Not defined	100	100	100
Radionuclidic purity				
Radionuclidic identification - Energy photons ϒ	The only gamma photons have energy of 0.511 MeV. A sum peak of 1.022 MeV may be observed	Comply	Comply	Comply
Half-life	19.9 to 20.9 min	20.1	20.3	20.3
Residual Solvents				
Ethanol	≤ 2500 mg/10 mL*	834.1	909.0	1172.8
Acetonitrile	≤ 4 mg/10 mL	0.0	0.0	0.0
Biological Tests				
Sterility[a]	No evidence of microbial growth should be found	Comply	Comply	Comply
Bacterial endotoxins[a]	≤ 175 IU /10 mL	Comply	Comply	Comply

* According to Ph. Eur., maximum 2.5g per administration taking the density (2.2.5) to be 0.790 g/mL[231].
[a] Product may be released for use before complexion of these tests.

Considering the results presented in **Table 3.9,** it is evident that the product can be produced with the required quality for human use.

3.3 Conclusions

Implementation of the [^{11}C]UCB-J synthesis process at ICNAS-P, was challenging mainly because of the complexity of the radiosynthesis, unlike any other process used by the group.

The effect of the solvent mixture was evaluated and the best conditions, using conventional heating, were achieved with the mixture DME/water, stirred at 80ºC for 10 minutes, yielding [^{11}C]UCB-J with 53.6 ± 0.4 % of RCY. The total synthesis time was 55 minutes, from EOB and 49 minutes from [^{11}C]CH_3I.

To optimize the [^{11}C]UCB-J process, microwave heating was tested during the ^{11}C-labelling reaction. The best results were obtained with the solvent mixture DME/H_2O (8:1) and the Power Cycling microwave heating method. The reaction was stirred during 4.73±0.86 minutes yielding [^{11}C]UCB-J with RCY of 53.03 ± 5.09 %, A_m of 369.7 ± 68.17 GBq/µmol and 100 % of the (*R*)-enantiomer.

With the microwave heating method, the total synthesis time was reduced to 49.7 minutes, with similar RCY's, a reduction that translated to 20% more activity produced.

The process was implemented at ICNAS-P and three runs of production and quality control were performed with all the batches conforming to the required specifications.

In summary, a robust automated and reproducible method was obtained that could be used for routine production.

Chapter 4

Conclusions and future perspectives

The biggest challenge of a radiopharmaceutical synthesis for PET imaging is the short half-life of the most common radionuclides, 109 and 20 minutes for ^{18}F and ^{11}C, respectively.

This PhD work had two main objectives:

1. First, the implementation, validation and improvement, by microwave heating, of a 6-[^{18}F]FDOPA synthesis process and its submission to the Portuguese pharmaceutical authorities to request a distribution authorization.
2. Second, the implementation and improvement of a [^{11}C]UCB-J synthesis process.

During the development of this work, a multistep 6-[^{18}F]FDOPA synthesis process, with RCY's of 28 ± 5.4% (ndc), and radiochemical purities ≥ 95 % performed in 90 minutes total synthesis time, was implemented.

Taking advantage of the knowledge/experience and high technical capacity of ICNAS-P, an innovative synthesis process of 6-[^{18}F]DOPA based in micro-wave technology was developed. Microwave technology is a very good tool to reduce the times and by-products of reactions. In radiochemistry, this is a very promising technology because of the reduced half-life of radionuclides.

So, to improve the already existent 6-[^{18}F]FDOPA synthesis methods, a new potential precursor was synthesised with yields of around 35 % and, microwave heating was used in key steps of the process, such as drying [^{18}F]fluoride, ^{18}F-fluorination and hydrolysis. In all these steps, reduction in the times, was observed. The use of microwave heating allowed a 25 % reduction in the global process time.

In the future, microwave heating could also be used in the ^{18}F-fluorination and hydrolysis steps of a recently developed Cu-catalyzed 6-[^{18}F]FDOPA synthesis processes, with very low RCY's and reaction times of around 10 minutes [110,111,113].

Also, the [^{11}C]UCB-J synthesis process was implemented at ICNAS-P, using conventional as well as microwave heating. The latter, required 49.7 minutes total synthesis time, instead of the 55 minutes necessary for conventional heating, with similar RCY's.

The obvious advantages of the microwave heating over conventional, not only observed in key steps of labelling with [^{18}F]fluoride, drying, ^{18}F-fluorination and, especially in hydrolysis of protecting groups, but also in Pd-catalyzed cross-coupling with [^{11}C]CH_3I, make this an interesting technology to apply in GMP routine production of several radiopharmaceuticals.

In future, this technology could be applied in the production of other radiopharmaceuticals, labelled with short lived radionuclides, or in the hydrolysis of protecting groups, which, generally,

takes long times to occur.

Moreover, the development of new synthesis modules which could include a microwave cavity instead of the traditional conventional oven, could facilitate the use of this technology in a routine GMP production of radiopharmaceuticals.

By the results and experience acquired during the development of this work, we don't doubt that microwave heating could have a great future in radiochemistry. However, due to the high costs of this technology, it's still expensive for most the PET centers.

Chapter 5

Experimental

The work was mostly performed at ICNAS-Produção Unipessoal, Lda (ICNAS-P). This company is owned of University of Coimbra, which produce a great variety of radiopharmaceuticals labelled with short-lived positron emitters and holds all necessary licenses for GMP pharmaceutical manufacturing. ICNAS-P, distributes radiopharmaceuticals at national level, produces for internal use, to be used in pre-clinical and clinical studies, and develops its own R&D projects. To produce radiopharmaceuticals, ICNAS-P is equipped with two IBA cyclotrons (Cyclone® 18/9 and Cyclone® KIUBE® variable energy), 2 fully equipped GMP Class C production labs, 5 Hot cells, 11 synthesis modules, one robotic arm for automatic dispensing of radiopharmaceuticals and, in course of this work, also a PETwave, a microwave to perform radiosynthesis. To perform the quality control of radiopharmaceuticals, the company also is equipped with 3 high performance liquid chromatography (HPLC) systems, 1 gas chromatograph (GC), 1 radio thin layer chromatograph (radio TLC) system, 1 dose calibrator and a High-Purity Germanium (HPGe) gamma spectrometer, in the quality control laboratory.

5.1 General considerations

All the manipulations of radioactive substances were performed under the standard requirements regarding radiological protection and safety. ALARA ("As Low As Reasonably Achievable") principle was always applied to prevent unnecessary exposure[254]. According to this, all experimental procedures were performed using personal protective equipment and lead barriers, and control of radiation exposure was performed with approved personal dosimeters, which are monthly checked, and their readings recorded.

All radiosynthesis was performed inside a shielded hot cell using remotely controlled modules. The process is controlled visually by the operator through a leaded-glass window and using specific software programs which monitors, in real time, activity, temperature, flow, pressure.

Whenever it is possible, tests, and methodology of analytical/quality control were performed according Eur. Ph.[252].

Implementation of the [^{18}F]FDOPA, **2.1**, synthesis was performed under Good Manufacturing Practices (GMP).

5.2 Reagents and solventes

All reagents and solvents were purchased from Merck (Darmstadt), ACROS Organic (New Jersey, USA), Alfa Aesar (Lancashire, United Kingdom) or Fisher Scientific (Waltham, Massachusetts, U.S.) and used without any further purification, unless otherwise noted.
Air and moisture sensitive reagents or solutions were handled under nitrogen atmosphere, in a vacuum system, or in a glove box.

Commercially available cassettes and reagents kits for [^{18}F]-FDOPA synthesis at the AllinOne® Synthesizer by Trasis were purchased from Trasis (Ans, Belgium).

4,5-dimethoxy-2-nitrobenzyl bromide (97 %), tris(dibenzylideneacetone)dipalladium(0), ($Pd_2(dba)_3$) and Tri(o-tolyl)phosphine ($P(o\text{-}tol)_3$) were purchased from Acros Organics (New Jersey, USA).

N-(Diphenylmethylene)glycine tert-butyl ester (99 %) and cesium hydroxide hydrate (99.9 %) were purchased from Alfa Aesar (Kandel, Germany).

Potassium iodine, potassium carbonate, dichloromethane, *n*-hexane, ethyl acetate, water, ethanol and acetonitrile HPLC grade was purchased from Fisher Chemical (U.K). Before use in chemical synthesis, dichloromethane, was distilled by a simple distillation. Each solvent was placed in a round-botton flask with calcium chloride anhydrous. The mixture was kept under reflux, for, at least, two hours (**Figure 5.1**). After distillation, the solvent is collected, passed through a column of basic alumina (grade I) and stored in a vial with activated molecular sieves.

Figure 5.1: Distillation system for solvent drying.

O-Allyl-N-(9-anthracenylmethyl)cinchonidium bromide (90 %), dimethylsulfoxide (DMSO), dimethylformamide (DMF), acetonitrile (ACN), 6-nitroveratraldhyde and hydriodic acid (57 %) were purchased from Merck Life Science (Darmstadt, Germany).

(*S*)-3-(5-Formyl-4-methoxymethoxy-2-nitro-phenyl)-2-(trityl-amino)-propionic acid tert-butyl ester, Kriptofix 2.2.2., tetrabutylammonium hydrogen carbonate (0.075M) – aqueous solution, stabilized with ethanol ($TBA.HCO_3$), (*R*)-3-(difluoroboranyl)-4-((2-oxo-4-(3,4,5-trifluorophenyl) pyrrolidine-1-yl) methyl)-pyridin-1-ium floride (BF_3-Dm-UCB-J), (*4R*)-1-[(3-methyl-4-pyridyl) methyl]-4-(3,4,5,-trifluorophenyl)pyrrolidine-2-one (UCB-J) were purchased from ABX Advanced biochemical compounds GmbH (Radeberg, Germany).

Minisart 0.2µm filters were purchased fom Sartorius (Göttingen, Germany).

Sep-Pack Acell Plus QMA Carbonate Plus light, Sep-Pack C18 plus short, Sep-Pack tC18 plus and Sep-Pack C18 plus light cartridges were purchased from Waters (Ireland).

Water for injections (WFI) and a saline solution (NaCl 0.9 %) were purchased from B.Braun (Queluz de Baixo, Portugal).

O^{18}-water enriched (Water-O-18 for PET, 98,0 %+, 50 g), ethanol for injection and HCl 4M solution were purchased from Rotem GmbH (Leipzig, Germany).

Sterile final product vials of 15mL and 100mL were purchased from Fluidómica (Cantanhede, Portugal).

Theodorico kit w and bulk vial syringe needles were purchased from Comecer (Castel Bolonhese RA, Italy).

5.3 Implementation of [^{18}F]FDOPA production at ICNAS-P

5.3.1 Production

6-[^{18}F]FDOPA multistep method, developed by Lemaire et. al[95] and automated by Trasis, was implementation and validated at ICNAS-Produção Unipessoal Lda.

Production validation was performed by 3 consecutive production runs, followed by quality control and stability tests.

The necessary documentation to submit to the authorities was generated, such as Standard Operating procedures (SOP's), registration documents, for production and Quality control, as well as packaging labels to primary, secondary, and tertiary containers.

Production was performed according GMP's, at a room classified as class C and filled in a hot cell classified as class A, by an aseptic process.

Trasis AllinOne® (Trasis, Belgium) synthesizer, presented in **Chapter 2** was equipped with

an HPLC system, composed by a Sunfire Prep C18, 5µm, 10x250mm column and a multi wavelength UV detector Knauer® (Berlin, Germany), controlled by the Supervision Software from Trasis (Ans, Belgium). Production is performed according the specific application manual-FDOPA,[189] supllied by Trasis.

5.3.2 Production procedure

To perform the production the following consumables, GMP grade, are required:

- Cassette, a disposable fluid pathway, which includes syringes, SPE cartridges, tubes, and connectors, supplied by Trasis, **Figure 5.2**.

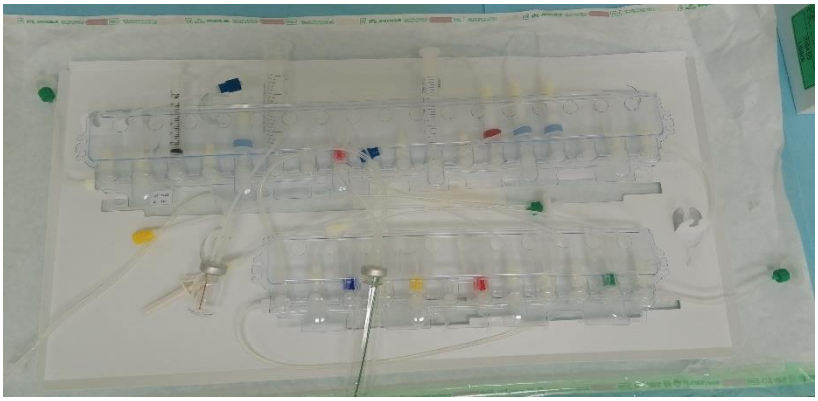

Figure 5.2: Cassette for the production of [^{18}F]FDOPA, supplied by Trasis.

- Reagents, which are supplied by Trasis, ready to use, in two packs, **Figure 5.3**.

Figure 5.3: Reagents kits and WFI water bags needed to perform the synthesis of 6-[^{18}F]FDOPA.

- 2 x 500 mL water bag for injections (WFI);
- 500 mL water HPLC grade;
- 500 mL ethanol HPLC grade;

- NaCl, 0,9 % solution;
- Theodorico kit W;
- Bulk vial syringe needle;
- 1 sterile final product vial of 100 mL (Bulk vial);
- At least 5 sterile final product vials (15mL);
- Filter 0.22 µm.

Before start, previous cassette is removed, wastes are empty, and the module was cleaned with a wipe of isopropanol 70 %. After, HPLC eluents are prepared and installed, **Figure 5.4.**

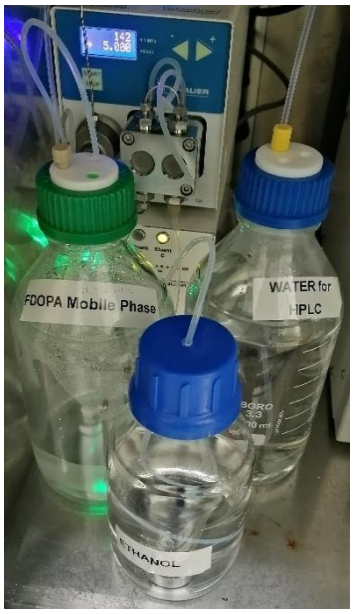

Figure 5.4: HPLC pump and [^{18}F]FDOPA mobile phase.

[^{18}F]FDOPA mobile phase, is prepared by mixing 2 syringes included in the reagents kit, 1mL of HPLC eluent excipients composed by ascorbic acid (250 ± 25 mg) and titriplex III (930 ± 50 mg) and 3 mL of HPLC eluent acetate buffer, composed by sodium acetate trihydrate (68 ± 1 mg), acetic acid (1 ± 0.05 mL) and WFI (2 ± 0.02 mL), with 500mL of WFI and placed at a bottle and installed in line A. Other 2 bottles, one with ethanol and other with water, HPLC grade, were also installed into lines B and C, respectively.

The dispensing and packaging are prepared before start production. This is performed at an automated robotic dispensing system, Theodorico® from Comecer, controlled by a specific software of Theodorico W®, **Figure 5.5.**

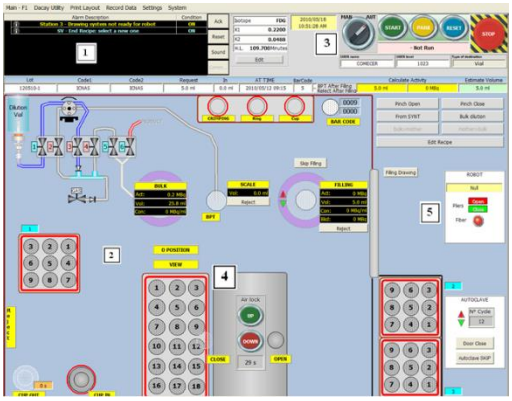

Figure 5.5: Theodorico W® control software.

In **Figure 5.6** we present a scheme of components of the outer and inner of Theodorico hot cell.

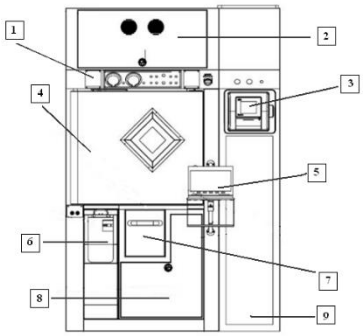

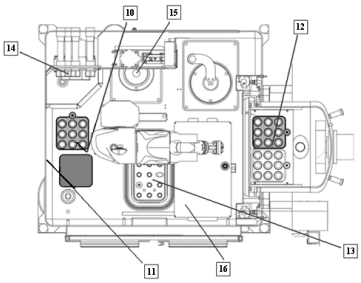

1- Control panel with pressure gauges.	9 - Access to autoclave deposits.
2- Ventilation system.	10 - Tray for deposit vials with [^{18}F]FDOPA solution.
3- Autoclave control panel.	11 – Position to rejected vials.
4- Shield door.	12 - Tray for deposit vials which will be autoclaved.
5- Theodorico W control software.	13 – Tray which transport the vials to the inner.
6- Dispensing system.	14 – Peristaltic pump.
7- Compressed air chamber.	15 – Bulk calibrator.
8- Access to technical compartment and electric panel.	16 – shielded door.

Figure 5.6: Schematic presentation of inside and outside of dispensing and packaging system (Outer-left, right-inner).

After remove the previous kit and clean the hot cell with isopropanol 70 %, a new Theodorico W kit was installed. In **Figure 5.7** we present the elements of the kit.

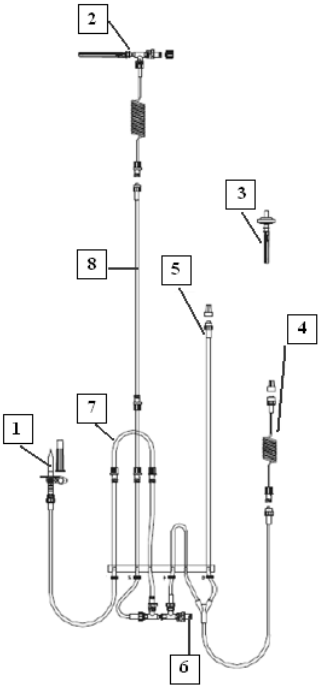

1-	Spike for saline solution bag.
2-	Filling needle.
3-	Ventilation needle for bulk vial.
4-	Connection to bulk vial.
5-	Connection to capillary tube where the radioactive solution will pass.
6-	Connection to valve to mix the mixture at bulk vial.
7-	Saline solution tube.
8-	[^{18}F]FDOPA solution.

Figure 5.7: Theodorico Kit W.

In **Figure 5.8** is presented the Theodorico kit W before (left) and after (right) installation.

Figure 5.8: Theodorico kit W before installation (left). Theodorico robotic arm after installation of Theodorico kit W (right).

After installation and before start production, at the software, activate the function “From SYNT” to open the valve until receive the 6-[^{18}F]FDOPA at bulk.

In Supervision Software®, chose at initial menu: “start synthesis”, after, select the script [^{18}F]FDOPA.UC**, Figure 5.9** to start synthesis and the script will order the module to execute a sequence of steps:

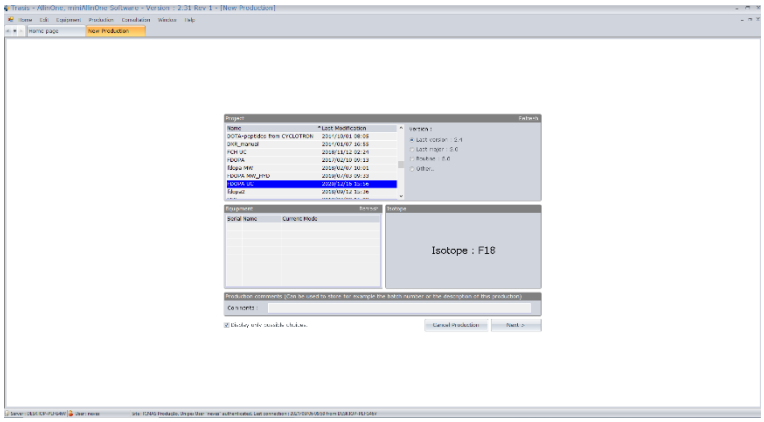

Figure 5.9: Script selected at Supervision Software®, to perform synthesis of 6-[^{18}F]FDOPA.

1. Machine tests were performed (syringe actuators, valves, pressure, vacuum, connections to the waste bottle, heaters).
2. It appears a message to “remove the previous cassette” if there is still any installed.
3. The synthesizer will move the syringe and rotary actuators to the correct positions to allow the placement of the new cassette.
4. Place the cassette (**Figure 5.10**).

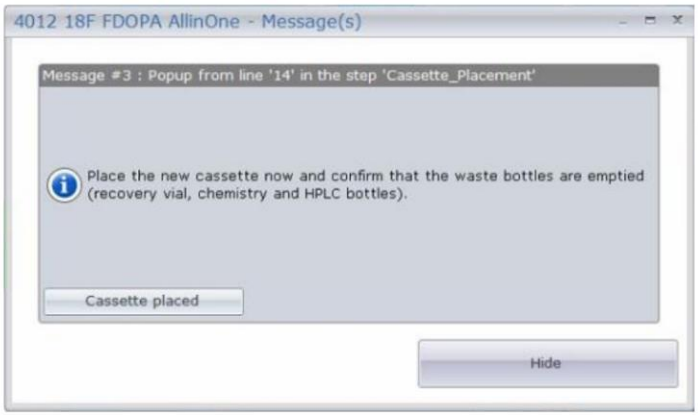

Figure 5.10: Cassette placement.

5. Star cassette tests, where is verified the correct placement of cassette, leaks-tightness of the connections, tubing, cassette and possible clogging of tubes, cartridges, or cassettes.
6. HPLC lines A, B and C priming.
7. Reagent's placement checklist appears, to assure that all the reagents were placed at the proper position, **Figure 5.11.**

Figure 5.11: Message of reagents placement.

8. After all the reagents are installed, the boxes must be filled to start the preliminary steps.
9. The alkylation vial is solubilized, tC18 cartridge is conditioned with 10 mL of ethanol and 10 mL of water, and the manifold is flushed and purged with nitrogen gas at high flow.
10. All the detectors are zeroed and a message to "Start Transfer" of [^{18}F]fluoride from cyclotron appears, **Figure 5.12**.

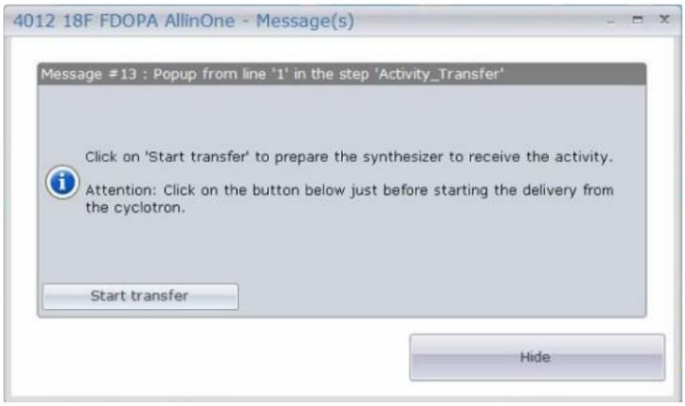

Figure 5.12: Message which indicates that machine is ready to receive [^{18}F]fluoride.

11. Cliquing in "Start transfer" to open the pinch valve in order to receive the radioactive solution.
12. Another message, "Activity received" appears**, Figure 5.13.**

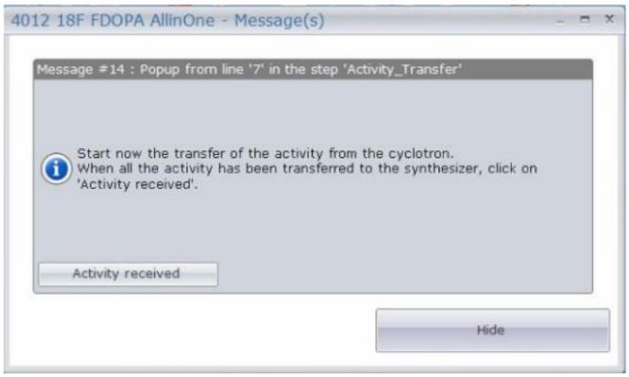

Figure 5.13: Message to click when all the activity is transferred.

13. Another pop up appears with the message “Start synthesis”, **Figure 5.14.**

Figure 5.14: Message which indicates that the machine is ready to start synthesis.

14. Press the button “Start Synthesis”.

No-carrier-added [^{18}F]fluoride was produced via the ^{18}O(p,n)^{18}F nuclear reaction by irradiation of [^{18}O]H_2O in a IBA Cyclone® 18/9 or in an IBA Cyclone® KIUVE® (variable energy) cyclotrons (Louvain-la-Neuve, Belgium). The [^{18}F]fluoride was transferred through lines to the hot cell in chemistry laboratory and is trapped on a QMA Sep-Pack light cartridge. The [^{18}F]fluoride was then eluted from the cartridge into the reaction vessel with 500 µL of a Kriptofix2.2.2 solution, composed by 250 µL of potassium carbonate in water (7 mg/250µL) and 250 µL of cryptand in acetonitrile (22 mg/250 µL). [^{18}F]fluoride was dried under a stream of nitrogen and vacuum for 5 minutes, at 110ºC to form the complex K[^{18}F]F K_{222}. The precursor **2.5** in *N*,*N*-dimethylformamide (20 mg/mL) was added to the dry salt and the ^{18}F-fluorination was performed at 165ºC for 5 minutes. After labelling, the reactor was cooled and diluted with 10 mL of water. This solution passed through a tC18 Sep-Pack cartridge, which is after washed with 10 mL of water and dried for 15 seconds with nitrogen.

Reduction of the [^{18}F]fluorinated aldehyde was performed at the tC18 cartridge, by passing an aqueous solution of $NaBH_4$ (3 mL, 18 mg) slowly through the cartridge. The column was washed with 5 mL of water and flushed, for 15 seconds, with a flow of nitrogen. After reduction, halogenation with 3 mL of HI 37 % was performed, at the same cartridge, by passing this acid slowly through the cartridge. Halogenation occurs for 2 minutes, yielding **2.9**. This product was then eluted from cartridge with dichloromethane (3 mL) to a second reactor. The excess of acid and water was removed by passing the solution through two potassium carbonate cartridges, located after tC18 and before the second reactor, where the enantioselective alkylation will occur.

To the reactor containing **2.9** in dichloromethane, a solution containing *N*-(diphenylmethylene)glycine tert-butyl ester, **2.11** (25mg) and the chiral phase-transfer catalyst (PTC) (2-3 mg) in 3 mL was added. After KOH (9M, 200 µL) were added to the same reactor, and this mixture was kept at room temperature for 6 minutes. Then, HI 57 % (10 mL) was added, and the dichloromethane evaporated at 100ºC during 1.7 minutes through a stream of nitrogen. After, the reactor was closed, and hydrolysis occurs for 16 minutes.

The reaction mixture was cooled to 50ºC, diluted with 5 mL of water, and injected in a 10 mL loop. To clean reactor and lines, then, more 2 mL and 1 mL were added to reactor and injected at loop. The total volume injected was 8 mL. HPLC purification was performed at a Waters Sunfire Prep C18 5µm – 10 x 250 mm (Waters, USA), using as mobile phase the solution already described.

15. The synthesis is performed without any intervention of the operator, until start the HPLC purification.
16. A message appears to inform the operator that the HPLC purification will starts, **Figure 5.15**.

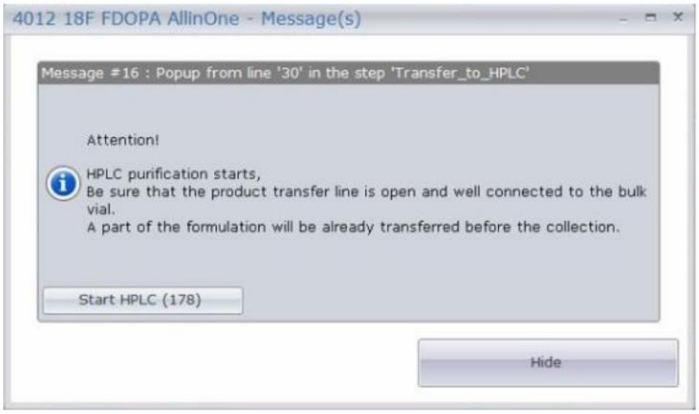

Figure 5.15: The reactional mixture is injected in the HPLC loop, and the machine is ready to start the HPLC purification.

17. After clicking in "Start HPLC" button, the trending view passes to the HPLC view and the collection line appears on the trending and, the button "Collection: Start" appears, **Figure 5.16.**

Figure 5.16: HPLC trending and collection button.

18. To collect 6-[^{18}F]FDOPA, click in "Start Collecting" when the collection line is close to the peak. Collection stops automatically after collecting 5.8mL.
19. Before collection, at specific software that
20. The collected product, the citrate buffer solution, composed by citric acid (36.5 mg), tri-sodium citrate (73.3 mg), NaCl (183.7 mg) and WFI (21 mL) formulation solvent, are transferred to the bulk vial.
21. After 300 seconds, the machine ends the flushing.
22. After 15 seconds the machine starts the steps: HPLC and cassette rising.
23. At the end, cassette is unlocked, and the production is finished.
24. A synthesis report is generated, which summarises the information about each production (steps, operator, process data, etc).

    In parallel with steps 22-24, the dispensing was performed at the Theodorico® System.
25. When all the activity arrives at the bulk vial, final product vials receipt is prepared, by selecting the function "Edit Recipe", **Figure 5.17,** where it will be indicating the desired activity or volume in each vial.

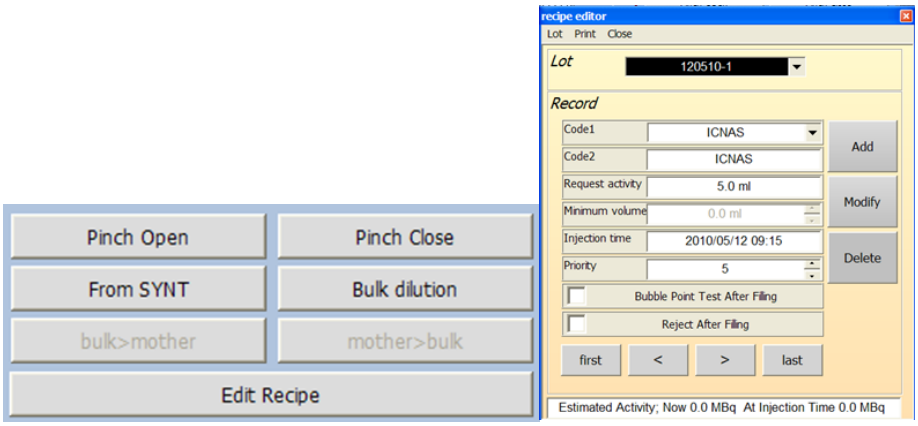

Figure 5.17: "Edit Recipe" menu at Theodorico W® control software.

26. The primary packaging labels are putted to the vials.
27. Through the function "down" and "up" of "Air Lock", transport the tray vials into the inner of automated dispenser and select, at the control panel, the positions of the empty vials.
28. Perform the Bubble Point Test (BPT).
29. Press button "START" to initialize the dispensing.
30. The robot initializes the primary packaging (vials) and send it to the secondary packaging (shielded container), which is closed after de vial dispensing.
31. When the button "Start/Stop blinks at green colour, put another shielded container and press the button, to dispense another vial, **Figure 5.18.**

Figure 5.18: Button Start/Stop.

32. The tertiary, and final, packaging was a plastic box where the shielded container was placed. Labels of the final packaging contains the identification of product, the pharmaceutical form, the volume, activity, and the identification of the final destiny.

Usually, starting with 113.0 ± 32.8 GBq at end of bombardment (EOB), 40.8 ± 14.3 GBq of 6-[^{18}F]FDOPA (n= 4) was obtained at end of synthesis (EOS), with 26.2 ± 8.8 % of

radiochemical yield (RCY). Total synthesis time is, usually 90 minutes.

5.3.3 Quality control of [^{18}F]FDOPA

Quality control of 6-[^{18}F]FDOPA was performed according the monograph 05/20189:2481, Fluorodopa (^{18}F) (Prepared by nucleophilic substitution) injection[180].

5.3.3.1 Determination of pH

The pH was measured using a pH meter JENWAY 3510 pH, from Bibby Scientific Limited (Staffordshire, UK) or strips with a pH range from 4.5-10.0, from Macherey-Nagel (Düren, Germany).

pH of 6-[^{18}F]FDOPA solution must be between 4.0 to 5.5.

5.3.3.2 Determination of Kryptofix$_{222}$

The presence of Kryptofix$_{222}$ was performed by a colorimetric semi-quantitative which allow to determine if the concentration of Kryptofix$_{222}$ in 6-[^{18}F]FDOPA solution (test solution) is lower than a solution with the maximum concentration allowed, 2.2 mg/10mL (reference solution). The test was performed at a TLC-SG plate which is dipped in an iodoplatine solution and dry for 12 hours.

To perform the analysis, 2.5 µL of the reference solution and 2.5 µL of the test solution were applied. After 1 minute of application, the plate is visualized. The central portion of the spot due to the test solution is not more intense than that of the spot due to the reference solution.

5.3.3.3 Chemical and radiochemical purities by HPLC

Chemical and radiochemical purities were determined by HPLC (*High Liquid Chromatography*) according to European Pharmacopoeia (Eur. Ph.). HPLC analysis was performed using an Agilent 1200 Series HPLC system from Agilent Technologies (USA) equipped with a multi wavelength UV detector and a GABIStar NaI(Tl) radiometric detector from Raytest Isotopenmessgeraete (Straubenhardt, Germany), an analytical column Xterra RP18 from Waters (USA), with dimensions of 250x4.6mm filled with protected silica with carbon chains and particle size of 3.5µm and an 20 µL loop injector, Rheodyne 7725i from Merck Life Science (Darmstadt, Germany).

Data acquisition and handling was performed using the Gina Star Chromatography Software Package.

To perform de analysis, is used, as mobile phase, an aqueous solution of trifluoroacetic acid

1.22 g/L (A) and acetonitrile (B), at a flow of 1 mL/min. The gradient is described in **Table 5.1.**

Table 5.1: Gradient used as HPLC eluent of [^{18}F]FDOPA method.

Time (min)	Mobile phase A (%)	Mobile phase B (%)
0.0	**98**	**2**
10.0	**98**	**2**
13.0	**95**	**5**
20.0	**95**	**5**
23.0	**5**	**95**
24.0	**98**	**2**
25.0	**98**	**2**

Before perform the analysis of [^{18}F]FDOPA test solution, a reference solution must be analysed. This solution contains 0.0115mg/mL of 6-fluorolevodopa 0.01mg/mL of *D*,*L*-DOPA (impurity D, according Eur. Ph.) and 0.005mg/mL of 6-hidroxy-*D*,*L*-DOPA (impurity E, according Eur. Ph.), to a final volume of 10 mL of mobile phase A (aqueous trifluoroacetic acid 1.22g/L).

To assure that the method is able to perform the analysis, injection of the reference solution was performed always before the analysis of test solution. Retention time of 6-fluorolevodopa is around 5 minutes and, the retention time of impurity *E* and impurity *D* are: 4.08 and 4.47 minutes, respectively.

Identification of product 6-[^{18}F]FDOPA was performed by the comparison of the radioactivity chromatogram with the reference solution. The principal peak in the radiochromatogram obtained with the test solution is similar in retention time to the peak corresponding to 6-fluorolevodopa in chromatogram of reference solution.

5.3.3.4 Enantiomeric purity

Enantiomeric purity is determined by HPLC, in the equipment described previously but using a chiral column, Crownpak CR(+) with dimensions of 150mm x 4.0mm with a silica-based filled modified with crown ethers. An aqueous solution of 2.9 g/L perchloric acid, isocratic, is used as mobile phase, at 1mL/min.

Before the analysis of product, two reference solutions must be analyzed. The first is a solution of 0.2 mg/mL of 6-fluorolevodopa in 10 mL of mobile phase and the other is a solution of 0.2 mg/mL of the racemic mixture *D,L*-6-fluorolevodopa in 10 mL of mobile phase.

Retention time of *L*-6-fluorolevodopa is around 7 minutes and of *D*-6-fluorolevodopa is around 5 minutes.

Retention times for reference solution:

D-FDOPA: 5.1 minutes

L-DOPA: 7.2 minutes

Test solution:

D-FDOPA: 5.3 minutes

L-DOPA: 7.2 minutes.

L-6-fluorolevodopa peak at chromatogram must be ≥ 96 % and *D*-6-fluorolevodopa ≤ 4 %.

5.3.3.5 Radiochemical purity by tin layer chromatography (TLC) – [^{18}F]fluoride

The radiochemical purity was determined by TLC-silica gel according the method B of Eur. Ph[252]. The system uses TLC silica gel 60 plates, with dimensions of 10x20 cm from Supelco, Merck Life Science (Darmstadt, Germany), as stationary phase, and a mixture of acetic acid and methanol, 1:9 (v/v) as mobile phase. Analysis must be performed with a suitable detector to determine the distribution of radioactivity.

To perform the chromatography, the plate is cut with the desired dimensions, a mark is made at 1cm from the bottom end at the center of plate, were, a 5 µL of sample was spotted (the origin). The plate was placed at a saturated chamber with mobile phase and is eluted until 2/3 of plate. At the end is dry over hot air and goes to the radiochromatograph. TLC plates were scanned on a MiniGita radioactivity TLC analyzer from Raytest **(**Straubenhardt, Germany**),** controlled by the software “miniGita Control”, **Figure 5.19**.

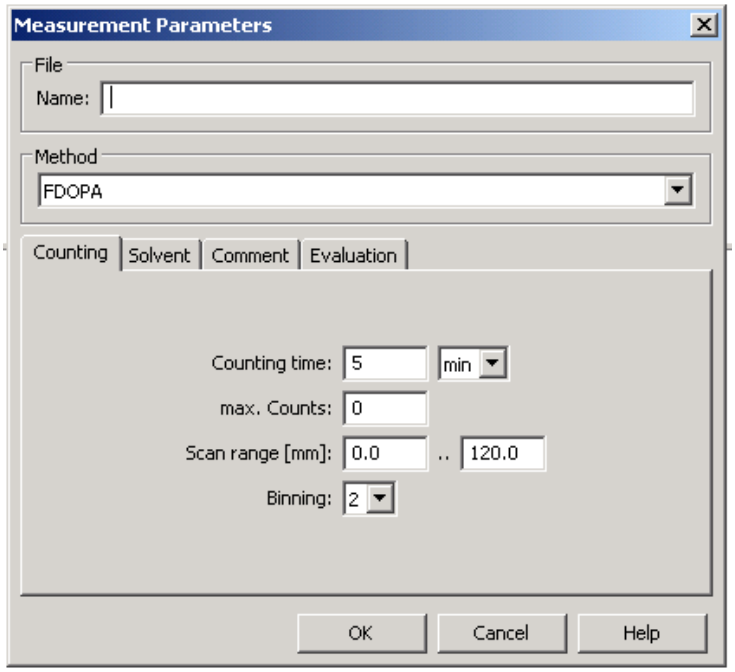

Figure 5.19: Software "miniGita Control".

Then the chromatogram acquisition, go to the software "GINA Star TLC" and open the file with the chromatogram acquired.

Rf [^{18}F]fluoride was 9.30 mm and of 6-[^{18}F]FDOPA was 42.86 mm.

[^{18}F]fluoride must be at, maximum, 5 % of total radioactivity.

5.3.3.6 Determination of residual solvents

Residual solvents are determined by gas chromatography (GC) at a gas chromatograph Agilent 6850 Series II, from Agilent technologies (Santa Clara, California, US).

Possible residual solvents of [^{18}F]FDOPA solution are ethanol, dichloromethane and *N*,*N*,-dimethylformamide. The analysis was performed using as a column HP-Fast Residual Solvent as stationary phase and helium as mobile phase.

The maximum limits to ethanol, dichloromethane and N,N-dimethylformamide are 2500mg/10 mL, 6.0 mg/10 mL and 8.8 mg / 10 mL, respectively.

5.3.3.7 Determination of radionuclidic purity

Radionuclidic purity is determined by the half-life, which is measured at a dose calibrator ISOMED 2010, from Nuklear-Medizintechnik GmbH (Dresden, Germany). Half-life of [^{18}F]fluoride is 109.8 minutes with an error of ± 5 %.

Another test to determine the radionuclidic purity is the gamma-ray spectrometry spectrum, performed at a High Purity Germanium (HPGe) radiation detector, model GEM30P4-76 from ORTEC (ORTEC, Tennessee, US), previously calibrated with ^{133}Ba and ^{154}Eu radioactive point like sources and keeping the dead-times inferior to 4 % during acquisition.

Acceptance criteria: The peaks in gamma spectrum corresponding to photons with energy different from 0.511 MeV or 1.022 MeV represents not more 0.1 % of the total radioactivity.

5.3.3.8 Determination of microbiologic purity

Bacterial endotoxins were determined at a spectrophotometer, endosafe®-PTS (Portable Test System), from Charles River Laboratories (Wilmington, Massachusetts, United States), based in the horseshoe crab-derived LAL (limulus amebocyte lysate) reagent, according to the following procedure:

1. Instrument Operation
   - The MENU key on the PTS keypad is pressed, to turn instrument on (Menu 5 turns instrument off).
   - The PTS Reader initiates a "SYSTEM SELF TEST" as it heats up to 37°C. This takes approximately 5 minutes.
   - The PTS Reader displays "SELF TEST OK" and then "INSERT CARTRIDGE".
2. Insert the cartridge

   Leave the the cartridge to come to room temperature in pouch and then, remove it. Then, it was inserted with the sample reservoirs facing up into slot at front of the PTS Reader. The cartridge was firmly pressed into the slot.
3. Insert the required information

   Operator identification, cartridge lot, calibration code, sample identification, and dilution factor. While this information is being entered, the cartridge is being pre-warmed.
4. Dispense the sample

   After all the test information is entered, the PTS reader displays "Add sample, press enter". 25 µL of sample were pipetted to all four sample reservoirs of the cartridge, the cartridge was inserted and is pressed "ENTER" on the PTS reader keypad

   Pumps draw sample aliquots into the test channels.

   Results are obtained in approximately 15 minutes.
5. Endotoxin test results
   - When the test is complete, the PTS reader gives an audible notification wich indicates that the assay is finished.
   - The endotoxin measurement and the assay acceptance criteria were

displayed on th screen.

- The PTS reader display alternate between the following results: Sample EU/mL; Sample % CV; Spike %CV; % Spike Recovery; Remove cartridge.

  The cartridge is removed.

Endotoxins must be less than 175 IU/10 mL.

Sterility tests were performed by an external entity, at Laboratorios Micro-Bios (Sant Joan Despi, Spain).

5.3.3.9 Determination of stability of [^{18}F]FDOPA solution

To determine an expiration date, quality control tests were performed after 12 hours. All the results are according to the specifications after this time. Longer times weren't tested due to the decay of radionuclide**.**

5.3.3.10 Determination molar activity (A_m) of [^{18}F]FDOPA

A_m of [^{18}F]FDOPA is calculated using a calibration curve, of concentration (mg/mL) in function of peak area (mAU*s). Calibration curve was obtained by injection of solutions of 6-fluorolevodopa with known concentrations in HPLC method of FDOPA already described in **Section 5.3.3.3**.

Solutions were prepared by dissolving 6-fluorolevodopa (5 mg) in mobile phase A (TFA 1.22 g/L) (1 mL). This solution (mother solution) was used to prepare the desired concentrations by consecutive dilutions. Concentrations of 0.12 mg/10 mL, 0.1 mg/10 mL, 0.07 mg/10 mL, 0.025 mg/10 mL, 0.01 mg/10 mL and 0.005 mg/10 mL were injected tree times.

Molar activity is given by the from the activity at EOS by the moles of 6-fluorolevodopa in GBq/µmol. Usually, the A_m obtained at ICNAS-P is of 467.10 ± 67.32 GBq/µmol (n = 4).

5.4 Synthesis of (*S*)-tert-butyl 3-(4,5-dimethoxy-2-nitrophenyl)-2-((diphenylmethylene)amino)propanoate (2.16)

5.4.1 General considerations

Organic synthesis and characterization of (*S*)-tert-butyl 3-(4,5-dimethoxy-2-nitrophenyl)-2-((diphenylmethylene)amino)propanoate**, 2.16** was performed by Inês Fonseca and Ivanna Hrynchak at Laboratory of Catalysis and Fine Chemistry, at Chemistry Department of Faculty of

Sciences and Technology of University of Coimbra. Reaction control and purification were performed at Radiochemistry and Cyclotron Laboratory at ICNAS – Produção Unipessoal, Lda.

Reaction and purification controls were performed by analytical High Performance Liquid Chromatography (HPLC). The analysis were performed on an Agilent 1200 Series HPLC system (Agilent Technologies, USA) equipped with a multi wavelength UV detector and a GABIStar NaI(Tl) radiometric detector (Raytest Isotopenmessgeraete GmbH, Straubenhardt, Germany). The injected volume was 20 μL and the wavelength of UV detector was 285 nm. Data analysis was performed with GinaX software from Raytest, using as stationary phase and a column XTerra®RP18, 5μm, 4.6x250mm (Waters, USA) and an isocratic mixture of acetonitrile/water, 70/30 as mobile phase.

Purification of the synthesized compound was performed by Flash chromatography at a PuriFlash® XS 420 (Interchim, França) and by semi-preparative at the AllinOne® synthesizer HPLC system, from Trasis (Belgium), equipped with a HPLC system, a multi wavelength UV detector (Knauer, Germany) at 254 nm, and a semipreparative column, Waters Sunfire Prep C18 5μm – 10 x 250 mm (Waters, USA).

Melting points were determined using a Büchi melting point apparatus in open capillaries. The infrared (IR) spectra were obtained using a ThermoNicolet IR380 FTIR and are reported as wavenumbers (cm^{-1}). 64 scans with a resolution of 2 cm^{-1} were collected for each sample. (Thermodynamics/Solid State Chemistry Group, Chemistry Department of Faculty of Sciences and Technology of University of Coimbra).

^{1}H and ^{13}C NMR spectra were recorded in $CDCl_3$ on Brucker Avance III spectrometer at 400 MHz and 100 MHz, respectively. Chemical shifts δ are reported in ppm relative to $CHCl_3$ (7.26 ppm for ^{1}H and 77.00 ppm for ^{13}C). For ^{1} H NMR, coupling constants *J* are given in Hz and the resonance multiplicity is described as s (singlet), d (doublet), t (triplet), q (quartet), m (multiplet), and br (broad). The analysis were performed at Nuclear Magnetic Ressonance Laboratory, Chemistry Department of Faculty of Sciences and Technology of University of Coimbra (Coimbra, Portugal).

High resolution mass spectrometry (HRMS) analyses were conducted on a Bruker Microtof equipped with selective ESI or MALDI detector (Unidade de Espectrometría de Masas e Proteómica from University of Santiago de Compostela, Spain). The abundance indicated for each mass number (m/z values) is given in percentage relative to the strongest peak of 100 % abundance (base peak).

The optical rotation value of the optical active compound was determined using automatic digital polarimeter Optical Activity AA-5 (Organic Chemistry Laboratory, Chemistry Department of Faculty of Sciences and Technology of University of Coimbra).

5.4.2 Synthesis of 2.16

2.16 was synthesized based in methodology already described in literature[95,97,186]. Following the general procedure, reaction conditions were optimized, being the best conditions the following:

4,5-dimethoxy-2-nitrobenzyl bromide (0.72 mmol, 0.200g) was added to a round bottom flask containing 14 mL of toluene at 40ºC. After, N-(Diphenylmethylene)glycine tert-butyl ester (0.58mmol, 0.171g), O-Allyl-*N*-(9-anthracenylmethyl)cinchonidium bromide (cPTC) (0.043mmol, 0.026g), KI (0.072, 0.012g), and 1.12 mL of CsOH.H2O 9M solution was added. the reaction was monitored after 1, 3, 16, 24 and 48 hours by HPLC, using an isocratic method, 70:30 Acetonitrile/H_2O, in a Xterra RP18 column (3.5 mm, 4.6x150 mm) from Waters at a flow rate of 1 mL/min and a wavelength (λ) of 285 nm. After 24 hours, no evolution was observed. At the best conditions selected, solution was stirred at 40ºC for 24 h.

Before analysis, the sample, as well as the final product **2.16**, was extracted with dichloromethane (DCM) (3 x 100 mL), dried over Na_2SO_4, filtered and the solvent evaporated to give a yellow solid.

To purify the product, two different techniques were tested, Flash Chromatography and Semi-preparative HPLC.

By Flash chromatography the column used was a flash column F0004-PF-C_{18}HP, tested with 2 gradients:

Gradient 1: starts with 10 % ACN and 90 % water, after 30 minutes, the percentages change to 90 % of ACN and 10 % water which is kept for 20 minutes.

Gradient 2: starts with 2 % ACN and 98 % water, until 8 minutes. Between 8 and 10 minutes, the gradient was change to 5 % of ACN and 95 % water. Between 15 and 20 minutes, changes to 95 % ACN and 5 % water, until 40minutes. Between 40 and 60 minutes the percentages go to 100 % of ACN.

The best purification conditions were obtained by HPLC with a semi-preparative C18 column (Waters Sunfire Prep C18 5µm – 10 x 250 mm), installed at Trasis AllinOne® module. The mobile phase was acetonitrile/H_2O (60/40), isocratic.

During the purification all the fractions were collected since the beginning of purification to the 36 minutes, and all were analysed by analytical HPLC. The fractions containing a percentage of product **2.16** higher tant 98 %, were collected between the 23 and 30 minutes, were going together, diluted in water, passed through a Sep-Pack® Plus C18 cartridge (previously activated with 10mL of ethanol followed by 10 mL of water). The product **2.16** is retained, the cartridge was dry by a stream of nitrogen and, then, the product is eluted with acetonitrile. The solvent was evaporated, yielding the product **2.16** as a yellow solid with 98 % of purity and 23 % yield.

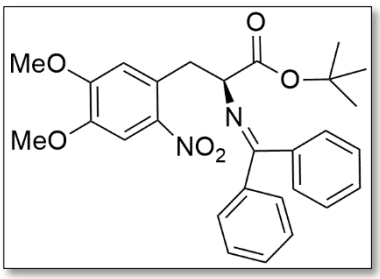

(**2.16**) Yield 23 % (8.34 mg, 0.017 mmol)

^{1}H NMR (400 MHz, $CDCl_3$): 1.45 (s, 9H); 3.32 (dd, *J*= 13.2, 9.7 Hz, 1H); 3.74 (s, 3H); 3.76 (dd, *J*= 13.2, 3.8 Hz, 1H); 3.91 (s, 3H); 4.37 (dd, *J*= 9.6, 3.7 Hz, 1H); 6.60 (d, *J*= 7.0 Hz, 2H); 6.80 (s, 1H); 7.24-7.36 (m, 7H); 7.53 (s, 1H); 7.59- 7.61 (m, 2H) ppm.

^{13}C NMR (100 MHz, $CDCl_3$): 28.1; 28.2; 37.0; 56.3; 56.4; 65.7; 81.5; 107.9; 115.7; 127.5; 128.1; 128.2; 128.4; 128.6; 128.8; 128.9; 130.2; 130.5; 132.5; 136.0; 139.2; 141.7; 147.5; 152.4; 170.6; 170.9 ppm.

HRMS (ESI-FIA-TOF): 491.2173 $[M+H]^+$ calculated for $C_{28}H_{30}N_2O_6\,H^+$ 491.2177.

$[\alpha]_D^{20}$ = -1.40 ± 0.05 ° (c1; CH_2Cl_2).

IR [ATR, cm^{-1}]: 2750 (CH aromatic); 2510 (CH); 2490 (C=N); 1800 (C=C aromatic); 1725 (CN); 1510(NO); 1225(CO).

m.p: 84-88ºC.

5.4.3 Stability tests of molecule 2.16

To study conditions of storage and manipulation of molecule **2.16**, stability tests were performed. The product was analysed by analytical HPLC, with the same conditions already described to reaction and purification control.

2.16 (15 mg, 7.35 mol), was kept for 2 days in acetonitrile (solvent used after purification) at -20ºC and after was analysed by HPLC. The purity of product was kept.

Then, the same solution was submitted to the microwave heating (1st method described in **Chapter 2**, **Table 2.10**), in acetonitrile. Then, the solvent was evaporated, the crude was diluted in DMF and the same microwave heating method was used. Adicionally, a 2nd microwave heating method, described in **Chapter 2**, **Table 2.10**, was also tested.

5.5 Microwave-assisted ^{18}F-fluorination

The radioactive products, of ^{18}F-fluorination, are manipulated behind a lead shielded window. The activity at end of synthesis (EOS) was measured with an ISOMED 1010 dose calibrator (Nuklear-Medizintechnik GmbH, Dresden, Germany).

No-carrier-added [^{18}F]fluoride was produced via the [^{18}O(p,n)^{18}F] nuclear reaction by irradiation of [^{18}O]H_2O (Water-O-18 for PET, 98,0 %+, 50g, Rotem Industries Ltd, Israel) in a IBA Cyclone® 18/9 or in an IBA Cyclone® KIUVE® (variable energy) cyclotrons (IBA RadioPharma Solutions, Louvain-la-Neuve, Belgium). Normally,

Microwave-assisted reactions were performed at a PETwave module from CEM (Mathews, U.S.) controlled by the Synergy Software (CEM, Mathews, US), while the corresponding reactions by conventional heating at AllinOne® synthesizer, from Trasis (Belgium) oven.

5.5.1 Microwave-assisted azeotropic ^{18}F-drying

Drying of [^{18}F]fluoride was performed with vacuum, nitrogen system located at the AllinOne® synthesizer (**Figure 5.20, A**). After drying, when the reactions were performed by conventional heating, were heated at 120ºC for 5 minutes, at the oven of Trasis module (**Figure 5.20, B**).

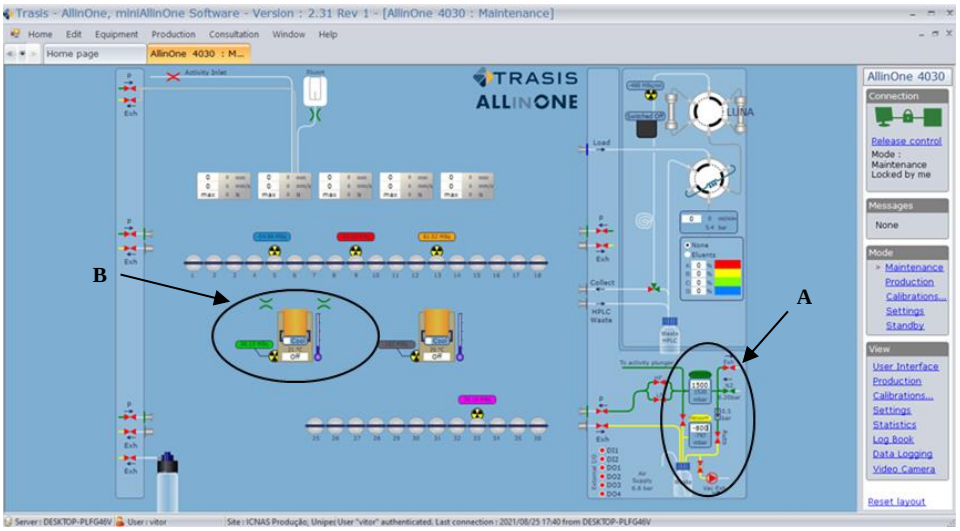

Figure 5.20: Trasis maintenance layout. System vacuum/nitrogen, **A**, and reactor, **B**.

Remote microwave cavity was located inside of a shielded MIP1-1P hot cell (**Figure 5.21, left),** while the microwave controller cable connected to the microwave cavity, is located outside the hot cell (**Figure 5.21, right**).

Figure 5.21: MIP1-1P hot cell, microwave system and microwave cavity of PETwave®.

All ^{18}F-fluorination reactions starts with production of [^{18}F]fluoride (≈0.25 ± 0.69 MBq, n = 29, 3mL) at a cyclotron, which is after send to a vial located at the blinded hot cell. [^{18}F]fluoride passed through a QMA column, which retains [^{18}F]fluoride, and [^{18}O]H_2O passed through the cartridge to a waste to be recovered. The column is dry by a nitrogen flow and after, and the [^{18}F]F^- was eluted to microwave reactor or Trasis reactor with a Cryptand solution, containing Kryptofix 2.2.2 (45.2 mg) in dry acetonitrile (0.3 mL) and K_2CO_3 (8.4 mg) in water (0.3 mL) or with commercially available TBA.HCO_3 aqueous solution (0.5 mL).

The residue was azeotropically dried in the microwave cavity. Different microwave heating methods, standard, dynamic, fixed power and power cycling (described in **Chapter 2**, **Section 2.6.1**) were tested in drying.

5.5.2 Microwave-assisted ^{18}F-fluorination of [^{18}F]FDOPA precursors

After dying, 20 mg of precursor to study (**2.5**, 6-nitroveratraldehyde, or **2.4**, (*S*)-3-(5-Formyl-4-methoxymethoxy-2-nitro-phenyl)-2-(trityl-amino)-propionic acid tert-butyl ester) dissolved in 0.5 or 1 ml of the solvent to test (DMF or DMSO), was added to the reactor in order

to perform the [^{18}F]fluorination, by microwave heating methods dynamic and Power Cycling (described in **Chapter 2**, **Section 2.5.2**).

At the end of reaction, a sample is collected, diluted with HPLC mobile phase andanalysed.

Chemical and radiochemical conversions were analyzed by analytical radio-HPLC, Agilent Technologies 1200 series (Santa Clara, California, United States) that is controlled for a GINAstar™ Software, from Elysia-Raytest (Elysia-Raytest GmbH, Straubenhardt, Germany). The HPLC system was equipped with an UV VIS detector (Diode Array G1315D), with a variable wavelength, and with a γ-radiation detector (Raytest, Gabi Star T1.0A).

Analysis of conversion of ^{18}F-fluorination of commercial 6-[^{18}F]FDOPA, precursors were performed at an analytical HPLC with an analytical column, XTerra®RP18, 5µm, 4.6x250mm (Waters, USA) as stationary phase and the following mobile phases, according with precursor:

2.5: isocratic, mixture of water/acetonitrile 70 % / 30 % at a flow of 1mL/min, as mobile phase. Rt (**2.5**) ≈ 3.3 minutes and Rt (**2.8**) ≈ 3.5 minutes.

2.4 and **2.16:** gradient of TFA 0.1 % (Mobile phase A) and ACN with TFA 0.1 % (Mobile phase B) **Table 5.2**. Rt (**2.4**) ≈18 min and Rt **(2.6)** ≈ 20 minutes.

Rt **(2.16**) ≈ 26.5 min

Table 5.2: Gradient used to determine the ^{18}F-Fluorination yield of **2.4** and **2.16**.

Time (min)	Mobile phase A (%)	Mobile phase B (%)
0.0	95	5
13.0	95	5
13.0	95	5
23.0	10	90
33.0	10	90
35.0	95	5
45.0	95	5

Radiochemical conversions were determined as the percentage of the desired product relatively all the other by-products in the chromatogram.

5.5.3 Hydrolysis of protected 6-nitro-*L*-DOPA hydrogensulfate and protected 6-nitro-formyl-DOPA

The precursor to hydrolyse, **2.16** or **2.4** (20 mg), dry or dissolved in the solvent to test, was placed in the microwave reactor and 1 mL of the acid, HCl 4M or HI, 37 %, was added. At the end of reaction, the crude was diluted in 10 mL of water and passed through a Sep-Pack C18 Plus short cartridge which retains the total and the partially hydrolysed products.

The conversions into the hydrolysed products were confirmed by HPLC by comparison of retention time (Rt) with the reference standards of 6-nitro-L-DOPA hydrogensulfate **2.20**, and the reference standard of 6-nitro-formyl-DOPA. HCl **2.19**, using the same analytical column described in the previous section as stationary phase and a isocratic mixture of ACN/water (70/30), at 254nm.

Rt (**2.4**)= 9.1 minutes

Rt (**2.19**)= 2.5 minutes

Rt (**2.16**)= 6.9 minutes

Rt (**2.20**)= 2.7 minutes

5.6 [^{11}C]UCB-J radiosynthesis

[^{11}C]UCB-J productions were performed based in procedures previously reported in literature[145,201–203].

5.6.1 Previous preparations

Before start synthesis, all the reagents, solvents, and ancillaries, must be prepared and installed inside of the hot cells.

Prior to each production, lines of Synthra [^{11}C]Choline module were purged and tested. Lines from porapack to Synthra reactor, or to microwave, and from Synthera Extension (when heating by conventional source) were purged with He and nitrogen for, at least, 30 minutes to avoid any contaminants from previous synthesis. 15 minutes before receive the activity, we proceed to the preparation of Synthra [^{11}C]Choline module. Liquid nitrogen was filled, and the HT oven was heated at 750ºC.

Solvent mixtures were degassed with nitrogen before being used to dissolve the reagents. Palladium catalyst ($Pd_2(dba)_3$) and phosphine ligand ($P(o\text{-}tol)_3$) are fractionated in a glove box.

5.6.2 Synthesis procedures

Hydrolysis of BF_3-Dm-UCB-J, 3.1

BF_3-Dm-UCB-J (1 ± 0.32 mg 2.7µmol) was weighed to a reactor vial, and 200 µL of methanol and 200 µL of HCl 1M were added. The via was closed and the mixture was kept at 60ºC for 1 hour. Then, the mixture was dry under a flow of nitrogen and vacuum to dryness. The solid was dissolved with 100 µL of the solvent mixture to be used in reaction.

The presence of species **3.1** and **3.2** in solution was confirmed by 1H-NMR and 19F-NMR.

Preparation of labelling reactor

To an Eppendorf weigh $Pd_2(dba)_3$ (1.6 ± 0.35 mg, 1.74 µmol), $P(o\text{-}tol)_3$ (3 ± 1.7 mg, 9.9 µmol) and K_2CO_3 (3 ± 1.73 mg, 30.4 µmol), n = 9. Add 350 µL of solvent mixture to test and transfer the contend to the Synthra or microwave reactor. Add the 100 µL of solution of BF_3-Dm-UCB-J, hydrolyzed or not, to the mixture. The mixture presents a dark red color. Keep the stirring at 30ºC until the mixture turn on light yellow. When the solution presents the desired color, the reactor (of Synthra or microwave cavity) is closed, the synthesis is initialized at Synthra, and the hot cell is closed to receive the $[^{11}C]CO_2$ and start the synthesis of $[^{11}C]CH_3I$.

Radiosynthesis of $[^{11}C]$UCB-J

Prior to each production, lines of Synthra $[^{11}C]$Choline module were purged and tested for flow and leak tightness. Lines from Porapack to reactor, and from Synthera Extension to reactor were purged with He and nitrogen for, at least, 30 minutes to avoid any contaminants from previous synthesis. 15 minutes before receive the activity, we proceed to the preparation of Synthra $[^{11}C]$Choline module. Liquid nitrogen dewar was filled, and the HT oven was heated at 750ºC.

$[^{11}C]CO_2$ was converted to $[^{11}C]CH_3I$, by gas phase approach, using the Synthra $[^{11}C]$Choline commercial module (Synthra GmbH, Hamburg, Germany), controlled by the software SynthraView version 2.0 (Synthra GmbH, Hamburg, Germany) via reduction to $[^{11}C]CH_4$ using a nickel catalyst/column followed by reaction of $[^{11}C]CH_4$ with I_2 at 750ºC during the recirculation after which $[^{11}C]CH_3I$ is trapped on the Porapack cartridge. When the activity is peaked, the $[^{11}C]CH_3I$ is released through a helium flow of 5 mL/min to the external reactor or to the remote microwave cavity. Then, the $[^{11}C]CH_3I$ is released to the Synthra reactor or microwave cavity to proceed with the radiolabelling reaction. When all $[^{11}C]CH_3I$ is released from porapack to reactor, this one is heated or submitted to the microwave heating. At the end of radiolabelling of $[^{11}C]$UCB-J, quenching of rection is performed with a commercially available IBA Synthera® Extension module, with a disposable kit inserted on a reusable cassette support.

The kit contains:

- a work syringe,

- a syringe with 1 mL of HCl 1M,
- one syringe with 2 ml of semi-preparative mobile phase (ammonium format 50mM, pH=10/ acetonitrile, 60/40),
- A tube connected to the nitrogen,
- A tube connected to the filtration vial,
- A tube to the filtration vial to pull the filtered solution,
- A tube connected to vial placed at another hot cell where, is the automated module Trasis AllinOne® (Ans, Belgium).

The quenching kit is the same when the reaction is performed by microwave or by conventional heating.

At end of reaction, HCl 1M (1mL) was added to the reactor and send to a vial through a minisart 0.2µm filter to remove all the solids present at reactional crude. The same procedure was repeated two times with addition of semi-preparative mobile phase pH=10 (adjusted with NH_3). Then, the solution was transferred to the hot cell were the purification and formulation will occur.

Purification of the product was performed with the Trasis AllinOne® synthesizer, using a dedicated cassette, composed by 3 in line manifolds, 3 work syringes, a syringe with semi-preparative mobile phase, a WFI bag, a dilution vial, a Sep-Pack C18 Plus light cartridge, 1mL of ethanol and 9 ml of NaCl 0.9 %.

When all the activity arrives to a vial, connected to the manifold, (From Synthera Extension), an order to the software was given and the purification starts with the injection of the content of this vial in semi-preparative loop. Then another 1 ml of mobile phase was injected to clean lines. The semi-preparative purification was performed at a semi-preparative column, SunFire®C18 OBD Prep Column, 10 mm x 250 mm, using a mixture of ammonium format 50mM and ACN (60/40) as mobile phase, 5 mL/min. The retention time of [^{11}C]-UCB-J was between 6 and 8 minutes.

The peak corresponding to [^{11}C]UCB-J was collected, diluted with 10 mL of water for injectables (WFI), and the resulting solution was passed through the Sep-Pack C18 Plus light cartridge, which is cleaned with 10 mL of WFI, dried with nitrogen and finally, was eluted with 1 mL of ethanol, to the final product vial, and reformulated with 9 mL of saline solution (NaCl, 0.9 %). All reported radiochemical yields (RCY'S) are decay corrected (dc) and based on [^{11}C]CH_3I.

The activity at end of synthesis (EOS) was measured with an ISOMED 1010 dose calibrator (Nuklear-Medizintechnik GmbH, Dresden, Germany).

5.6.3 Quality Control of [^{11}C]UCB-J

Quality control of [^{11}C]UCB-J was adapted from an already described previously in literature[202].

The tests realized after each production were the following:

- Visual inspection was performed behind a lead shielded window.
- The activity at end of synthesis (EOS) was measured with an ISOMED 1010 dose calibrator (Nuklear-Medizintechnik GmbH, Dresden, Germany).
- The pH of product was determined using a pH Meter 3510 Jenway (United Kingdom).
- Chemical and radiochemical purities were analyzed by analytical radio-HPLC, Agilent Technologies 1200 series (Santa Clara, California, United States) that is controlled for a GINAstar™ Software, from Elysia-Raytest (Elysia-Raytest GmbH, Straubenhardt, Germany), using a Waters XBridge, C18, 5um (4.6x150mm column) as stationary phase and a mixture of ACN/sodium dihydrogen phosphate 10mM (40/60) as mobile phase, at 1mL/min. The HPLC system was equipped with an UV VIS detector (Diode Array G1315D), with a wavelength of 254 nm, and with a γ-radiation detector (Raytest, Gabi Star T1.0A). Radiochemical purity was determined as the percentage of the [^{11}C]UCB-J peak and chemical purity was determined by quantification and relative comparison of the corresponding UV absorbance peaks of the QC samples and the reference standards of know concentrations (10 ug /dose for UCB-J and 1.5 µg / dose for desmethylUCB-J). This limits was based in animal toxicity studies[202].
- Enantiomeric purity was analyzed by HPLC with the same HPLC already described but using a chiral column, Chiralpack IA-3, 3µm, 4.6 x 150 mm using as mobile phase a mixture of 75 % of *n*-hexane, 25 % of ethanol and 0.1 % of triethylamine. The retention time of (*S*)-enantiomer is about 07:46 and of (*R*)-enantiomer is about 09:41.
- Molar activity (A_m) was determined by the ratio of radioactivity in GBq and the amount of UCB-J (µmol) at the end of synthesis (EOS).
- Residual solvents (ethanol and acetonitrile) were determined at an Agilent Technologies 6850 gas chromatograph controlled by a GINAstar™ Software, from Elysia-Raytest.
- Radionuclidic identification- Energy photons γ, was determined by gamma-ray spectrometry at a High Purity Germanium (HPGe) radiation detector.

- Bacterial endotoxins content was determined using the LAL test, performed in the Endosafe® PTS™ portable testing system (Charles River Laboratories, Massachusetts, USA).
- Sterility test was performed in an external certified laboratory.

Bacterial endotoxins and sterility tests may be performed after the release of product.

Tests as visual inspection, pH, half-life, radionuclidic identification, bacterial endotoxins and sterility were performed according the same procedures described in **Section 5.3.3**, for Quality Control of 6-[^{18}F]FDOPA.

References

1. Stone-Elander, N., Elander, J.-O. Thorell, A.F. *PET Chemistry The Driving Force in Molecular Imaging*. (Springuer, 2007).

2. Wong, F.C., Kim, E.E. A review of molecular imaging studies reaching the clinical stage. *Eur. J. Radiol.* **70**, 205–211 (2009).

3. Saga T, Koizumi M, Furukawa T, Yoshikawa K,F.Y. Radiopharmaceuticals for positron emission tomography. *Cancer Sci.* **100**, 375–381 (2009).

4. Pedroso de Lima, A., Abrunhosa, A., Dourado, A., Oliveira, A.D., Guerreiro, C., Costa, D.C., Alves, F.J.C., Caramelo, F.J., Araújo, H., Pedroso de Lima, J.J., Botelho, F.M., Prata, I., Ferreira, N.C., Crespo, P., Gordo, P.M. Radiofármacos: Desenvolvimento e Principais Aplicações. in *Física em Medicina Nuclear. Temas e Aplicações* (ed. Lima, J. J. P.) 119–157 (2008).

5. Suzuki, M., Doi, H., Koyama, H., Zhang, Z., Hosoya, T., Onoe, H., Watanabe, Y. Pd0-mediated rapid cross-coupling reactions, the rapid C-[^{11}C]methylations, revolutionarily advancing the syntheses of short-lived PET molecular probes. *Chem. Rec.* **14**, 516–541 (2014).

6. Hutton, B.F. Physics applied to radiopharmacy: imaging instruments for nuclear medicine. in *Sampson's Textbook of Radiopharmacy* (ed. Tony Theobald) 61–84 (Pharmaceutical Press, 2011).

7. Radvanyi, P., Villain, J. The discovery of radioactivity. *Comptes Rendus Phys.* **18**, 544–550 (2017).

8. McQuarrie, S. Production of radionuclides. in *Sampson's Textbook of Radiopharmacy* (ed. Tony Theobald) 73–84 (2011).

9. Alves, F.J.C.O. Ciclotrão e a Produção de Radionuclídeos. in *Física em Medicina Nuclear. Temas e Aplicações* (ed. Pedrosp de Lima, J. J.) 25–90 (2008).

10. Silindir, M., Özer, A.Y. Recently developed radiopharmaceuticals for Positron Emission Tomography (PET). *Fabad J. Pharm. Sci.* **33**, 153–162 (2008).

11. Lau, J., Rousseau, E., Kwon, D., Lin, K.S., Bénard, F., Chen, X. Insight into the development of PET radiopharmaceuticals for oncology. *Cancers (Basel).* **12**, (2020).

12. Pichler, V., Berroteŕan-Infante, N., Philippe, C., Vraka, C., Klebermass, E. M., Balber, T., Pfaff, S., Nics, L., Mitterhauser, M., Wadsak, W. An overview of pet radiochemistry, part 1: The covalent labels ^{18}F, ^{11}C, and ^{13}N. *J. Nucl. Med.* **59**, 1350–1354 (2018).

13. Theobold, T. What is radiopharmacy? in *Sampson's Textbook of Radiopharmacy* (ed. Theobald, T.) 1–7 (2011).

14. Wadsak, W., Mitterhauser, M. Basics and principles of radiopharmaceuticals for PET/CT. *Eur. J. Radiol.* **73**, 461–469 (2010).

15. Blower, P.J. Radiopharmaceutical chemistry: basic concepts. in *Sampson's Textbook of Radiopharmacy* (ed. Tony Theobald) 87–123 (Pharmaceutical Press, 2011).

16. Allott, L., Aboagye, E.O. Chemistry Considerations for the Clinical Translation of Oncology PET Radiopharmaceuticals. *Mol. Pharm.* **17**, 2245–2259 (2020).

17. O'Keefe, D.S., Bacich, D.J., Huang, S.S., Heston, W.D.W. A perspective on the evolving story of PSMA biology, PSMA-based imaging, and endoradiotherapeutic strategies. *J. Nucl. Med.* **59**, 1007–1013 (2018).

18. Kozikowski, A.P., Nan, F., Conti, P., Zhang, J., Ramadan, E., Bzdega, T., Wroblewska, B., Neale, J.H., Pshenichkin, S., Wroblewski, J.T. Design of remarkably simple, yet potent urea-based inhibitors of glutamate carboxypeptidase II (NAALADase). *J. Med. Chem.* **44**, 298–301 (2001).

19. Aboagye, E.O., Luthra, S.K., Brady, F., Poole, K., Anderson, H., Jones, T., Boobis, A., Burtles, S.S., Price, P. Cancer research UK procedures in manufacture and toxicology of radiotracers intended for pre-phase I positron emission tomography studies in cancer patients. *Br. J. Cancer* **86**, 1052–1056 (2002).

20. Silberstein, E.B. Prevalence of adverse reactions to positron emitting radiopharmaceuticals in nuclear medicine. *J. Nucl. Med.* **39**, 2190–2192 (1998).

21. Vallabhajosula, S., Solnes, L., Vallabhajosula, B. A broad overview of positron emission tomography radiopharmaceuticals and clinical applications: What is new? *Semin. Nucl. Med.* **41**, 246–264 (2011).

22. Elsinga, P.H. Present and future of PET-radiopharmaceuticals. *Nucl. Med. Rev.* **15**, 13–16 (2012).

23. Almuhaideb, A., Papathanasiou, N., Bomanji, J. ^{18}F-FDG PET/CT imaging in oncology. *Ann. Saudi Med.* **31**, 3–13 (2011).

24. Minn, H., Kauhanen, S., Seppanen, M., Nuutila, P. ^{18}F-FDOPA: A Multiple-Target Molecule. *J. Nucl. Med.* **50**, 1915–1918 (2009).

25. Glaudemans, A.W.J.M., Enting, R.H., Heesters, M.A.A.M., Dierckx, R.A.J.O., Van Rheenen, R.W.J., Walenkamp, A.M.E. Slart, R.H.J.A. Value of ^{11}C-methionine PET in imaging brain tumours and metastases. *Eur. J. Nucl. Med. Mol. Imaging* **40**, 615–635 (2013).

26. Rabinovici, A.J. Furst, J.P. O'Neil, C.A. Racine, E.C. Mormino, S.L. Baker, S. Chetty, P. Patel, T.A. Pagliaro, W.E. Klunk, C.A. Mathis, H.J. Rosen, B.L. Miller, W.J.J. ^{11}C-PIB PET imaging in Alzheimer disease and frontotemporal lobar degeneration. *Neurology* **68**, 1205–1212 (2007).

27. Becker, G., Dammicco, S., Bahri, M.A., Salmon, E. The rise of synaptic density PET imaging. *Molecules* **25**, (2020).

28. Grassi, I., Nanni, C., Allegri, V., Morigi, J.J., Montini, G.C., Castellucci, P., Fanti, S. The clinical use of PET with [^{11}C]-acetate. *Am. J. Nucl. Med. Mol. Imaging* **2**, 33–47 (2012).

29. Mikołajczak, R., Garnuszek, P. Radiopharmaceuticals in cardiology. *Nucl. Med. Rev.* **15**, 39–45 (2012).

30. Rinnab, L., Simon, J., Hautmann, R.E., Cronauer, M.V., Hohl, K., Buck, A.K., Reske, S.N., Mottaghy, F.M. [^{11}C]choline PET/CT in prostate cancer patients with biochemical recurrence after radical prostatectomy. *World J. Urol.* **27**, 619–625 (2009).

31. Bois, F., Noirot, C., Dietemann, S., Mainta, I.C., Zilli, T., Garibotto, V., Walter, M.A. [^{68}Ga]Ga-PSMA-11 in prostate cancer: a comprehensive review. *Am. J. Nucl. Med. Mol. Imaging* **10**, 349–374 (2020).

32. Ambrosini, V., Campana, D., Bodei, L., Nanni, C., Castellucci, P., Allegri, V., Montini, G.C., Tomassetti, P., Paganelli, G., Fanti, S. ^{68}Ga-DOTANOC PET/CT clinical impact in patients with neuroendocrine tumors. *J. Nucl. Med.* **51**, 669–673 (2010).

33. Comission Européene. Good Manufacturing Practice, Medicinal Products for Human and Veterinary Use. 1–8 https://ec.europa.eu/health/documents/eudralex/vol-4_en (2008).

34. European Comission. Eudralex Volume 4 Annex 3 Manufacture of Radiopharmaceuticals Release for public. *Eur. Com. J.* 1–8 (2008).

35. Gillings, N., Hjelstuen, O., Ballinger, J., Behe, M., Decristoforo, C., Elsinga, P., Ferrari, V., Peitl, P.K., Koziorowski, J., Laverman, P., Mindt, T.L., Neels, O., Ocak, M., Patt, M.,

Todde, S. Guideline on current good radiopharmacy practice (cGRPP) for the small-scale preparation of radiopharmaceuticals. *EJNMMI Radiopharm. Chem.* **6**, (2021).

36. Niazi, S. EudraLex Volume 4 Annex 1. *Guidelines to Good Manufacturing Practice Medicinal Products for Human and Veterinary* vol. 2008 79–92 https://ec.europa.eu/health/sites/default/files/files/eudralex/vol-4/2008_11_25_gmp-an1_en.pdf (2009).

37. Bouin, A.S., Wierer, M. Quality standards of the European Pharmacopoeia. *J. Ethnopharmacol.* **158**, 454–457 (2014).

38. European Pharmacopoeia. Radiopharmaceutical Preparations. *Eur. Pharmacopoeia* 884–887 (2008).

39. Coenen, H.H. Coenen, H.H., Gee, A.D., Adam, M., Antoni, G., Cutler, C.S., Fujibayashi, Y., Jeong, J.M. Mach, R.H., Mindt, T.L., Pike, V.W., Windhorst, A.D. Consensus nomenclature rules for radiopharmaceutical chemistry — Setting the record straight. *Nucl. Med. Biol.* **55**, v–xi (2017).

40. Gupta, M., Eugene, W. W. L. *Microwaves and Metals*. *Microwaves and Metals* (2011). doi:10.1002/9780470822746.

41. Mishra, R.R., Sharma, A.K. Microwave-material interaction phenomena: Heating mechanisms, challenges and opportunities in material processing. *Compos. Part A Appl. Sci. Manuf.* **81**, 78–97 (2016).

42. Silva, A.M.G., Pinto, J. Avanços na Síntese Química: Síntese Assistida por Micro-ondas. (2012).

43. Gedye, R., Smith, F., Westaway, K., Ali, H. Baldisera, L. Laberge, L., Roussel, J. The use of microwave ovens for rapid organic synthesis. *Tetrahedron Lett.* **27**, 279–282 (1986).

44. Giguere, R.J., Bray, T.L., Duncan, S.M., Majetich, G. Application of commercial microwave ovens to organic synthesis. *Tetrahedron Lett.* **27**, 4945–4948 (1986).

45. Nain, S., Singh, R., Ravichandran, S. Importance of Microwave Heating In Organic Synthesis. *Adv. J. Chem. A* **2**, 94–104 (2019).

46. Kappe, C.O. Controlled Microwave Heating in Modern Organic Synthesis. *Angew. Chem. Int. Ed* **43**, 6250–6284 (2004).

47. Stass, D.V., Woodward, J.R., Timmel, C.R., Hore, P.J., McLauchlan, K.A.

Radiofrequency magnetic field effects on chemical reaction yields. *Chem. Phys. Lett.* **329**, 15–22 (2000).

48. Stone-Elander, S., Elander, N., Thorel, J.-O., Fredriksson, A. Microwaving in ^{18}F Chemistry: Quirks and Tweaks. in *PET Chemistry Driving Force in Molecular Imaging* (eds. Schubiger, P. A., Lehmann, L., Friebe, M.) 243–269 (Springer Berlin Heidelberg New York, 2007).

49. Schanche, J.-S. Microwave synthesis solutions from Personal Chemistry. *Mol. Divers.* **7**, 293–300 (2003).

50. Hwang, D.-R., Moerlein, S.M., Lang, L., Welch, M. J. *Application of Microwave Technology to the Synthesis of Short-lived Radiopharmaceuticals*. *J. CHEM. SOC., CHEM. COMMUN.* https://pubs.rsc.org/en/content/articlepdf/1987/c3/c39870001799 (1987).

51. Stone-Elander, S., Elander, N. Fast Chemistry in Microwave Fields: Nucleophilic ^{18}F-Radiofluorinations of Aromatic Molecules. *Appl. Radiat. Isot.* **44**, 889–893 (1993).

52. Taylor, M.D., Roberts, A.D., Nickles, R.J. Improving the yield of 2-[^{18}F]fluoro-2-deoxyglucose using a microwave cavity. *Nucl. Med. Biol.* **23**, 605–609 (1996).

53. Elander, N., Jones, J.R., Lu, S.-Y., Stone-Elander, S. Microwave-enhanced radiochemistry. *Chem. Soc. Rev* **29**, 239–249 (2000).

54. Stone-Elander, S., Elander, N.S. Microwave applications in radiolabelling with short-lived positron-emitting. *J. Label. Compd. Radiopharm.* **45**, 715–746 (2002).

55. Fredriksson, A., Stone-Elander, S. Rapid microwave-assisted cleavage of methyl phenyl ethers: New method for synthesizing desmethyl precursors and for removing protecting groups. *J. Label. Compd. Radiopharm.* **45**, 529–538 (2002).

56. CEM Corporation. *PETwave Manual*. (2018).

57. Chen, K., Li, Z., Conti, P.S. Microwave-assisted one-pot radiosynthesis of 2'-deoxy-2'-[^{18}F]fluoro-5-methyl-1-β-d-arabinofuranosyluracil ([18F]-FMAU). *Nucl. Med. Biol.* **39**, 1019–1025 (2012).

58. Kumar, P., Ortlieb, R.K. Gupta, A.I., Wiebe, L. Microwave-assisted Radiosynthesis of the Hypoxia Marker 1-α-*D*-(5-Deoxy-5-[^{18}F]fluoroarabinofuranosyl)-2-nitroimidazole ([^{18}F]FAZA). Curr Radiopharm. **7**(1),49-56 (2014).

59. Teodoro, R., Wenzel, B., Oh-Nishi, A., Fischer, S., Peters, D., Suhara, T., Deuther-Conrad, W., Brust, P. A high-yield automated radiosynthesis of the alpha-7 nicotinic receptor radioligand [^{18}F]NS10743. *Appl. Radiat. Isot.* **95**, 76–84 (2015).

60. Ravert, H. T., Holt, D. P., Gao, Y., Horti, A. G. & Dannals, R. F. Microwave-assisted radiosynthesis of [^{18}F]ASEM, a radiolabeled α-7-nicotinic acetylcholine receptor antagonist. *J. Label. Compd. Radiopharm.* **58**, 180–182 (2015).

61. Guo, N., Alagille, D., Tamagnan, G., Price, R.R., Baldwin, R. M. Microwave-induced nucleophilic [^{18}F]fluorination on aromatic rings: Synthesis and effect of halogen on [^{18}F]fluoride substitution of meta-halo (F, Cl, Br, I)-benzonitrile derivatives. *Appl. Radiat. Isot.* **66**, 1396–1402 (2008).

62. Berroterán-Infante, N., Kalina, T., Fetty, L., Janisch, V., Velasco, R., Vraka, C., Hacker, M., Haug, A.R., Pallitsch, K., Wadsak, W., Mitterhauser, M. (*R*)-[^{18}F]NEBIFQUINIDE: A promising new PET tracer for TSPO imaging. *Eur. J. Med. Chem.* **176**, 410–418 (2019).

63. Scott, P.J.H., Shao, X. Fully automated, high yielding production of N-succinimidyl 4-[^{18}F]fluorobenzoate ([^{18}F]SFB), and its use in microwave-enhanced radiochemical coupling reactions. *J. Label. Compd. Radiopharm.* **53**, 586–591 (2010).

64. Hou, S., Phung, D.L., Lin, W., Wang, M., Liu, K., Shen, C.K. Microwave-assisted One-pot Synthesis of N-succinimidyl-4-[^{18}F]fluorobenzoate ([^{18}F]SFB). *J. Vis. Exp.* 1–16 (2011).

65. Wuest, F., Berndt, M., Kniess, T. Carbon-11 Labelling Chemistry Based upoun [11C]Methyl Iodide. in *PET Chemistry The Driving Force in Molecular Imaging* (eds. Schubiger, P. A., Lehmann, L., Friebe, M.) 183–212 (Springuer, 2007).

66. Coenen, H.H. Fluorine-18 Labelling Methods: Features and Possibilities of Basic Reactions. in *PET Chemistry Driving Force in Molecular Imaging* (eds. G., S., Lessl, M. & Friebe, M.) (Springer-Verlag Berlin Heidelberg, 2007).

67. Snell A.H. Minutes of the Pasadena Meeting 1936: A new radioactive isotope of fluoride. *Proc. Am. Phys. Soc. Phys Rev* **51**, 143 (1937).

68. Volker, J., Hodge, H., Wilson, H., SN, V.V. The adsorption of fluorides by enamel, dentin, bone and hydroxyapatite as show by the radioactive isotope. *J Biol Chem* **134**, 543–548 (1940).

69. Deng, X., Rong, J., Wang, L., Vasdev, N., Zhang, L., Josephson, L., Liang, S.H. Chemistry

for Positron Emission Tomography : Recent Advances in ^{11}C-, ^{18}F-, ^{13}N-, and ^{15}O-Labeling Reactions. *Angew. Chem. Int. Ed* **58**, 2580–2605 (2019).

70. Hess, E., Blessing, G., Coenen, H.H., Qaim, S.M. Improved target system for production of high purity [^{18}F]fluorine via the ^{18}O(p,n)^{18}F reaction. *Appl. Radiat. Isot.* **52**, 1431–1440 (2000).

71. Bergman, J., Solin, O. Fluorine-18-labeled fluorine gas for synthesis of tracer molecules. *Nucl. Med. Biol.* **24**, 677–683 (1997).

72. Miller, P.W., Long, N.J., Vilar, R., Gee, A.D. Synthesis of ^{11}C, ^{18}F, ^{15}O, and ^{13}N radiolabels for positron emission tomography. *Angew. Chemie - Int. Ed.* **47**, 8998–9033 (2008).

73. Teare, H., Robins, E.G., Årstad, E., Luthra, S.K., Gouverneur, V. Synthesis and reactivity of [^{18}F]-N-fluorobenzenesulfonimide. *Chem. Commun.* 2330–2332 (2007) doi:10.1039/b701177f.

74. Teare, H., Robins, E.G., Kirjavainen, A., Forsback, S., Sandford, G., Solin, O., Luthra, S.K., Gouverneur, V. Radiosynthesis and evaluation of [^{18}F]Selectfluor bis(triflate). *Angew. Chemie - Int. Ed.* **49**, 6821–6824 (2010).

75. Cortés González, M. A., Nordeman, P., Bermejo Gómez, A., Meyer, D.N., Antoni, G., Schou, M., Szabó, K.J. Fluoro-benziodoxole: A no-carrier-added electrophilic fluorinating reagent. Rapid, simple radiosynthesis, purification and application for fluorine-18 labelling. *Chem. Commun.* **54**, 4286–4289 (2018).

76. Tredwell, M., Gouverneur, V. ^{18}F labeling of arenes. *Angew. Chemie - Int. Ed.* **51**, 11426–11437 (2012).

77. Vries, E.F.J. De, Luurtsema, G., Bru, M., Elsinga, P.H., Vaalburg, W. Fully automated synthesis module for the high yield one- pot preparation of 6-[^{18}F]Fluoro- L-DOPA. *Appl. Radiat. Isot.* **51**, 389–394 (1999).

78. Diksic, M., Farrokhzad, S. New Synthesis of Fluorine-18-Labeled by Cleaving the Carbon-Silicon Bond with Fluorine . *J Nucl Med.* 26, 1314-1318 (1985).

79. Adam, M.J., Jivan, S. Synthesis and purification of L-6-[^{18}F]fluorodopa. *Int. J. Radiat. Appl. Instrumentation. Part A. Appl. Radiat. Isot.* **39**, 1203–1206 (1988).

80. Luxen, A., Perlmutter, M., Bida, G.T., Moffaert, G.V., Cook, J.S., Satyamurthy, N., Phelps, M.E., Barrio, J.R. Remote, semiautomated production of 6-[^{18}F]fluoro-*L*-dopa for

human studies with PET. *Int. J. Radiat. Appl. Instrumentation. Part A. Appl. Radiat. Isot.* **41**, 275–281 (1990).

81. Chaly, T., Bandyopadhayay, D., Matacchieri, R., Belakhleff, A., Dhawan, V., Takikawa, S., Margouleff, D., Eidelberg, D. A disposable synthetic unit for the preparation of 3-O-methyl-6-[^{18}F]fluorodopa using a regioselective fluorodemercuration reaction. *Appl. Radiat. Isot.* **45**, 25–30 (1994).

82. Namavari, M., Bishop, A., Satyamurthy, N., Bida, G., Barrio, J.R. Regioselective radiofluorodestannylation with [^{18}F]F2 and [^{18}F]CH3COOF: A high yield synthesis of 6-[^{18}F]fluoro-*L*-dopa. *Int. J. Radiat. Appl. Instrumentation. Part A. Appl. Radiat. Isot.* **43**, 989–996 (1992).

83. Dolle, F., Demphel, S., Hinnen, F., Fournier, D., Vaufrey, F., Crouzel, C. 6-[^{18}F]Fluoro-L-DOPA by radiofluorodestannylation : A short and simple synthesis of a new labelling precursor. *J. Label. Compd. Radiopharm.* **41**, 105–114 (1998).

84. Füchtner, F., Angelberger, P., Kvaternik, H., Hammerschmidt, F., Simovc, B.P., Steinbach, J. Aspects of 6-[^{18}F]fluoro-L-DOPA preparation: precursor synthesis, preparative HPLC purification and determination of radiochemical purity. *Nucl. Med. Biol.* **29**, 477–481 (2002).

85. Stenhagen, I.S.R., Kirjavainen, A.K., Forsback, S.J., Jørgensen, C.G., Robins, E.G., Luthra, S.K., Solin, O., Gouverneur, V. Fluorination of an arylboronic ester using [^{18}F]selectfluor bis(triflate): Application to 6-[^{18}F]fluoro-*L*-DOPA. *Chem. Commun.* **49**, 1386–1388 (2013).

86. John Gatley, S., Shaughnessy, W.J. Production of ^{18}F-labeled compounds with ^{18}F-produced with a 1-MW Research reactor. *Int. J. Appl. Radiat. Isot.* **33**, 1325–1330 (1982).

87. Schlyer, D.J., Bastos, M.A.V., Alexoff, D., Wolf, A.P. Separation of [^{18}F]fluoride from [^{18}O]water using anion exchange resin. *Int. J. Radiat. Appl. Instrumentation. Part* **41**, 531–533 (1990).

88. Schlyer, D. J., Firouzbakht, M. L., Wolf, A. P. Impurities in the [^{18}O]water target and their effect on the yield of an aromatic displacement reaction with [^{18}F]fluoride. *Appl. Radiat. Isot.* **44**, 1459–1465 (1993).

89. Coenen, H. H., Schüller, M., Stöcklin, G., Klatte, B., Knöchel, A. Preparation of N.C.A. [^{17}-^{18}F]fluoroheptadecanoic acid in high yields via aminopolyether supported, nucleophilic fluorination. *J. Label. Compd. Radiopharm.* **23**, 455–466 (1986).

90. Hamacher, K., Coenen, H.H., Stöcklin, G. Efficient Stereospecific Synthesis of No-Carrier-Added 2-[^{18}F]-Fluoro-2-Deoxy-D-Glucose Using Aminopolyether Supported Nucleophilic Substitution. *J. Nucl. Med.* **27**, (1986).

91. Shiue, C. -Y, Watanabe, M., Wolf, A.P., Fowler, J.S., Salvadori, P. Application of the nucleophilic substitution reaction to the synthesis of No‐carrier‐added [^{18}F]fluorobenzene and other ^{18}F-labeled aryl fluorides. *J. Label. Compd. Radiopharm.* **21**, 533–547 (1984).

92. Karramkam, M., Hinnen, F., Bramoullé, Y., Jubeau, S., Dollé, F. Ortho-[^{18}F]fluoronitrobenzenes by no-carrier-added nucleophilic aromatic substitution with K[^{18}F]F-K_{222} - A comparative study. *J. Label. Compd. Radiopharm.* **45**, 1103–1113 (2002).

93. Van Dort, M.E., Yang, D.J., Kilbourn, M.R., Gole, D.J., Kalir, A., Domino, E.F., Young, A.B., Wieland, D. M. Synthesis of [^{18}F]phencyclidines for glutamate receptor mapping. *J. Label. Compd. Radiopharm.* **26**, 346–347 (1989).

94. Neves, A.C.B., Hrynchak, I., Fonseca, I., Alves, V.H.P., Pereira, M.M., Falcão, A., Abrunhosa, A.J Advances in the automated synthesis of 6-[^{18}F]Fluoro-L-DOPA. *EJNMMI Radiopharm. Chem.* **6**, (2021).

95. Lemaire, C., Gillet, S., Guillouet, S., Plenevaux, A., Aerts, J., Luxen, A. Highly enantioselective synthesis of no-carrier-added 6-[18F]fluoro-L-dopa by chiral phase-transfer alkylation. *European J. Org. Chem.* 2899–2904 (2004).

96. Wagner, F. M., Ermert, J., Coenen, H. H. Three-step, 'one-pot' radiosynthesis of 6-fluoro-3,4-dihydroxy-l- phenylalanine by isotopic exchange. *J. Nucl. Med.* **50**, 1724–1729 (2009).

97. Libert, L.C., Franci, X., Plenevaux, A.R., Ooi, T., Maruoka, K., Luxen, A.J., Lemaire,

C. F. Production at the Curie Level of No-Carrier-Added 6-^{18}F-Fluoro-L-Dopa. *J. Nucl. Med.* **54**, 1154–1161 (2013).

98. Lemaire, C., Damhaut, P., Plenevaux, A., Comar, D. Enantioselective Synthesis of 6-[fluorine-18]-fluoro-L-DOPA from no-carrier-added fluorine-18-fluoride. *J. Nucl. Med.* **35**, 1996–2002 (1994).

99. Pike, V.W., Aigbirhio, F.I. Reactions of cyclotron-produced [^{18}F]fluoride with diaryliodonium salts - A novel single-step route to no-carrier-added [^{18}F]fluoroarenes. *J.*

Chem. Soc. Chem. Commun. 2215–2216 (1995).

100. DiMagno, S.G. Fluorination of aromatic ring systems. US; US20110313170 A1, (2011).

101. Edwards, R., Westwell, A.D., Daniels, S., Wirth, T. Convenient synthesis of diaryliodonium salts for the production of [^{18}F]F-DOPA. *European J. Org. Chem.* **2015**, 625–630 (2015).

102. Ross, T.L., Ermert, J., Hocke, C., Coenen, H.H. Nucleophilic ^{18}F-fluorination of heteroaromatic iodonium salts with no-carrier-added [^{18}F]fluoride. *J. Am. Chem. Soc.* **129**, 8018–8025 (2007).

103. Chun, J.H., Lu, S., Lee, Y.S., Pike, V.W. Fast and high-yield microreactor syntheses of ortho -substituted [^{18}F]Fluoroarenes from reactions of [^{18}F]Fluoride ion with diaryliodonium salts. *J. Org. Chem.* **75**, 3332–3338 (2010).

104. Lee, Y.-S., Hodoscek, M., Chun, J.-H., Pike, V.W. Conformational structure and energetics of 2-methylphenyl(2'-methoxyphenyl)iodonium chloride: evidence for solution clusters. *Chem. Eur. J.* **16**, 10418–10423 (2014).

105. Rotstein, B.H., Stephenson, N.A., Vasdev, N., Liang, S.H. Spirocyclic hypervalent iodine(III)-mediated radiofluorination of non-activated and hindered aromatics. *Nat. Commun.* **5**, 1–7 (2014).

106. Lee, E., Hooker, J.M., Ritter, T. Nickel-mediated oxidative fluorination for PET with aqueous [^{18}F] fluoride. *J. Am. Chem. Soc.* **134**, 17456–17458 (2012).

107. Neumann, K., Qin, L., Vavere, A., Snyder, S., DiMagno, S. New rapid fluorination process for the production of carrier free-^{18}F 6-[^{18}F]FDA and 6-[^{18}F]-L-DOPA. *J. Nucl. Med.* **53**, (2012).

108. Tredwell, M., Preshlock, S.M., Taylor, N.J., Gruber, S., Huiban, M., Passchier, J., Mercier, J., Génicot, C., Gouverneur, V. A General Copper-Mediated Nucleophilic ^{18}F Fluorination of Arenes. *Angew. Chemie Int. Ed.* **53**, 7751–7755 (2014).

109. Ichiishi, N., Brooks, Allen F., Topczewski, J.J., Rodnick, M.E., Sanford, M.S., Scott,

P.J.H. Copper-Catalyzed [^{18}F]Fluorination of (Mesityl)(aryl)iodonium Salts. *Org. Lett.* **16**, 3224–3227 (2014).

110. Mossine, A. V., Tanzey, S.S., Brooks, A.F., Makaravage, K.J., Ichiishi, N., Miller, J.M., Henderson, B.D., Erhard, T., Bruetting, C., Skaddan, M.B., Sanford, M. S., Scoot, P.J.H

One-pot synthesis of high molar activity 6-[^{18}F]fluoro-*L*-DOPA by Cu-mediated fluorination of a BPin precursor. *Org. Biomol. Chem.* **17**, 8701–8705 (2019).

111. Mossine, A.V., Tanzey, S.S., Brooks, A.F., Makaravage, K.J., Ichiishi, N., Miller, J.M., Henderson, B.D., Erhard, T., Bruetting, C., Skaddan, M.B., Sanford, M.S., Scoot, P.J.H. Synthesis of high-molar-activity [^{18}F]6-fluoro-*L*-DOPA suitable for human use via Cu-mediated fluorination of a BPIN precursor. *Nat. Protoc.* **15**, 1742–1759 (2020).

112. Makaravage, K.J., Brooks, A.F., Mossine, A. V, Sanford, M.S., Scott, P.J.H. Copper-Mediated Radiofluorination of Arylstannanes with [^{18}F]KF. *Org. Lett.* **18**, 5440–5443 (2016).

113. Zarrad, F., Zlatopolskiy, B.D., Krapf, P., Zischler, J., Neumaier, B. A practical method for the preparation of ^{18}F-labeled aromatic amino acids from nucleophilic [^{18}F]fluoride and stannyl precursors for electrophilic radiohalogenation. *Molecules* **22**, (2017).

114. Belanger, A.P., Pandey, M.K., Degrado, T.R. Microwave-assisted radiosynthesis of [^{18}F]fluorinated fatty acid analogs. *Nucl. Med. Biol.* **38**, 435–441 (2011).

115. Ponde, D.E., Dence, C.S., Schuster, D.P., Welch, M.J. Rapid and reproducible radiosynthesis of [^{18}F]FHBG. *Nucl. Med. Biol.* **31**, 133–138 (2004).

116. Elie, J., Vercouillie, J., Arlicot, N., Lemaire, L., Bidault, R., Bodard, S., Hosselet, C., Deloye, J.B., Chalon, S., Emond, P., Guilloteau, D., Buron, F., Routier, S. Design of selective COX-2 inhibitors in the (aza)indazole series. Chemistry, in vitro studies, radiochemistry and evaluations in rats of a [^{18}F]PET tracer. *J. Enzyme Inhib. Med. Chem.* **34**, 1–7 (2019).

117. Shi, J., Afari, G., and Bhattacharyya, S. Rapid synthesis of [^{18}F]fluoroestradiol: remarkable advantage of microwaving over conventional heating. *J. Label Compd. Radiopharm* **57**, 790–736 (2014).

118. Wolf, A.P., Redvanly, C.S. Carbon-11 and radiopharmaceuticals. *Int. J. Appl. Radiat. Isot.* **28**, 29–48 (1977).

119. Ferrieri, R.A., Wolf, A.P. The Chemistry of Positron Emitting Nucleogenic (Hot) Atoms with Regard to Preparation of Labelled Compounds of Practical Utility. *Radiochim. Acta* **34**, 69–84 (1983).

120. Schirbel, A., Holschbach, M.H., Coenen, H.H. N.C.A.[^{11}C]CO_2 as a safe substitute for phosgene in the carbonylation of primary amines. *J. Label Compd. Radiopharm* **42**, 537–

551 (1999).

121. Felicini, C., Någren, K., Berton, A., Pascali, G., Salvadori, P.A. Development of an automated modular system for the synthesis of [^{11}C]acetate. *Nucl. Med. Commun.* **31**, 1033–1039 (2010).

122. Dahl, K., Halldin, C., Schou, M. New methodologies for the preparation of carbon-11 labeled radiopharmaceuticals. *Clin. Transl. Imaging* **5**, 275–289 (2017).

123. Långström, B., Lundqvist, H. The preparation of ^{11}C-methyl iodide and its use in the synthesis of ^{11}C-methyl-*L*-methionine. *Int. J. Appl. Radiat. Isot.* **27**, 357–363 (1976).

124. Larsen, P., Ulin, J., Dahlstrøm, K., Jensen, M. Synthesis of [^{11}C]iodomethane by iodination of [^{11}C]methane. *Appl. Radiat. Isot.* **48**, 153–157 (1997).

125. Någren, K., Müller, L., Halldin, C., Swahn, C.G., Lehikoinen, P. Improved synthesis of some commonly used PET radioligands by the use of [^{11}C]methyl triflate. *Nucl. Med. Biol.* **22**, 235–239 (1995).

126. Jewett, D.M. A simple synthesis of [^{11}C]methyl triflate. *Int. J. Rad. Appl. Instrum. A.* **43**, 1383–1385 (1992).

127. Pascali, C., Bogni, A., Itawa, R., Cambiè, M., Bombardieri, E. [^{11}C]Methylation on a C18 Sep-Pak cartridge: a convenient way to produce [N-methyl-^{11}C]choline. *J. Label Compd. Radiopharm* **43**, 195–203 (2000).

128. Wilson, A.A., Garcia, A., Jin, L., Houle, S. Radiotracer synthesis from [^{11}C]-iodomethane: a remarkably simple captive solvent method. *Nucl. Med. Biol.* **27**, 529–532 (2000).

129. Comar, D., Crouzel, C., Maziere, M. Synthesis and metabolism of ^{11}C-chlorpromazine methiodide. *Radiopharm Labeled Coumpd* 461–469 (1973).

130. Långström, B., Lundqvist, H. The preparation of ^{11}C-methyl iodide and its use in the synthesis of ^{11}C-methyl-L-methionine. *Int. J. Appl. Radiat. Isot.* **27**, 357–363 (1976).

131. Matarrese, M.,M. Soloviev, D., Todde, S., Neutro, F., Petta, P., Carpinelli, A., Brüssermann, M., Galli Kienle, M., Fazio, F. Preparation of [^{11}C] radioligands with high specific radioactivity on a commercial PET tracer synthesizer. *Nucl. Med. Biol.* **30**, 79–83 (2003).

132. Link, J.M., Krohn, K.A., Clark, J.C. Production of [^{11}C]CH_3I by single pass reaction of

[^{11}C]CH_4 with I_2. *Nucl. Med. Biol.* **24**, 93–97 (1997).

133. Wuest, F., Berndt, M., Kniess, T. Carbon-11 Labeling Chemistry Based upoun [^{11}C]Methyl Iodide. in *PET Chemistry The Driving Force in Molecular Imaging* (eds. Schubiger, P. A., Lehmann, L., Friebe, M.) 183–212 (Springer-Verlag Berlin Heidelberg, 2007).

134. Nagren, K., Halldin, C. Methylation of Amide and Thiol Functions with (^{11}C)Methyl Triflate, as Exemplified by [^{11}C]NMSP, [^{11}C]Flumazenil and [^{11}C]methionine. *J. Label. Compd. Radiopharm.* 831–841 (1998).

135. Wilson, A.A., Garcia, A., Chestakova, A., Kung, H., Houle, S. A rapid one-step radiosynthesis of the β-amyloid imaging radiotracer N-methyl-[^{11}C]2-(4′ -methylaminophenyl)-6-hydroxybenzothiazole ([^{11}C]-6-OH-BTA-1). *J. Label. Compd. Radiopharm.* **47**, 679–682 (2004).

136. Neves, M. da G.P.M.S., Simões, M.M.Q., Cavaleiro, J.A.S. Carbon-carbon bond formation mediated by palladium (0). in *Catalysis from Theory to Application* (eds. Figueiredo, J. L., Pereira, M. M. & Faria, J.) 355–378 (Imprensa Universidade de Coimbra, 2008).

137. Hostetler, E.D., Terry, G.E., Burns, H.D. An improved synthesis of substituted [^{11}C]toluenes via Suzuki coupling with [^{11}C]methyl iodide. *J. Label. Compd. Radiopharm.* **48**, 629–634 (2005).

138. Doi, H. Pd-mediated rapid cross-couplings using [11C]methyl iodide: Groundbreaking labeling methods in 11C radiochemistry. *J. Label. Compd. Radiopharm.* **58**, 73–85 (2015).

139. Doi, H., Ban, I., Nonoyama, A., Sumi, K., Kuang, C., Hosoya, T., Tsukada, H., Suzuki, M. Palladium(0)-mediated rapid methylation and fluoromethylation on carbon frameworks by reacting methyl and fluoromethyl iodide with aryl and alkenyl boronic acid esters: Useful for the synthesis of [^{11}C]CH_3-C- and [^{18}F]FCH2-C- Containing PET tracers. *Chem. - A Eur. J.* **15**, 4165–4171 (2009).

140. Takashima-Hirano, M., Takashima, T., Katayama, Y., Wada, Y., Sugiyama, Y., Watanabe, Y., Doi, H., Suzuki, M. Efficient sequential synthesis of PET Probes of the COX-2 inhibitor [^{11}C]celecoxib and its major metabolite [^{11}C]SC-62807 and in vivo PET evaluation. *Bioorg. Med. Chem.* **19**, 2997–3004 (2011).

141. Kanazawa, M., Furuta, K., Doi, H., Mori, T., Minami, T., Ito, S., Suzuki, M., Synthesis of an acromelic acid a analog-based ^{11}C-labeled PET tracer for exploration of the site of

action of acromelic acid a in allodynia induction. *Bioorganic Med. Chem. Lett.* **21**, 2017–2020 (2011).

142. Ijuin, R., Takashima, T., Watanabe, Y., Sugiyama, Y., Suzuki, M. Synthesis of [^{11}C]dehydropravastatin, a PET probe potentially useful for studying OATP1B1 and MRP2 transporters in the liver. *Bioorganic Med. Chem.* **20**, 3703–3709 (2012).

143. Watanabe, Y., Takahashi, K., Hosoya, T., Onoe, K., Doi, H., Nagata, H., Hiramatsu, T., Li, X.L., Watanabe, Y., Wada, Y., Takashima, T., Suzuki, M., Onoe, H. ^{11}C-Cetrozole: An improved C-[^{11}C]-methylated pet probe for aromatase imaging in the brain. *J. Nucl. Med.* **55**, 852–857 (2014).

144. Andersen, V.L., Herth, M.M., Lehel, S., Knudsen, G. M., Kristensen, J.L. Palladium-mediated conversion of para-aminoarylboronic esters into para-aminoaryl-^{11}C-methanes. *Tetrahedron Lett.* **54**, 213–216 (2013).

145. Nabulsi, N. B., Mercier, J., Holden, D., Carr, S., Najafzadeh, S., Vandergeten, M.C., Lin, S.F., Deo, A., Price, N., Wood, M., Lara-Jaime, T., Montel, F., Laruelle, M., Carson, R.E., Hannestad, J., Huang, Y. Synthesis and preclinical evaluation of ^{11}C-UCB-J as a PET tracer for imaging the synaptic vesicle glycoprotein 2A in the brain. *J. Nucl. Med.* **57**, 777–784 (2016).

146. Hamill, T.G., Krause, S., Ryan, C., Bonnefous, C., Govek, S., Seiders, T.J., Cosford, N.D.P., Roppe, J., Kamenecka, T., Patel, S., Gibson, R.E., Sanabria, S., Riffel, K., Eng, W., King, C., Yang, X., Green, M.D., O'Malley, S.S., Hargreaves, R., Burns, H.D. Synthesis, characterization, and first successful monkey imaging studies of metabotropic glutamate receptor subtype 5 (mGluR5) PET radiotracers. *Synapse* **56**, 205–216 (2005).

147. Howes, O.D., Montgomery, A.J., Asselin, M.C., Murray, R.M., Grasby, P.M., Mcguire, P. KMolecular imaging studies of the striatal dopaminergic system in psychosis and predictions for the prodromal phase of psychosis. *Br. J. Psychiatry* **191**, s13–s18 (2007).

148. Bose, S.K., Turkheimer, F.E., Howes, O.D., Mehta, M.A., Cunliffe, R., Stokes, P.R., Grasby, P.M. Classification of schizophrenic patients and healthy controls using [^{18}F] fluorodopa PET imaging. *Schizophr Res* **106**, 148–155 (2008).

149. Brooks, D.J., Frey A.K., Marek, K.L., Oakes, D., Paty, D., Prentice, R., Shults, C.W., Stoessl, A.J. Assessment of neuroimaging techniques as biomarkers of the progression of Parkinson's disease. *Exp. Neurol.* **184**, 68–79 (2003).

150. Oldendorf, W. Stereospecificity of blood-brain barrier permeability to amino acids. *Am J*

Physiol. 967–969 (1973).

151. Pretze, M., Wängler, C., Wängler, B. 6-[^{18}F]fluoro-L-DOPA: A well-established neurotracer with expanding application spectrum and strongly improved radiosyntheses. *Biomed Res. Int.* **2014**, 12 (2014).

152. Heiss, W. D., Wienhard, K., Wagner, R., Lanfermann, H., Thiel, A., Herholz, K., Pietrzyk, U. F-Dopa as an amino acid tracer to detect brain tumors. *J. Nucl. Med.* **37**, 1180–2 (1996).

153. Neels, O.C., Koopmans, K. P., Jager, P. L., Vercauteren, L., van Waarde, A., Doorduin, J., Timmer-Bosscha, H., Brouwers, A.H., de Vries, E.G.E., Dierckx, R.A.J.O., Kema, I.P., Elsinga, P.H. Manipulation of [^{11}C]-5-Hydroxytryptophan and 6-[^{18}F]Fluoro-3,4-Dihydroxy-*L*-Phenylalanine Accumulation in Neuroendocrine Tumor Cells. *Cancer Res.* **68**, 7183–7190 (2008).

154. Jager, P.L., Chirakal, R., Marriott, C.J., Brouwers, A.H., Koopmans, K.P., Gulenchyn, K.Y. 6-L-^{18}F-fluorodihydroxyphenylalanine PET in neuroendocrine tumors: basic aspects and emerging clinical applications. *J. Nucl. Med.* **49**, 573–586 (2008).

155. Balogova, S., Talbot, J. N., Nataf, V., Michaud, L., Huchet, V., Kerrou, K., Montravers, F. ^{18}F-Fluorodihydroxyphenylalanine vs other radiopharmaceuticals for imaging neuroendocrine tumours according to their type. *Eur. J. Nucl. Med. Mol. Imaging* **40**, 943–966 (2013).

156. Chondrogiannis, S., Cristina Marzola, M., Al-Nahhas, A., Venkatanarayana, T.D., Mazza, A., Opocher, G., Rubello, D. Normal biodistribution pattern and physiologic variants of ^{18}F-DOPA PET imaging. *Nucl. Med. Commun.* **34**, 1141–1149 (2013).

157. Martiniova, L., Cleary, S., Lai, E.W., Kiesewetter, D.O., Seidel, J., Dawson, L.F., Phillips, J.K., Thomasson, D., Chen, X., Powers, J.F., Kvetnansky, R., Pacak, K.. Usefulness of [^{18}F]-DOPA for PET imaging in a mouse model of phechoromocytoma. *Nucl Med Biol* **39**, 215–226 (2012).

158. Rischke, H.C., Benz, M.R., Wild, D., Mix, M., Dumont, R., Campbell, D., Seufert, J., Wiech, T., Rossler, J., Weber, W., Neumann, H. P. H., Rössler, J., Weber, W., Neumann, H.P.H. Correlation of the Genotype of Paragangliomas and Pheochromocytomas with Their Metabolic Phenotype on 3,4-Dihydroxy-6-^{18}F-Fluoro-*L*-Phenylalanin PET. *J. Nucl. Med.* **53**, 1352–1358 (2012).

159. Koopmans, K.P., Neels, O.C., Kema, I.P., Elsinga, P.H., Sluiter, W.J., Vanghillewe, K., Brouwers, A.H., Jager, P.L., De Vries, E.G.E. Improved staging of patients with carcinoid

and islet cell tumors with ^{18}F-dihydroxy-phenyl-alanine and ^{11}C-5-hydroxy-tryptophan positron emission tomography. *J. Clin. Oncol.* **26**, 1489–1495 (2008).

160. Edwards, R., Wirth, T. 6-fluoro-3,4-dihydroxy-L-phenylalanine - Recent modern syntheses for an elusive radiotracer. *J. Label. Compd. Radiopharm.* **58**, 183–187 (2015).

161. G. Firnau, C. Nahmias, S.G. [^{18}F]5-Fluoro-DOPA with Reactor-Produced Fluorine-18. *Int. J. Appl. Radiat. Isot.* **160**, 182 (1973).

162. Firnau, G., Chirakal, R., Garnett, E.S. Aromatic radiofluorination with [^{18}F] fluorine gas : 6-[^{18}F] fluoro-L-dopa. *J Nuci Med* **25**, 1228–1233 (1984).

163. Tierlinq, T., Hamacher, K., Coenen, H. H. & Gmbh, F. J. A New Nucleophilic Asymmetric Synthesis. *J. Label. Cpd. Radiopharm* **44**, 146–147 (2001).

164. Rene-Martin., Baumgart, D., Huebner, S., Juettler, S., Saul, S., Clausnitzer, A., Mollitor, J., Smits, R., Hoepping, A., Mueller, M. First SPE Method for Routine Production of Nucleophilic [^{18}F]-L-DOPA. *J. Label. Compd. Radiopharm.* **56**, S126 (2013).

165. Diksic, M., Farrokhzad, S. New synthesis of fluorine-18-labeled 6-fluoro-L-dopa by cleaving the carbon-silicon bond with fluorine. *J. Nucl. Med.* **26**, 1314–8 (1985).

166. Bishop, A., Satyamurthy, N., Bida, G., Barrio, J.R. Chemical reactivity of the ^{18}F electrophilic reagents from the ^{18}O(p,n)^{18}F gas target systems. *Nucl. Med. Biol.* **23**, 559–565 (1996).

167. Füchtner, F., Steinbach, J. Efficient synthesis of the ^{18}F-labelled 3-O-methyl-6-[^{18}F]fluoro-L-DOPA. *Appl. Radiat. Isot.* **58**, 575–578 (2003).

168. Luxen, A., Guillaume, M., Melega, W.P., Pike, V.W., Solin, O., Wagner, R. Production of 6-[^{18}F]fluoro-l-DOPA and its metabolism in vivo—a critical review. *Int. J. Radiat. Appl. Instrumentation. Part B. Nucl. Med. Biol.* **19**, 149–158 (1992).

169. Adam, M.J., Ruth, T.J., Grierson, J.R., Abeysekera, B., Pate, B.D. Routine Synthesis of L- [^{18}F] 6-Fluorodopa with Fluorine- 18 Acetyl Hypofluorite. 1462–1466 (1986).

170. Koopmans, K.P., Brouwers, A.H., Hooge, M.N., Horst-Schrivers, A.N.V.D., Kema, I.P., Wolffenbuttel, B.H., De Hooge, M.N., Bruce H., De Vries, E.G., Jager, P.L. Carcinoid crisis after injection of 6-^{18}F-fluorodihydroxyphenylalanine in a patient with metastatic carcinoid. *J. Nucl. Med.* **46**, 1240–3 (2005).

171. Kuik, W.-J., Kema, I.P., Brouwers, A.H., Zijlma, R., Neumann, K.D., Dierckx, R.A.J.O.,

DiMagno, S.G., Elsinga, P.H. In Vivo Biodistribution of No-Carrier-Added 6-^{18}F-Fluoro-3,4-Dihydroxy-L-Phenylalanine (^{18}F-DOPA), Produced by a New Nucleophilic Substitution Approach, Compared with Carrier-Added ^{18}F-DOPA, Prepared by Conventional Electrophilic Substitution. *J. Nucl. Med.* **56**, 106–112 (2015).

172. Füchtner, F., Preusche, S., Maeding, P., Zessin, J., Steinbach, J. Factors affecting the specific activity of [^{18}F]fluoride from a [^{18}O]water target. *Nuklearmedizin* **47**, 116–119 (2008).

173. Ding, Y.-S., Shiue, C.-Y., Fowler, J.S., Wolf, A.P., Plenevaux, A. No-carrier-added (NCA) aryl [^{18}F]fluorides via the nucleophilic aromatic substitution of electron-rich aromatic rings. *J. Fluor. Chem.* **48**, 189–206 (1990).

174. Guillaume, M., Cantineau, R., Cantineu, M. L. No-carrier-added regioselective preparation of 6-^{18}F-fluoro-L-dopa. 1247–1252 (1990).

175. Lemaire, C., Guillaume, M., Cantineau, R., Plenevaux, A., Christiaens, L. An approach to the asymmetric synthesis of l-6-[^{18}F]fluorodopa via NCA nucleophilic fluorination. *Int. J. Radiat. Appl. Instrumentation. Part A. Appl. Radiat. Isot.* **42**, 629–635 (1991).

176. Lemaire, C., Plenevaux, A., Cantineau, R., Christiaens, L., Guillaume, M., Comar, D. Nucleophilic enantioselective synthesis of 6-[^{18}F]Fluoro-l-dopa via two chiral auxiliaries. *Appl. Radiat. Isot.* **44**, 737–744 (1993).

177. Reddy, G.N., Haeberli, M., Beer, H.F., Schubiger, A.P. An improved synthesis of no-carrier-added (NCA) 6-[^{18}F]Fluoro-*L*-DOPA and its remote routine production for PET investigations of dopaminergic systems. *Appl. Radiat. Isot.* **44**, 645–649 (1993).

178. Najafi, A. Measures and pitfalls for successful preparation of 'no carrier added' asymmetric 6-[^{18}F]fluor-*L*-dopa from ^{18}F-fluoride ion. *Nucl. Med. Biol.* **22**, 395–397 (1995).

179. Horti, A., Redmond, D.E., Soufer, R. No-carrier-added (NCA) synthesis of 6-[^{18}F]fluoro-L-DOPA using 3,5,6,7,8,8a-hexahydro-7,7,8a-trimethyl-[6S-(6α, 8α, 8αβ)]-6,8-methano-2H-1,4-benzoxazin-2-one. *J. Label. Compd. Radiopharm.* **36**, 409–423 (1995).

180. European Pharmacopoiea. Fluorodopa (18F) (Prepared by nucleophilic substitution) Injection. in *European Pharmacopoeia* 6534–6537 (European Pharmacopoeia, 2019).

181. Kaneko, S., Ishiwata, K., Hatano, K., Omura, H., Ito, K., Senda, M. Enzymatic synthesis of no-carrier-added 6-[^{18}F]fluoro-l-dopa with β-tyrosinase. *Appl. Radiat. Isot.* **50**, 1025–

1032 (1999).

182. Guillouet, S.C., Lemaire, G., Bonmarchand, L., Zimmer, Bars, D. Large scale production of 6-[^{18}F]fluoro-L-DOPA in a semi-automated system. *JournalofLabelledCompounds Radiopharm.* **44**, S868–S870 (2001).

183. Zhang, L., Tang, G., Yin, D., Tang, X., Wang, Y. Enantioselective synthesis of no-carrier-added (NCA) 6-[^{18}F]fluoro-L-DOPA. *Appl. Radiat. Isot.* **57**, 145–151 (2002).

184. Shen, B., Ehrlichmann, W., Uebele, M., Machulla, H.-J., Reischl, G. Automated synthesis of n.c.a. [^{18}F]FDOPA via nucleophilic aromatic substitution with [^{18}F]fluoride. *Appl. Radiat. Isot.* **67**, 1650–1653 (2009).

185. Krasikova, R.N., Zaitsev, V.V., Ametamey, S.M., Kuznetsova, O.F., Fedorova, O.S., Mosevich, I.K., Belokon, Y.N., Vyskočil, Š, Shatik, S.V., Nader, M., Schubiger, P.A Catalytic enantioselective synthesis of ^{18}F-fluorinated α-amino acids under phase-conditions using (S)-NOBIN. *Nucl. Med. Biol.* **31**, 597–603 (2004).

186. Corey, E.J., Xu, F., Noe, M.C.A Rational Approach to Catalytic Enantioselective Enolate Alkylation Using a Structurally Rigidified and Defined Chiral Quaternary Ammonium Salt under Phase Transfer Conditions. *J. Am. Chem. Soc.* **119**, 12414–12415 (1997).

187. Lemaire, C., Gillet, S., Guillouet, S., Plenevaux, A., Aerts, J., Luxen, A. Highly Enantioselective Synthesis of No ‐ Carrier ‐ Added 6 ‐ [^{18}F]Fluoro ‐ L ‐ dopa by Chiral Phase ‐ Transfer Alkylation. *Eur. J. Org. Chem.* 2899–2904 (2004).

188. Lemaire, C., Libert, L., Plenevaux, A., Aerts, J., Franci, X., Luxen, A. Fast and reliable method for the preparation of ortho- and para-[^{18}F]fluorobenzyl halide derivatives: Key intermediates for the preparation of no-carrier-added PET aromatic radiopharmaceuticals. *J. Fluor. Chem.* **138**, 48–55 (2012).

189. Date, R. *AllinOne Specific application manual [^{18}F] FDOPA.*

190. Poniger, S.S. Automated Nucleophilic Radiosynthesis of [^{18}F] FDOPA with a modified iPHASE FlexLab Module Ya-Yao Huang , Stan Poniger , Chia-Ling Tsai ,. in *22nd ISRS* (2017).

191. Pretze, M., Franck, D., Kunkel, F., Foßhag, E., Wängler, C., Wängler, B. Evaluation of two nucleophilic syntheses routes for the automated synthesis of 6-[^{18}F]fluoro-L-DOPA. *Nucl. Med. Biol.* **45**, 35–42 (2017).

192. Hormuzdi, S.G., Filippov, M.A., Mitropoulou, G., Monyer, H., Bruzzone, R. Electrical

synapses: A dynamic signaling system that shapes the activity of neuronal networks. *Biochim. Biophys. Acta - Biomembr.* **1662**, 113–137 (2004).

193. Proper, E.A., Oestreicher, A.B., Jansen, G.H., Veelen, C.W.M.V., Van Rijen, P.C., Gispen, W.H., De Graan, P.N.E. Immunohistochemical characterization of messy fibre sprouting in the hippocampus of patients with pharmaco-resistant temporal lobe epilepsy. *Brain* **123**, 19–30 (2000).

194. Robinson, J.L., Molina-Porcel, L., Corrada, M.M., Raible, K., Lee, E. B., Lee, V.M.Y., Kawas, C.H., Trojanowski, J.Q. Perforant path synaptic loss correlates with cognitive impairment and Alzheimer's disease in the oldest-old. *Brain* **137**, 2578–2587 (2014).

195. Glantz, L., Lewis, D. Decreased dendritic spine density on prefrontal cortical pyramidal neurons in schizophrenia. *Arch Gen Psychiatry* **57**, 65–73 (2000).

196. Tang, G., Gudsnuk, K., Kuo, S.-H., Cotrina, M.L., Sosunov, G.R.A., Sonders, M.S., Kanter, E., Castagna, C., Yamamoto, A., Yue, Z., Arancio, O., Bradley S.P.F.C., Dwork, A.J., Goldman, J., Sulzer, D. Loss of mTOR-dependent macroautophagy causes autistic-like synaptic pruning deficits. *Neuron* **83**, 1131–1143 (2014).

197. Kang, H., Voleti, B., Hajszan, T. Decreased expression of synapse-related genes and loss of synapses in major depressive disorder. *Nat. Med.* **18**, 1413–1417 (2012).

198. Cybulska, K., Perk, L., Booij, J., Laverman, P., Rijpkema, M. Huntington's disease: A review of the known PET imaging biomarkers and targeting radiotracers. *Molecules* **25**, 1–21 (2020).

199. Cai, H.J., Mangner, T., Muzik, O., Wang, M.-W., C. Chugani, D., T. Chugani, H., Radiosynthesis of ^{11}C-Levetiracetam: A Potential Marker for PET Imaging of SV2A Expression. *ACS Med. Chem. Lett.* **5**, 1152–1155 (2014).

200. Lyseng-Williamson, K.A. Levetiracetam: A review of its use in epilepsy. *Drugs* **71**, 489–514 (2011).

201. Rokka, J., Schlein, E., Eriksson, J. Improved synthesis of SV2A targeting radiotracer [^{11}C]UCB-J. *EJNMMI Radiopharm. Chem.* **4**, (2019).

202. Sephton, M.S., Miklovicz, T., Russell, J.J., Doke, A., Li, L., Boros, I., Aigbirhio, F.I.Automated radiosynthesis of [^{11}C]UCB-J for imaging synaptic density by positron emiss ion tomography. *J. Label. Compd. Radiopharm.* **63**, 151–158 (2020).

203. Onega, M., Ching, H., Roble, A. Highly improved and GMP compliant synthesis of ^{11}C-

UCB-J: in situ generation of boronic acid precursor. in *European journal of nuclear medicine and molecular imaging* . **44** S528 (2017).

204. Sergio, E., Mark, L., Alf, T., Sprycha, M., Buchanan, T., Mestdagh, N., Kenda, B., Mercier, J., Laurent, P., Gillard, M., Tytgat, D., Gunnar, A. [^{11}C]UCB-A, a novel PET tracer for synaptic vesicle protein 2 A. *Nucl Med Biol* **43**, 325–332 (2016).

205. Bretin, F., Warnock, G., Bahri, M. Preclinical radiation dosimetry for the novel SV2A radiotracer [^{18}F]UCB-H. *EJNMMI Radiopharm. Res* **3**, 35 (2013).

206. Finnema, S., Nabulsi, N., Mercier, J. Kinetic evaluation and test-retest reproducibility of [^{11}C]UCB-J, a novel radioligand for positron emission tomography imaging of synaptic vesicle glycoprotein 2A in humans. *J Cereb Blood Flow Metab* **38**, 2041–2052 (2017).

207. Finnema, S., Nabulsi, N., Eid, T. Imaging synaptic density in the living human brain. *Sci Transl Med* **8**, 348–396 (2016).

208. Bertoglio, D., Verhaeghe, J., Miranda, A., Kertesz, I., Cybulska, K., Korat, Š., Wyffels, L., Stroobants, S., Mrzljak, L., Dominguez, C., Liu, L., Skinbjerg, M., Munoz-Sanjuan, I., Staelens, S. Validation and noninvasive kinetic modeling of [^{11}C]UCB-J PET imaging in mice. *J. Cereb. Blood Flow Metab.* **40**, 1351–1362 (2020).

209. Martiniova, L., Cleary, S., Lai, E.W., Kiesewetter, D.O., Seidel, J., Dawson, L.F., Phillips, J.K., Thomasson, D., Chen, X., Eisenhofer, G., Powers, J.F., Kvetnansky, R.,Pacak, K. Usefulness of [^{18}F]-DA and [^{18}F]-DOPA for PET imaging in a mouse model of pheochromocytoma. *Nucl. Med. Biol.* **39**, 215–226 (2012).

210. The World Health Report 2001: Mental Disorders affect one in four people. https://www.who.int/news/item/28-09-2001-the-world-health-report-2001-mental-disorders-affect-one-in-four-people.

211. Darbà, J., Marsà, A. Exploring the current status of neuroendocrine tumours: A population-based analysis of epidemiology, management and use of resources. *BMC Cancer* **19**, 1–7 (2019).

212. Mohnike, K., Blankenstein, O., Minn, H., Mohnike, W., Fuchtner, F., Otonkoski, T. [^{18}F]-DOPA Positron Emission Tomography for Preoperative Localization in Congenital Hyperinsulinism. *Horm. Res. Paediatr.* **70**, 65–72 (2008).

213. European Commission. Council Directive 65/66/EEC. *Off. J. Eur. Communities* 20–24 (1965).

214. Council Directive 89/343/EEC of 3 May 1989 extending the scope of Directives 65/65/EEC and 75/319/EEC and laying down additional provisions for radiopharmaceuticals - Legislation - Legislation - VLEX 843284635. https://eu.vlex.com/vid/council-directive-89-343-843284635.

215. Note for guidance in radiopharmaceuticals. (1990).

216. European Parliament & Council. 2001/83/Ec. *Dir* 172 (2001).

217. European Commission. Directive 2003/63/EC. *Off. J. Eur. Union* **L**, 46–94 (2003).

218. European Commission. Commission Directive 2003/94/EC. *Off. J. Eur. Union* **L 262**, 1–33 (2003).

219. The European Parliament and the Council of the European Union. Directive 2004/27/EC, of 31 March 2004 amending Directive 2001/83/EC on the Community code relating to medicinal products for human use. *Off. J. Eur. Union* **L**, 34–57 (2004).

220. Comittee for human medicinal products. Guideline on radiopharmaceuticals. Stability studies on rFVIIIFc drug substance. 1–14 http://www.emea.europa.eu (2007).

221. Medicines Agency, E. Guideline on the non-clinical requirements for. **44**, 1–10 (2018).

222. Ministério da Saúde. Decreto-Lei n.º 72/91, de 8 de Fevereiro. *Diário da Repub.* **1**, 618–634 (1991).

223. Infarmed. Deliberação n.º 1497/2004 , de 7 de Dezembro - Define as condições exigidas aos fornecedores de matérias-primas para a prescrição e a preparação de medicamentos manipulados. *Diário da Républica* 1–2 (2004).

224. Ministério da Saúde. DL nº 176/2006 de 30 de agosto. *Diário da República 1ª série* 6297–6303 (2006).

225. Infarmed. Decreto-Lei n.º176 de 30 de Agosto de 2006. *Diário da República* 1–250 (2006).

226. Ministério da Saúde. Portaria nº 594/2004, 2004-06-02. *Legis. Farm. Compil.* **129**, 3441–5 (2004).

227. EudraLex - Volume 4 - Good Manufacturing Practice (GMP) guidelines | Public Health. https://ec.europa.eu/health/documents/eudralex/vol-4_en.

228. Castillo Meleán, J., Ermert, J., Coenen, H.H. A three-step radiosynthesis of 6-[^{18}F]fluoro-

L-meta-tyrosine starting with [^{18}F]fluoride. *J. Label. Compd. Radiopharm.* **58**, 133–140 (2015).

229. Kobayashi, S., Tanaka, H., Amii, H., Uneyama, K. A new finding in selective Baeyer-Villiger oxidation of α-fluorinated ketones; a new and practical route for the synthesis of α-fluorinated esters. *Tetrahedron* **59**, 1547–1552 (2003).

230. European Pharmacopoiea. Fluorodopa (18F) (Prepared by electrophilic substitution) injection. in *European Pharmacopoeia 8.0*.

231. 5.4 Residual Solvents. in *European Pharmacopoeia 9.0*.

232. Fluorodopa (18F)(prepared by nucleophilic substitution) Injection. in *Pharmeuropa 29.2* 156–161 (2017).

233. Mossine, A.V., Brooks, A.F., Ichiishi, N., Makaravage, K.J., Sanford, M.S., Scott, P.J.H. Development of customized [^{18}F] fluoride elution techniques for the enhancement of copper-mediated late-stage radiofluorination. *Sci. Rep.* **7**, 1–9 (2017).

234. Maruoka, K., Ooi, T. Enantioselective amino acid synthesis by chiral phase-transfer catalysis. *Chem. Rev.* **103**, 3013–3028 (2003).

235. Lygo, B., Andrews, B.I., Crosby, J., Peterson, J.A. Asymmetric alkylation of glycine imines using in situ generated phase-transfer catalysts. *Tetrahedron Lett.* **43**, 8015–8018 (2002).

236. Kano, T., Kumano, T., Sakamoto, R., Maruoka, K. Stereoselective synthesis of cyclic amino acids via asymmetric phase-transfer catalytic alkylation. *Org. Biomol. Chem.* **11**, 271–278 (2013).

237. Dolling, U.H., Davis, P., Grabowski, E.J.J. Efficient catalytic asymmetric alkylations. 1. Enantioselective synthesis of (+)-indacrinone via chiral phase-transfer catalysis. *J. Am. Chem. Soc.* **106**, 446–447 (2002).

238. O'Donnell, M.J., Bennett, W.D., Wu, S. The stereoselective synthesis of .alpha.-amino acids by phase-transfer catalysis. *J. Am. Chem. Soc.* **111**, 2353–2355 (2002).

239. Lygo, B., Wainwright, P.G. A new class of asymmetric phase-transfer catalysts derived from Cinchona alkaloids - Application in the enantioselective synthesis of α-amino acids. *Tetrahedron Lett.* **38**, 8595–8598 (1997).

240. Chester, W. Instruction Manual For CROWNPAK CR (+) / CR (-).

241. Maruoka, K. Practical Aspects of Recent Asymmetric Phase-Transfer Catalysis. *Organic Process Research & Development*. **12**, 679–697 (2008).

242. Lygo, B., Andrews, B.I. Asymmetric phase-transfer catalysis utilizing chiral quaternary ammonium salts: Asymmetric alkylation of glycine imines. *Acc. Chem. Res.* **37**, 518–525 (2004).

243. Starks, C.M., Liotta, C.L., Halpern, M.E. Basic Concepts in Phase-Transfer Catalysis. In: *Phase-Transfer Catalysis*. (Springer, 1994).

244. Ooi, T., Kameda, M., Maruoka, K. Molecular design of a C2-symmetric chiral phase-transfer catalyst for practical asymmetric synthesis of α-amino acids. *J. Am. Chem. Soc.* **121**, 6519–6520 (1999).

245. Ooi, T., Ohara, D., Fukumoto, K., Maruoka, K. Importance of chiral phase-transfer catalysts with dual functions in obtaining high enantioselectivity in the Michael reaction of malonates and chalcone derivatives. *Org. Lett.* **7**, 3195–3197 (2005).

246. Lygo, B., Allbutt, B., James, S. R. Identification of a highly effective asymmetric phase-transfer catalyst derived from α-methylnaphthylamine. *Tetrahedron Lett.* **44**, 5629–5632 (2003).

247. Lygo, B. Enantioselective synthesis of dityrosine and isodityrosine via asymmetric phase-transfer catalysis. *Tetrahedron Lett.* **40**, 1389–1392 (1999).

248. Lygo, B., Crosby, J., Peterson, J.A. Enantioselective synthesis of bis-α-amino acid esters via asymmetric phase-transfer catalysis. *Tetrahedron Lett.* **40**, 1385–1388 (1999).

249. Ooi, T., Maruoka, K. Recent advances in asymmetric phase-transfer catalysis. *Angew. Chemie - Int. Ed.* **46**, 4222–4266 (2007).

250. Stone-Elander, S., Elander, N. Microwave applications in radiolabelling with short-lived positron-emitting radionuclides. *J. Label. Compd. Radiopharm.* **45**, 715–746 (2002).

251. Stone-Elander, S., Elander, N. Microwave cavities: Some parameters affecting their use in radiolabelling reactions. *Int. J. Radiat. Appl. Instrumentation. Part A. Appl. Radiat. Isot.* **42**, 885–887 (1991).

252. Blanc, P. European Pharmacopoeia. *Br. Med. J.* **2**, 192 (1964).

253. Becker, G., Warnier, C., Serrano, M.E., Bahri, M.A., Mercier, J., Lemaire, C., Salmon, E., Luxen, A., Plenevaux, A. Pharmacokinetic Characterization of [^{18}F]UCB-H PET

Radiopharmaceutical in the Rat Brain. *Mol. Pharm.* **14**, 2719–2725 (2017).

254. Radiation Studies - CDC: ALARA. https://www.cdc.gov/nceh/radiation/alara.html.